

NASA Contractor Report

STRAIN ENERGY RELEASE RATE AS A FUNCTION OF TEMPERATURE AND PRELOADING HISTORY UTILIZING THE EDGE DELAMINATION FATIGUE TEST METHOD

Richard S. Zimmerman and Donald F. Adams

Composite Materials Research Group
University of Wyoming
Laramie, Wyoming 82071

Contract NAG-1-674

February 1989

(NASA-CR-184966) STRAIN ENERGY RELEASE RATE
AS A FUNCTION OF TEMPERATURE AND PRELOADING
HISTORY UTILIZING THE EDGE DELAMINATION
FATIGUE TEST METHOD Contractor Report, Jul.
1986 - Oct. 1988 (Wyoming Univ.) 270 p

N89-21286

Unclas
0204574

63/39

Report Documentation Page

1. Report No.		2. Government Accession No.		3. Recipient's Catalog No.	
4. Title and Subtitle Strain Energy Release Rate as a Function of Temperature and Preloading History Utilizing the Edge Delamination Fatigue Test Method				5. Report Date February 1989	
				6. Performing Organization Code	
7. Author(s) Richard S. Zimmerman and Donald F. Adams				8. Performing Organization Report No. UW-CMRG-R-89-106	
				10. Work Unit No.	
9. Performing Organization Name and Address Composite Materials Research Group University of Wyoming P. O. Box 3295 Laramie, WY 82071				11. Contract or Grant No. NAG-1-674	
				13. Type of Report and Period Covered Contractor Report July 1986 - October 1988	
12. Sponsoring Agency Name and Address National Aeronautics and Space Administration NASA-Langley Research Center Hampton, VA 23665				14. Sponsoring Agency Code	
15. Supplementary Notes Technical Monitor: Dr. T. Kevin O'Brien Fatigue and Fracture Branch - NASA-Langley Research Center					
16. Abstract Static laminate and tension-tension fatigue testing of IM7/8551-7 composite materials was performed. The Edge Delamination Test (EDT) was utilized to evaluate the temperature and preloading history effect on the critical strain energy release rate (G_c). Static and fatigue testing was performed at room temperature and 180°F (82°C). Three preloading schemes were used to precondition fatigue test specimens prior to performing the normal tension-tension fatigue EDT testing. Computer software was written to perform all fatigue testing while monitoring the dynamic modulus to detect the onset of delamination and record the test information for later retrieval and reduction.					
17. Key Words (Suggested by Author(s)) edge delamination test (EDT) strain energy release rate (G_c) tension-tension fatigue modulus decay carbon fiber-reinforced/epoxy composite				18. Distribution Statement	
19. Security Classif. (of this report)		20. Security Classif. (of this page)		21. No. of pages 270	
				22. Price	

REPORT UW-CMRG-R-89-106

STRAIN ENERGY RELEASE RATE AS A FUNCTION
OF TEMPERATURE AND PRELOADING HISTORY
UTILIZING THE EDGE DELAMINATION FATIGUE TEST METHOD

RICHARD S. ZIMMERMAN
DONALD F. ADAMS

FEBRUARY 1989

TECHNICAL REPORT
NASA-LANGLEY RESEARCH CENTER
GRANT NO. NAG-1-674

COMPOSITE MATERIALS RESEARCH GROUP
DEPARTMENT OF MECHANICAL ENGINEERING
UNIVERSITY OF WYOMING
LARAMIE, WYOMING 82071-3295

PREFACE

This final report presents the results of a research program, initiated in July 1986, sponsored by the National Aeronautics and Space Administration under Grant No. NAG-1-674 (University of Wyoming Project No. 5-32474). The NASA Technical Monitor was Dr. T. Kevin O'Brien, Fatigue and Fracture Branch, Materials Division, NASA-Langley Research Center.

All work was performed by the Composite Materials Research Group (CMRG) within the Department of Mechanical Engineering at the University of Wyoming. Co-principal investigators were Mr. Richard S. Zimmerman, Staff Engineer, and Dr. Donald F. Adams, Professor. Making significant contributions to this program were Mr. Michael Borgman and Ms. Janice Atkins, undergraduate students in Mechanical Engineering and members of the CMRG.

Use of commercial products or names of manufacturers in this report does not constitute official endorsement of such products or manufacturers, either expressed or implied, by the National Aeronautics and Space Administration.

TABLE OF CONTENTS

Section	Page
1. INTRODUCTION	1
2. SUMMARY	3
3. SPECIMEN FABRICATION AND TEST PROCEDURES	10
3.1 Material	10
3.2 Static Test Procedures	10
3.2.1 Static Tension	11
3.2.2 In-Plane Iosipescu Shear	13
3.2.3 Transverse Coefficient of Thermal Expansion	13
3.3 Tension-Tension Edge Delamination Fatigue Procedure.	13
3.4 Dye-Enhanced X-ray and Optical Photography	21
3.5 Temperature and Relative Humidity Measurement	22
4. TEST RESULTS	23
4.1 Fiber and Void Volume	23
4.2 Static Tension	23
4.3 In-Plane Iosipescu Shear	26
4.4 Transverse Coefficient of Thermal Expansion.	26
4.5 Tension-Tension Edge Delamination Fatigue	27
4.6 X-ray and Optical Photography	34
5. CONCLUSIONS	43
REFERENCES	45
APPENDIX A Individual Static Test Results	47
APPENDIX B Individual Tension-Tension Fatigue Results	151

SECTION 1

INTRODUCTION

The edge delamination test (EDT) is a mixed-mode fracture test method comprised of components of a tensile mode and a sliding or interlaminar shear mode of delamination (Mode I and Mode II). It was initially developed by Pagano and Pipes to characterize interlaminar fracture toughness in composite laminates and provide a method to determine their relative damage tolerance and toughness [1,2]. The EDT has been further developed by O'Brien and most recently has been proposed as a standard test method by the American Society for Testing and Materials (ASTM) [3,4].

The edge delamination specimen develops interlaminar normal stresses at the free edges when loaded in tension. These stresses, caused by large Poisson's ratio mismatches between plies, cause the specimen to delaminate at the ply interface with the highest interlaminar normal stress. The delamination is controlled by a combination of Mode I and Mode II. Several different laminate types have been used to perform this test, with varying percentages of Mode I and Mode II components based on the layup and material system [2,3]. O'Brien has also developed a finite element computer program to quantify the contribution of each mode in the EDT for the purpose of predicting material behavior related to damage tolerance and fracture toughness [3].

The EDT method is normally performed under static tensile loading but can be performed under tension-tension fatigue loading. Fatigue loading allows the determination of dynamic fracture toughness

properties due to the cyclic loading. The purpose of this study was to measure effects of temperature and preloading history on critical strain energy release rate (G_C) determined using the edge delamination test method (EDT) in tension-tension fatigue. Tension-tension fatigue testing at two test temperatures was performed on IM7/8551-7 carbon fiber-reinforced epoxy composite specimens laid up in the $[\pm 35/0/90]_s$ orientation. Some edge delamination specimens were fatigue tested with no preconditioning while others were preconditioned using one of two methods, i.e., a high mean load for 1000 cycles or a high spike load. Static tests to determine in-plane lamina properties and static edge delamination tests were also performed on IM7/8551-7 material.

SECTION 2

SUMMARY

All test specimens were fabricated and tested by the Composite Materials Research Group (CMRG) from cured panels supplied by NASA-Langley. The complete test matrix is given in Tables 1 and 2.

Static lamina testing was performed to generate in-plane material properties necessary to calculate the critical strain energy release rate (G_C) values measured in edge delamination tests (EDT). Static EDT were conducted to allow comparisons with dynamic EDT results. Transverse coefficient of thermal expansion (CTE) tests were also performed. Tension-tension fatigue testing was performed using the EDT method with three types of preconditioning of the test specimens.

Average axial and transverse tensile, edge delamination, and in-plane Iosipescu shear results are presented in Figures 1 through 4 as a function of test temperature. Average tabulated data are given in Section 4 and individual specimen data and stress-strain plots are presented in Appendix A.

Figure 1 shows the axial tensile test results for the IM7/8551-7 carbon fiber-reinforced/epoxy material. Figures 1a through 1c show that there were minimal differences in the longitudinal material properties between the two test temperatures. Figure 2 presents the transverse tensile material properties measured. Slightly more variation was seen in the transverse tensile material properties because of specimen configuration and material variations at the two test temperatures. These differences are discussed in detail in Section 4. Critical strain energy release rate (G_C) calculated from the static EDT results

TABLE 1

Test Matrix for Static Tests

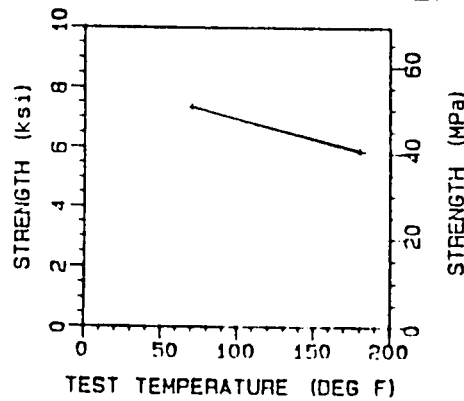
Test Method	Test Temperature (°F)	
	75	180
	<u>Test Replicates</u>	
Axial Tension	5	5
Transverse Tension	5	5
In-Plane Iosipescu Shear	5	5
[±35/0/90] _s Edge Delamination	5	5
Transverse Coefficient of Thermal Expansion (-40°F to 250°F)	3	
	43 Specimens	

TABLE 2

Test Matrix for Edge Delamination
Fatigue Tests at 10 Hz, R = 0.1

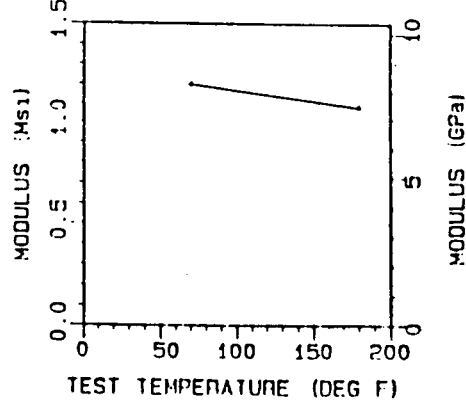
Fatigue Curve Type	Test Temperature (°F)	Specimen Replicates
Baseline Sine Wave (no preconditioning)	75	20
	180	20
High Load Spike in 1st Cycle (70 percent of ultimate load)	75	20
	180	20
High Mean Load Sine Wave (First 1000 cycles at 70 percent of ultimate peak load)	75	20
(First 1000 cycles at 60 percent of ultimate peak load)	180	20
Runout to 10 ⁶ Cycles Typical		120 Specimens
Runout to 10 ⁷ Cycles One Test/Curve		

STATIC TENSILE STRENGTH



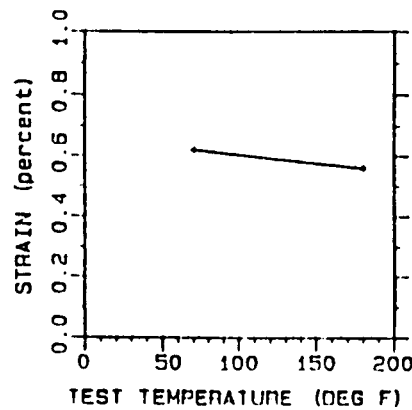
a) Static Axial Tensile Strength

STATIC TENSILE MODULUS



b) Static Axial Tensile Modulus

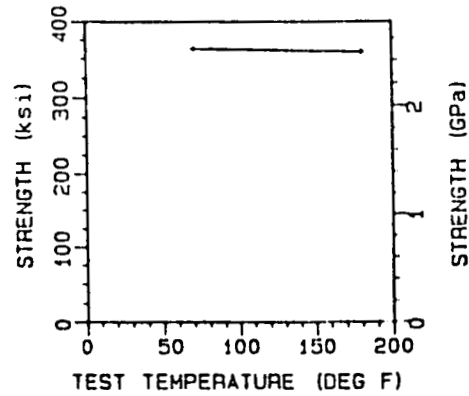
ULTIMATE TENSILE STRAIN



c) Static Axial Tensile Ultimate Strain

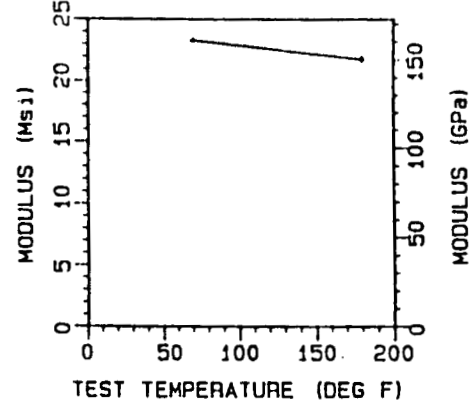
Figure 1. Average Static Axial Tensile Results for the IM7/8551-7 Carbon/Epoxy Unidirectional Composite as a Function of Temperature.

STATIC TENSILE STRENGTH



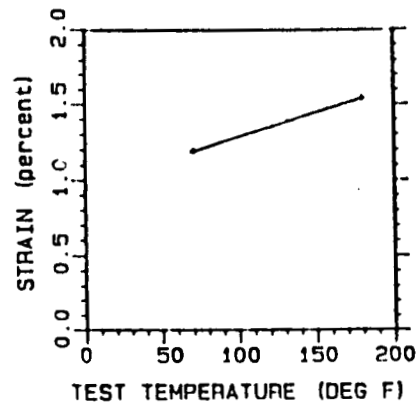
a) Static Transverse Tensile Strength

STATIC TENSILE MODULUS



b) Static Transverse Tensile Modulus

ULTIMATE TENSILE STRAIN



c) Static Transverse Tensile Ultimate Strain

Figure 2. Average Static Transverse Tensile Results for the IM7/8551-7 Carbon/Epoxy Unidirectional Composite as a Function of Temperature.

decreased slightly at the higher test temperature, as seen in Figure 3. In-plane Iosipescu shear properties are shown in Figure 4. Shear strength and modulus values decreased slightly at the higher test temperature. Ultimate shear strain variation with temperature could not be determined due to saturation of the strain gage rosettes at both test temperatures. Transverse CTE was measured for the IM7/8551-7 material.

Six complete fatigue curves were generated using EDT specimens. Three fatigue curves were generated at room temperature and three at 180°F (82°C), all at 10 Hz, using a sinusoidal waveform and a load ratio R equal to 0.1. Three preconditioning load histories (described in Section 3) were used to determine their effects on G_C . A laminated plate computer program (AC3) was used to calculate the sub-laminate modulus required for the calculation of the stiffness contribution in the strain energy release rate equation [12]. Cycles to delamination were reduced significantly after specimens had been preconditioned with the 1000 cycle high mean loading. Less effect on number of cycles to delamination was measured when a high spike loading precondition was performed prior to the fatigue loading. Values of G_C were higher at the elevated test temperature when the same precondition history fatigue curves were compared. This effect on G_C was the reverse of that seen in the static G_C data.

Section 3 discusses the test procedures and test apparatuses for all testing performed. Section 4 presents average test results for static and fatigue testing performed. Conclusions are given in Section 5. Individual test results are given in Appendices A and B.

STRAIN ENERGY RELEASE RATE

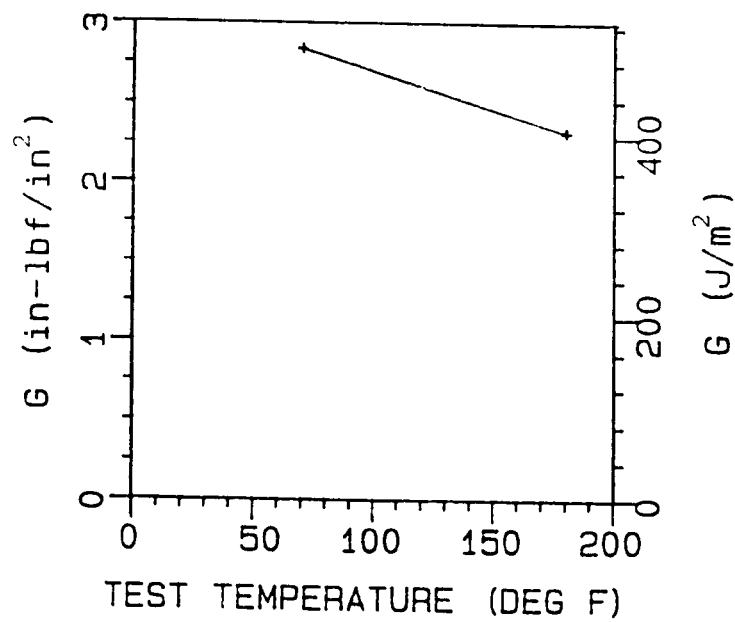
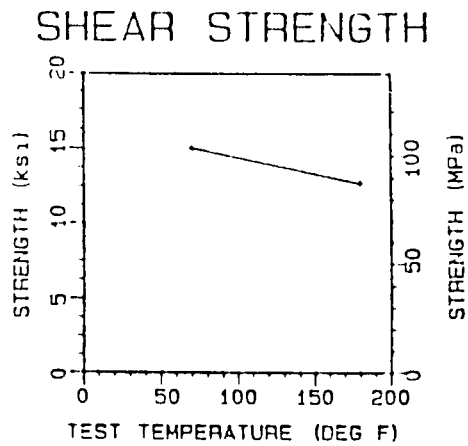
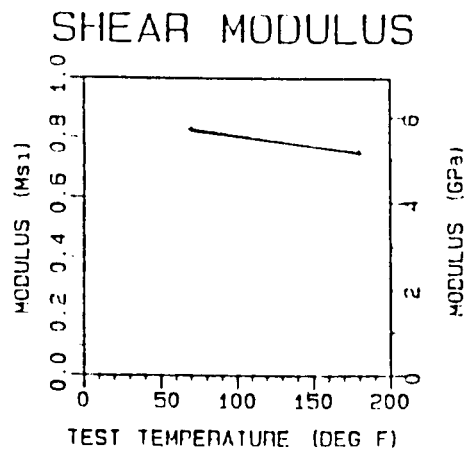


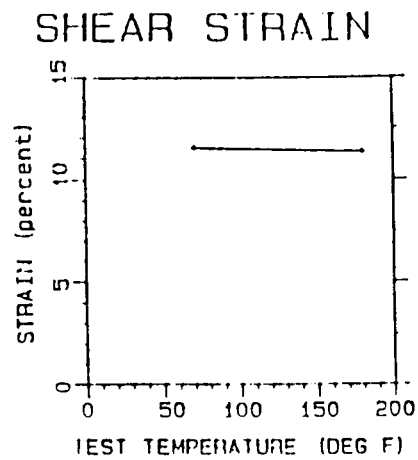
Figure 3. Average Static Critical Strain Energy Release Rate for IM7/8551-7 Carbon/Epoxy Unidirectional Composite as a Function of Temperature.



a) Static In-plane Iosipescu Shear Strength



b) Static In-plane Iosipescu Shear Modulus



c. Static In-plane Iosipescu Shear Strain

Figure 4. Average In-plane Iosipescu Shear Results for IM7/8551-7 Carbon/Epoxy Unidirectional Composite as a Function of Temperature.

SECTION 3

SPECIMEN FABRICATION AND TEST PROCEDURES

3.1 Material

The material system chosen by NASA-Langley for this study was IM7/8551-7 carbon fiber-reinforced epoxy. It is a relatively new material system manufactured by Hercules Aerospace, Salt Lake City, Utah. The IM7 is a high strength, medium modulus carbon fiber (683 ksi (4.71 GPa), 41.0 Msi (283 GPa)) [4]. The 8551-7 is a rubber-toughened epoxy with good G_{IC} toughness properties (5.5 in-lb/in² (958 J/m²)) [5]. All materials used in this program were supplied by NASA-Langley in flat plate form. Six inch (152.4 mm) square panels were supplied in the edge delamination test layup ($[\pm 35/0/90]_S$) and three different thickness unidirectional layups ($[0]_8$, $[0]_{12}$, and $[0]_{20}$). Enough material was supplied to complete six edge delamination fatigue curves and all required static tests.

3.2 Static Test Procedures

All specimens were cut from the supplied panels utilizing an abrasive cut-off wheel mounted on a surface grinder. Water cooling was used to ensure that the material did not overheat during the cutting process.

Acid digestion fiber volume determinations were performed on all panels. The procedure given in ASTM Standard Test Method D3171-76 was followed, where a 70% nitric acid was used to dissolve the matrix from the fibers using a hot plate to heat the samples to approximately 170°F (75°C) to speed up the reaction time [6]. The 8551-7 toughened epoxy

dissolved at a slower rate than usually seen in this procedure on previously studied epoxies.

All static tests were conducted using a computer-controlled Instron Model 1125 electromechanical testing machine. A BEMCO Model FTU 3.0 environmental chamber was used to achieve the 180°F (82°C) test temperature. A crosshead rate of 0.08 in/min (2 mm/min) was used for all static testing except the edge delamination testing, which was performed at 0.04 in/min (1 mm/min).

3.2.1 Static Tension

Guidelines in ASTM Standard Test Procedure D3039-76 were followed for all static tension testing [7]. Conventional wedge action grips were utilized to load specimens for all static tension testing. Static axial tension test specimens were 6 in. (152 mm) long, 0.5 inch (12.7 mm) wide, and approximately 0.04 in. (1.0 mm) thick. Longer specimens are normally used for axial tension (9 in. (229 mm)) but the supplied panels limited the specimen length to the smaller dimension. Glass/epoxy circuit board material end tabs 1.5 in. (38 mm) long were bonded to each specimen using a two-part epoxy adhesive. The adhesive was Techkits A-12 (Techkits, Inc., Demarest, New Jersey). It is used extensively for bonding tabbing material to composite specimens and has good material properties up to 350°F (177°C). Axial strains were measured using a 2 inch (50.8 mm) gage length Instron extensometer, allowing complete stress-strain curves to be generated. Lateral strains were measured with a 0.5 inch (12.7 mm) gage length extensometer on the axial tension test specimens, allowing for the calculation of Poisson's ratio.

Transverse tension test specimens were 6 in. (152 mm) long, 0.75 in. (19 mm) wide, and 0.115 in. (2.9 mm) or 0.040 in. (1.0 mm) thick. Not all transverse tension specimens could be cut from the same thickness panel due to the small panel dimensions. None of the supplied panels were large enough to accommodate all the required ten transverse tension specimens. The five room temperature test specimens were cut from the 0.115 in. (2.9 mm) thick $[0]_{20}$ panel while the five elevated temperature test specimens were cut from a 0.04 inch (1.0 mm) thick $[0]_8$ panel. End tabs were not used with these specimens. Axial strains were measured using a 2 inch (50.8 mm) gage length Instron extensometer, allowing complete stress-strain curves to be generated. Transverse strains were not measured on the transverse tension specimens.

Edge delamination test (EDT) specimens were 6 in. (152 mm) long, 0.5 inch (12.7 mm) wide, and approximately 0.04 in. (1.0 mm) thick. This specimen geometry was used for previous edge delamination testing for NASA-Langley at the University of Wyoming [10]. Other geometries can be used for this test method as described by O'Brien and Carlsson and Pipes in references [3,14]. The smaller specimen configuration was used in this program to allow more specimens to be fabricated. Approximately 1.0 inch (25.4 mm) of each end of the EDT specimens was held in the grip area, leaving 4 in. (102 mm) between the grips. Axial strains were measured using a 2 inch (50.8 mm) gage length Instron extensometer, allowing complete stress-strain curves to be generated. Lateral strains were measured with a 0.5 inch (12.7 mm) gage length extensometer, allowing for the calculation of Poisson's ratio for the static EDT tests.

3.2.2 In-Plane Iosipescu Shear

In-plane Iosipescu shear test specimens were 3 in. (76.2 mm) long, 0.75 in. (19.1 mm) wide, and approximately 0.06 in. (1.6 mm) thick. Opposing 90° notches were cut on each edge of the specimens to a depth of 0.15 in. (3.8 mm). The notches were cut using a silicon-carbide grinding wheel dressed to the 90° angle with a 0.05 in. (1.3 mm) radius at the bottom of the notch.

Loads were applied to all in-plane shear specimens using a Wyoming Iosipescu shear test fixture. Shear strains were measured with a Measurements Group No. EP-13-062TH-120 two-element rosette strain gage mounted between the notches of the specimens. Complete shear stress-shear strain curves were generated for all Iosipescu shear specimens.

3.2.3 Transverse Coefficient of Thermal Expansion (CTE)

The transverse CTE test specimens were 5 in. (127 mm) long, 0.375 in. (9.5 mm) wide, and 0.115 in. (2.9 mm) thick. No axial coefficient of thermal expansion specimens were tested in this program.

Transverse CTE tests were performed using a microprocessor-controlled quartz-tube dilatometer in conjunction with a linear-variable differential transformer (LVDT). The specimens were exposed to thermal excursions between -40°F (-40°C) and 250°F (120°C). Data were acquired on the heat-up portion of the thermal cycles only. Two thermal cycles each were completed on the three specimens tested.

3.3 Tension-Tension Edge Delamination Fatigue Procedure

All fatigue tests were performed on an Instron Model 1321 biaxial servo-hydraulic testing machine using a 10 Hz sinusoidal excitation

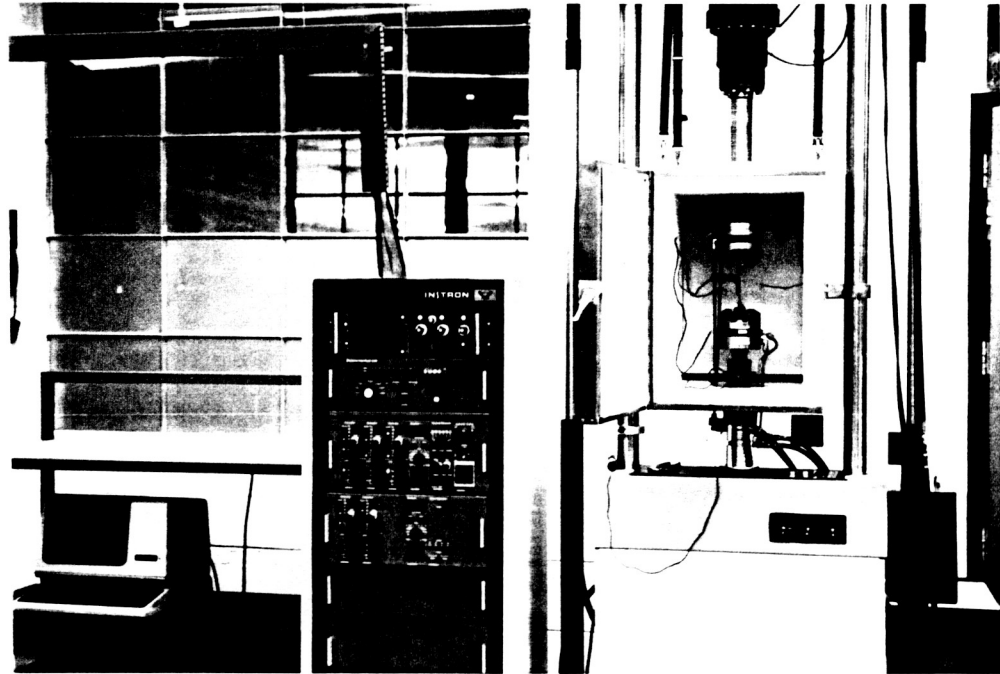
waveform and a load ratio R (ratio of minimum to maximum applied cyclic loading) approximately equal to 0.1. Axial strains were measured using a 2 inch (50.8 mm) gage length Instron extensometer. The extensometer knife edges were bonded to the EDT specimens using Devcon 5-minute two-part epoxy to ensure that the measured strains were not affected by slippage of the knife edges on the specimens' surface during the fatigue test.

Model 647.02S hydraulic grips manufactured by MTS, Inc., Minneapolis, Minnesota, were used to grip specimens for all edge delamination fatigue testing. The grips were equipped with special high temperature seals and actuating fluid system to allow usage up to 350°F (177°C). They have a load capacity of 5500 pounds (25 kN), which was sufficient to perform all EDT fatigue testing.

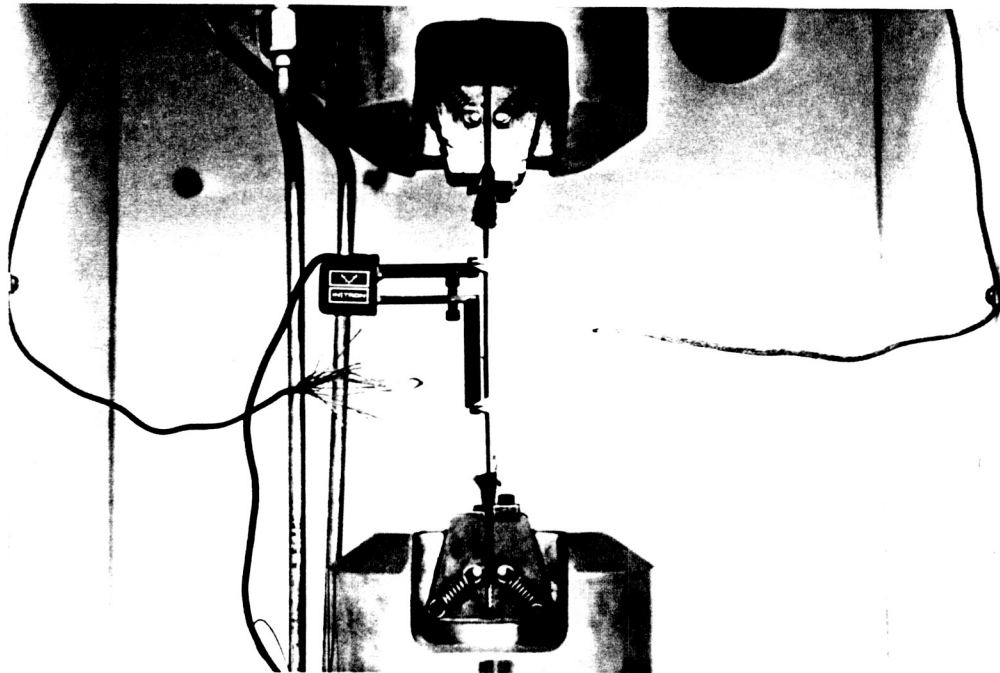
An Applied Test Systems, Inc. Series 2911 environmental chamber was used to achieve the required 180°F (82°C) test temperature. Chamber temperature was measured using a Type "E", Chromel-Constantan, thermocouple placed near the test specimen. Figure 5 shows the tension-tension fatigue test configuration used with the environmental chamber in place.

Six complete fatigue curves were generated using the EDT method while monitoring the dynamic modulus of the specimens. Three fatigue curves were generated at room temperature and three at elevated temperature, 180°F (82°C). The three fatigue curves at each temperature were generated using different preloading schemes prior to the normal sinusoidal fatigue test. One curve at each test temperature consisted of a normal sinusoidal loading to specimen delamination with no preload history (normal baseline curve). One curve at room temperature was

ORIGINAL PAGE IS
OF POOR QUALITY



a) Overall View of EDT Fatigue Test Setup



b) Close-up View of EDT Fatigue Test Setup

Figure 5. Edge Delamination Fatigue Test Configuration Showing Extensometer Mounted on EDT Specimen, Hydraulic Grips, Environmental Chamber, Instron Model 1321 Testing Machine, and Controls Cabinet.

generated with normal sinusoidal loading to delamination after the specimens had been subjected to a high cyclic load to 70 percent of ultimate load for 1000 cycles (high mean load curve). The elevated temperature fatigue curve with a high mean load for 1000 cycles was performed to only 60 percent of ultimate load because the EDT specimens delaminated before the 1000 cycles were completed at 70 percent of ultimate load. This precluded the possibility for further fatigue loading. The third fatigue curves at both test temperatures were generated after the EDT specimens had been subjected to a maximum load of 70 percent of ultimate load for one cycle (spike load curve).

The fatigue test procedure for all testing was quite complicated and required a great deal of time and effort to perfect. The application computer programs necessary to calibrate and perform the testing were written by the CMRG in Fortran 77 computer language on a PDP 11/24 minicomputer. The application programs interfaced with an Instron Machine Driver (IMD) to perform the required subroutine calls to control the test machine and to acquire the data during each fatigue test. The Instron Machine Driver is written in the Macro-11 computer language and is supported by Instron Corporation, Canton, Massachusetts. It consists of numerous machine control subroutines and data acquisition subroutines interfaced with the Instron testing machine hardware. Data recorded during each fatigue test were load, strain, stroke, and cycle count.

The application computer programs also performed many calculations and decisions based on the status of the fatigue test, such as to continue with the test if the specimen was intact, or stop the test if the specimen had delaminated causing a loss of stiffness. The decision

to continue or suspend testing was based on the dynamic modulus calculated during the test. The dynamic modulus was calculated using a linear regression curve-fit technique. The lowest stress level during a cycle (σ_{\min}) was found and the slope of the stress-strain curve was calculated over the next 20 data stress-strain pairs. If the calculated dynamic modulus had decreased by 5 percent or more from the initial calculated modulus, signifying delamination, then the computer would stop the fatigue test. Storage of data was accomplished using a logarithmic scheme similar to that used in previous modulus decay fatigue testing for NASA-Langley [8,9]. Table 5 gives the data storage progression used in this program.

There were five major steps required to prepare for and perform an EDT fatigue test. Step 1 was to calibrate the load, strain, and stroke

Table 5

DATA STORAGE PROGRESSION

Cycle Range	Cycle Increment Between Disk Storage
1 to 100	1
101 to 1000	10
1001 to 10,000	100
10,001 to 100,000	1,000
100,101 to 1,000,000	10,000
1,000,001 to 10,000,000	100,000

transducers to the appropriate values required. This step was performed periodically during the testing to verify that calibration values had not changed for the three transducers and their respective amplifiers.

Step 2 was to calibrate the computer with the three transducer outputs. This step was performed to ensure the computer had stored the current transducer calibrations before each fatigue test.

Step 3 was to perform a preliminary fatigue test using a square wave excitation on a specimen with similar stiffness to the actual test specimen. A square wave excitation was used to set the load transducer gain level for optimum control and response of the Instron test machine at each load level as described in the Instron Machine Operation Manual [11]. Step 3 was critical because of the limited load control response of the Instron 1321 at the 10 Hz cycling frequency. After setting the gain level to the optimum level, the computer program calculated the appropriate amount of computer control overprogramming necessary to ensure the loads transmitted to the specimen were close to the desired values. The mass of the torsional actuator below the linear actuator was very detrimental to the performance of the Instron Model 1321 test machine at the 10 Hz cycling frequency, but was fully compensated for by this load command overprogramming in the application computer program. The stiffness of the composite material specimens being tested was low enough and the inertia of the load frame actuator high enough to require a command overprogramming of 10 to 20 percent for all fatigue tests.

Step 4 was performed on only those specimens subjected to a pretest load history. The high mean load EDT specimens were tension-tension fatigue tested for 1000 cycles at a maximum peak load equal to 70 percent of ultimate load in the room temperature case, and 60 percent of

ultimate load in the 180°F (82°C) case. The lower peak load precondition used for the elevated temperature specimens was necessary to prevent the delamination of the specimens prior to completing the full 1000 cycles. The spike load EDT specimens were cycled once to a peak load of 70 percent of ultimate prior to being subjected to the normal sinusoidal loading. It was not necessary to reduce the spike peak load level for the elevated temperature specimens because they did not delaminate during the one cycle at the 70 percent peak load level.

Performance of the actual tension-tension fatigue test on the edge delamination specimen at a particular stress level was Step 5. This step included performing the fatigue test between two predetermined stress values until delamination occurred and the specimen calculated dynamic modulus had decreased by at least 5 percent from the initial calculated value. Figure 6 shows a typical modulus decay curve. All modulus decay curves are included in Appendix B. When the dynamic modulus decreased to less than 95 percent of the original calculated value, the computer suspended the fatigue test and ramped to zero load. As Figure 6 shows, the drop in modulus was easily determined from the data. The critical strain value (ϵ_c) used in the G_c calculation was determined by looking at these curves and picking the location of the onset of delamination as the point where the modulus started to decrease to the minimum value for that test. At least one specimen for each fatigue curve was tested to 10^7 cycles to investigate material behavior at longer than normal fatigue test runout (typically 10^6 cycles). Optical inspection of test specimens, after the computer had suspended the tests, always revealed they had delaminated on one or both free edges.

MODULUS DECAY CURVE

IM 7 / 8551-7

SINGLE SPIKE AT 70% ULTIMATE - ROOM TEMPERATURE (23 C)

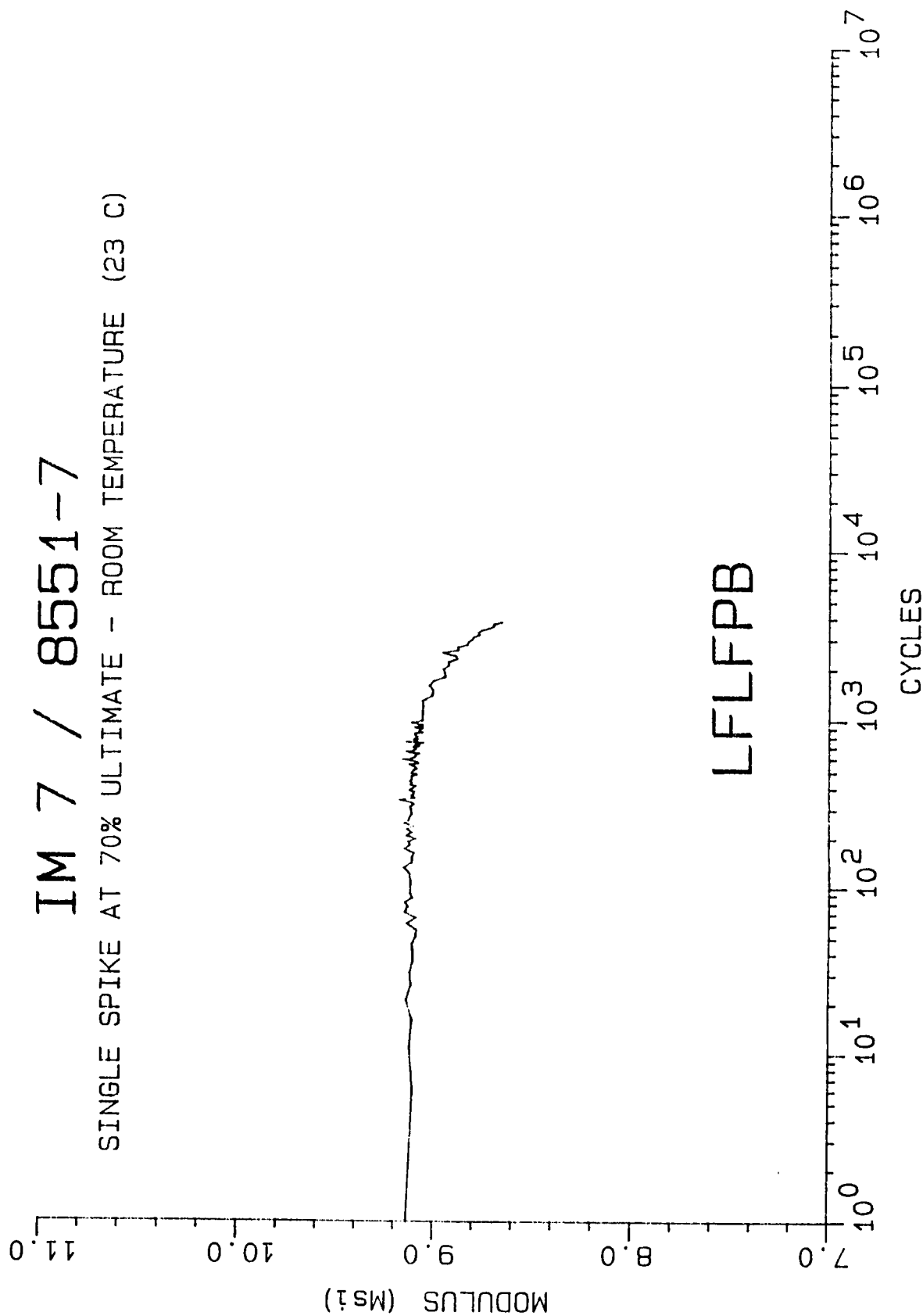


Figure 6. Typical Modulus Decay Curve Used to Determine Onset of Delamination.

Specimen data files were then transferred from the PDP11/24 to a VAX 11/750 minicomputer for reduction and plotting after test completion. Complete test results are presented in Section 4.

3.4 Dye-Enhanced X-Ray and Optical Photography

Dye-enhanced x-ray and optical photographs were taken of some of the specimens, to document the extent of the delaminations. A PANTEK Model HF75 Industrial X-ray unit was used to take all radiographs. This unit was designed especially for low density materials such as composites. The dye was the same used for previous work for NASA-Langley [10]. The mixture formula used is as follows:

60 gm	ZnI ₂ (Zinc Iodide)
10 ml	Isopropyl Alcohol
10 ml	Deionized Water
1 ml	Kodak "Photo-Flo", Wetting Agent

Polaroid Type 55 sheet film was used for all x-ray photographs. Settings on the x-ray controls were adjusted to result in good contrast for better interpretation of the photographs. The control settings were 17 kilovolts (kV), 12 milliamps (mA), 20 seconds exposure time, and 17 inch (432 mm) film focal distance (FFD). Two specimens from each EDT fatigue curve were radiographed. These radiographs are presented in Section 4.

3.5 Temperature and Relative Humidity Measurement

Temperature and relative humidity measurements were recorded during most of the fatigue testing phase in the test laboratory using a Cole-Parmer Model 8368-50 hygrothermograph. Charts were changed periodically during the testing phase. Relative humidity ranged from 12 to 20 percent while laboratory temperature ranged from 68° to 86°F (20° to 30°C).

SECTION 4

TEST RESULTS

4.1 Fiber and Void Volume Results

All IM7/8551-7 panels supplied by NASA-Langley had a fiber volume of approximately 60 percent. The $[0]_8$ and $[\pm 35/0/90]_S$ panels had slightly higher fiber volumes than the $[0]_{12}$ and $[0]_{20}$ panels (62 percent versus 59 percent). Void volumes were typically less than 1 percent except for the EDT panels where 1.2 to 4.7 percent voids were measured. Individual tabulated fiber and void volume data are given in Appendix A.

4.2 Static Tension Test Results

All average static test results are given in Table 4. Individual static test results are given in Appendix A. Static tensile test results for the two test temperatures indicate the moderate elevated temperature, i.e., 180°F (82°C), had some effect on the material behavior.

A slight decrease in axial tensile strength, and axial Young's modulus, and an increase in ultimate axial tensile strain and major Poisson's ratio were measured at the elevated test temperature, possibly due to the higher test temperature causing slight softening of the matrix material.

Transverse tensile test results indicate that the IM7/8551-7 material had lower strength and stiffness properties at the elevated test temperature. Because the specimens tested at the two different

TABLE 4

Average Static Test Results for IM7/8551-7
Carbon Fiber-Reinforced Epoxy Composite Material

Test Method	Test Temperature (°F)	Ultimate Strength (ksi) (MPa)	Modulus (Msi) (GPa)	Ultimate Strain (percent)	Poisson's Ratio	Stress at Delamination (ksi) (MPa)	Strain at Delamination (percent)	Strain Energy Release Rate $\frac{(\text{in-lb})}{(\text{in}^2)}$ $\frac{(\text{J})}{(\text{m}^2)}$
Axial Tension	75	363	23.3	2505	160.7	1.19	0.18	
	180	359	21.8	2475	150.3	1.54	0.36	
Transverse Tension	75	7.3	51	1.20	8.2	0.62		
	180	5.9	41	1.08	7.4	0.56		
In-Plane Tension	75	15.0	104	0.83	5.7	>11.50		
	180	12.7	88	0.75	5.2	>11.30		
Edge Delamination [$\pm 35/0/90$] _s	75	106.6	735	9.85	67.9	1.16	0.20	2.84 497
	180	109.4	754	9.99	68.9	1.45	0.45	2.32 406

temperatures were cut from different panels and were of different thicknesses, an independent temperature effect could not be determined. The overall effect of specimen configuration and test temperature was seen as a decrease in transverse tensile strength and modulus and ultimate transverse tensile strain values at the higher test temperature.

Static EDT results indicate that the IM7/8551-7 material was almost 20 percent tougher at room temperature than at the elevated test temperature. Critical strain energy release rate (G_C) values were slightly lower at the elevated temperature due to the lower measured critical strain at delamination (ϵ_C) and the lower stiffness values for the laminates. Equation (1) was used to calculate G_C :

$$G_C = \frac{1}{2} \epsilon_C^2 t (E_{lam} - E^*) \quad (1)$$

where G_C = critical strain energy release rate

ϵ_C = axial strain at delamination onset

t = laminate thickness

E_{lam} = initial laminate modulus

E^* = laminate modulus if completely delaminated along one or more interfaces

Strain at delamination onset (ϵ_C) was determined from the EDT stress-strain curves at the point where the curve began to deviate from linear behavior. E_{lam} was determined by calculating the initial tangent modulus for the static EDT specimens. Values for ϵ_C and E_{lam} are given in Table 4. The delaminated modulus (E^*) was calculated using Equation (2):

$$E^* = \frac{8E_{[\pm 35/0]_S} + 2E_{22}}{8} \quad (2)$$

No $[\pm 35/0]_S$ sub-laminate material was supplied to measure the stiffness values required to calculate the G_C values. Laminated Plate Theory Program AC3 was used to calculate the stiffness values for the sub-laminate used in the E^* calculations [12]. The E_{22} value was determined by calculating the initial tangent modulus from the transverse tensile tests. Appropriate values for each test temperature were used in all calculations.

4.3 In-Plane Iosipescu Shear Test Results

Average in-plane shear test results are presented in Table 4. Individual tabulated results and plotted results are given in Appendix A. Significant differences were seen in shear test results at the two test temperatures. Shear strength decreased by 25 percent and shear modulus decreased by 10 percent at the higher test temperature. Ultimate shear strains could not be determined due to saturation of the strain gage rosettes used to measure shear strain on the Iosipescu shear test specimens. Shear strains measured were quite nonlinear for this material system at both test temperatures.

4.4 Transverse Coefficient of Thermal Expansion (CTE) Results

Average transverse CTE results are presented here. Individual tabulated and plotted transverse CTE results are presented in Appendix A. The average transverse CTE value for the IM7/8551-7 material was $19.4 \mu\epsilon/^\circ\text{F}$ ($34.8 \mu\epsilon/^\circ\text{C}$). This value is quite typical for most carbon fiber/epoxy material systems. No unusual behavior was seen

in the thermal expansion testing results. No axial thermal expansion testing was conducted in this program due to the dilatometer equipment not being able to adequately measure the extremely small displacements in the axial direction for carbon fiber/epoxy composites.

4.5 Tension-Tension Edge Delamination Fatigue Results

Six complete fatigue curves were generated using the EDT method subjected to sinusoidal excitation loading at 10 Hz, $R = 0.1$, at various stress levels. Three of the fatigue curves were generated at room temperature and three at elevated temperature, 180°F (82°C). Three different specimen preconditioning methods were used to prepare the EDT test specimens for cyclic fatigue loading. One curve at each test temperature was generated using a normal sinusoidal loading to specimen delamination with no pretest load history (baseline curves). One curve at room temperature was generated with normal sinusoidal loading after the specimen had been subjected to a high cyclic load to 70 percent of ultimate load for 1000 cycles (high mean load curves). The elevated temperature precondition, with the high mean load for 1000 cycles, was performed to only 60 percent of ultimate load. The EDT specimens delaminated before the 1000 cycles were completed at 70 percent, precluding the need for further fatigue loading. The third fatigue curve at both test temperatures was generated after the EDT specimens had been subjected to 70 percent of ultimate load for one cycle only (spike load).

Figures 7 through 9 illustrate the temperature effect on G_C for each of the three load preconditions. Figure 7 shows the two normal fatigue curves generated at different temperatures. Figures 8 and 9

STRAIN ENERGY RELEASE RATE AT ONSET OF DELAMINATION

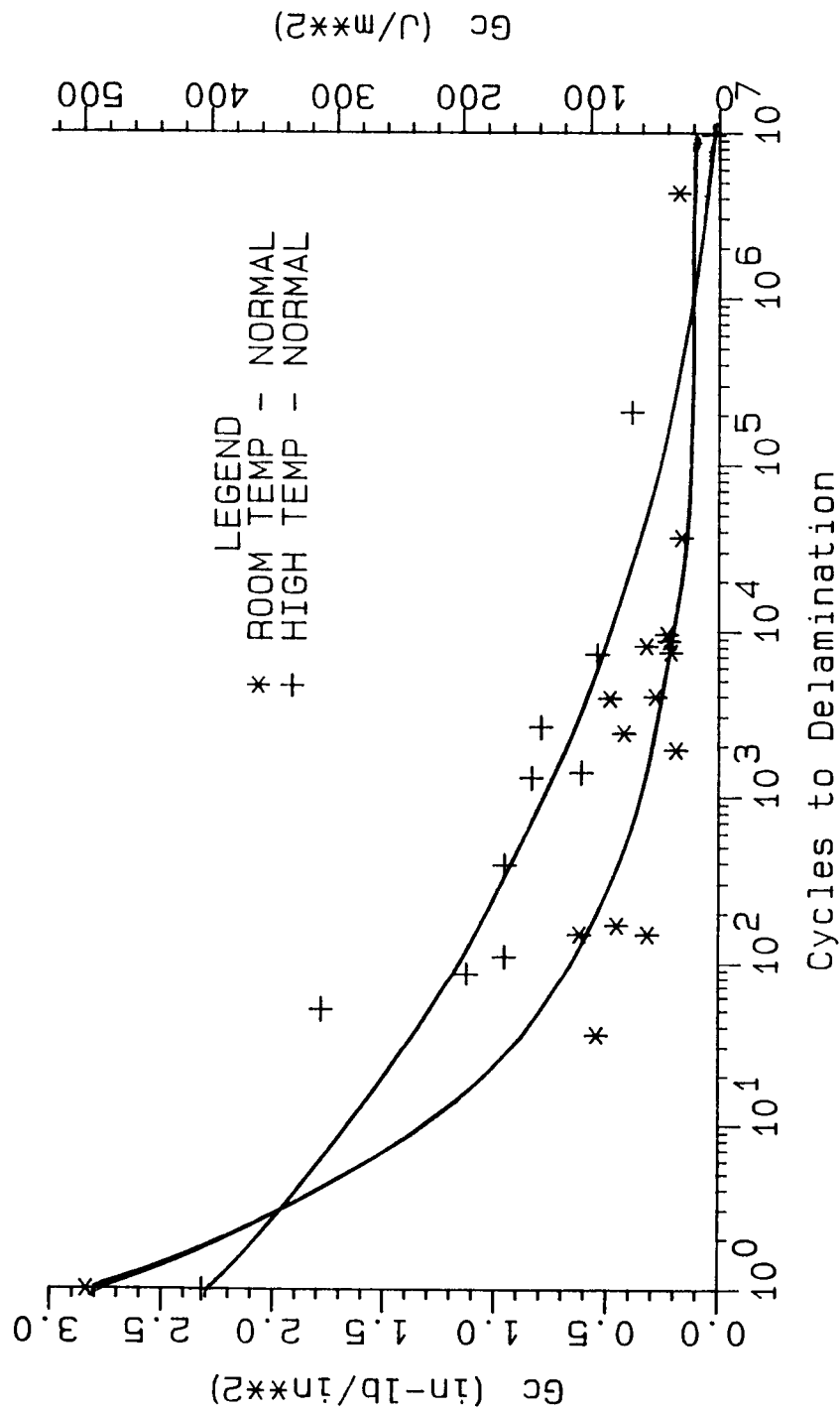


Figure 7. Critical Strain Energy Release Rate for IM7/8551-7 [$+35/0/90$]_s Laminates with No Precondition as a Function of Temperature.

STRAIN ENERGY RELEASE RATE AT ONSET OF DELAMINATION

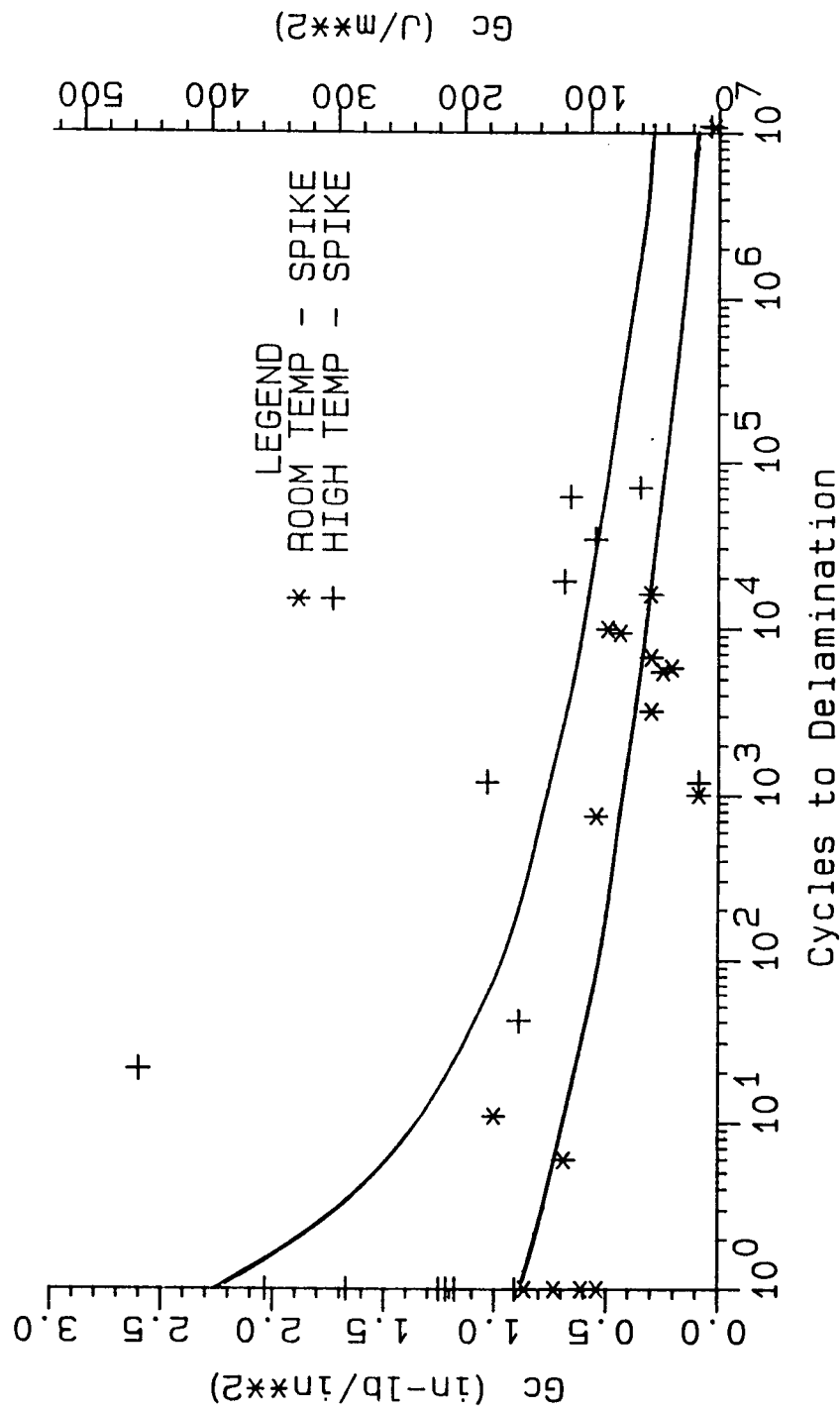


Figure 8. Critical Strain Energy Release Rate for IM7/8551-7 [$+35/0/90$]_s Laminates with High Spike Load Precondition as a Function of Temperature.

STRAIN ENERGY RELEASE RATE AT ONSET OF DELAMINATION

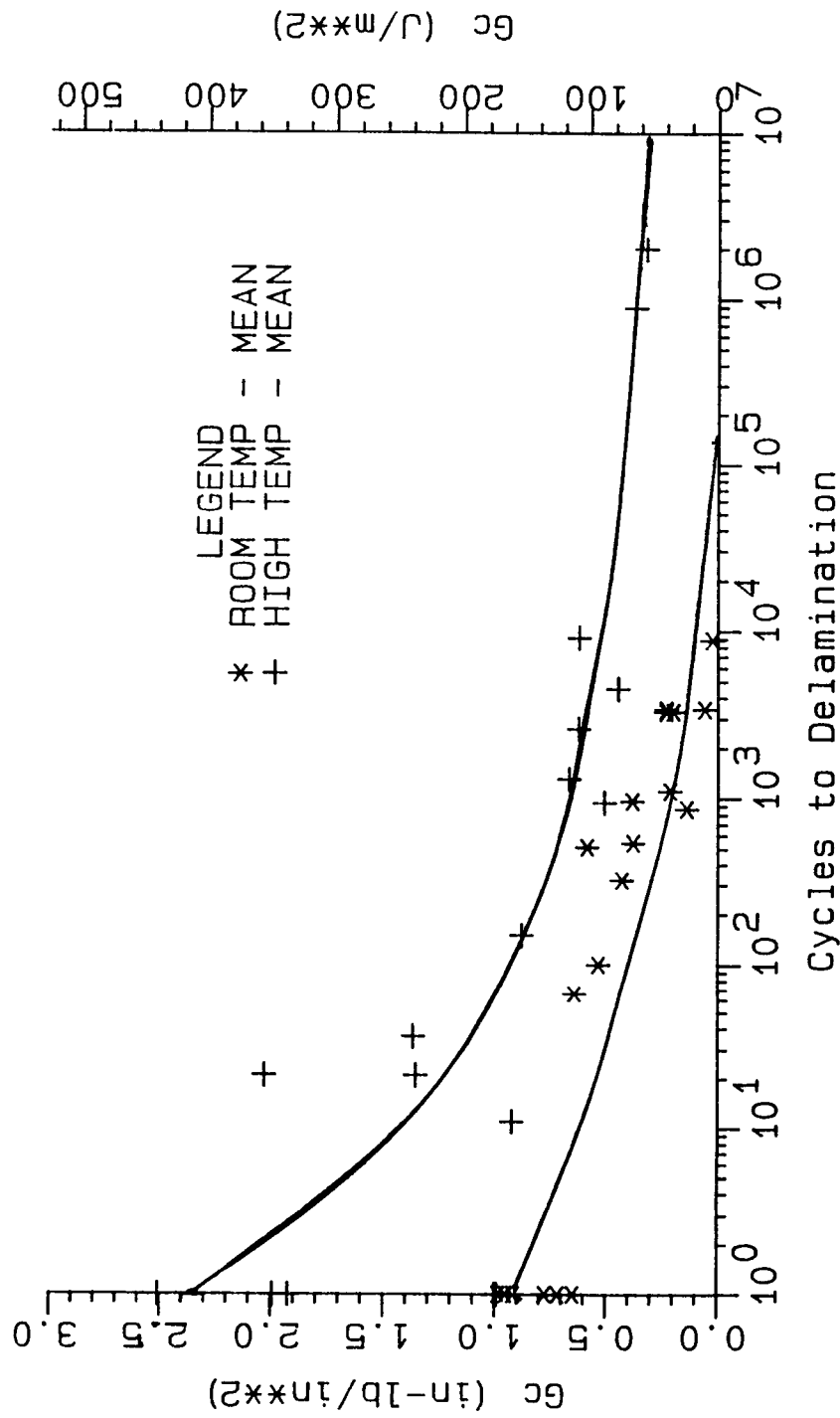


Figure 9. Critical Strain Energy Release Rate for IM7/8551-7 [+35/0/90]_s Laminates with High Mean Load for 1000 Cycles Precondition as a Function of Temperature.

show the high spike and high mean load precondition fatigue curves at the two test temperatures, respectively. The elevated temperature curve in all three of these figures indicates that higher dynamic G_C values were calculated independent of precondition method, for comparable cycles to delamination.

Comparisons of room temperature fatigue G_C values at low numbers of cycles with static G_C data (Table 4) indicate that the dynamic G_C values are much lower (a factor of two) than those generated under static loading at room temperature. Elevated temperature dynamic G_C values at a low number of cycles to delamination indicate much more consistent values compared with elevated temperature static G_C values.

The normal, high spike load, and high mean load curves at the room test temperature and elevated test temperature are plotted in Figures 10 and 11, respectively. Figure 10 indicates that there are significant effects due to the preloading history at room temperature. The two precondition loading curves indicate that damage incurred by the specimen is worse for the high mean load precondition than for the high spike precondition. At room temperature, nearly three decades fewer cycles were seen in the high mean precondition curve than the normal curve data. The spike precondition curve at room temperature indicates that approximately two decades fewer cycles to delamination were measured compared to the normal fatigue curve. Precondition comparisons in Figure 11 show that the effects were reduced significantly at the higher test temperature. Little difference could be seen between the three fatigue curves at the 180°F (82°C) test temperature after passing 10-100 cycles.

STRAIN ENERGY RELEASE RATE AT ONSET OF DELAMINATION

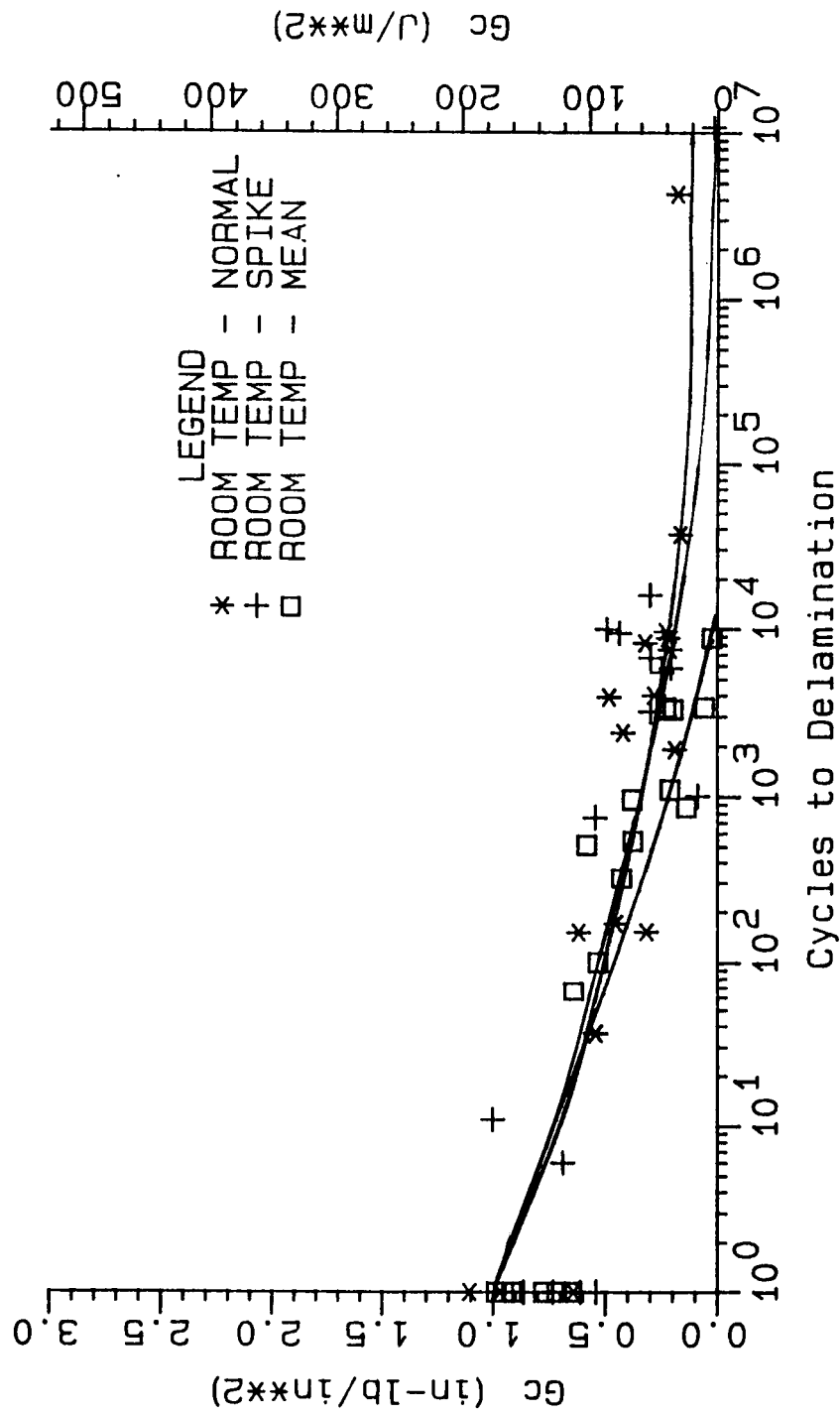


Figure 10. Critical Strain Energy Release Rate for IM7/8551-7 [₊35/0/90]_s Laminates at Room Temperature as a Function of Precondition.

STRAIN ENERGY RELEASE RATE AT ONSET OF DELAMINATION

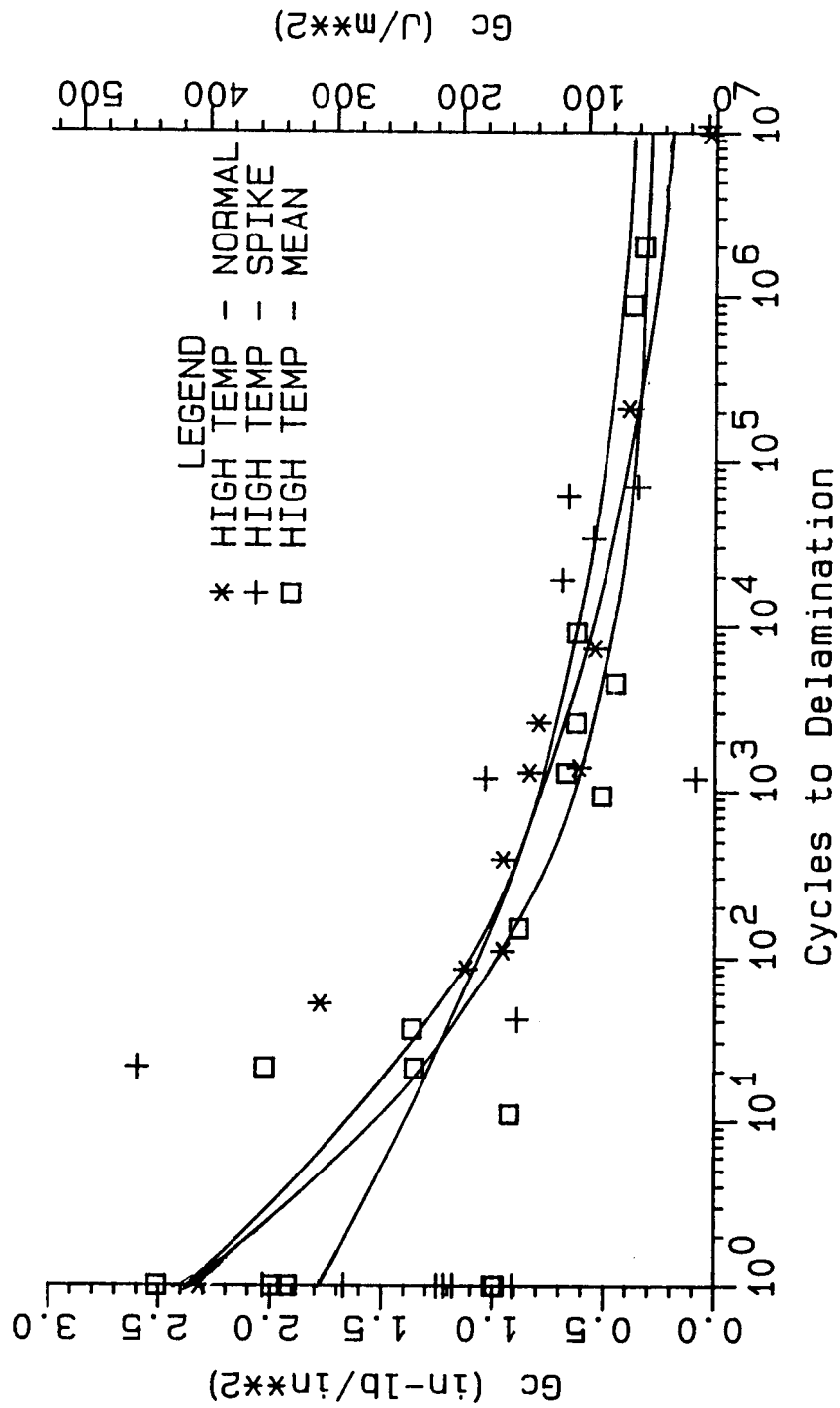


Figure 11. Critical Strain Energy Release Rate for IM7/8551-7 [$+35/0/90$] Laminates at Elevated Temperature (180°F (82°C)) as a Function of Precondition.

4.6 X-ray and Optical Photograph Results

Dye-penetrant enhanced x-rays and optical photographs were taken of some of the failed EDT specimens to document the extent of the delaminations. The x-ray opaque dye was composed of the materials listed in Section 3.5 at the given mixing ratios. Figures 12 through 17 are dye-penetrant enhanced x-rays of two specimens from each fatigue curve. At least two specimens from each fatigue curve were x-rayed to see if there were any differences in delamination zones due to temperature or the load history variations used for the fatigue testing. One specimen with less than 100 cycles and one with more than 10,000 cycles were x-rayed from each fatigue curve. The delamination zones appear as darkened areas in the radiographs. Number of cycles to delamination, temperature, and load precondition did not seem to affect the delamination zone size or appearance. Darkened areas at the points of extensometer attachment were due to the glue lines absorbing the dye and are not caused by actual damage to the specimens.

Optical photographs were taken of specimen edges to document the delamination crack at the free edge. Figures 18 and 19 are optical photographs of two specimen edges showing typical edge delamination cracks. The delamination occurred at the 0/90 interfaces in all cases, and wandered back and forth between the 0° plies within the 90° plies along the length of the specimens. This behavior was as expected for the $[\pm 35/0/90]_s$ layup used in this program. No variations in delaminations were seen between the different test temperatures or preloading history specimens to indicate any visible effect on the delamination crack path.

ORIGINAL PAGE IS
OF POOR QUALITY

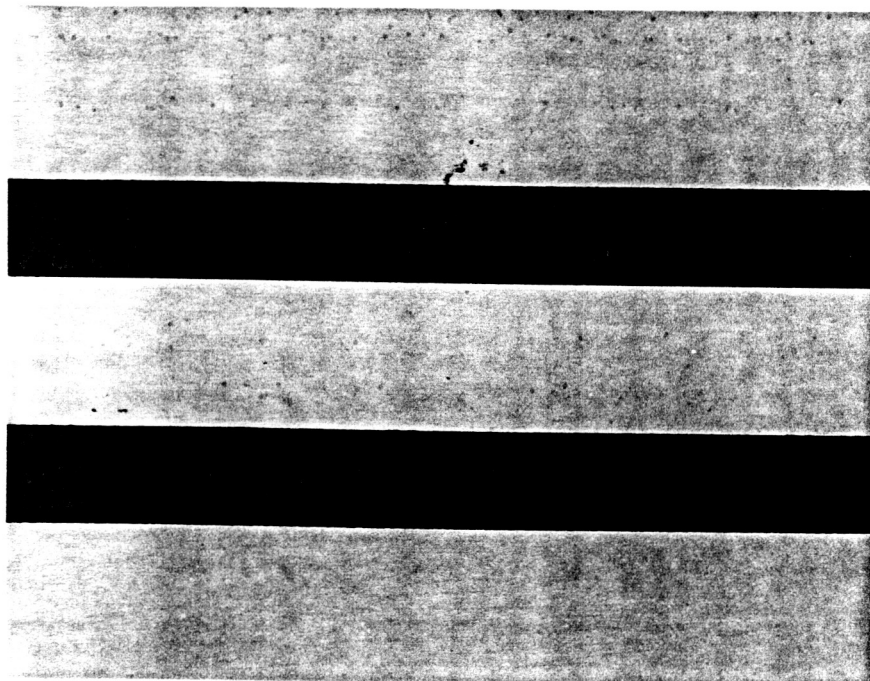


Figure 12. Dye-enhanced X-ray Photograph of Two EDT Fatigue Failed Specimens at Room Temperature, No Precondition.

Top: Specimen No. LFLESA - 36 Cycles to Delamination.

Bottom: Specimen No. LFLLSA - 950 Cycles to Delamination.

ORIGINAL PAGE IS
OF POOR QUALITY

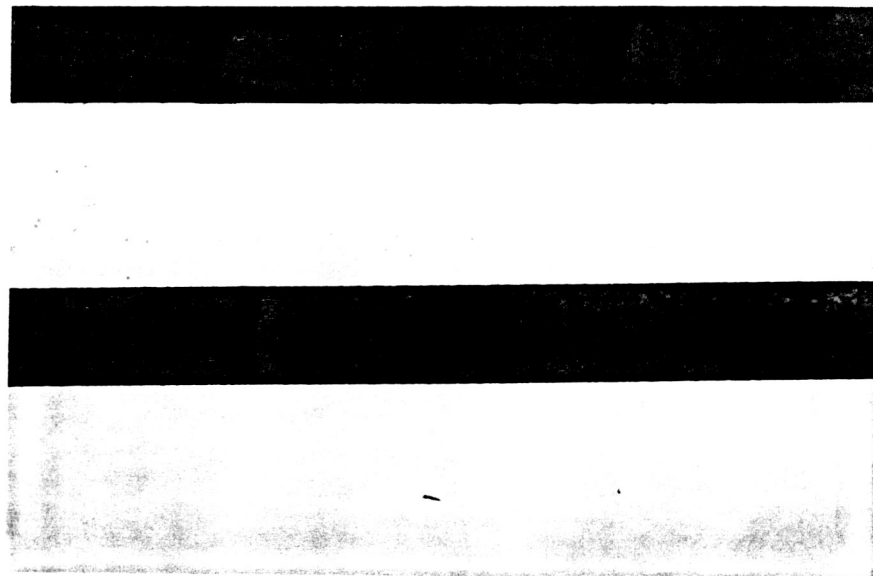


Figure 13. Dye-enhanced X-ray Photograph of Two EDT Fatigue Failed Specimens at Room Temperature, High Spike Load Precondition.

Top: Specimen No. LFLDPA - 1 Cycle to Delamination.

Bottom: Specimen No. LFLNPB - 1000 Cycles to Delamination.

ORIGINAL PAGE IS
OF POOR QUALITY

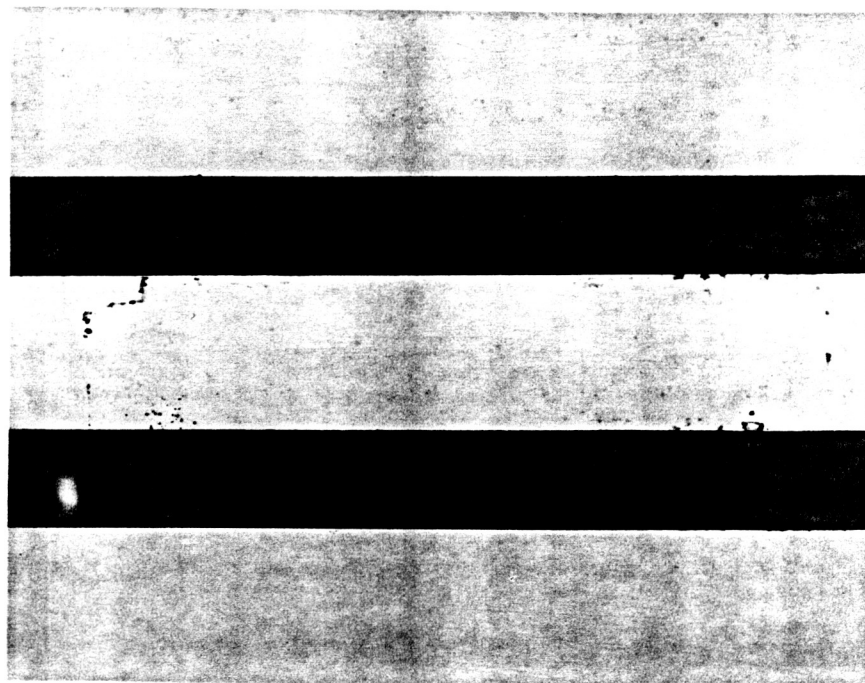


Figure 14. Dye-enhanced X-ray Photograph of Two EDT Fatigue Failed Specimens at Room Temperature, High Mean Load Precondition.

Top: Specimen No. LFLDMB - 66 Cycles to Delamination.

Bottom: Specimen No. LFLDMA - 3300 Cycles to Delamination.

ORIGINAL PAGE IS
OF POOR QUALITY

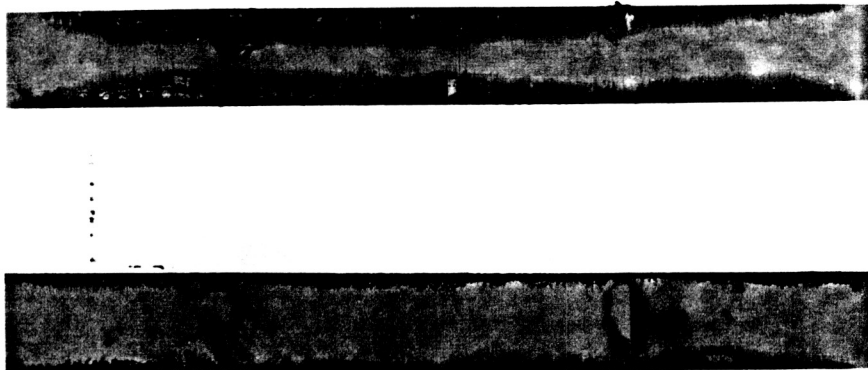


Figure 15. Dye-enhanced X-ray Photograph of Two EDT Fatigue Failed Specimens at 180°F (82°C), No Precondition.

Top: Specimen No. LFHESA - 51 Cycles to Delamination.

Bottom: Specimen No. LFHMSB - 210,000 Cycles to Delamination.

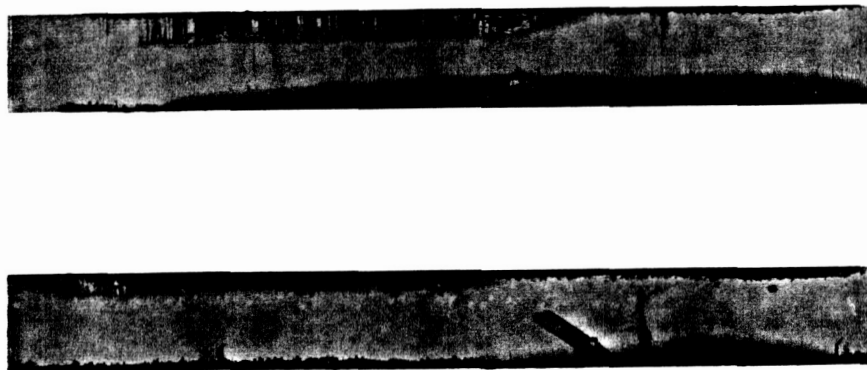


Figure 16. Dye-enhanced X-ray Photograph of Two EDT Fatigue Failed Specimens at 180°F (82°C), High Spike Load Precondition.

Top: Specimen No. LFHEPA - 1 Cycle to Delamination.

Bottom: Specimen No. LFHMPA - 70,000 Cycles to Delamination.

ORIGINAL PAGE IS
OF POOR QUALITY

ORIGINAL PAGE IS
OF POOR QUALITY

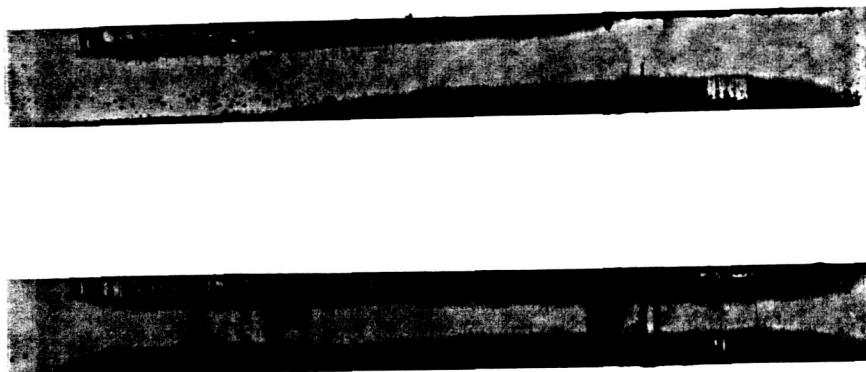


Figure 17. Dye-enhanced X-ray Photograph of Two EDT Fatigue Failed Specimens at 180°F (82°C), High Mean Load Precondition.

Top: Specimen No. LFHFMA - 1 Cycle to Delamination.

Bottom: Specimen No. LFHMMA - 890,000 Cycles to Delamination.

ORIGINAL PAGE IS
OF POOR QUALITY

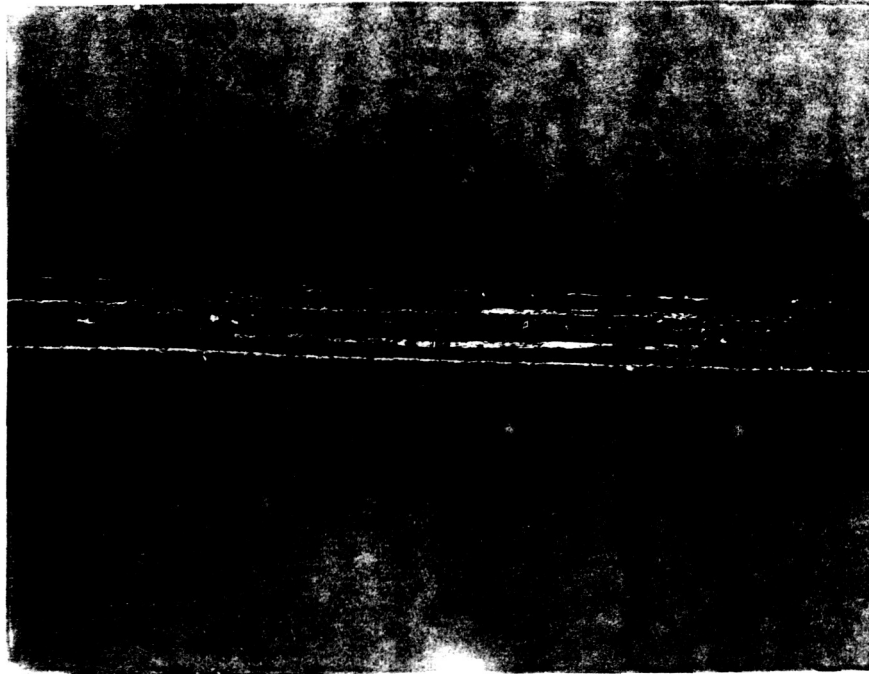


Figure 18. Optical Photograph of Failed EDT Fatigue Specimen Showing a Crack at the Free Edge in the 90° Plies.

ORIGINAL PAGE IS
OF POOR QUALITY



Figure 19. Optical Photograph of Failed EDT Fatigue Specimen Showing a Crack on the Free Edge in the 90° Plies.

SECTION 5

CONCLUSIONS

Static lamina, static edge delamination, and tension-tension fatigue edge delamination testing was performed on IM7/8551-7 carbon fiber-reinforced/epoxy. Static lamina test results indicated some reduction in material properties from the elevated test temperature on this material system. Matrix-dependent material properties (shear, transverse tension, and EDT) measured at the elevated test temperature were typically lower than those measured at room temperature. Higher test temperatures could be used for future testing to identify an upper use temperature for this material system. The IM7/8551-7 performed well at the 180°F (82°C) test temperature. Static test results indicated that the G_C of this material system was quite good compared to other material systems previously tested [5,6]. Results from this test program should allow the finite element analysis used by O'Brien to predict the contributions of G_{IC} and G_{IIC} to G_C for this material [3].

At room temperature, EDT fatigue results indicated lower G_C values (half of static values) were measured compared to static G_C values. All three preconditions resulted in lower G_C at room temperature. EDT fatigue testing at the 180°F (82°C) test temperature indicated that comparable values of G_C were measured compared to static EDT values.

Effects on G_C at elevated temperature due to preconditioning test specimens were minimal. Only at the high stress level/low number of cycles portion of the fatigue curves was there much variation in G_C between the different load preconditioning data. The high mean load and high spike load curves resulted in G_C values lower than the no

precondition curve values up to about 100 cycles. Elevated temperature data from the three precondition curves approached the same G_C value at runout (10^7 cycles).

The room temperature G_C values at equal number of cycles from the three precondition curves were quite different after 10,000 cycles. The three room temperature curves showed a strong influence of the precondition method used with the high mean load having the lowest G_C values and the no precondition G_C values being the highest values at greater than 10,000 cycles. Number of cycles to delamination was reduced by three to four decades compared with the no precondition case after specimens had been preconditioned at room temperature by the high mean level method. Two to three fewer decades of cycles to delamination were measured after preconditioning with the single high spike loading compared with the no precondition case.

Optical photographs showed that the delamination crack on the free edge of specimens did not vary due to test temperature or precondition. Dye-enhanced radiographs taken of delaminated specimens showed that no discernible differences could be attributed to the two different test temperatures or three preconditions.

REFERENCES

1. R.B. Pipes and N.J. Pagano, "Interlaminar Stresses in Composite Laminates under Uniform Axial Extension," Journal of Composite Materials, Vol. 4, 1970, pp. 538-548.
2. N.J. Pagano and R.B. Pipes, "Some Observations on the Interlaminar Strength of Composite Laminates," International Journal of Mechanical Sciences, Vol. 15, 1973, pp. 679-688.
3. T.K. O'Brien, "Characterization of Delamination Onset and Growth in a Composite Laminate," Damage in Composite Materials, ASTM STP 775, American Society for Testing and Materials, Philadelphia, Pennsylvania, 1982, pp. 140-167.
4. T.K. O'Brien and N.J. Johnston, "A Simple Test for the Interlaminar Fracture Toughness of Graphite/Epoxy Laminates," Proceedings of the 27th National SAMPE Symposium, May 1982, Reno, Nevada, p. 401-415.
5. "MagnaMite Graphite Fiber, Type IM7," Data Sheet 868, Hercules, Inc., Wilmington, Delaware, 1988.
6. "Hercules Prepreg Tape Materials Characterization Data Package," Hercules Composite Products Group, Magna, Utah, November 1988.
7. "Standard Test Method for Fiber Content of Resin-Matrix Composites by Matrix Digestion," ASTM Standard Test Method D-3171-76 (Reapproved 1982), 1988 ASTM Annual Book of Standards, Section 15, Volume 15.03, American Society for Testing and Materials, Philadelphia, Pennsylvania, 1988, pp. 122-124.
8. "Standard Test Method for Tensile Properties of Fiber-Reinforced Composites," ASTM Standard Test Method D-3039-76 (Reapproved 1982), 1988 ASTM Annual Book of Standards, Section 15, Volume 15.03, American Society for Testing and Materials, Philadelphia, Pennsylvania, 1988, pp. 117-121.
9. E.M. Odom and D.F. Adams, "Stiffness Reductions During Tensile Fatigue Testing of Graphite/Epoxy Angle-Ply Laminates," NASA Contractor Report 166019, National Aeronautics and Space Administration, Washington, D.C., November 1982.
10. R.S. Zimmerman, D.F. Adams, and E.M. Odom, "Load Ratio and Frequency Effects on Strain Energy Release Rate During Tensile Fatigue Testing Utilizing the Edge Delamination Test," Report UWME-DR-401-109-1, Department of Mechanical Engineering, University of Wyoming, December 1984.

11. Operation Manual for 2150 Controllers, Manual No. 11-1-12, Instron Corporation, Canton, Massachusetts, 1977, pp. 2.4-2.6.
12. Standard Tests for Toughened Resin Composites, NASA Reference Publication 1092, Revised Edition, Compiled by ACEE Composites Project Office, NASA-Langley Research Center, Hampton, Virginia, 1983, pp. 7-14.
13. Advanced Composites Design Guide, Vol. II-Analysis, Air Force Flight Dynamics Laboratory, Dayton, Ohio, January 1973, pp. 2.B.1.1-2.B.1.29.
14. L.A. Carlsson, and R.B. Pipes, Experimental Characterization of Advanced Composite Materials, Prentice-Hall, Inc., Englewood Cliffs, New Jersey, 1987.

APPENDIX A

INDIVIDUAL STATIC TEST RESULTS

Table A1

Individual Fiber and Void Volume Results for
IM7/8551-7 Composites

Plate Layup	Fiber Volume (V_f) (Percent)	Void Volume (V_v) (Percent)
[0] ₈	62.9	4.8
	64.1	1.7
	<u>63.0</u>	<u>0.9</u>
	Average	2.5
Std. Dev.	0.6	2.1
[0] ₁₂	59.6	0.7
	60.1	0.4
	<u>59.8</u>	<u>0.6</u>
	Average	0.6
Std. Dev.	0.2	0.2
[0] ₂₀	57.9	0.8
	57.8	1.0
	<u>58.0</u>	<u>4.1</u>
	Average	2.0
Std. Dev.	0.1	1.8
[±35/0/90] _s	62.7	1.2
	61.8	2.8
	<u>62.4</u>	<u>4.7</u>
	Average	2.9
Std. Dev.	0.5	1.8

Table A2

Individual Static Axial Tensile Results
for IM7/8551-7 Composites

Specimen Name	Test Temperature (°F)	Tensile Strength (ksi)	(GPa)	Tensile Modulus (Msi)	(GPa)	Ultimate Strain (Percent)	Poisson's Ratio
NLOTD2	75	372	2.56	23.9	165	1.5	0.168
3		383	2.64	23.8	164	0.6*	0.186
4		341	2.35	21.7	150	1.9	0.174
5		231*	1.59*	24.7	170	0.8*	0.200
6		<u>358</u>	<u>2.47</u>	<u>22.3</u>	<u>154</u>	<u>1.3</u>	<u>0.189</u>
Average		364	2.51	23.3	161	1.5	0.183
Std. Dev.		18	0.12	1.2	8	0.3	0.013
NLFSH1	180	321	2.21	22.1	152	1.2*	0.419*
2		364	2.51	21.4	148	1.6	0.404
3		367	2.53	21.3	147	1.5	0.345
4		369	2.54	21.8	150	1.5	0.345
5		<u>372</u>	<u>2.56</u>	<u>22.5</u>	<u>155</u>	<u>1.5</u>	<u>0.337</u>
Average		359	2.47	21.8	150	1.5	0.358
Std. Dev.		21	0.15	0.5	3	0.1	0.031

*Not included in Average or Standard Deviation

Table A3

Individual Static Transverse Tensile Results
for IM7/8551-7 Composites

Specimen Name	Test Temperature	Tensile Strength		Tensile Modulus		Ultimate Strain
	(°F)	(ksi)	(GPa)	(Msi)	(GPa)	(Percent)
NLTDD0	75	6.84	47.8	1.19	8.2	0.58
1		7.56	52.1	1.15	7.9	0.67
2		7.61	52.5	1.21	8.3	0.64
3		2.80*	19.3*	1.15	7.9	0.22*
4		7.40	51.0	1.21	8.3	0.62
5		<u>7.30</u>	<u>50.3</u>	<u>1.27</u>	<u>8.8</u>	<u>0.59</u>
Average		7.34	50.7	1.20	8.2	0.62
Std. Dev.		0.03	1.86	0.05	0.3	0.04
NTTD21	180	3.84*	26.5*	1.07	7.4	0.37*
22		4.72	32.5	1.05	7.2	0.46
23		5.05	34.8	1.05	7.2	0.53
24		6.20	42.7	1.08	7.4	0.60
25		6.50	44.8	1.11	7.6	0.62
26		6.63	45.7	1.09	7.5	0.65*
27		<u>6.19</u>	<u>42.7</u>	<u>1.09</u>	<u>7.5</u>	<u>0.60</u>
Average		5.88	40.5	1.08	7.4	0.56
Std. Dev.		0.80	5.5	0.02	0.2	0.07

*Not included in Average and Standard Deviation

Table A4

Individual In-Plane Iosipescu Shear Results
for IM7/8551-7 Composites

Specimen Name	Test Temperature (°F)	Shear Strength		Shear Modulus		Ultimate Strain (Percent)
		(ksi)	(GPa)	(Msi)	(GPa)	
NFIRD1	75	16.1	111	0.86	6.0	11.9
2		14.9	103	0.87	6.0	11.9
3		15.8	109	0.83	5.7	11.9
4		15.5	107	0.83	5.7	10.3
5		<u>12.8</u>	<u>88</u>	<u>0.76</u>	<u>5.2</u>	<u>5.4*</u>
Average		15.0	104	0.83	5.7	11.5
Std. Dev.		1.3	9	0.05	0.3	0.8
NFIHD1	180	12.4	85	0.81	5.6	11.4
2		10.1*	70*	0.77	5.3	5.9*
3		13.3	91	0.76	5.3	11.3
4		13.1	90	0.78	5.4	11.3
5		<u>12.3</u>	<u>85</u>	<u>0.62</u>	<u>4.2</u>	<u>11.3</u>
Average		12.7	88	0.75	5.2	11.3
Std. Dev.		0.5	3	0.08	0.6	0.1

*Not included in Average or Standard Deviation

Table A5
Individual Static Edge Delamination Test Results
for IM7/8551-7 Composites

Specimen Name	Test Temperature (°F)	Thickness (in)	Ultimate Strength (ksi)	Modulus Strength (Msi)	Strength Delamination (ksi)	Strength Delamination (MPa)	Critical Strain Energy Release Rate (in-lbf/in ²)	Critical Strain Energy Release Rate (J/m ²)	Strain at Delamination (percent)	Poisson's Ratio	
NLDTD1	75	0.042	108	9.0	62.0	93*	641*	3.95*	692*	0.99*	0.196
2		0.043	99	9.6	66.2	93*	641*	3.85*	675*	0.97	0.138*
3		0.044	99	9.7	66.9	79	545	2.62	459	0.79	0.168
4		0.044	120	10.1	69.6	92	634	3.59	628	0.93	0.211
5		0.044	94	10.2	70.3	81	558	2.91	509	0.83	0.183
6		0.042	115	9.6	66.2	75	517	2.37	416	0.77	0.258*
7		0.043	108	9.9	68.3	78	538	2.70	473	0.81	0.232
8		0.044	<u>111</u>	<u>10.8</u>	<u>74.5</u>	<u>62*</u>	<u>428*</u>	<u>1.38*</u>	<u>241*</u>	<u>0.57*</u>	<u>0.267*</u>
Average			107	9.9	68.0	81	558	2.84	497	0.85	0.198
Std. Dev.			9	0.5	3.7	7	45	0.46	80	0.08	0.025
NLDTD21	180	0.045	112	9.9	68.3	72	496	2.32	406	0.73	0.388
22		0.044	109	10.8	74.5	70	483	1.94	339	0.67	0.564*
23		0.045	108	10.1	69.6	81	558	2.98	521	0.83	0.471
24		0.045	108	9.4	64.8	65	448	2.03	355	0.68	0.421
25		0.045	<u>110</u>	<u>9.7</u>	<u>66.9</u>	<u>81</u>	<u>558</u>	<u>3.27*</u>	<u>573*</u>	<u>0.87</u>	<u>0.415</u>
Average			109	10.0	68.8	74	509	2.32	405	0.76	0.424
Std. Dev.			2	0.5	3.6	7	48	0.47	82	0.09	0.035

*Not included in Average or Standard Deviation

TABLE A6

Lamina and Laminate Material Properties
for IM7/8551-7 Composites

Test Temperature
75°F (25°C) 180°F (82°C)

[0]_s (Input Properties From Static Tests Used in AC3)

E_{11}	=	23.3 Msi (160.7 GPa)	21.1 Msi (145.5 GPa)
E_{22}	=	1.2 Msi (8.3 GPa)	1.1 Msi (7.6 GPa)
G_{12}	=	0.83 Msi (5.7 GPa)	0.75 Msi (5.2 GPa)
ν_{12}	=	0.180	0.370

[±35/0/90]_s (Predicted Properties From AC3)

E_x	=	11.1 Msi (76.5 GPa)	10.3 Msi (71.0 GPa)
E_y	=	7.6 Msi (52.4 GPa)	7.1 Msi (49.0 GPa)
G_{xy}	=	3.1 Msi (21.4 GPa)	2.9 Msi (20.0 GPa)
ν_{xy}	=	0.311	0.332

[±35/0]_s (Predicted Properties From AC3)

E_x	=	11.8 Msi (81.4 GPa)	10.9 Msi (75.2 GPa)
E_y	=	2.3 Msi (15.9 GPa)	2.1 Msi (14.5 GPa)
G_{xy}	=	3.9 Msi (26.9 GPa)	3.6 Msi (24.8 GPa)
ν_{xy}	=	1.093	1.140

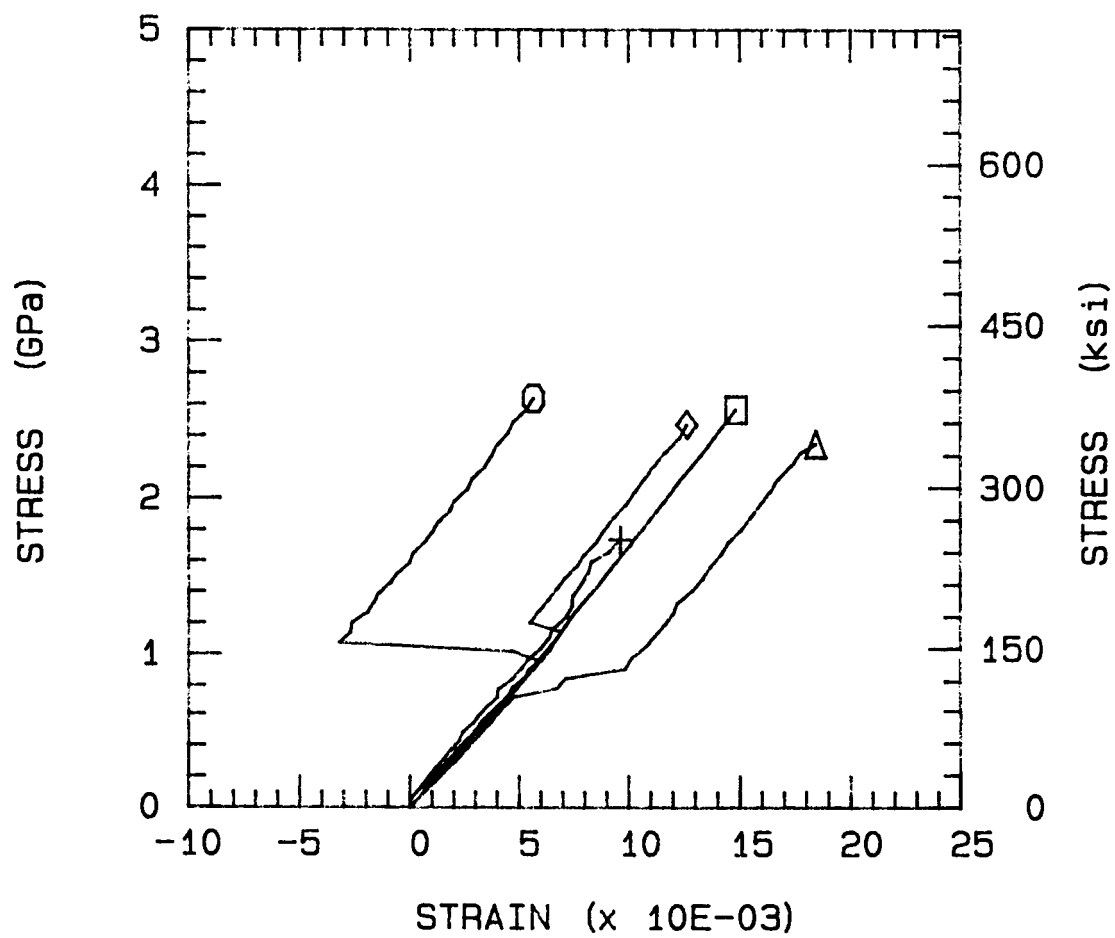
E^*	=	9.18 Msi (63.3 GPa)	8.41 Msi (58.0 GPa)
-------	---	---------------------	---------------------

(Calculated Using AC3 and Equation 2)

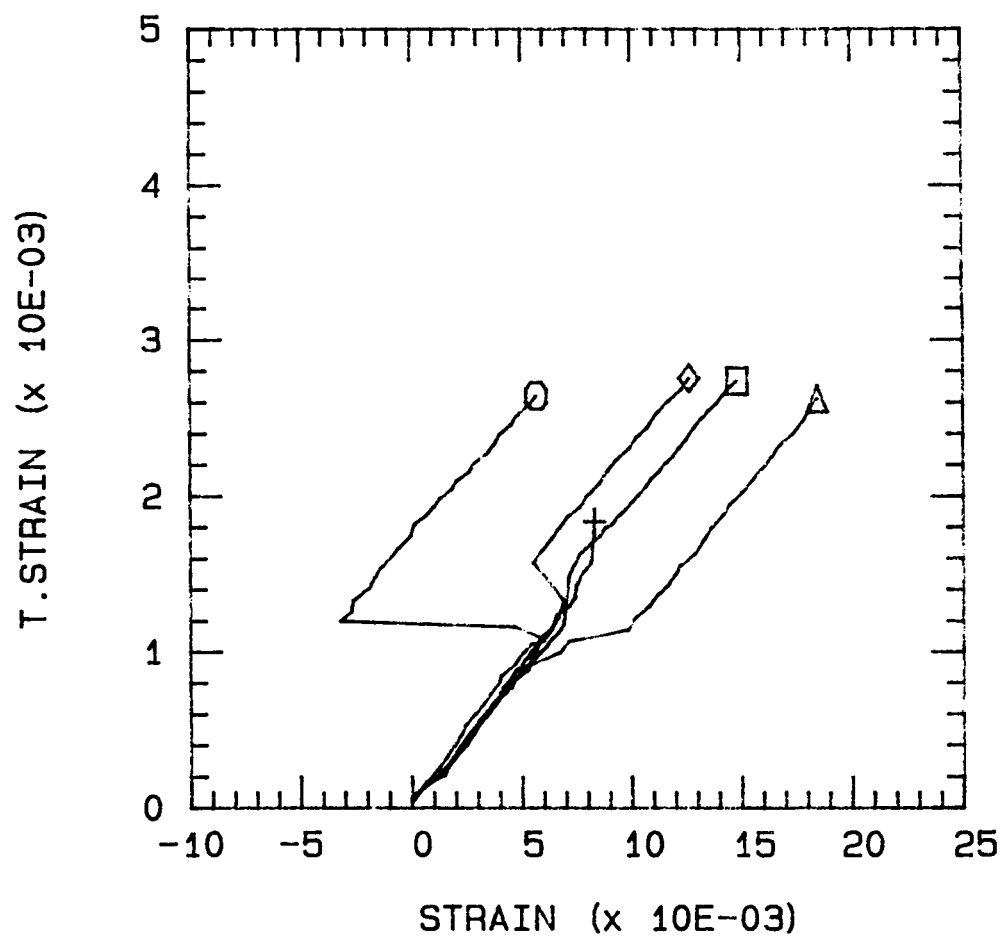
E_{lam}	=	9.85 Msi (67.9 GPa)	9.99 Msi (68.9 GPa)
-----------	---	---------------------	---------------------

(Measured Static EDT Initial Tangent Modulus)

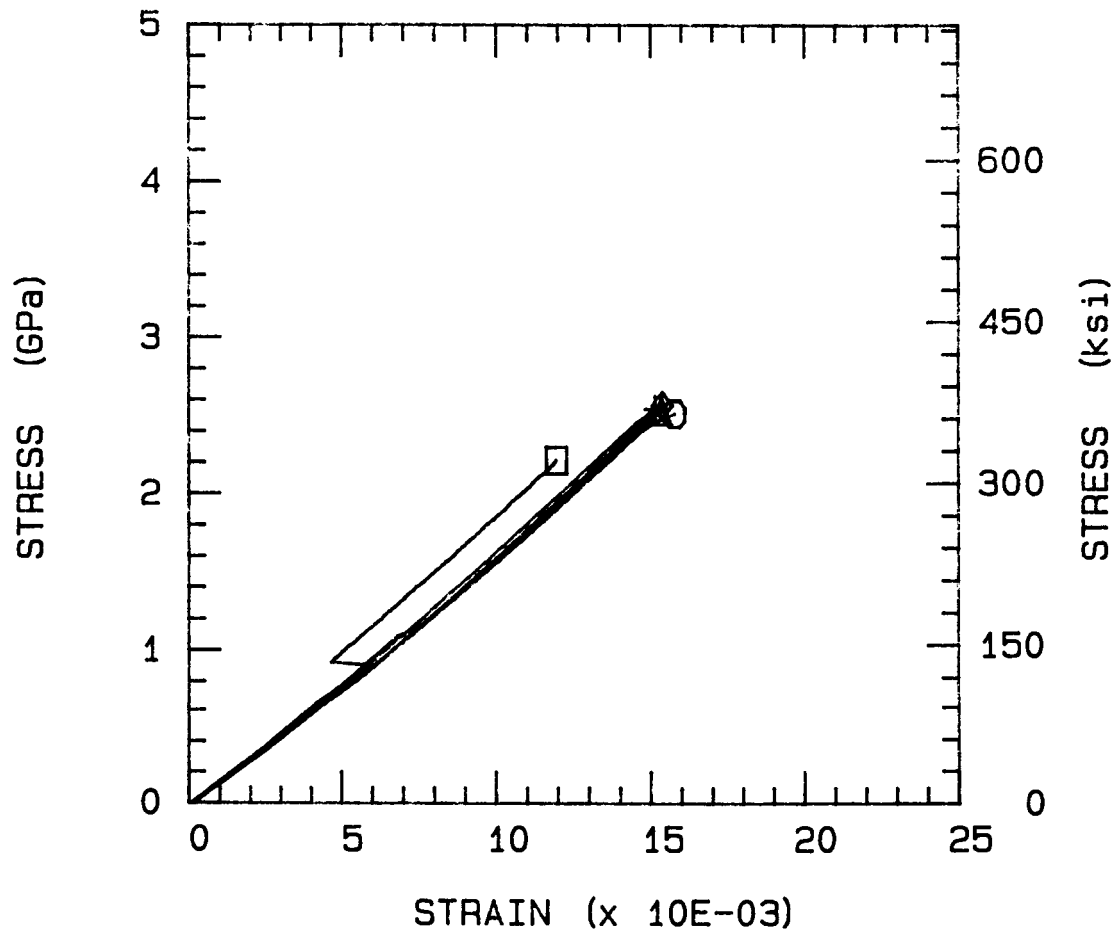
AXIAL TENSION 23 DEG C



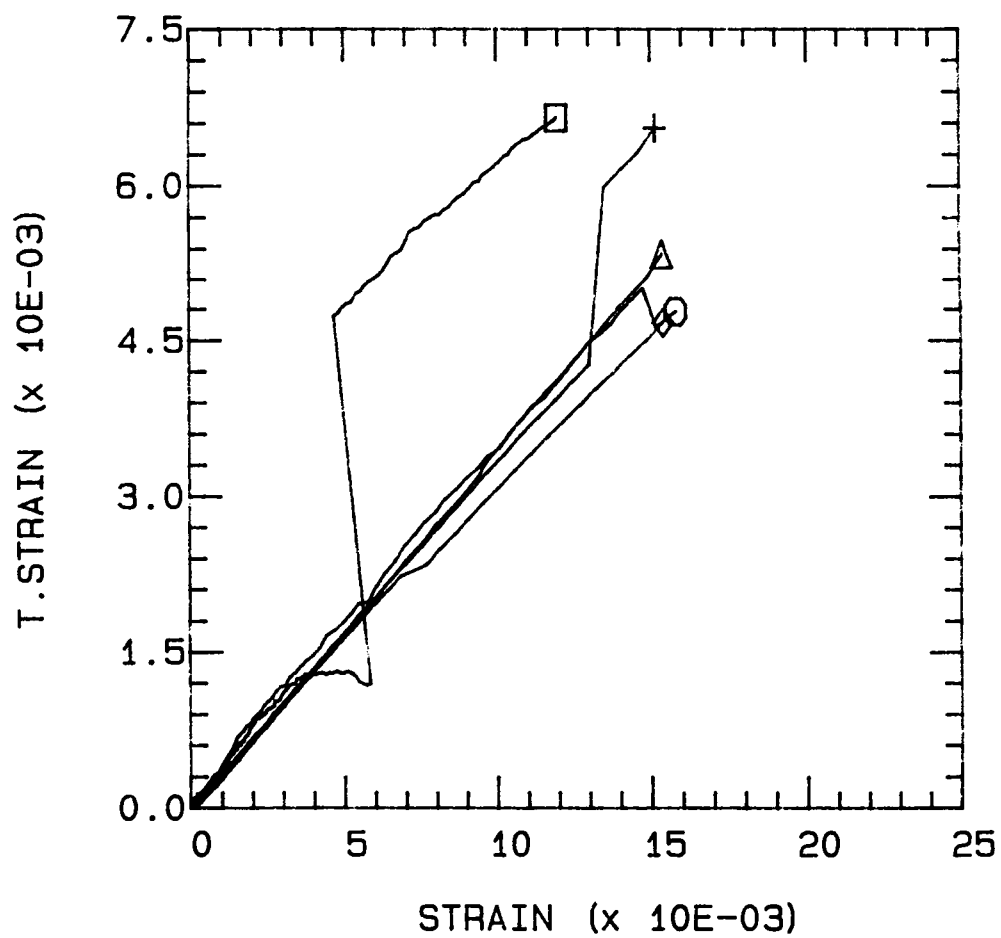
AXIAL TENSION 23 DEG C



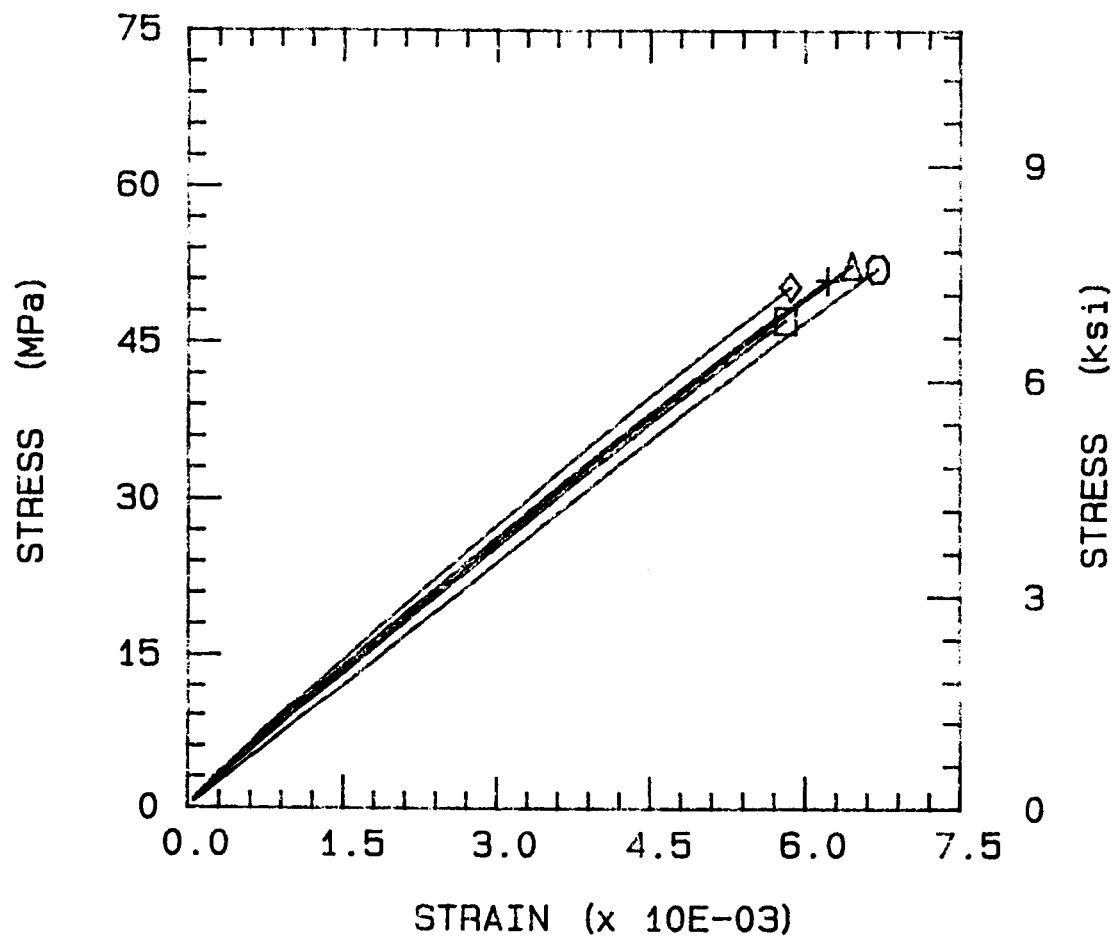
AXIAL TENSION 82 DEG C



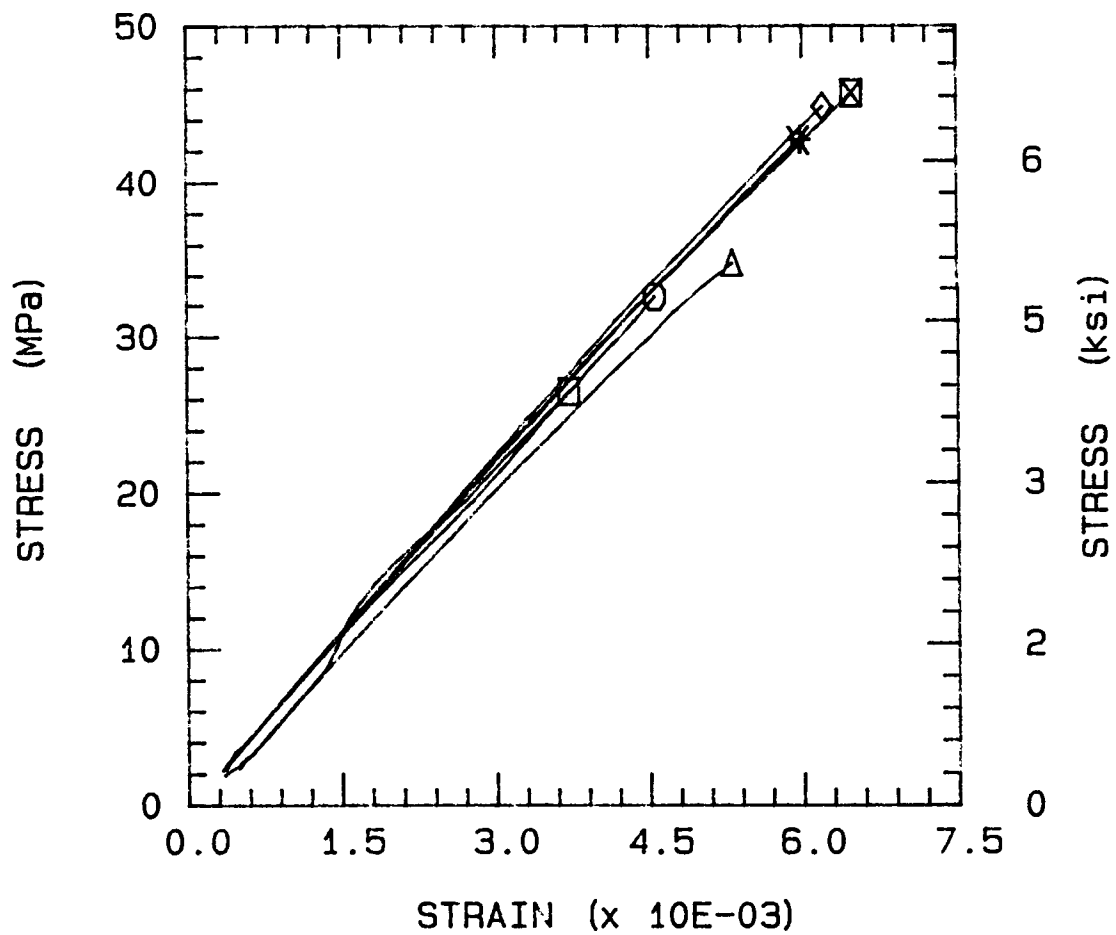
AXIAL TENSION 82 DEG C



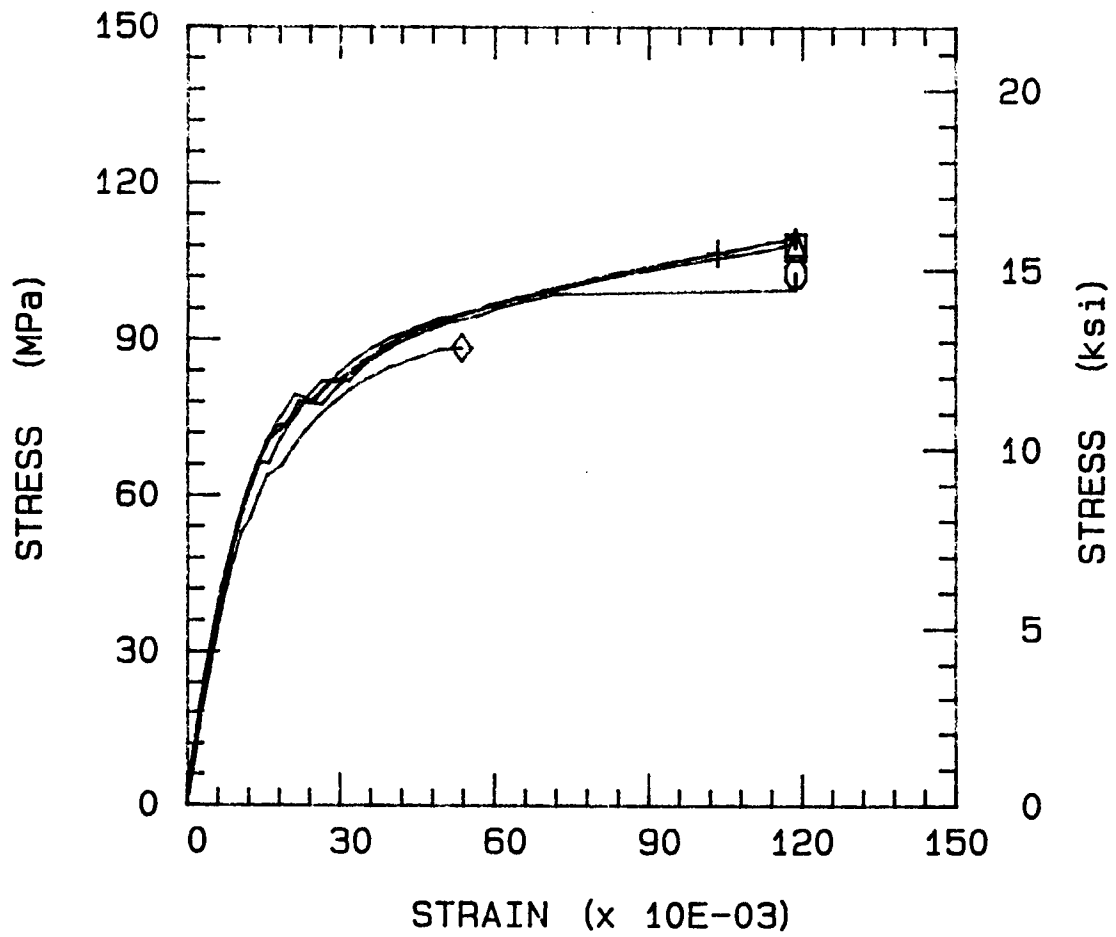
TRANSVERSE TENSION 23 DEG C



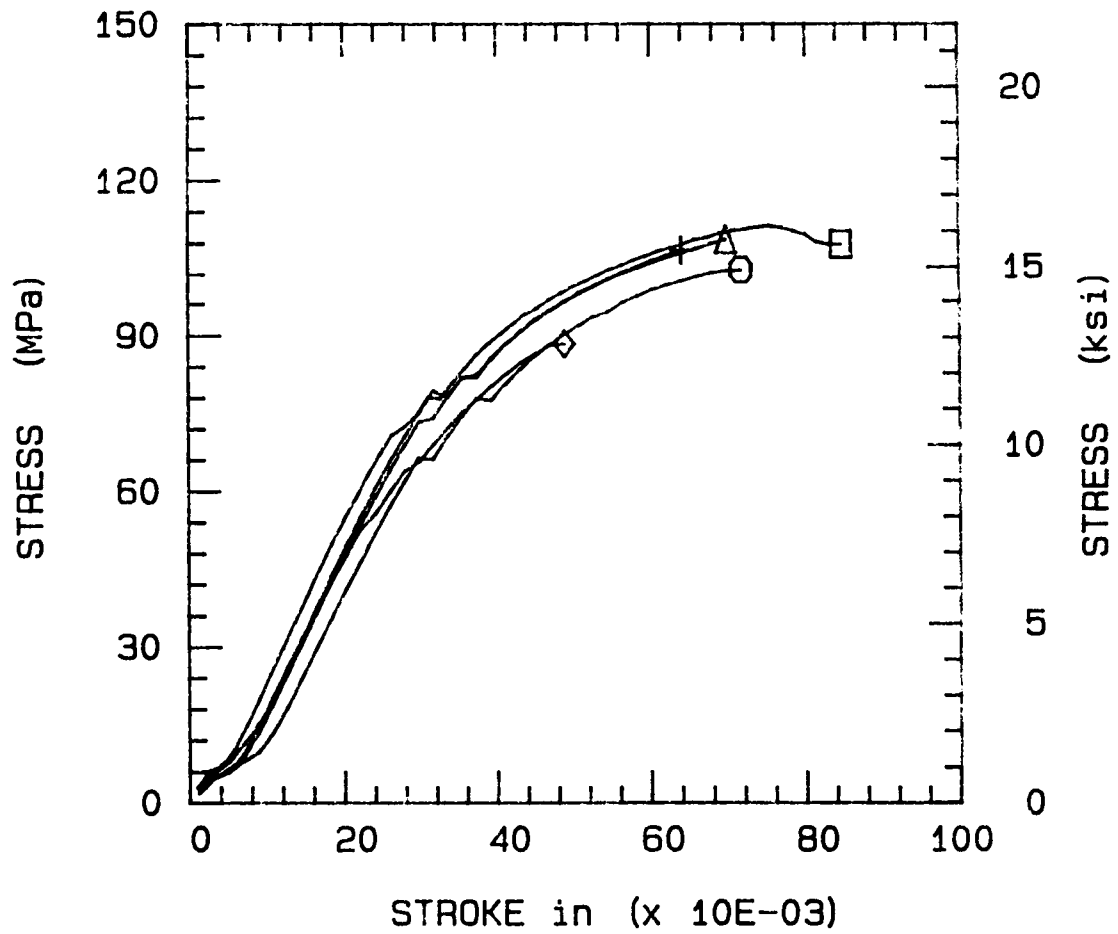
TRANSVERSE TENSION 82 DEG C



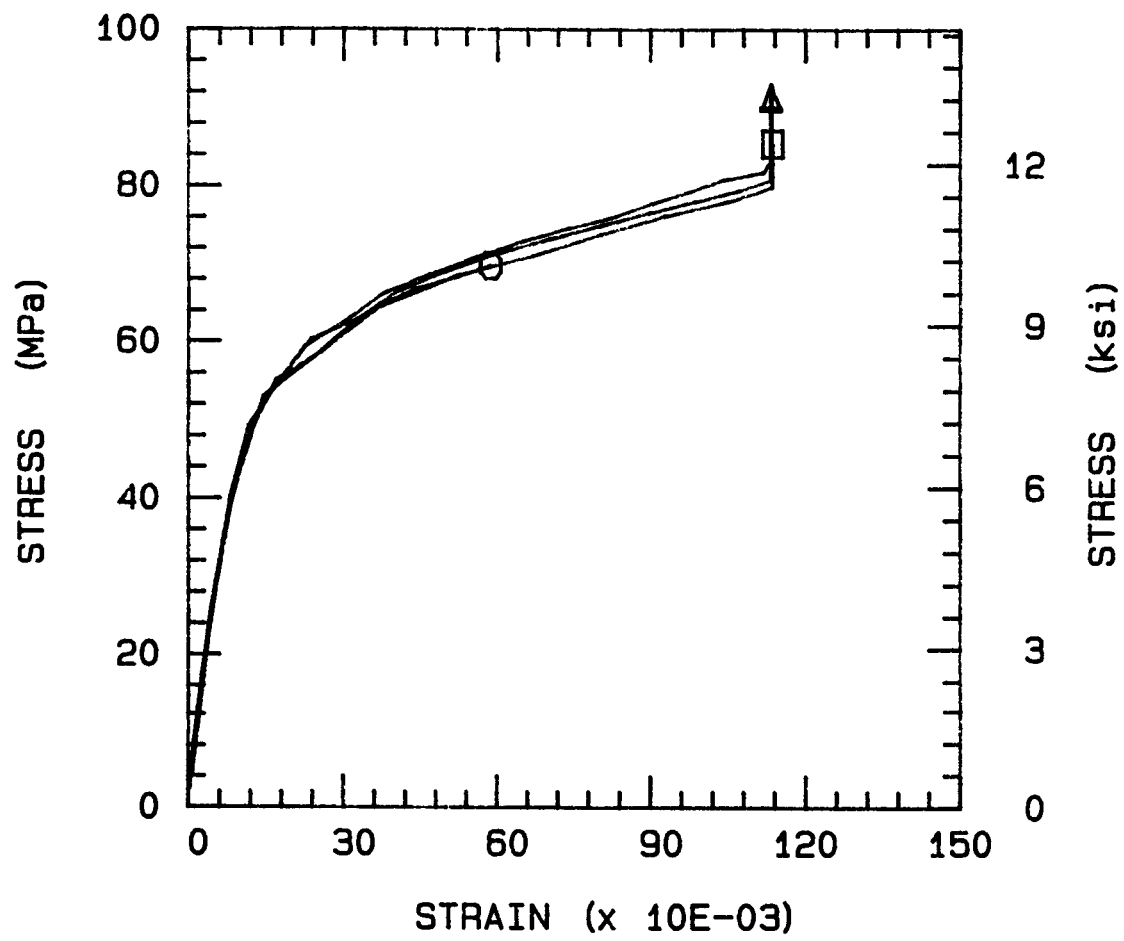
IOSIPESCU SHEAR 23 DEG C



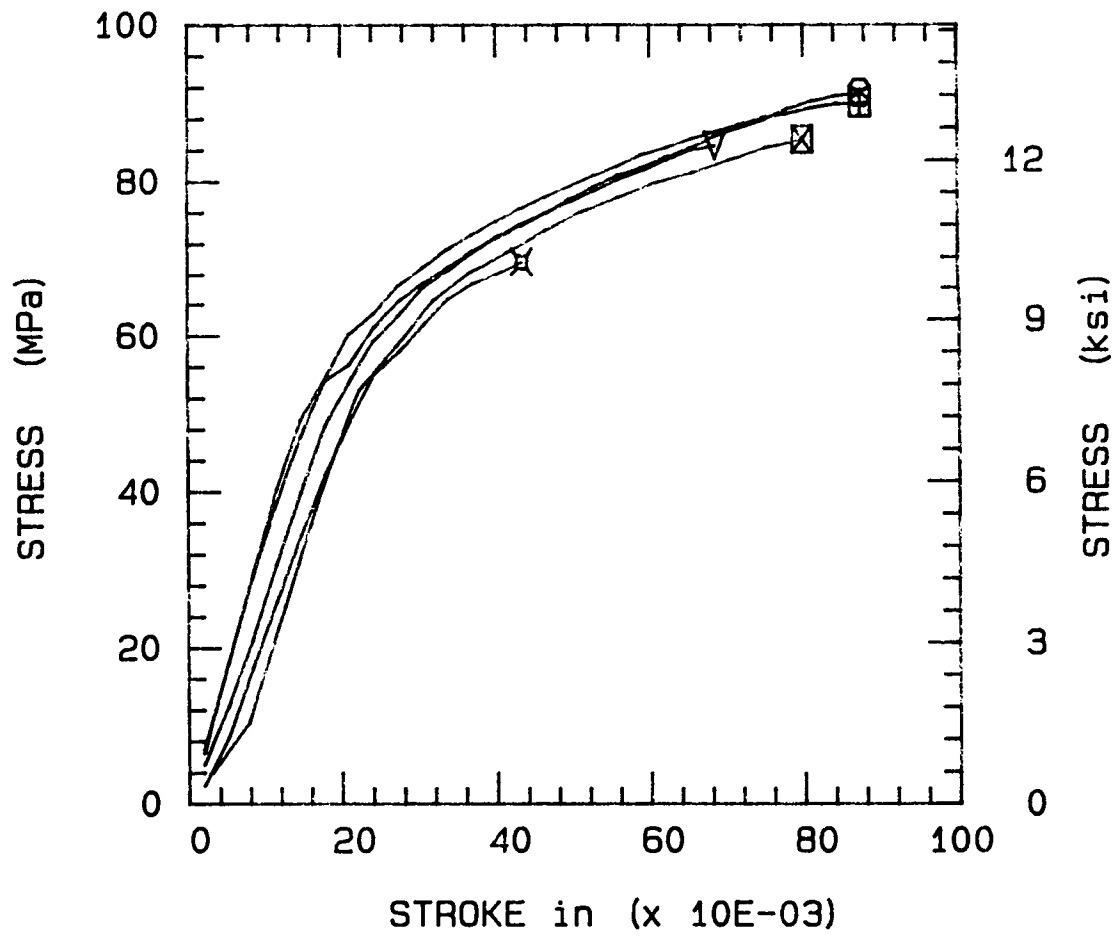
IOSIPESCU SHEAR 23 DEG C



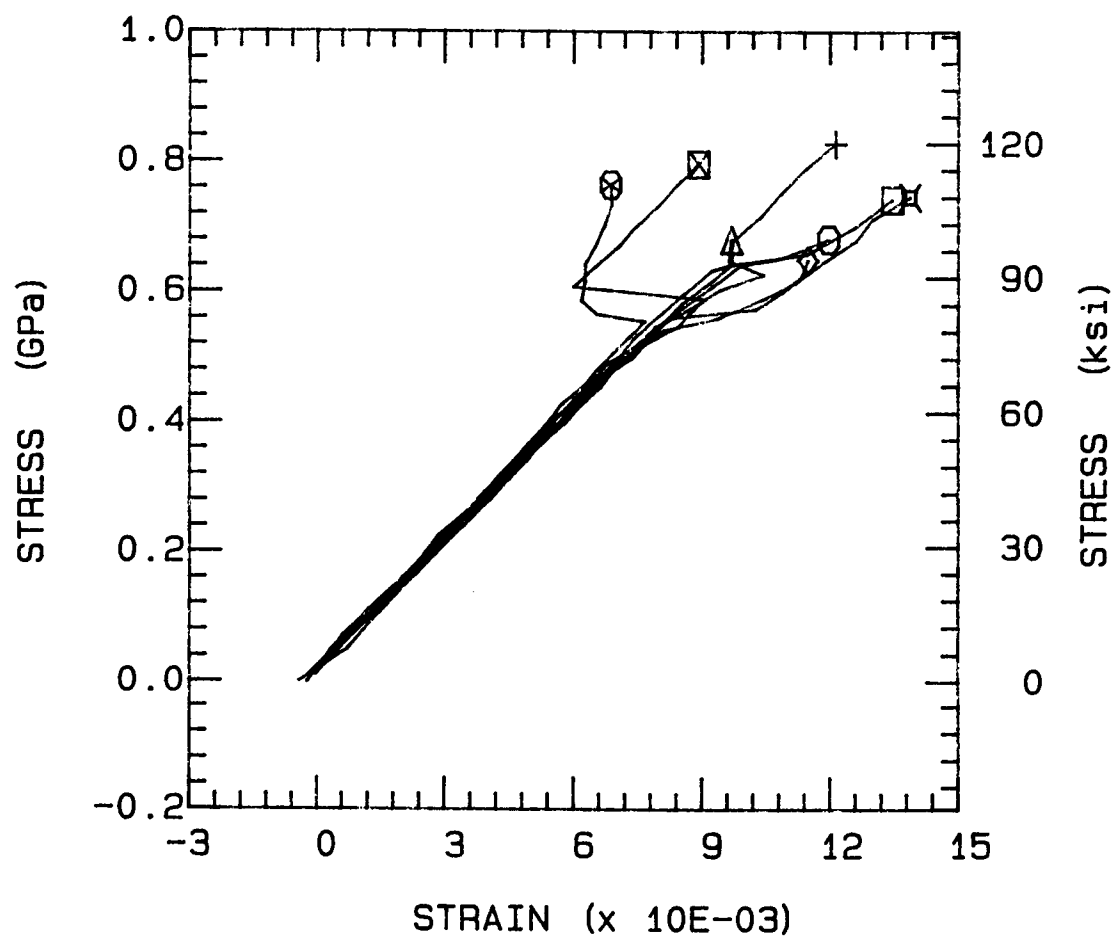
IOSIPESCU SHEAR 82 DEG C



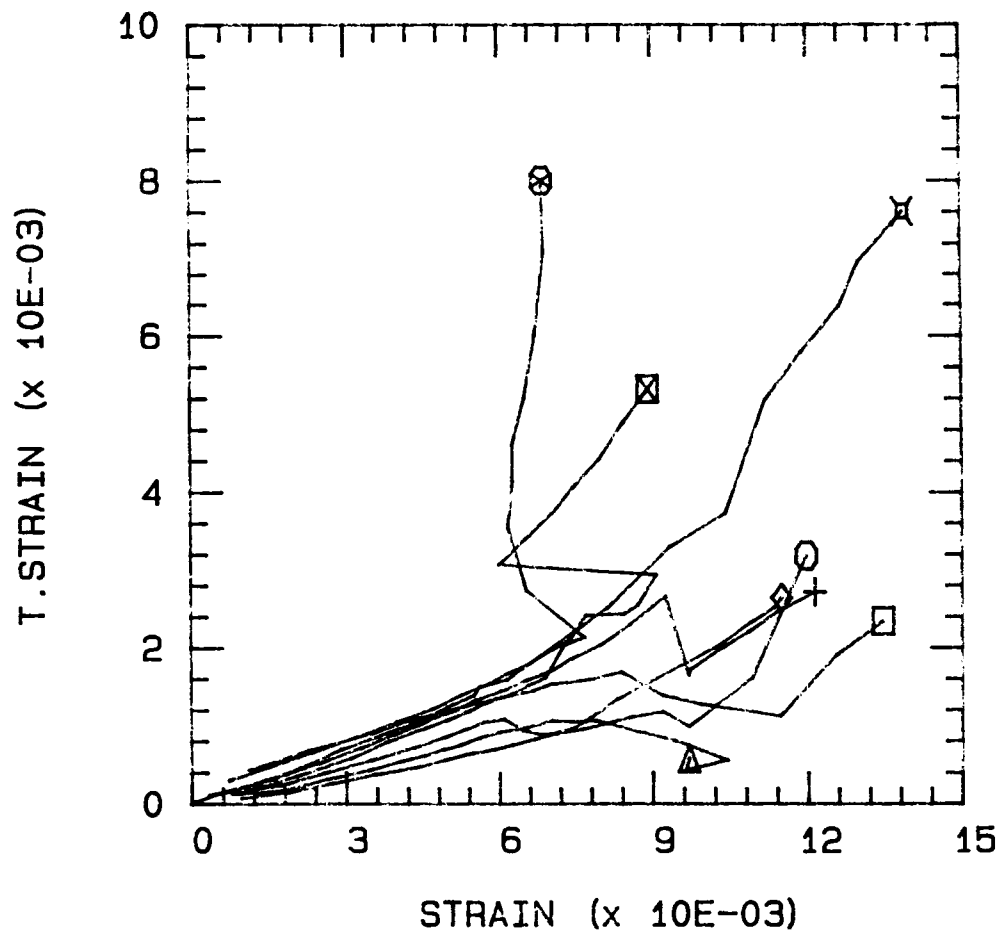
IOSIPESCU SHEAR 82 DEG C



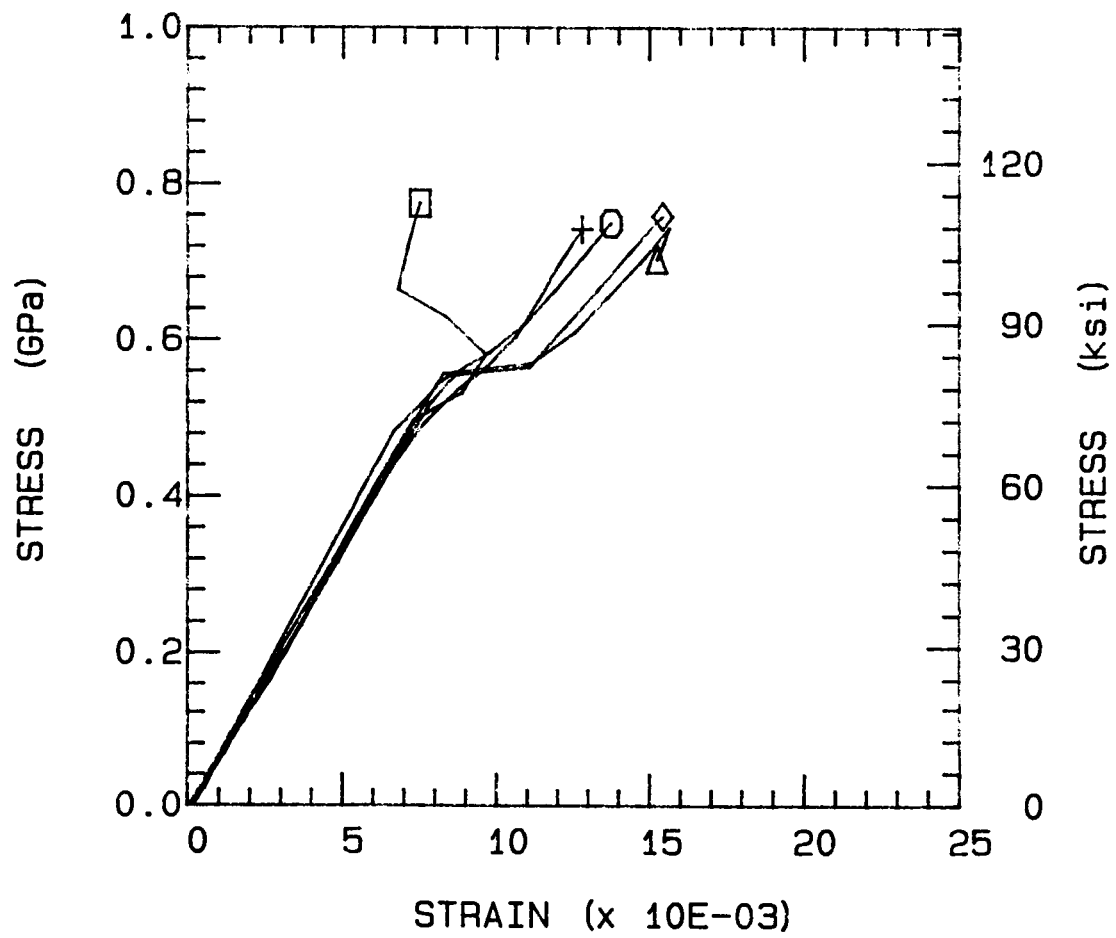
EDGE DELAMINATION 23 DEG C



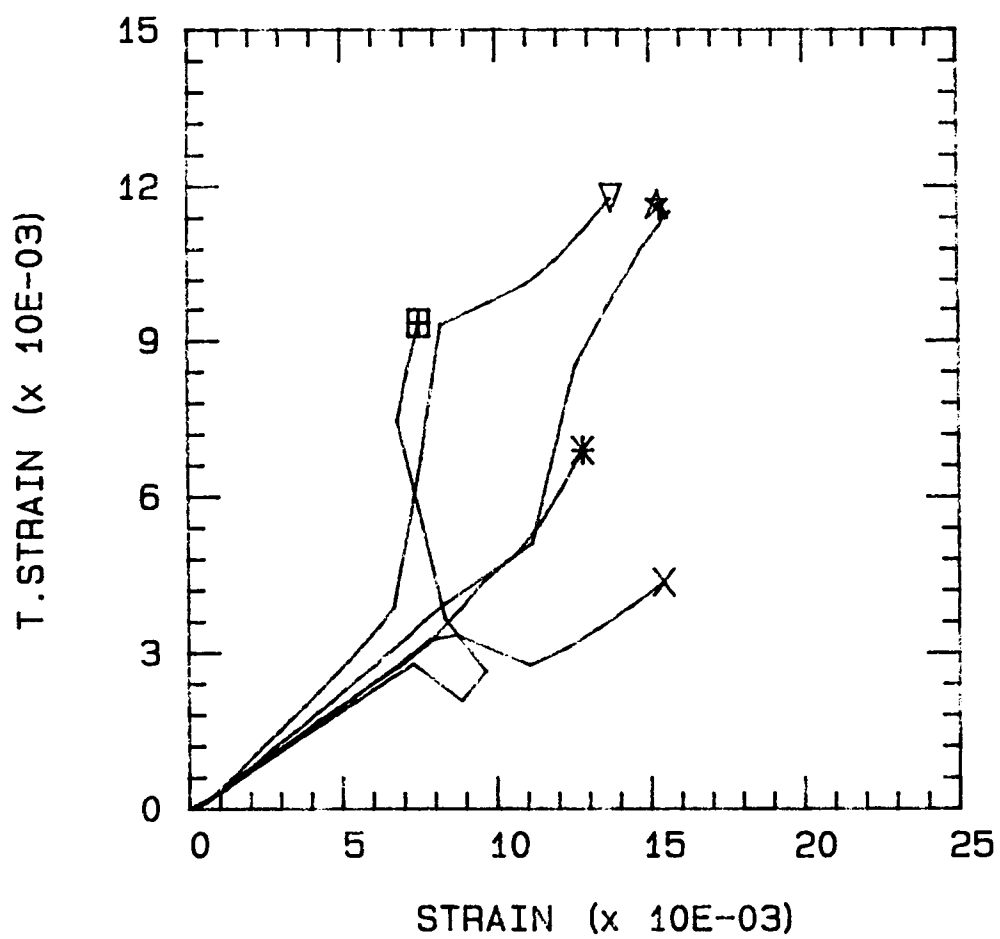
EDGE DELAMINATION 23 DEG C



EDGE DELAMINATION 82 DEG C



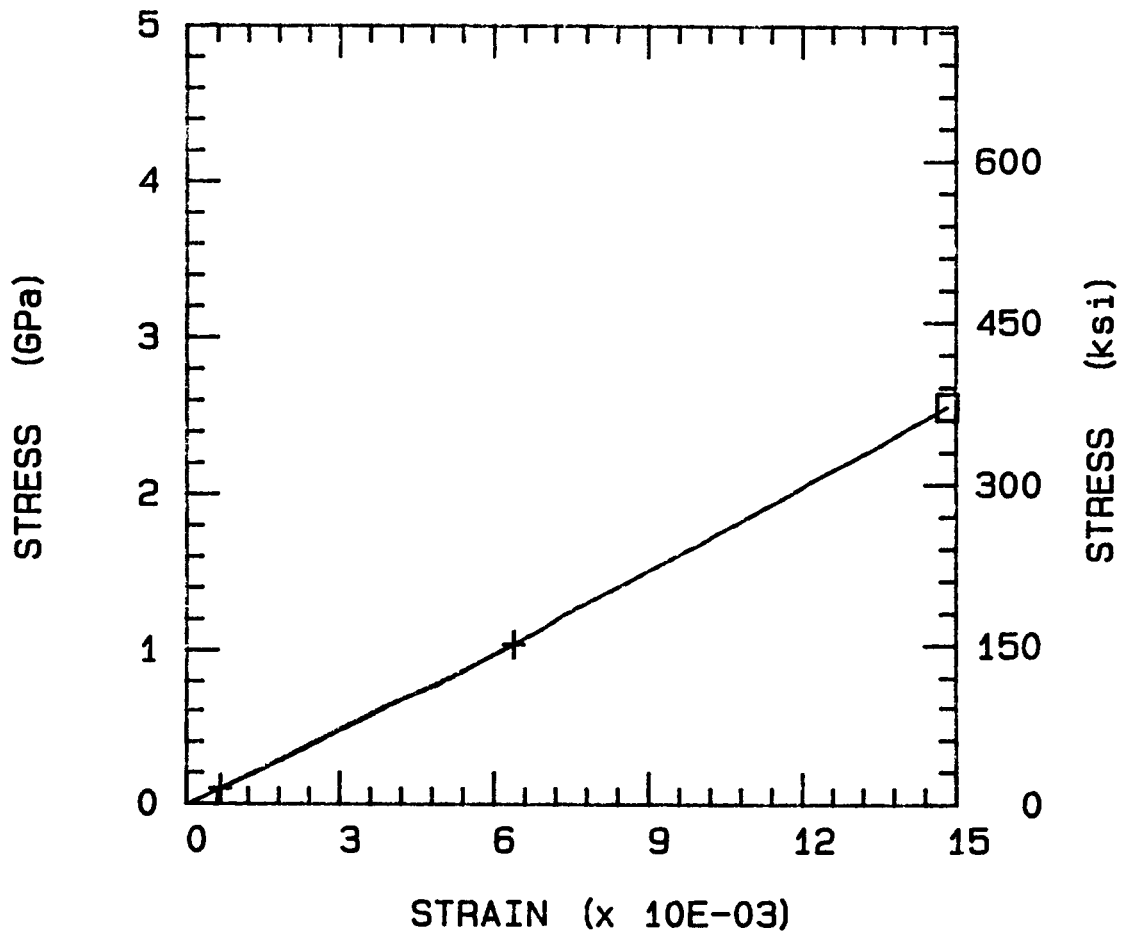
EDGE DELAMINATION 82 DEG C



NLOTD2.TEN

ULT. STRESS = 372.000 ksi

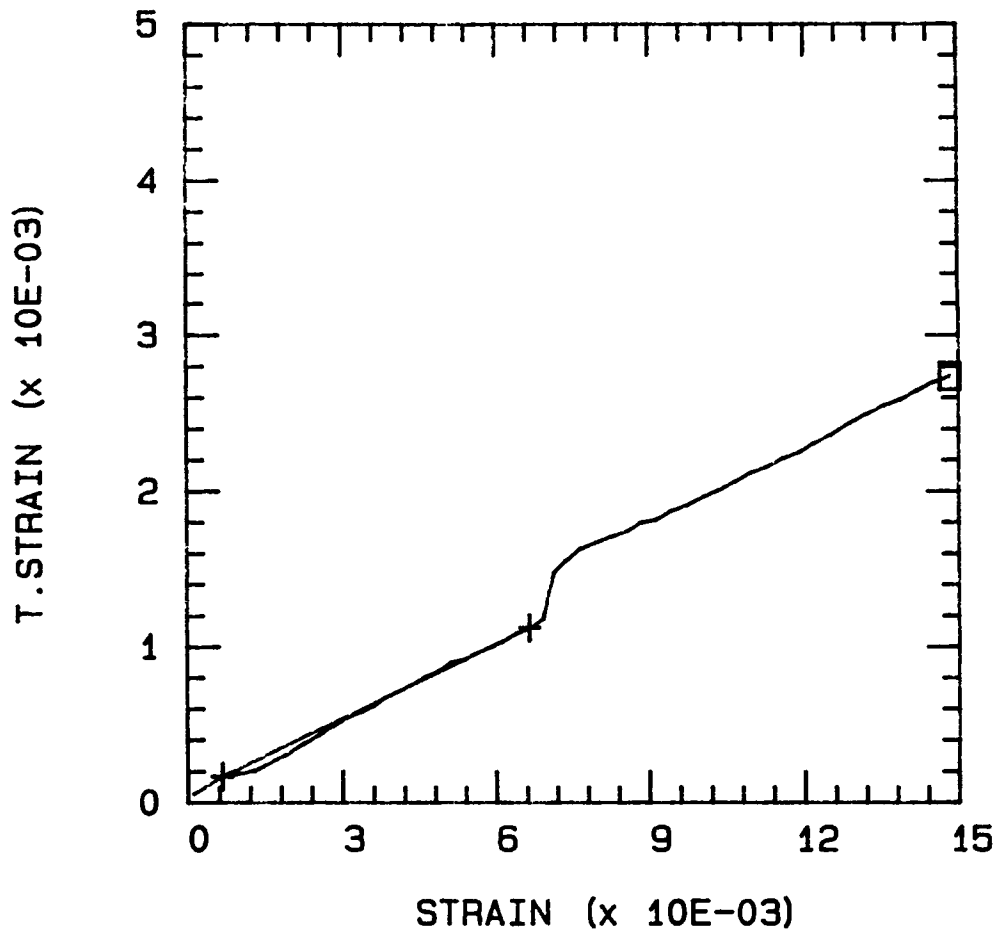
TEMP = 23.0 DEG. C MOD = 23.894 Msi



NLOTD2.TEN

ULT. STRESS = 372.000 ksi

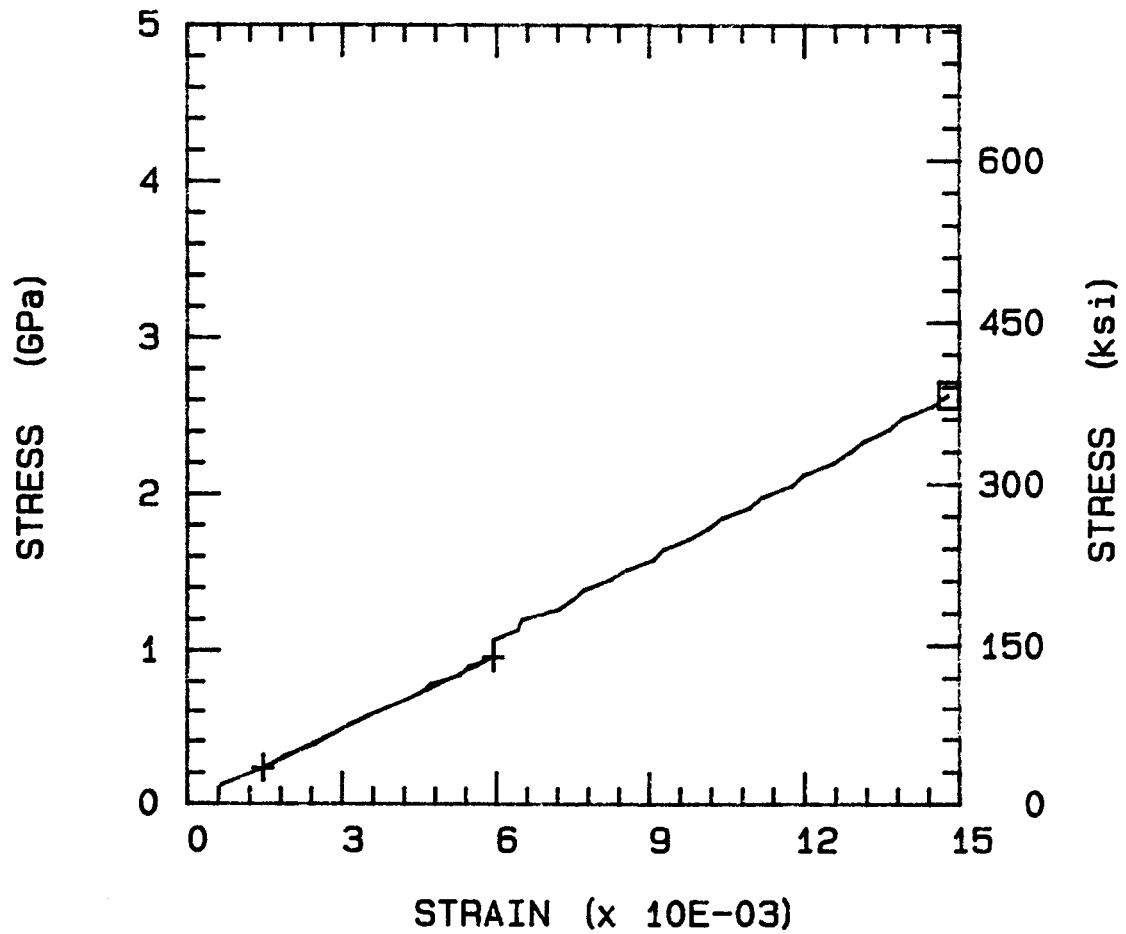
TEMP = 23.0 DEG. C NU = 0.168



NL0TD3.TEN

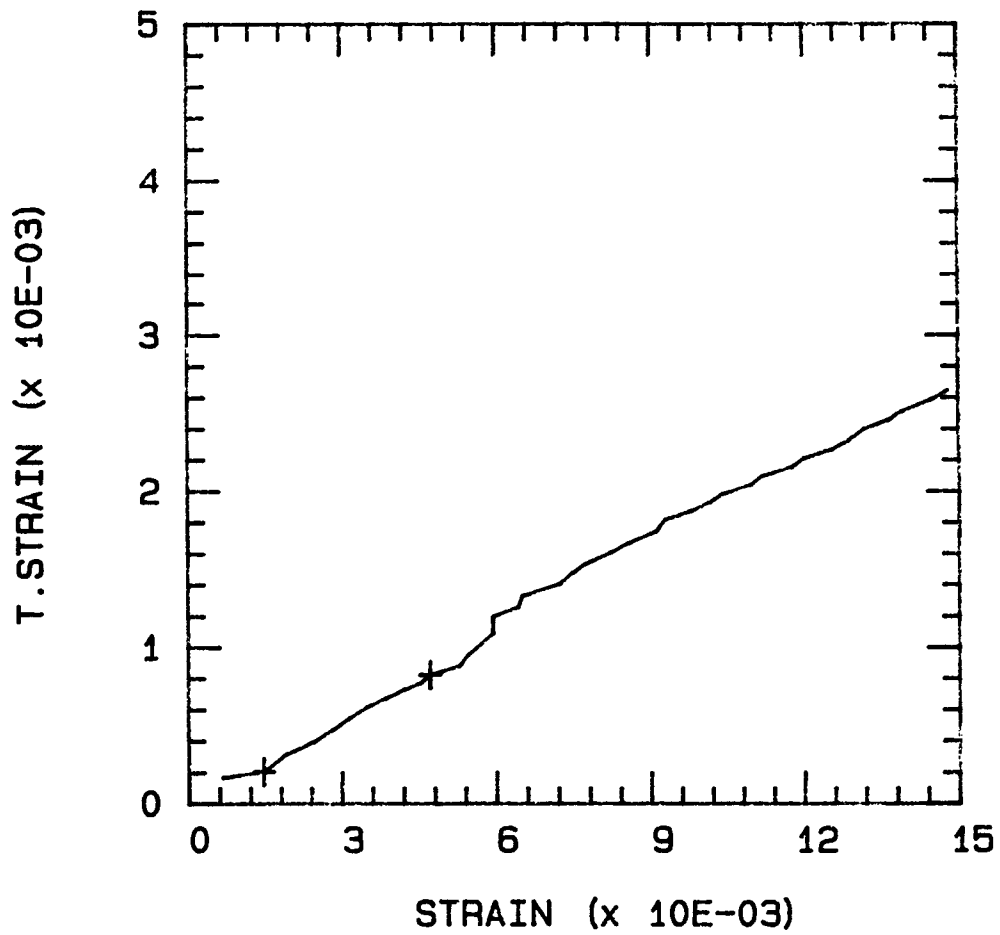
ULT. STRESS = 382.500 ksi

TEMP = 23.0 DEG. C MOD = 23.844 Msi



NLOTD3.TEN

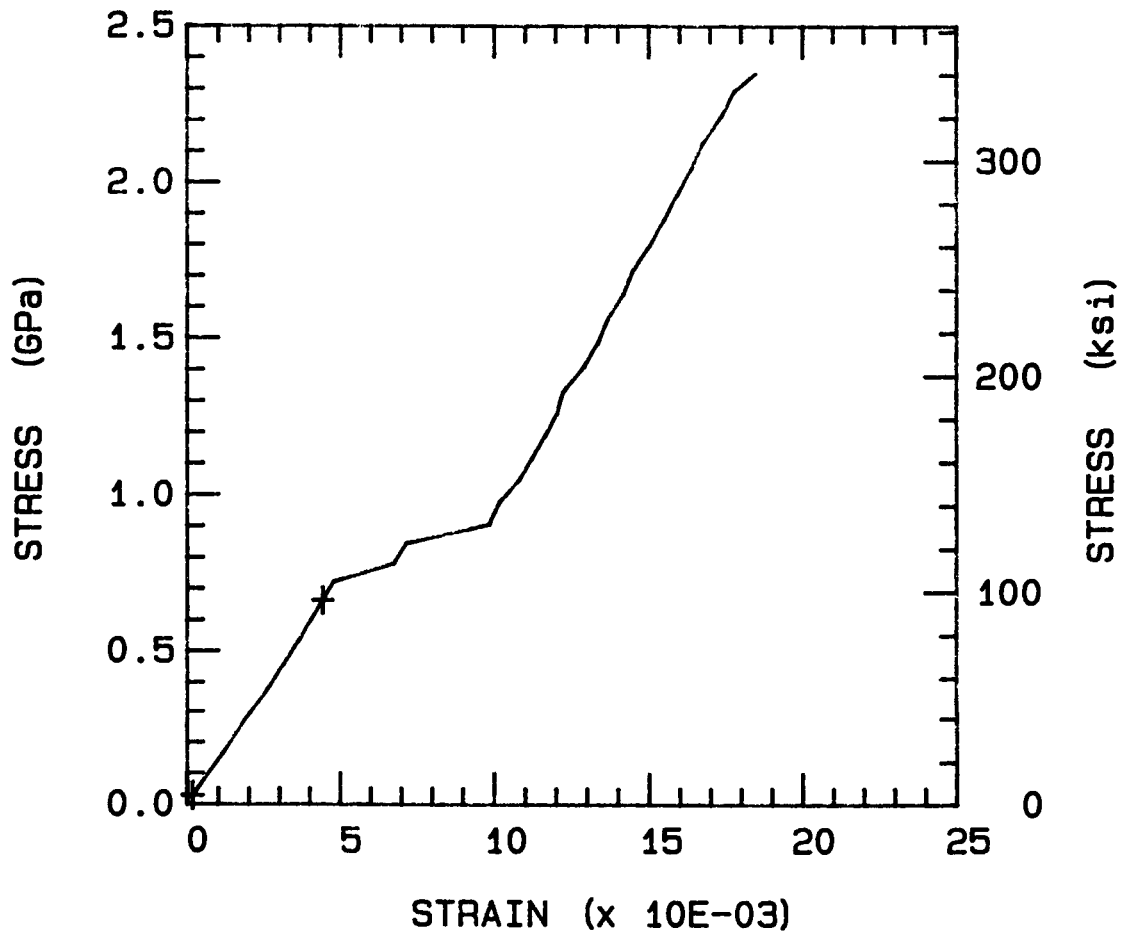
ULT. STRESS = 382.500 ksi
TEMP = 23.0 DEG. C NU = 0.186



NLOTD4.TEN

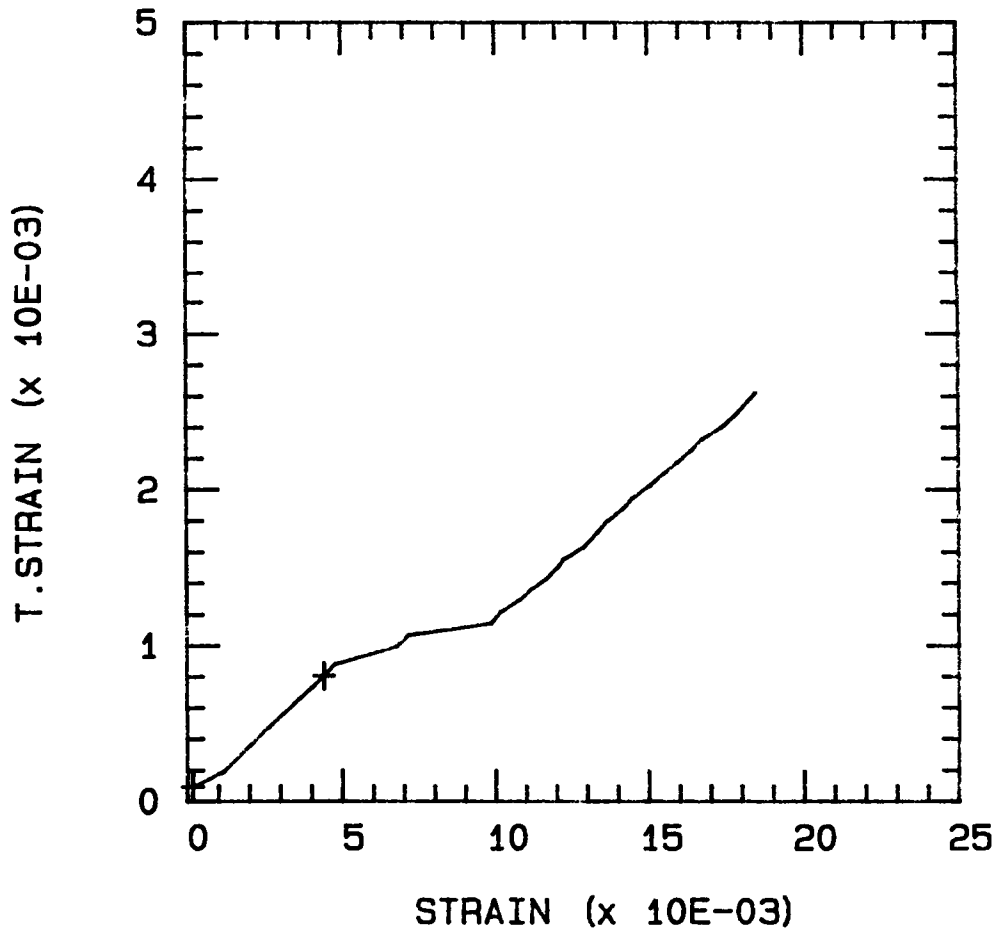
ULT. STRESS = 340.700 ksi

TEMP = 23.0 DEG. C MOD = 21.679 Msi



NLOTD4.TEN

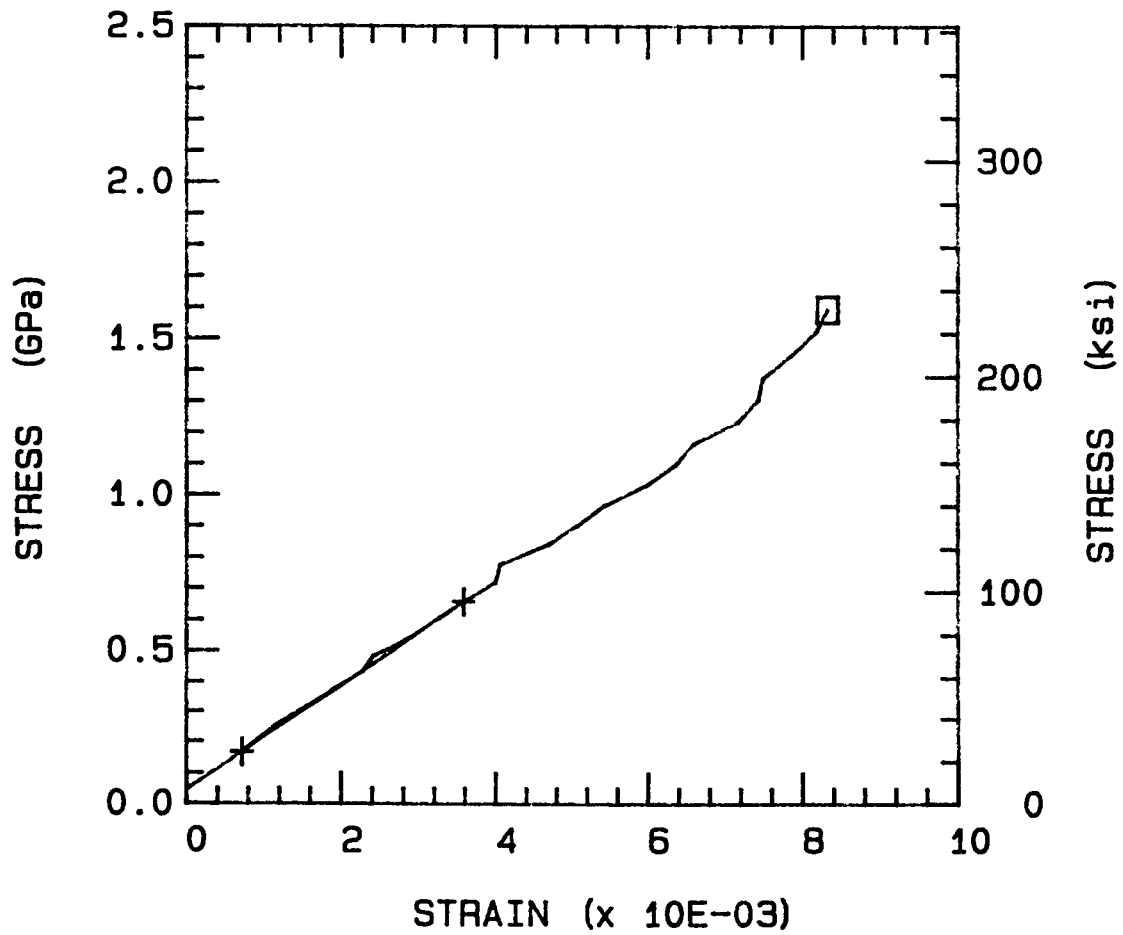
ULT. STRESS = 340.700 ksi
TEMP = 23.0 DEG. C NU = 0.174



NL0TD5.TEN

ULT. STRESS = 231.200 ksi

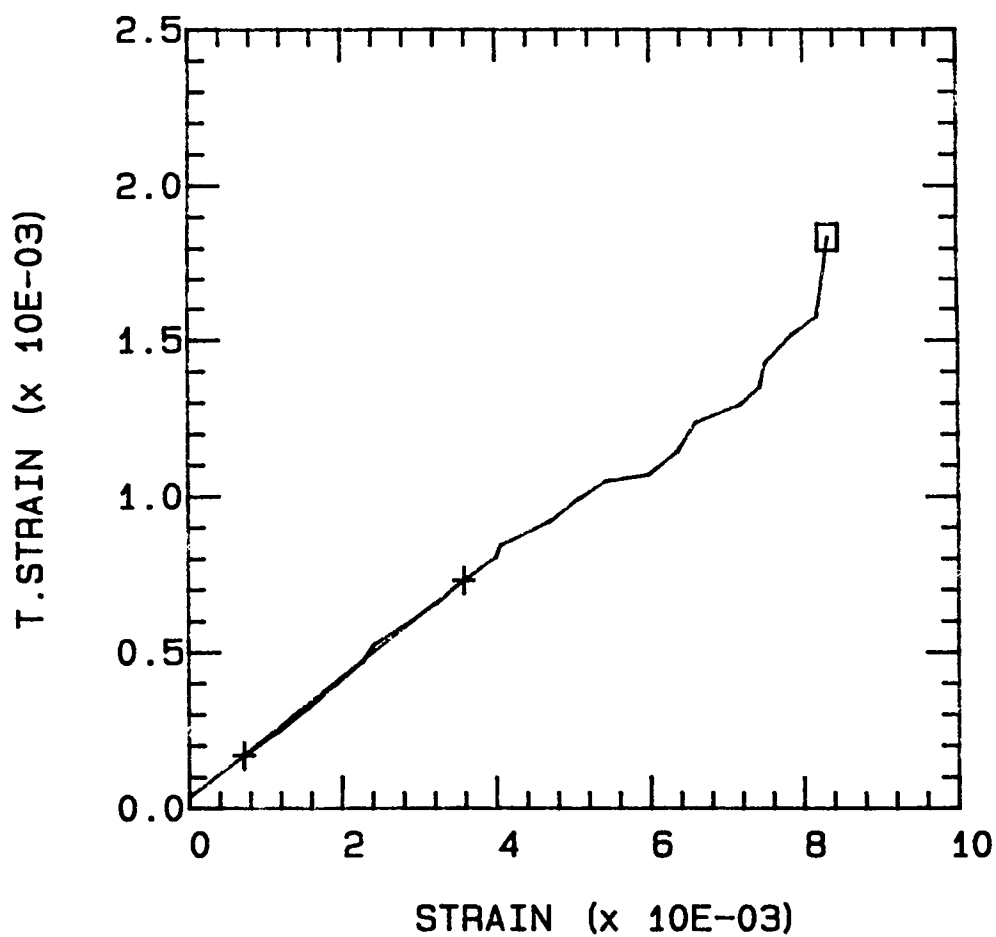
TEMP = 23.0 DEG. C MOD = 24.672 Msi



NLOTD5.TEN

ULT. STRESS = 231.200 ksi

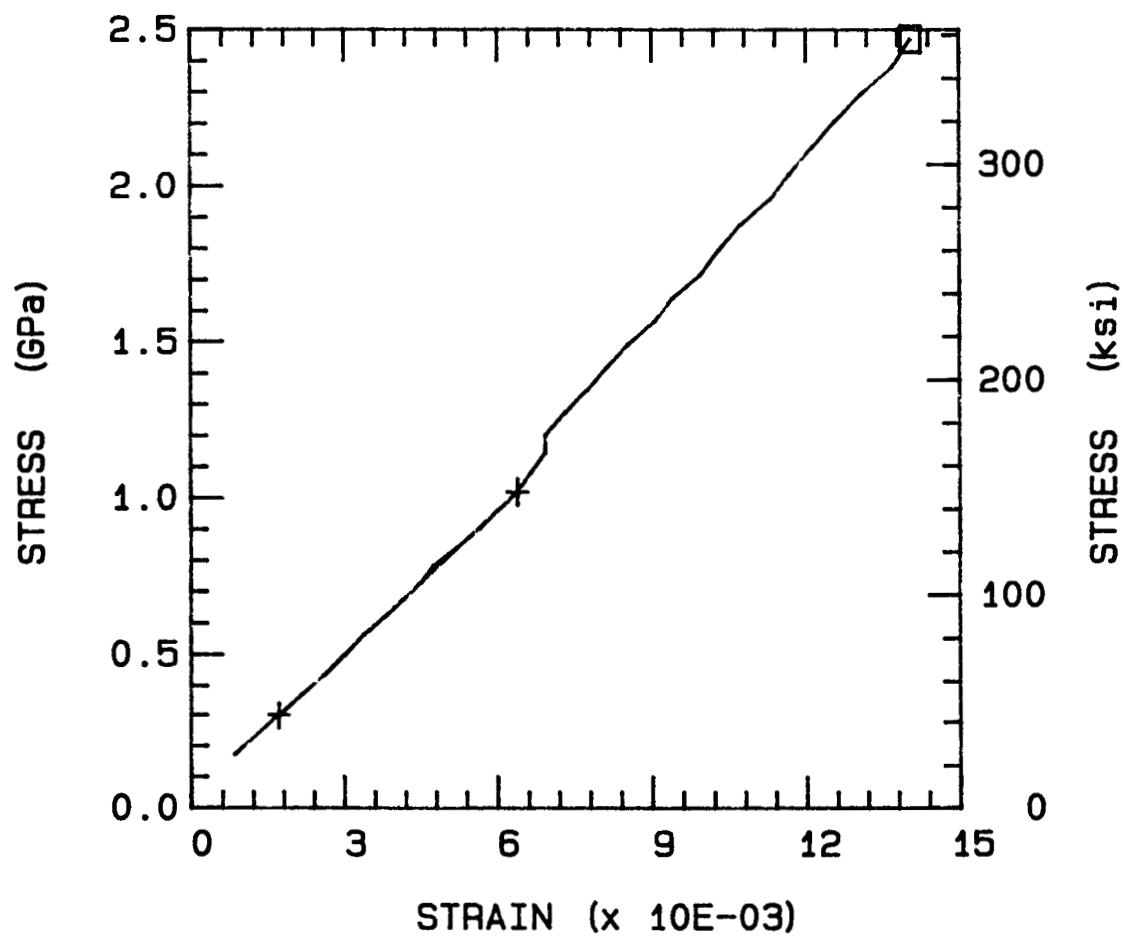
TEMP = 23.0 DEG. C NU = 0.200



NLOTD6.TEN

ULT. STRESS = 358.300 ksi

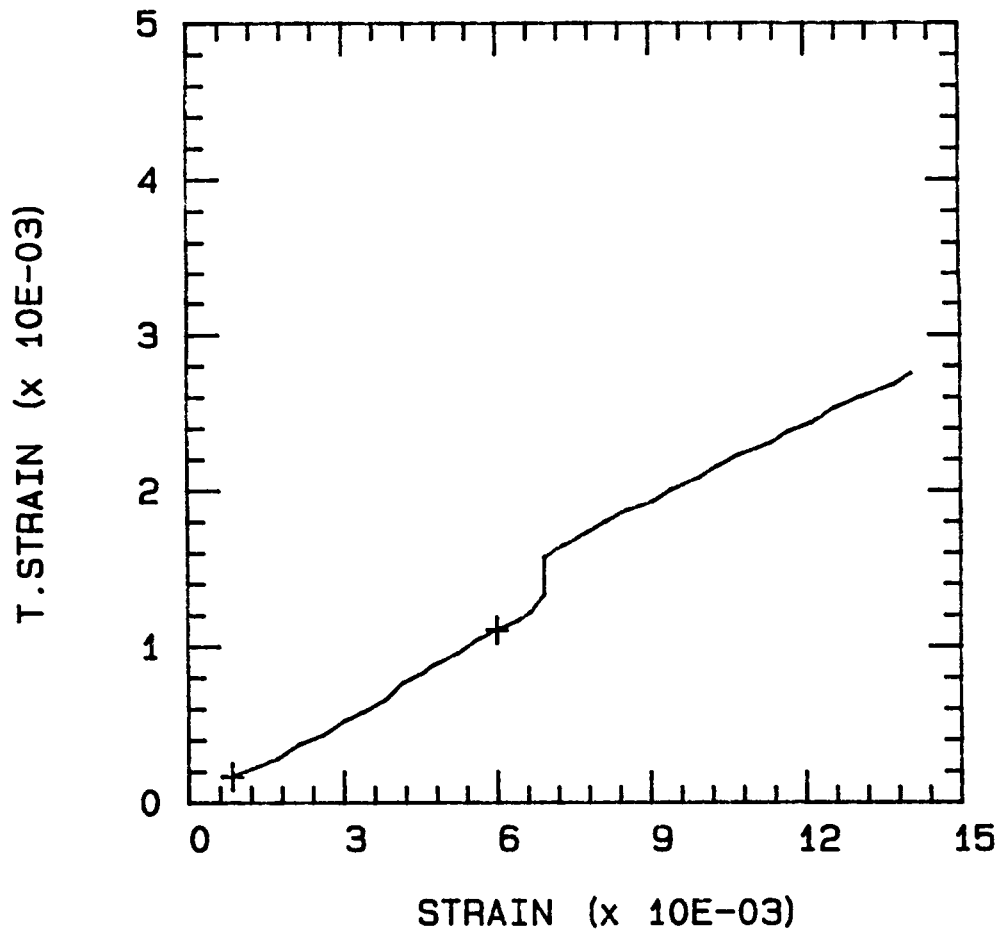
TEMP = 23.0 DEG. C MOD = 22.318 Msi



NLOTD6.TEN

ULT. STRESS = 358.300 ksi

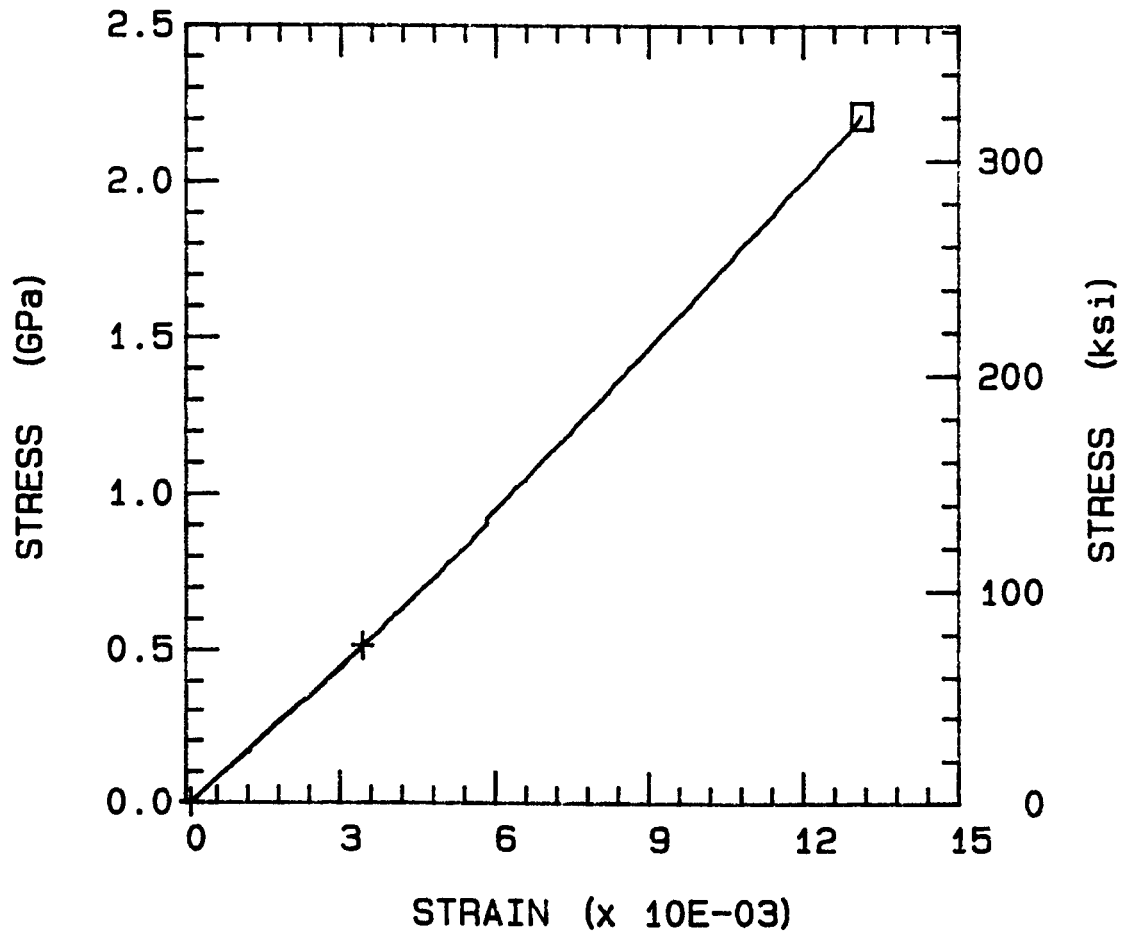
TEMP = 23.0 DEG. C NU = 0.189



NLFSH1.TEN

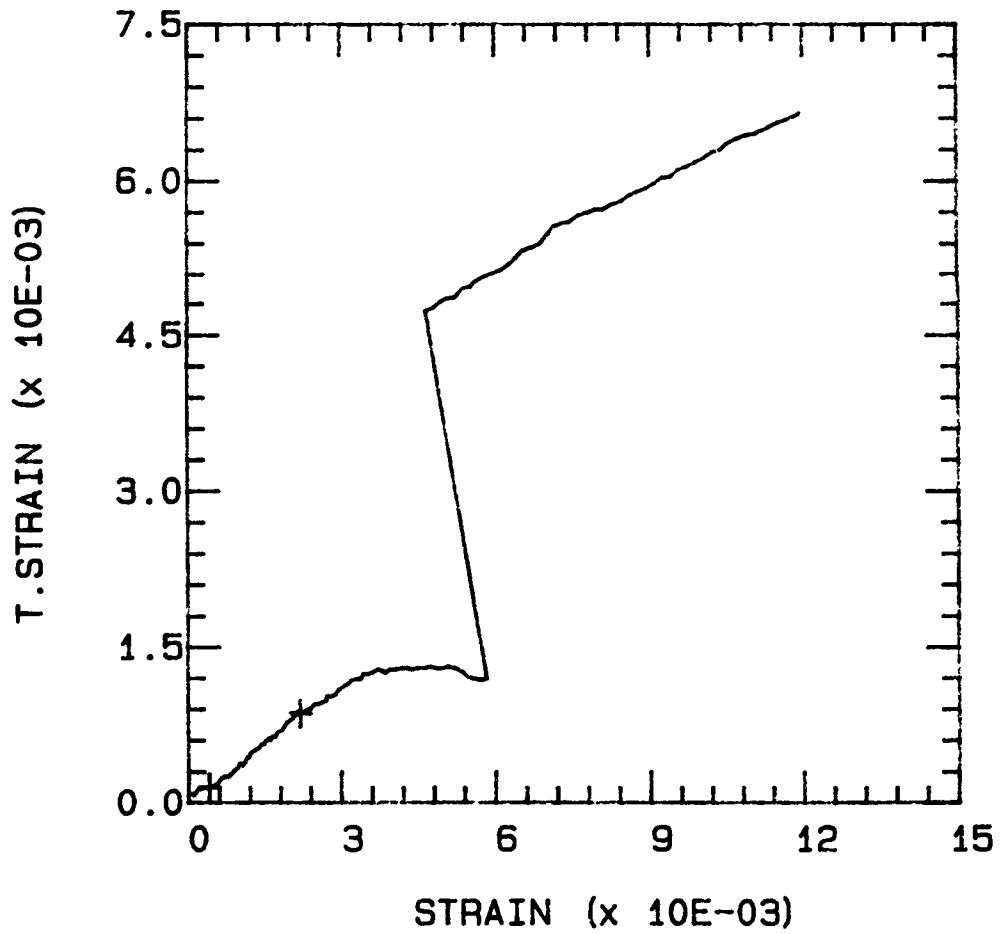
ULT. STRESS = 320.800 ksi

TEMP = 82.0 DEG. C MOD = 22.138 Msi



NLFSH1.TEN

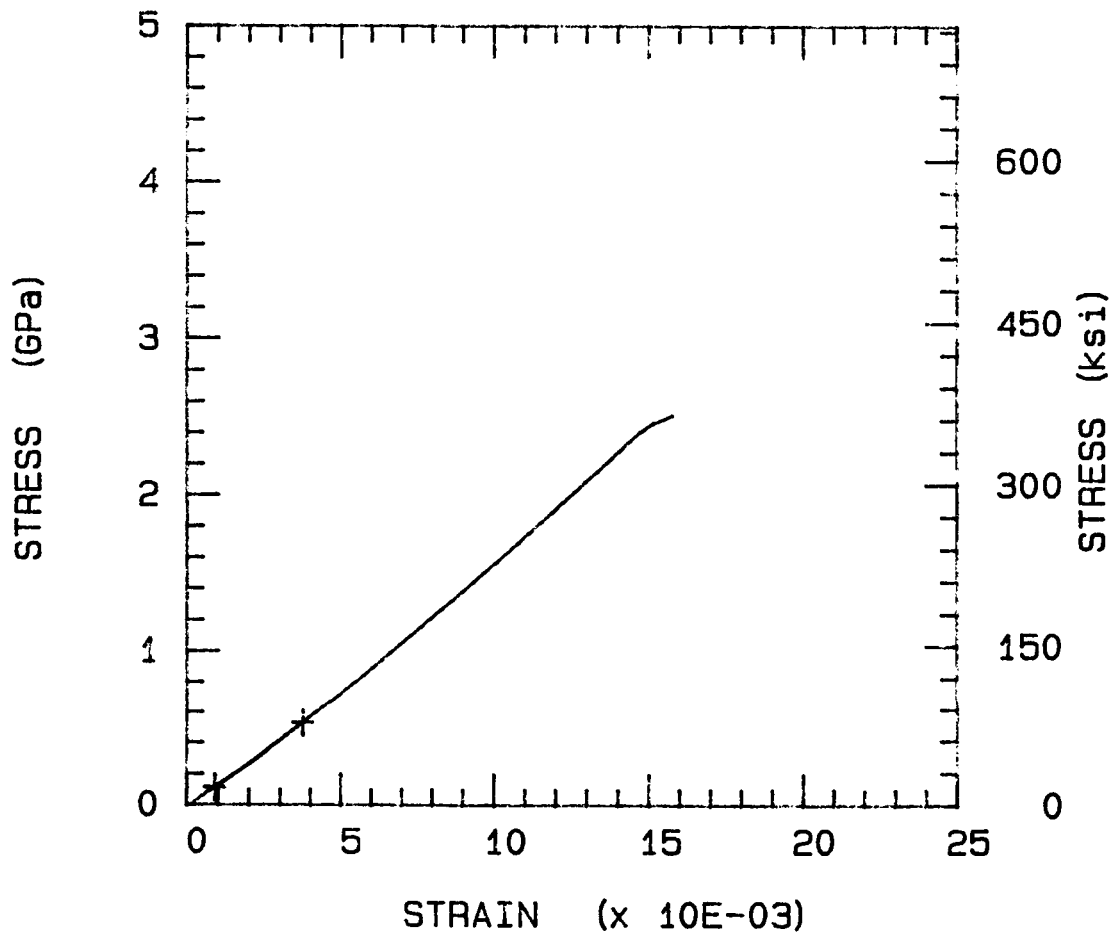
ULT. STRESS = 320.800 ksi
TEMP = 82.0 DEG. C NU = 0.419



NLFSH2.TEN

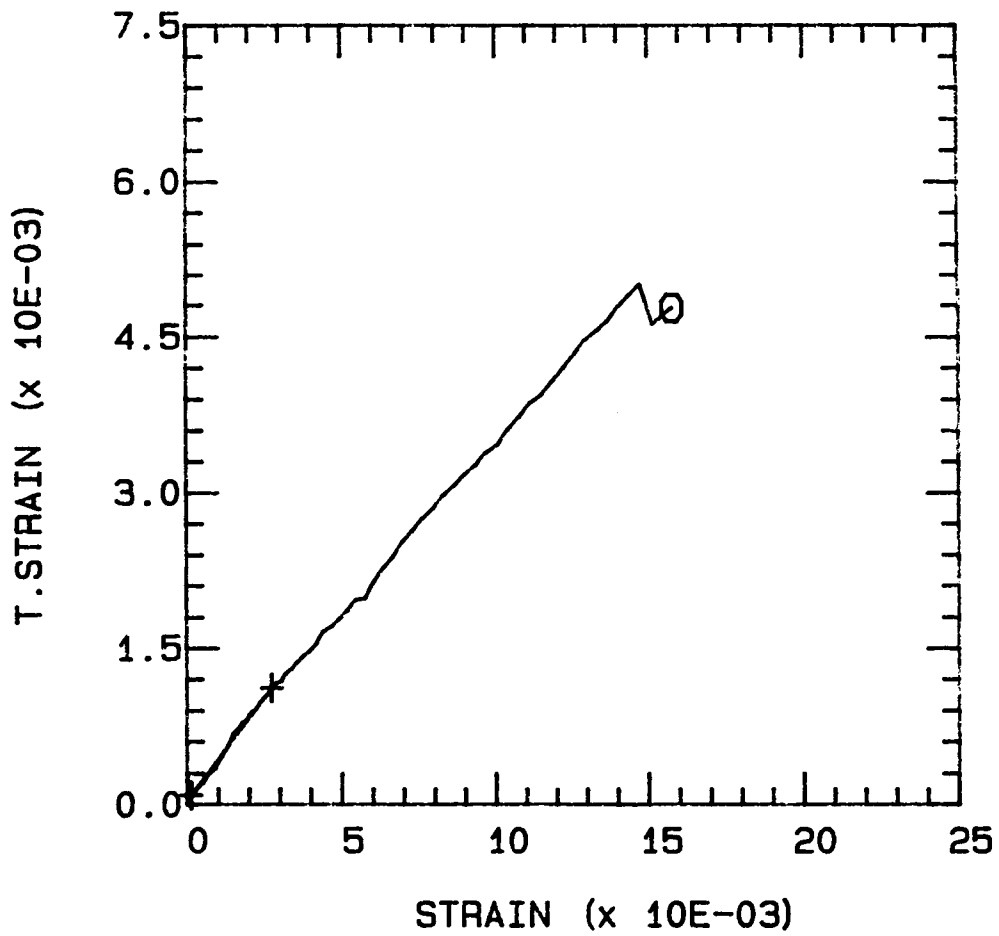
ULT. STRESS = 364.300 ksi

TEMP = 82.0 DEG. C MOD = 21.357 Msi



NLFSH2.TEN

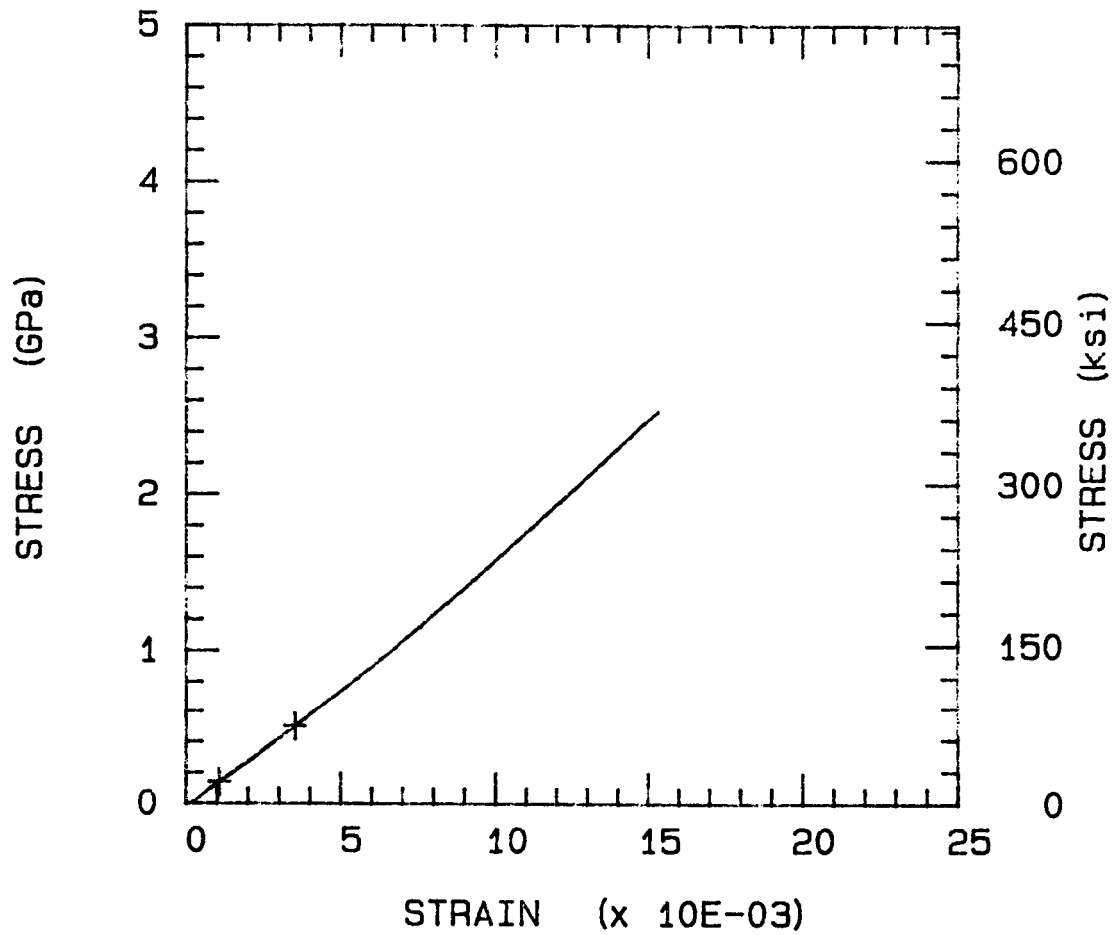
ULT. STRESS = 364.300 ksi
TEMP = 82.0 DEG. C NU = 0.404



NLFSH3.TEN

ULT. STRESS = 366.700 ksi

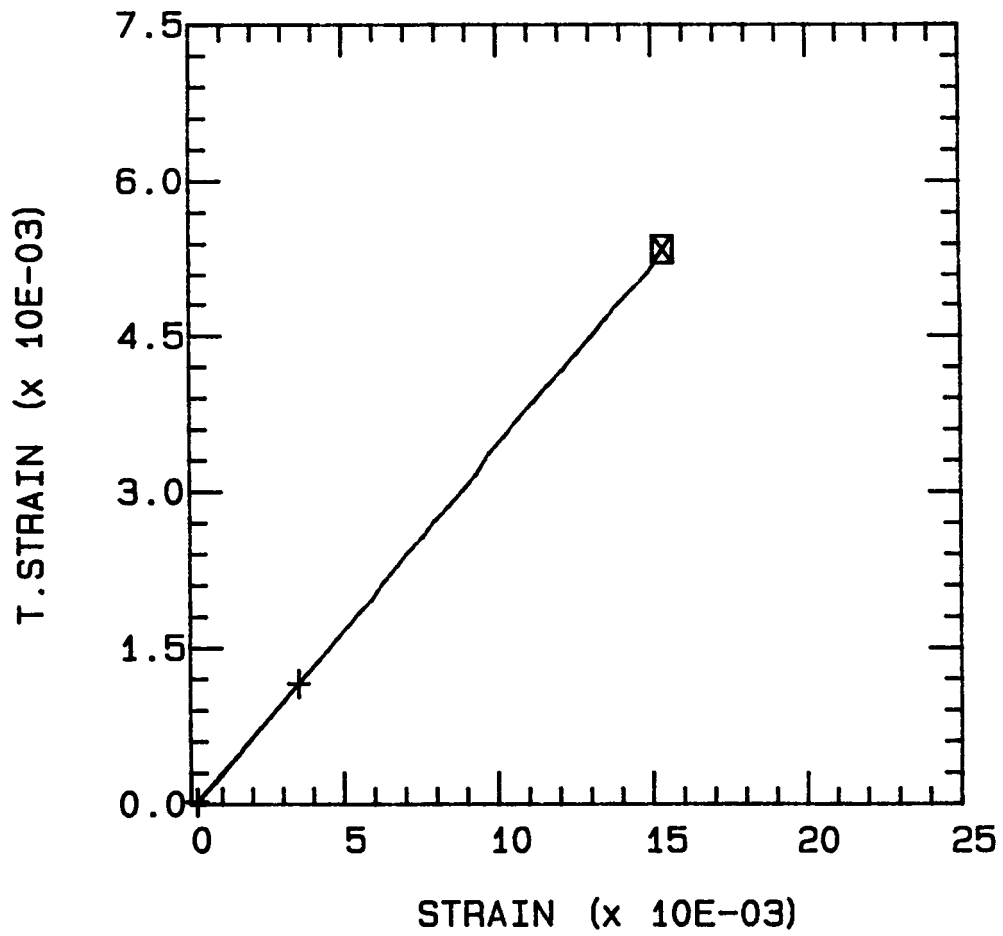
TEMP = 82.0 DEG. C MOD = 21.345 Msi



NLFSH3.TEN

ULT. STRESS = 366.700 ksi

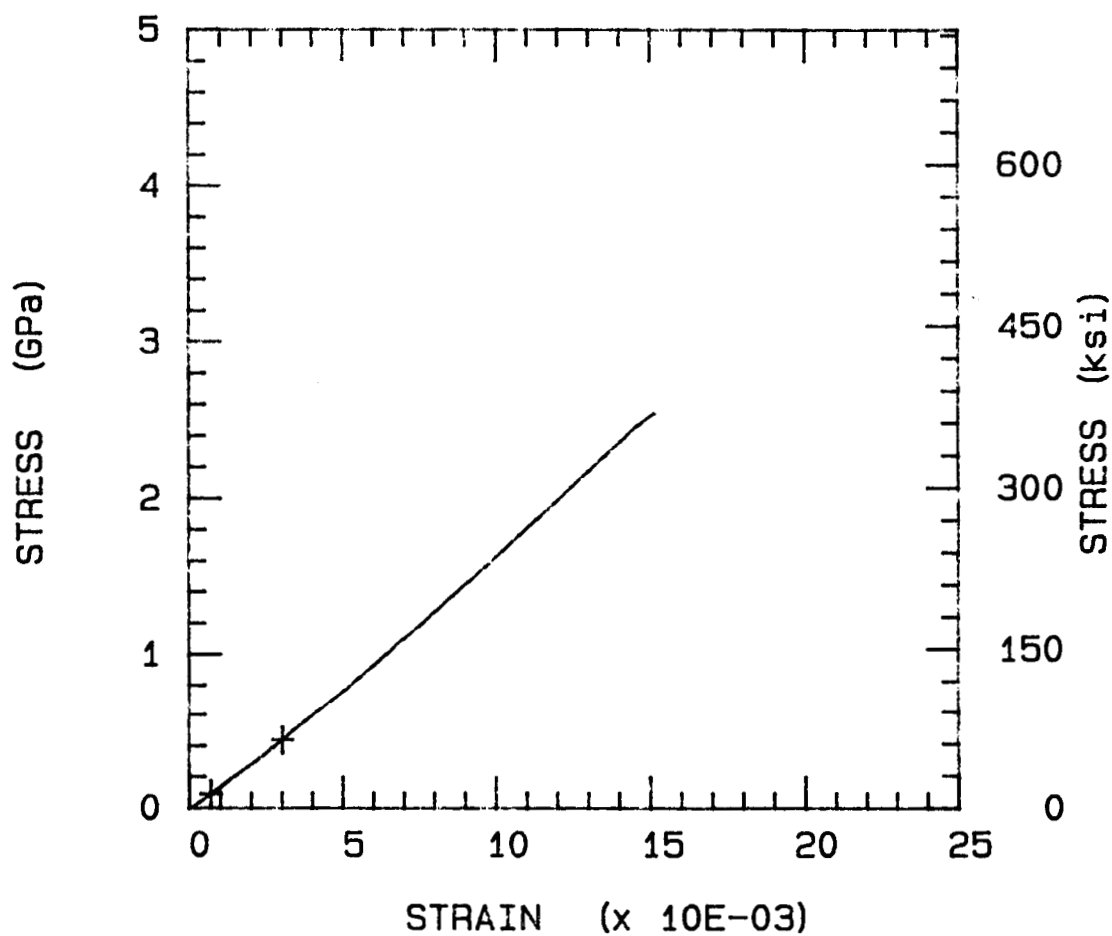
TEMP = 82.0 DEG. C NU = 0.345



NLFSH4.TEN

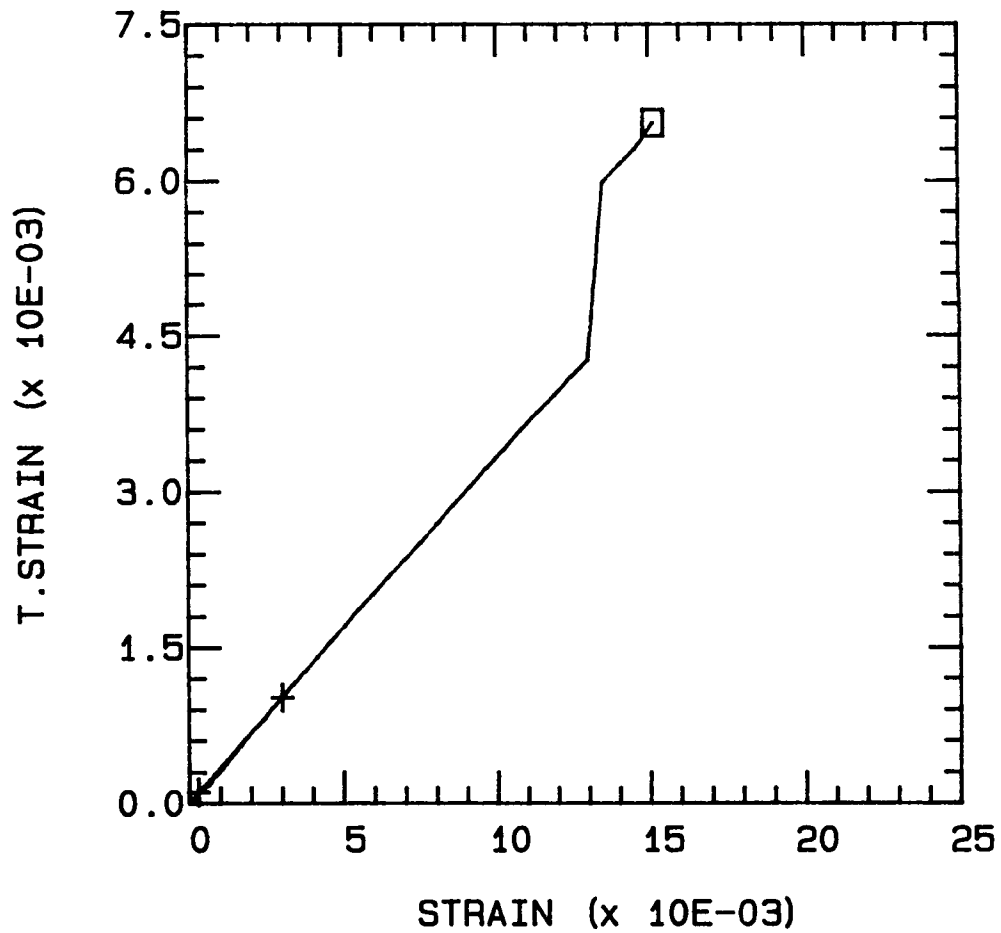
ULT. STRESS = 368.500 ksi

TEMP = 82.0 DEG. C MOD = 21.787 Msi



NLFSH4.TEN

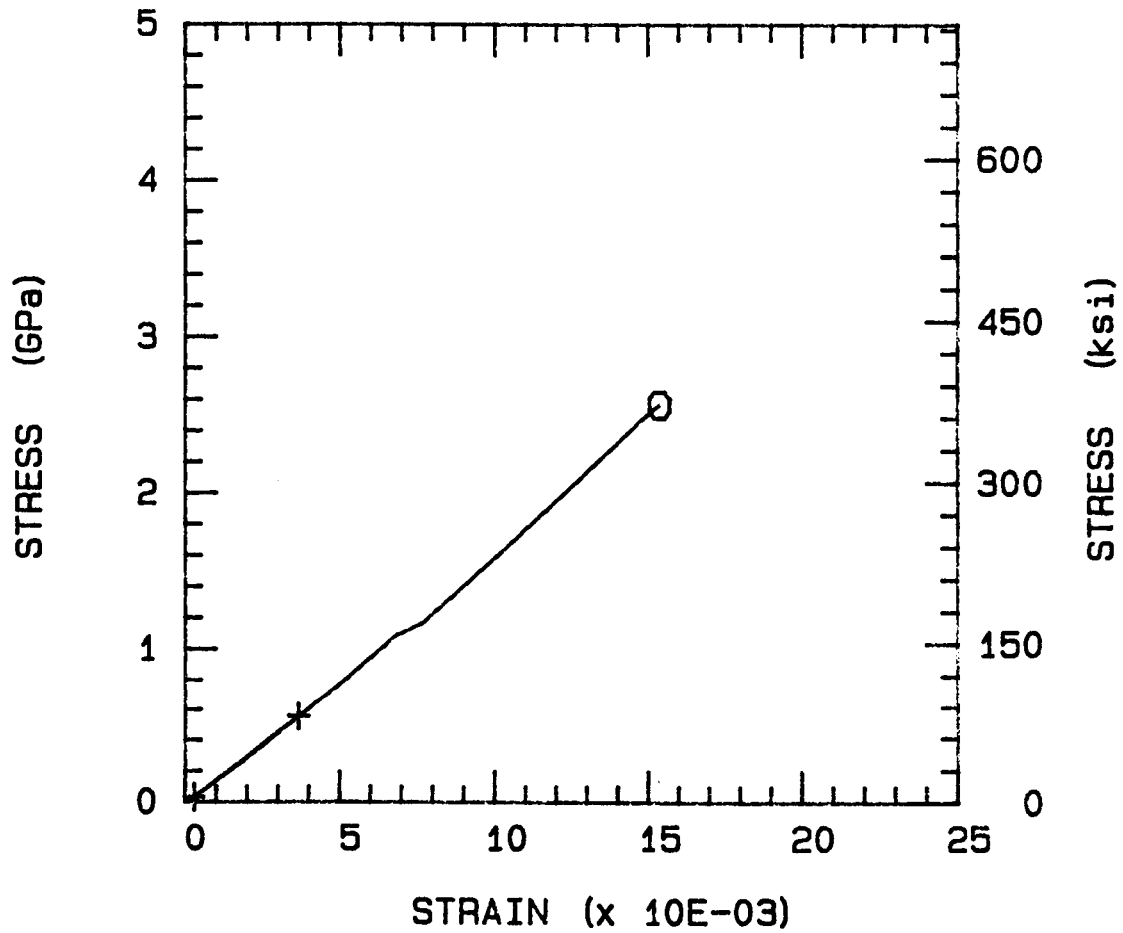
ULT. STRESS = 368.500 ksi
TEMP = 82.0 DEG. C NU = 0.345



NLFSH5.TEN

ULT. STRESS = 372.300 ksi

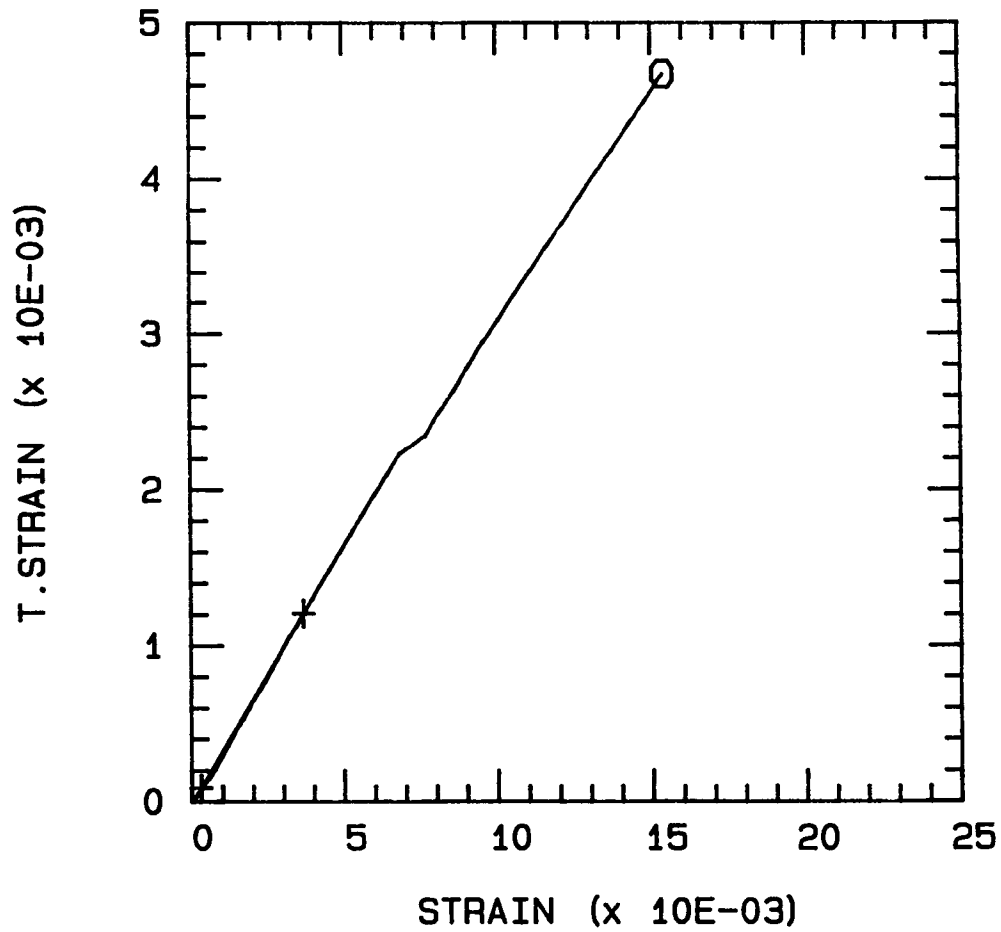
TEMP = 82.0 DEG. C MOD = 22.448 Msi



NLFSH5.TEN

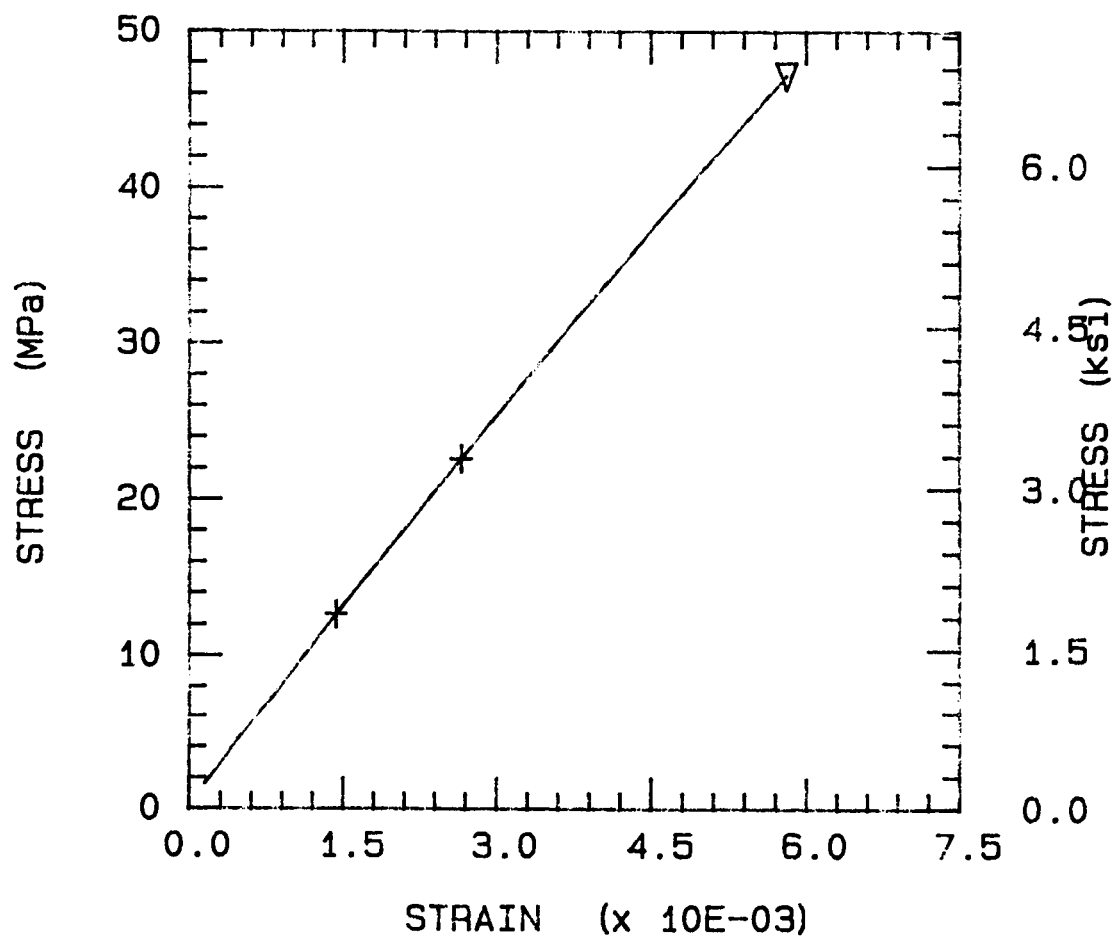
ULT. STRESS = 372.300 ksi

TEMP = 82.0 DEG. C NU = 0.337



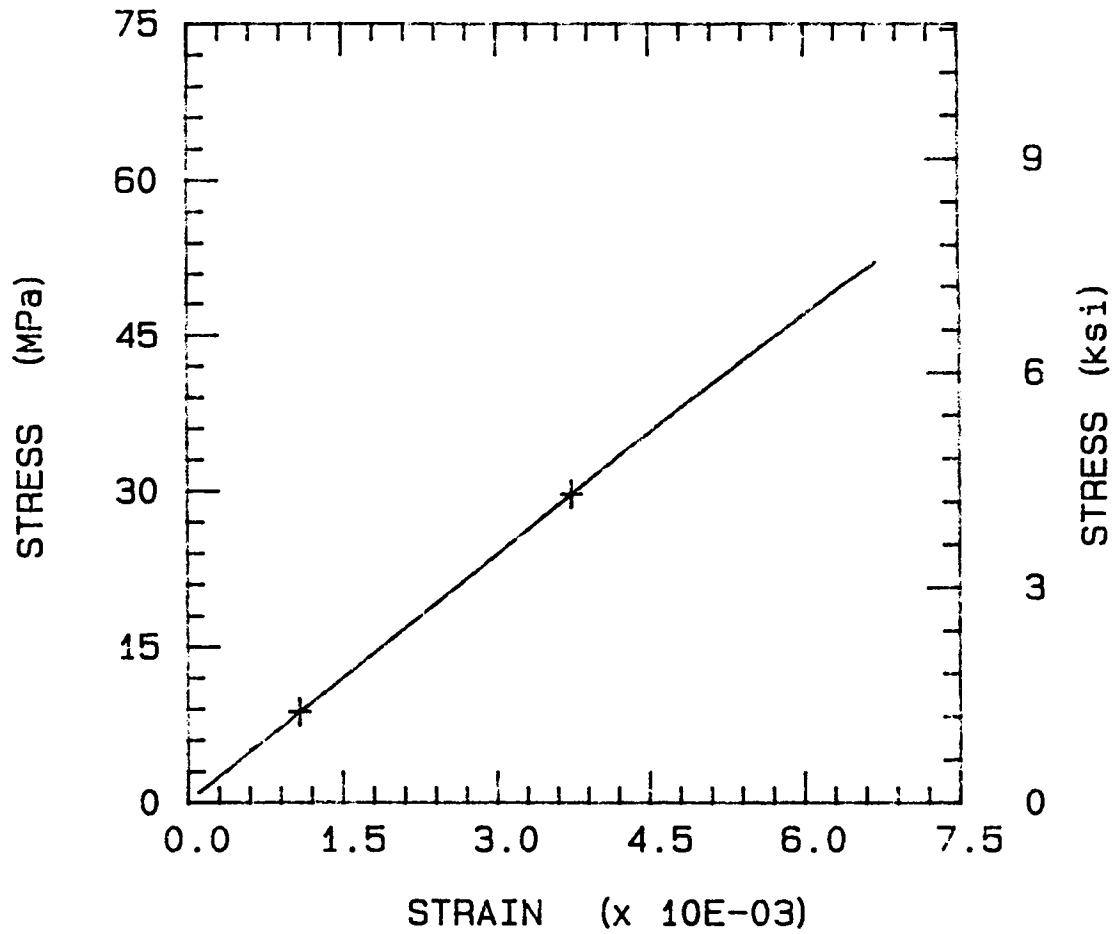
NLTTDO.TEN

ULT. STRESS = 6.838 ksi
TEMP = 23.0 DEG. C MOD = 1.186 Msi



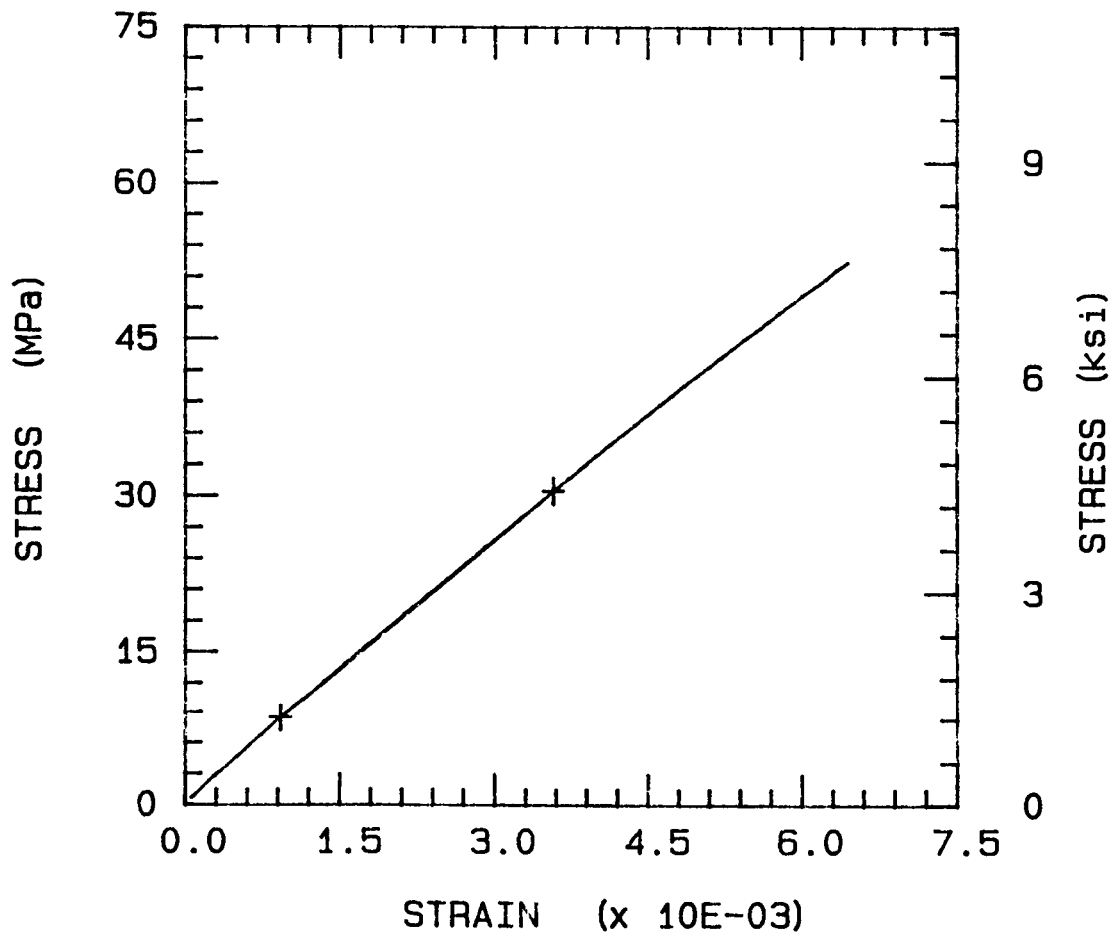
NLTTD1.TEN

ULT. STRESS = 7.560 ksi
TEMP = 23.0 DEG. C MOD = 1.149 Msi



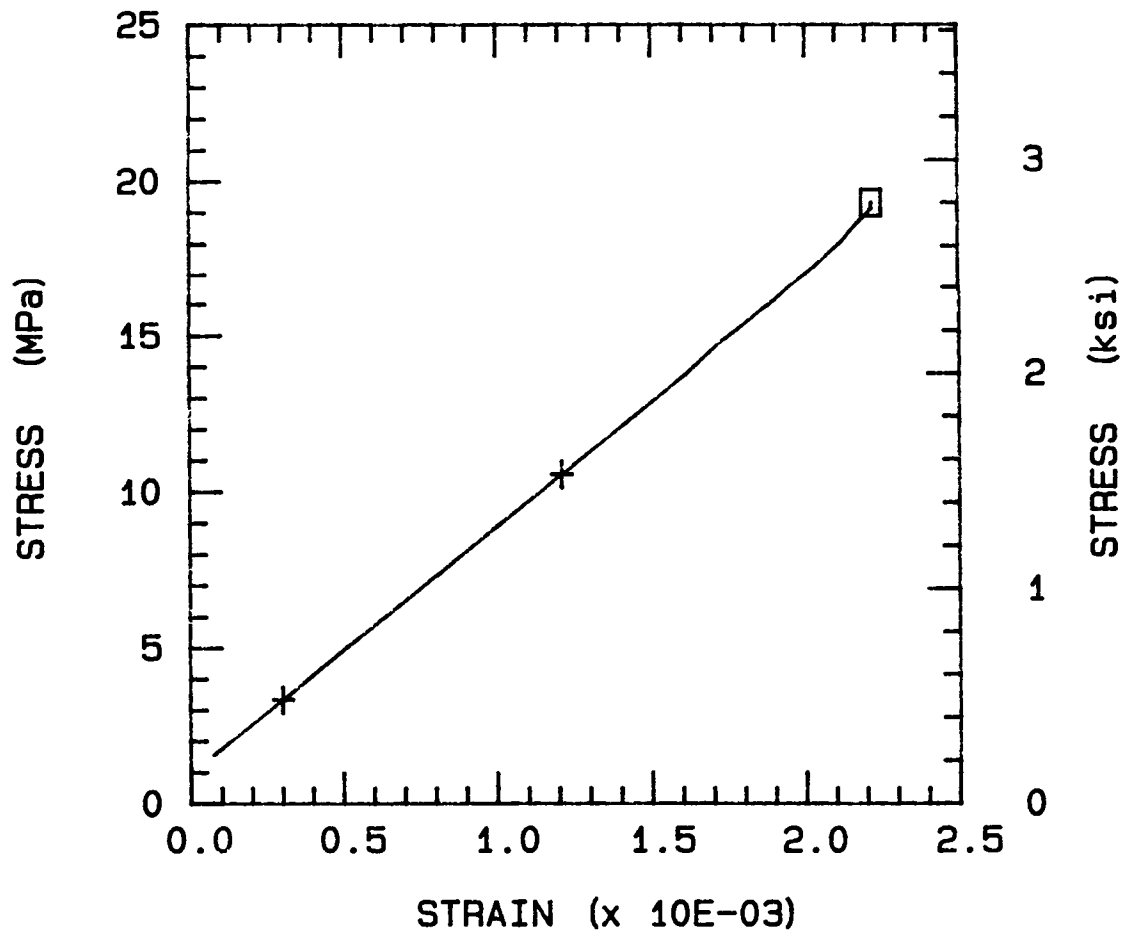
NLTTD2.TEN

ULT. STRESS = 7.607 ksi
TEMP = 23.0 DEG. C MOD = 1.205 Msi



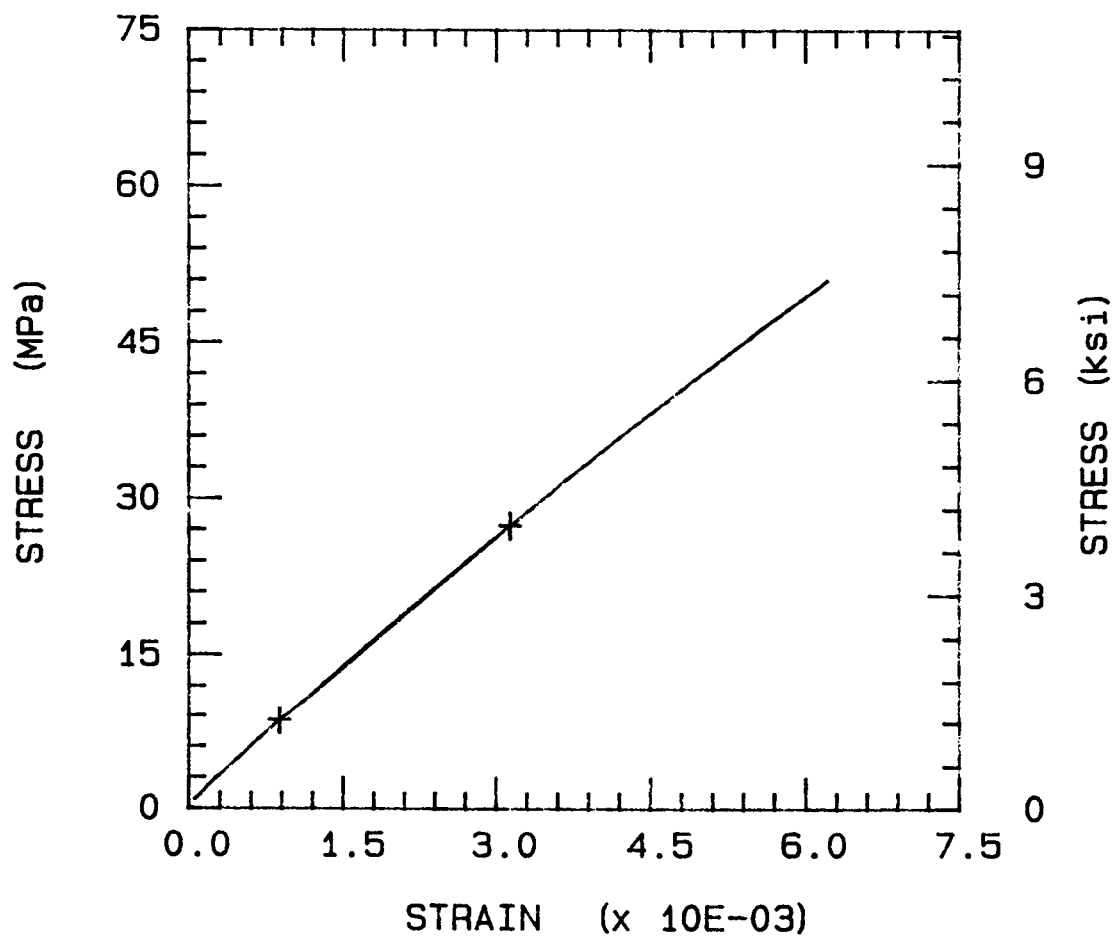
NLTTD3.TEN

ULT. STRESS = 2.801 ksi
TEMP = 23.0 DEG. C MOD = 1.152 Msi



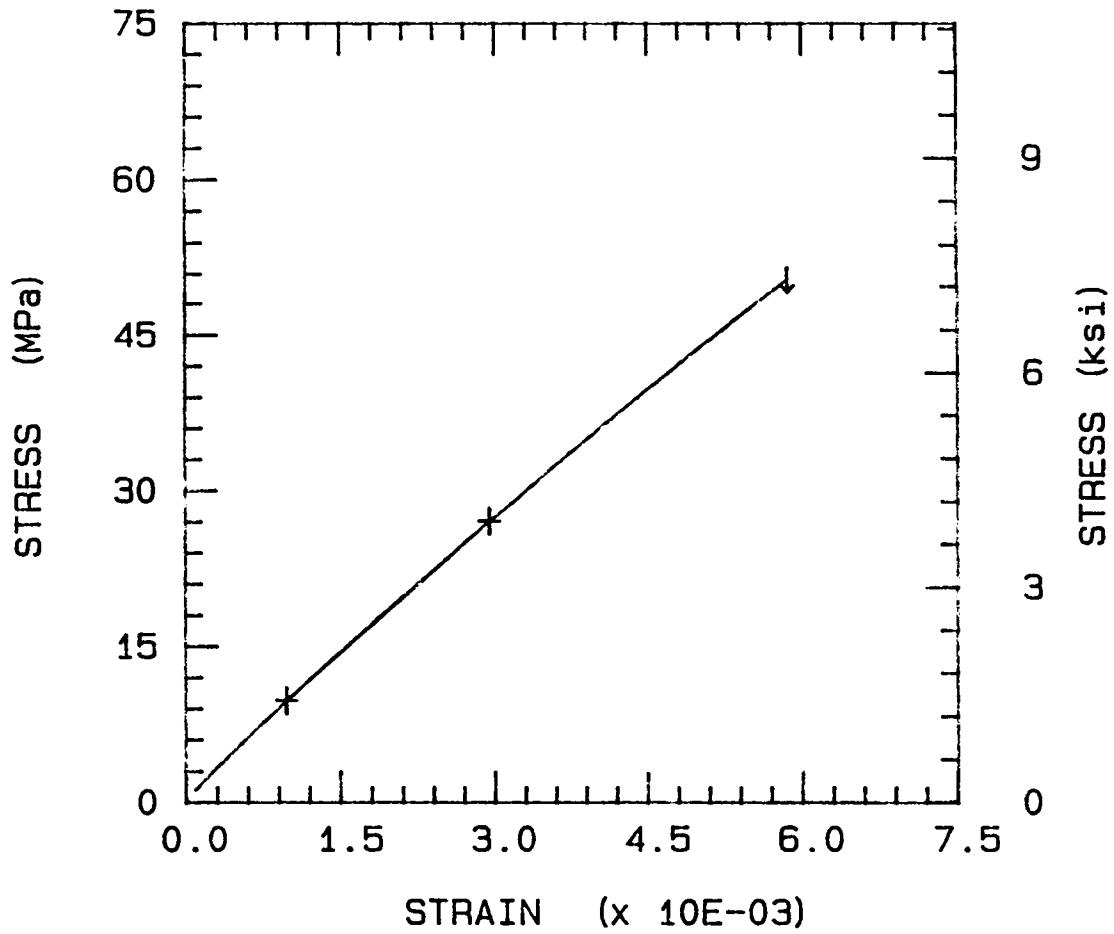
NLTTD4.TEN

ULT. STRESS = 7.397 ksi
TEMP = 23.0 DEG. C MOD = 1.211 Msi



NLTTD5.TEN

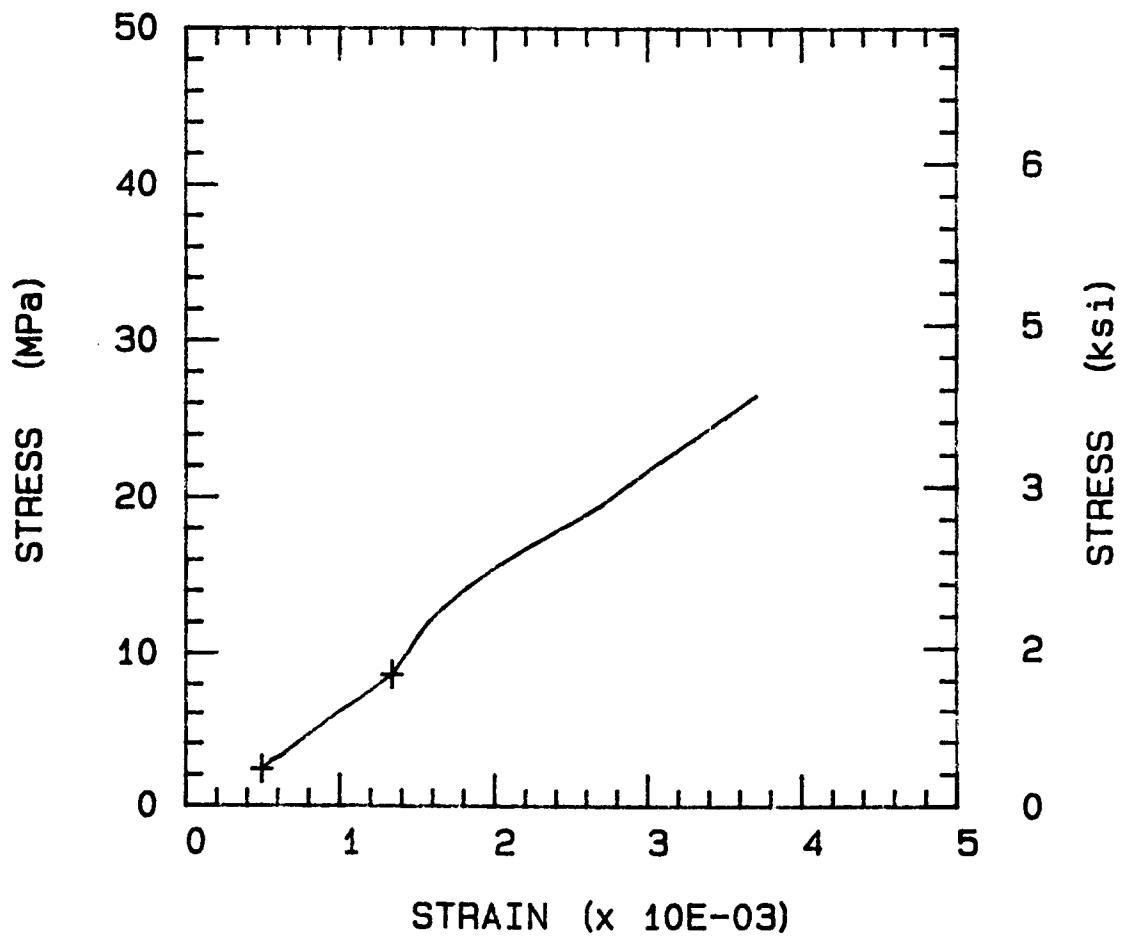
ULT. STRESS = 7.304 ksi
TEMP = 23.0 DEG. C MOD = 1.269 Msi



NTTD21.TEN

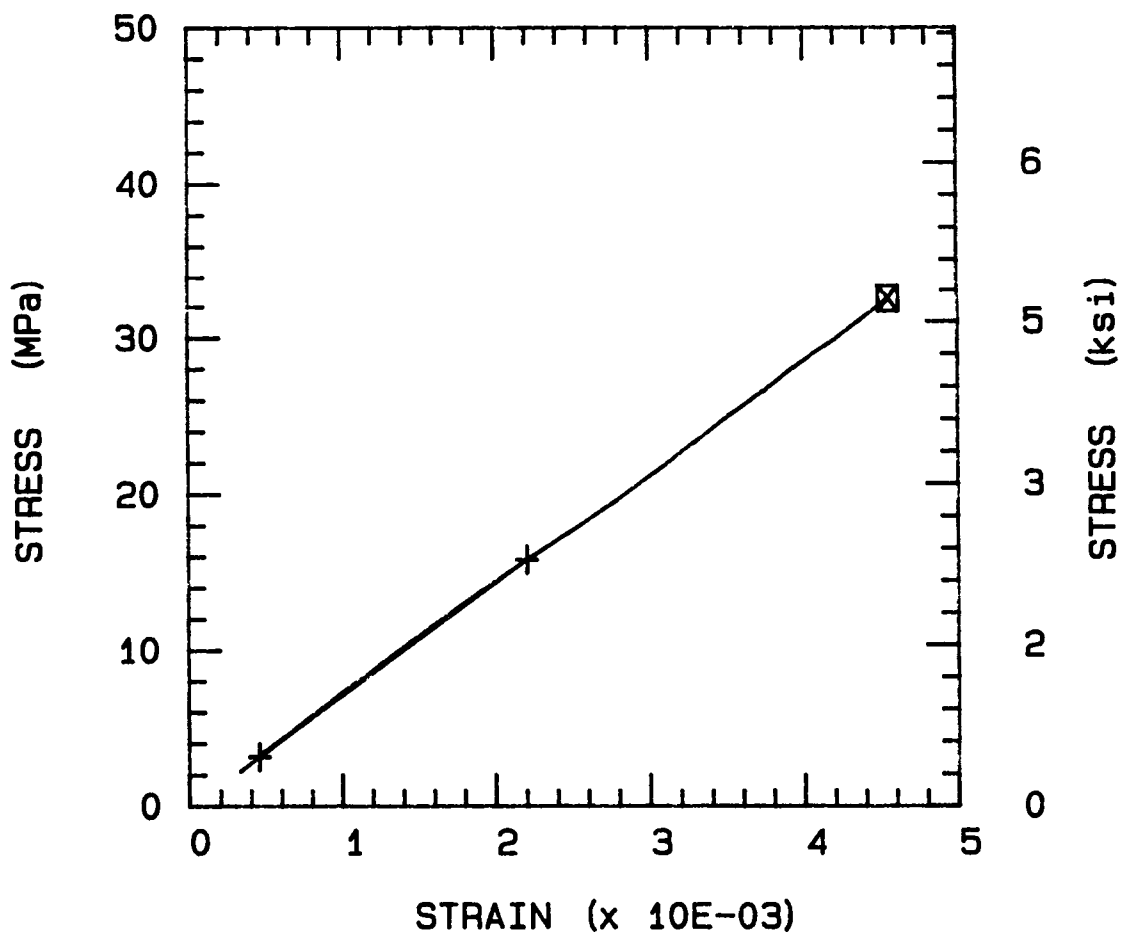
ULT. STRESS = 3.843 ksi

TEMP = 82.0 DEG. C MOD = 1.067 Msi



NTTD22.TEN

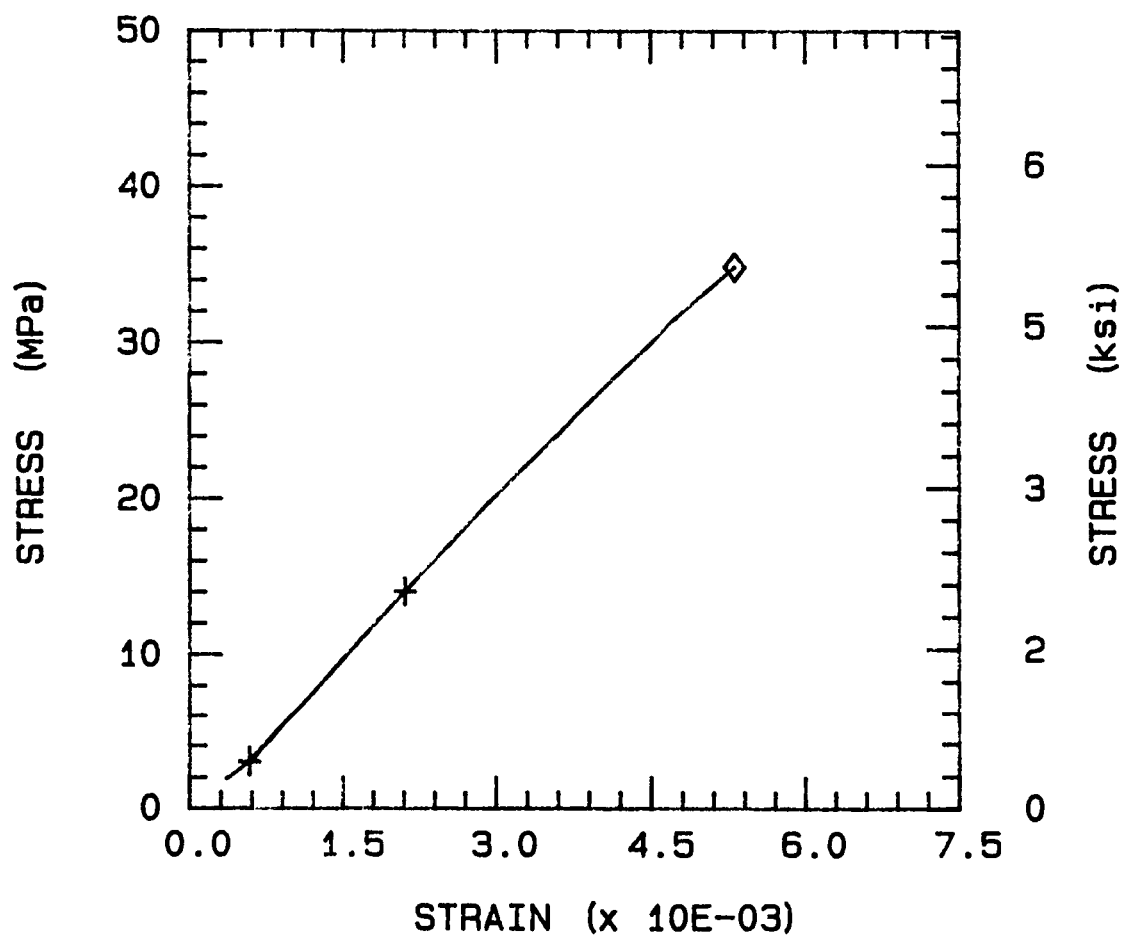
ULT. STRESS = 4.722 ksi
TEMP = 82.0 DEG. C MOD = 1.051 Msi



NTTD23.TEN

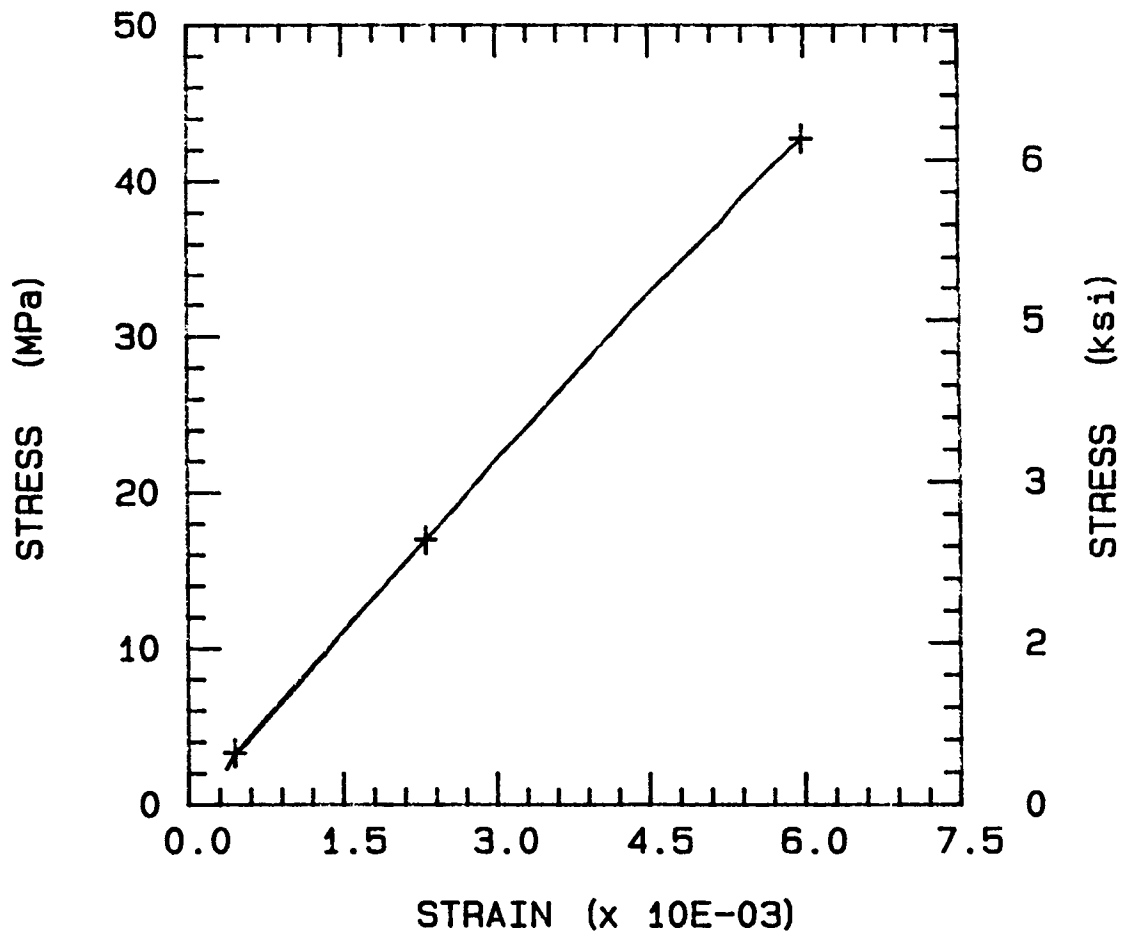
ULT. STRESS = 5.053 ksi

TEMP = 82.0 DEG. C MOD = 1.053 Msi



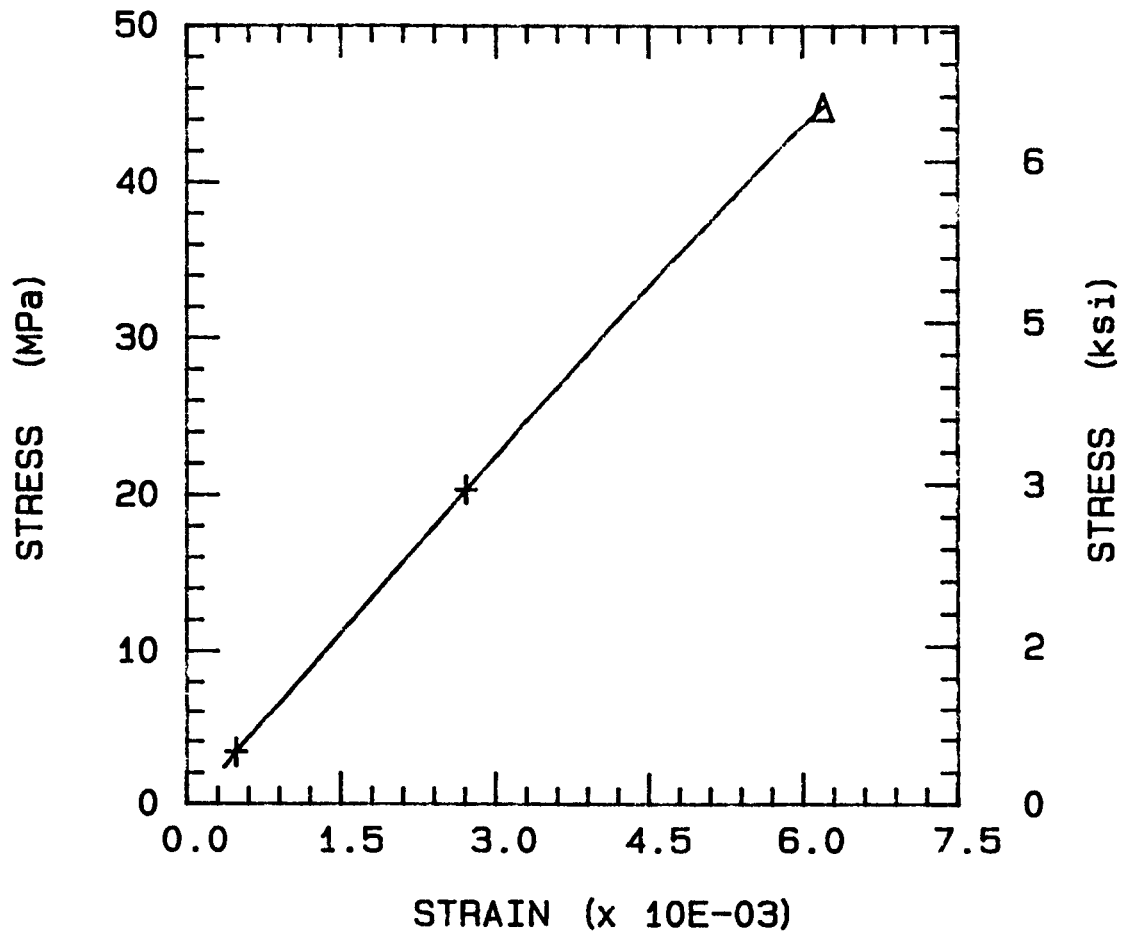
NTTD24.TEN

ULT. STRESS = 6.200 ksi
TEMP = 82.0 DEG. C MOD = 1.076 Msi



NTTD25.TEN

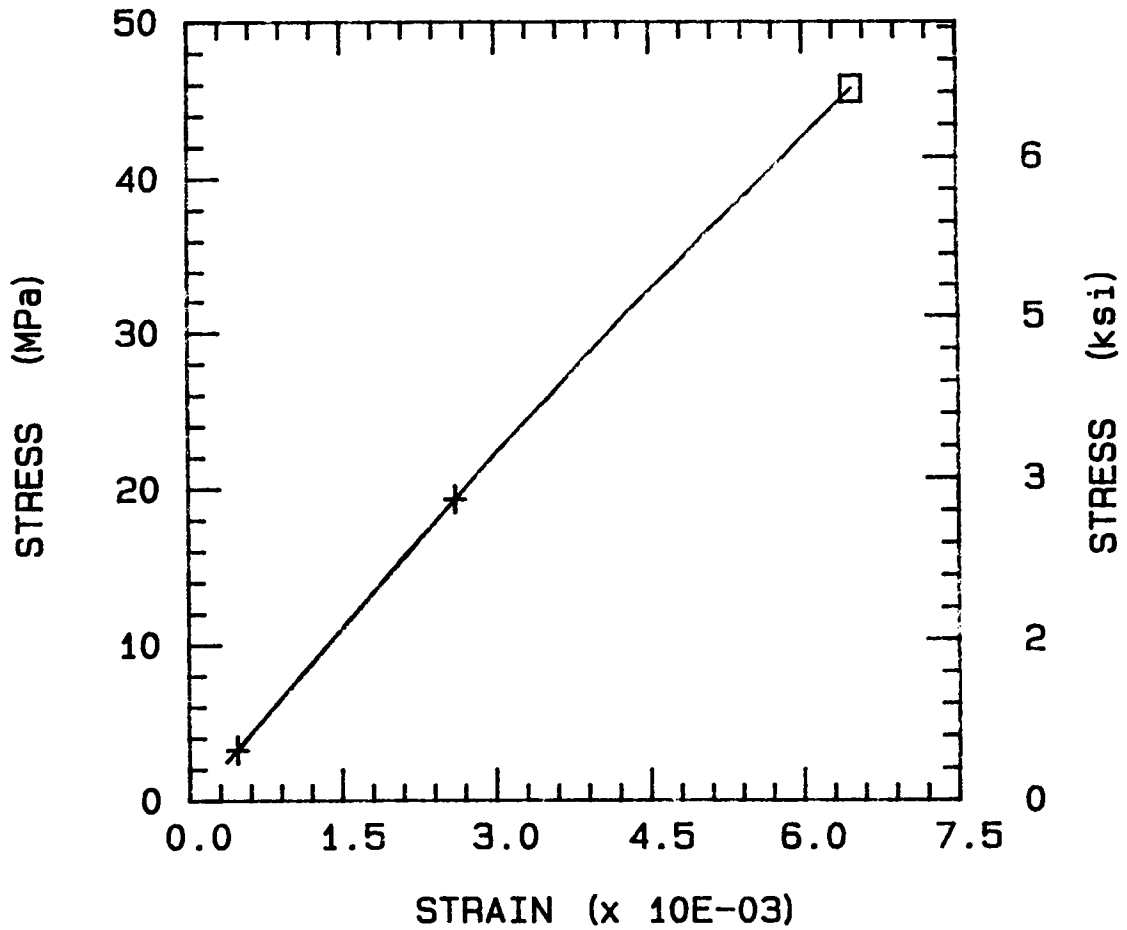
ULT. STRESS = 6.504 ksi
TEMP = 82.0 DEG. C MOD = 1.106 Msi



NTTD26.TEN

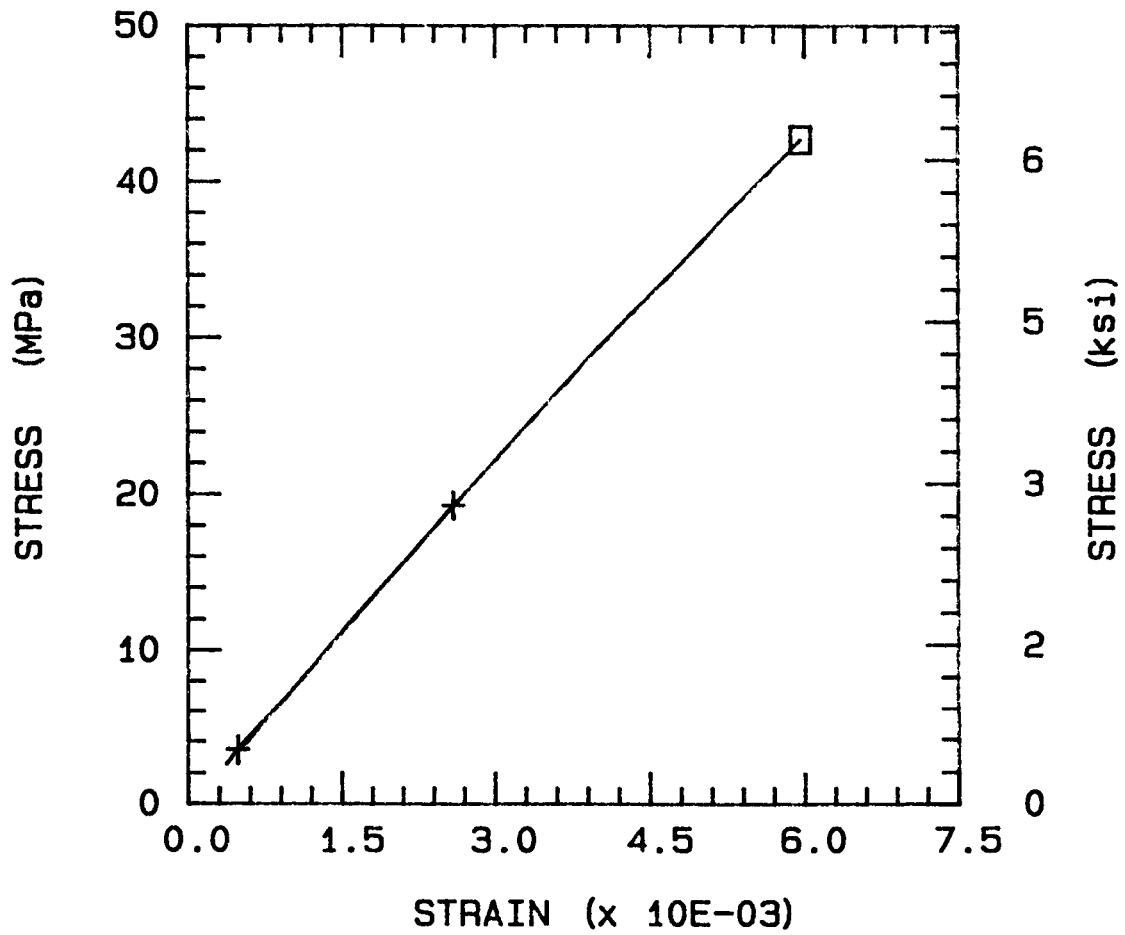
ULT. STRESS = 6.631 ksi

TEMP = 82.0 DEG. C MOD = 1.094 Msi



NTTD27.TEN

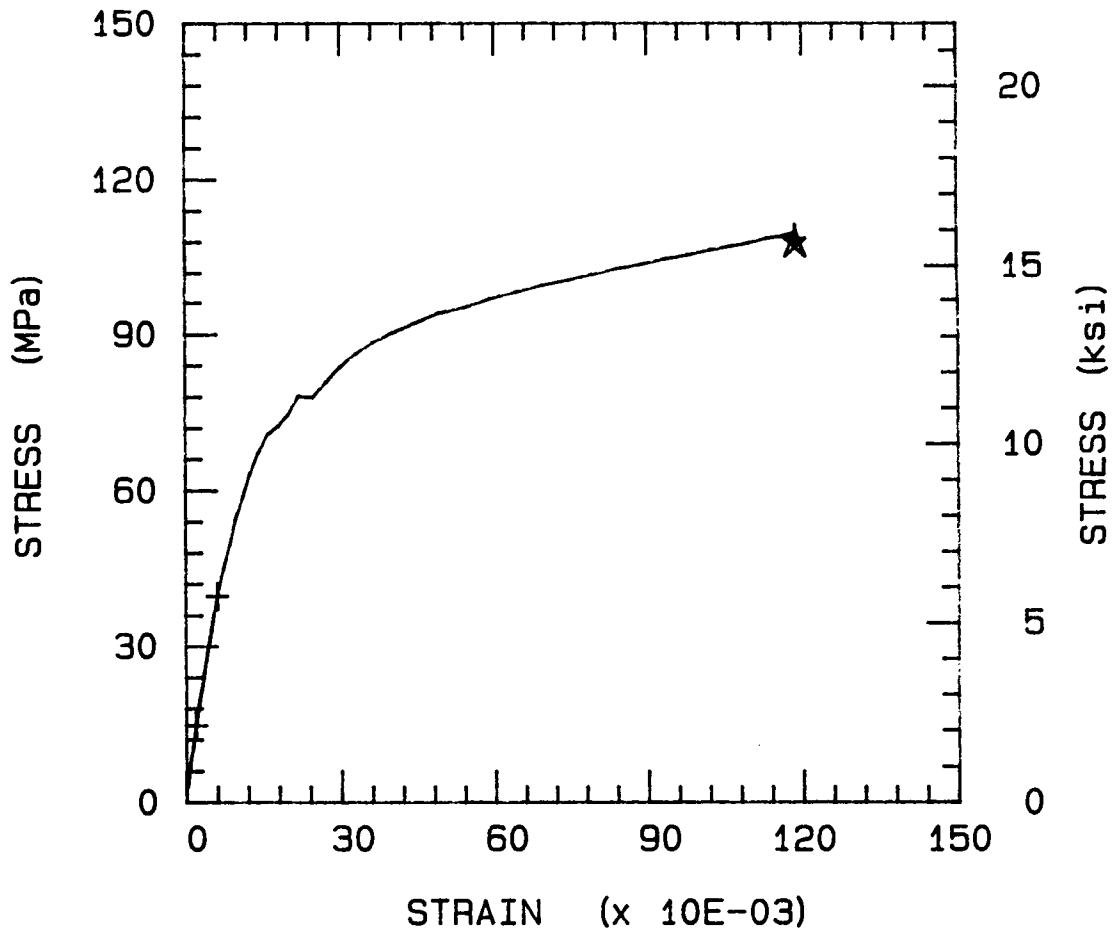
ULT. STRESS = 6.192 ksi
TEMP = 82.0 DEG. C MOD = 1.088 Msi



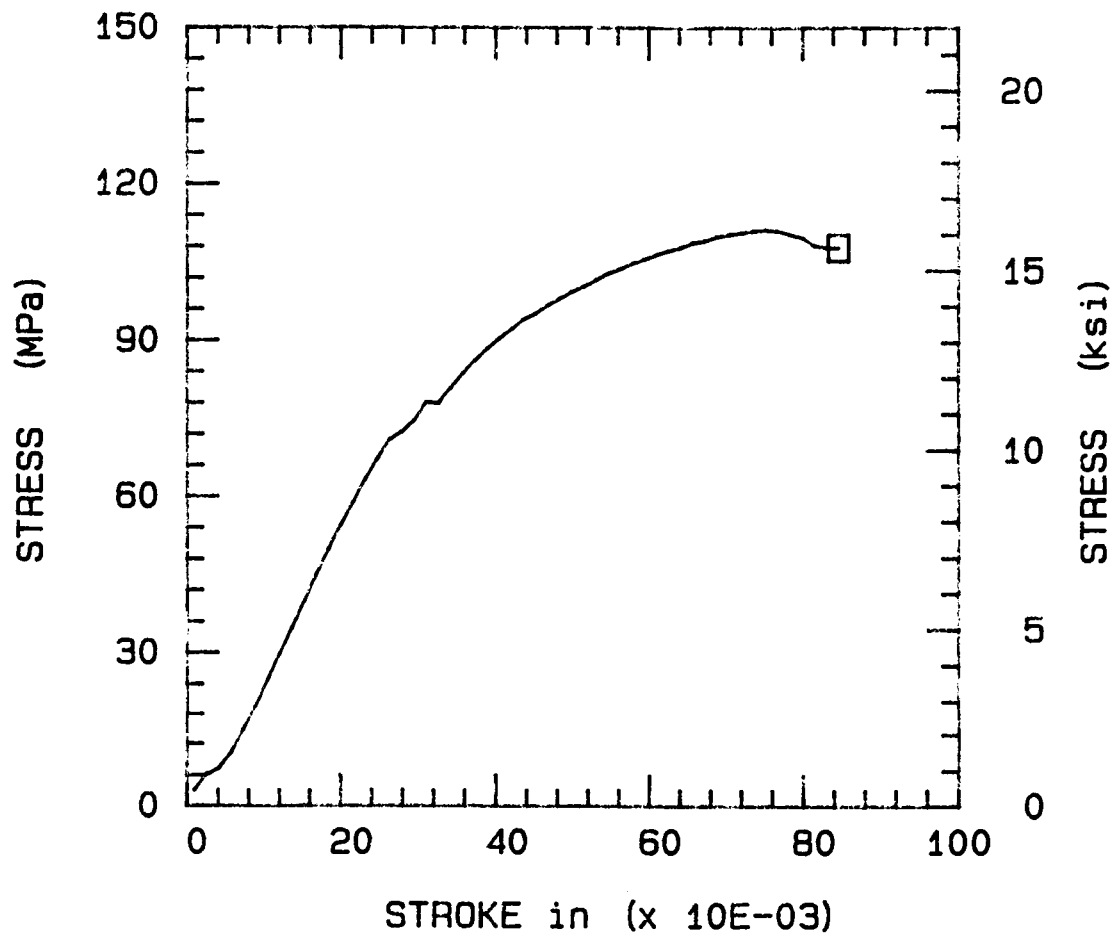
NFIRD1.IOS

ULT. STRESS = 16.140 ksi

TEMP = 24.0 DEG. C MOD = 0.863 Msi

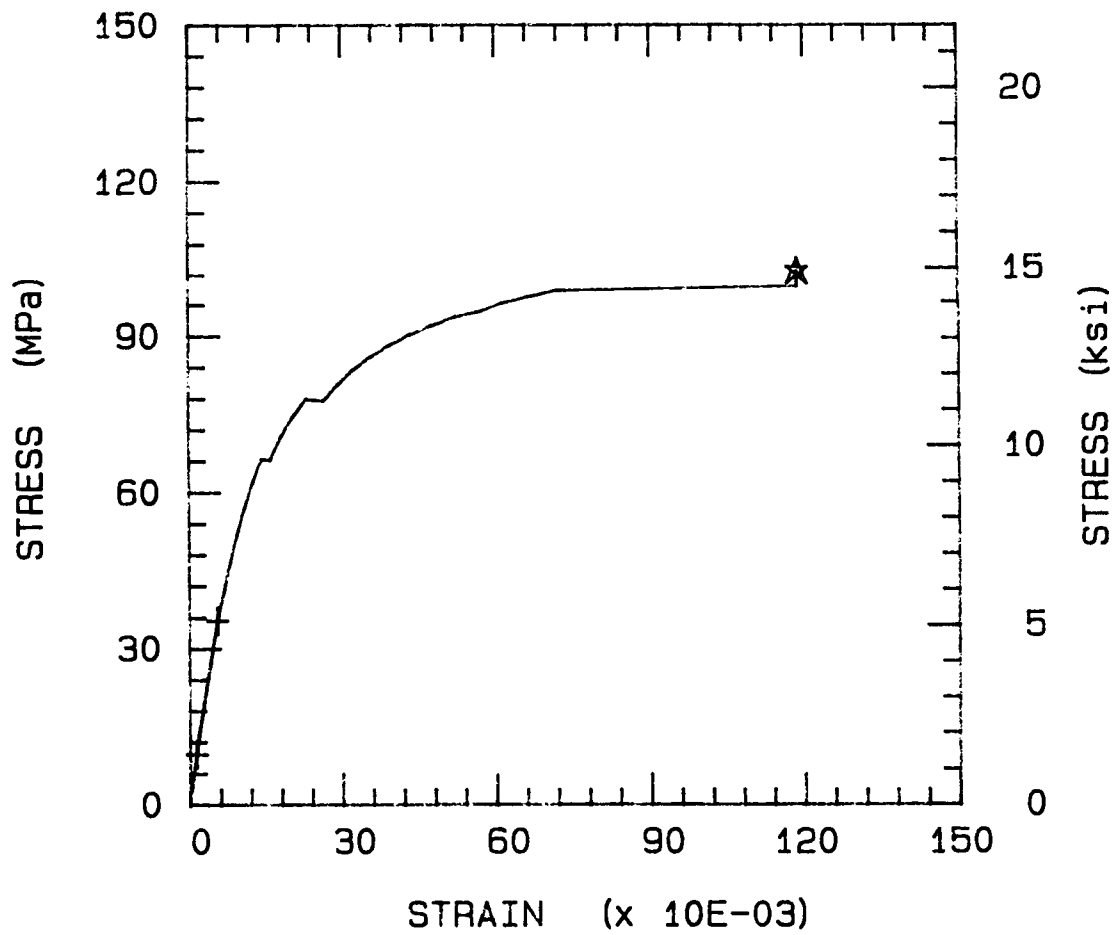


NFIRD1.IOS

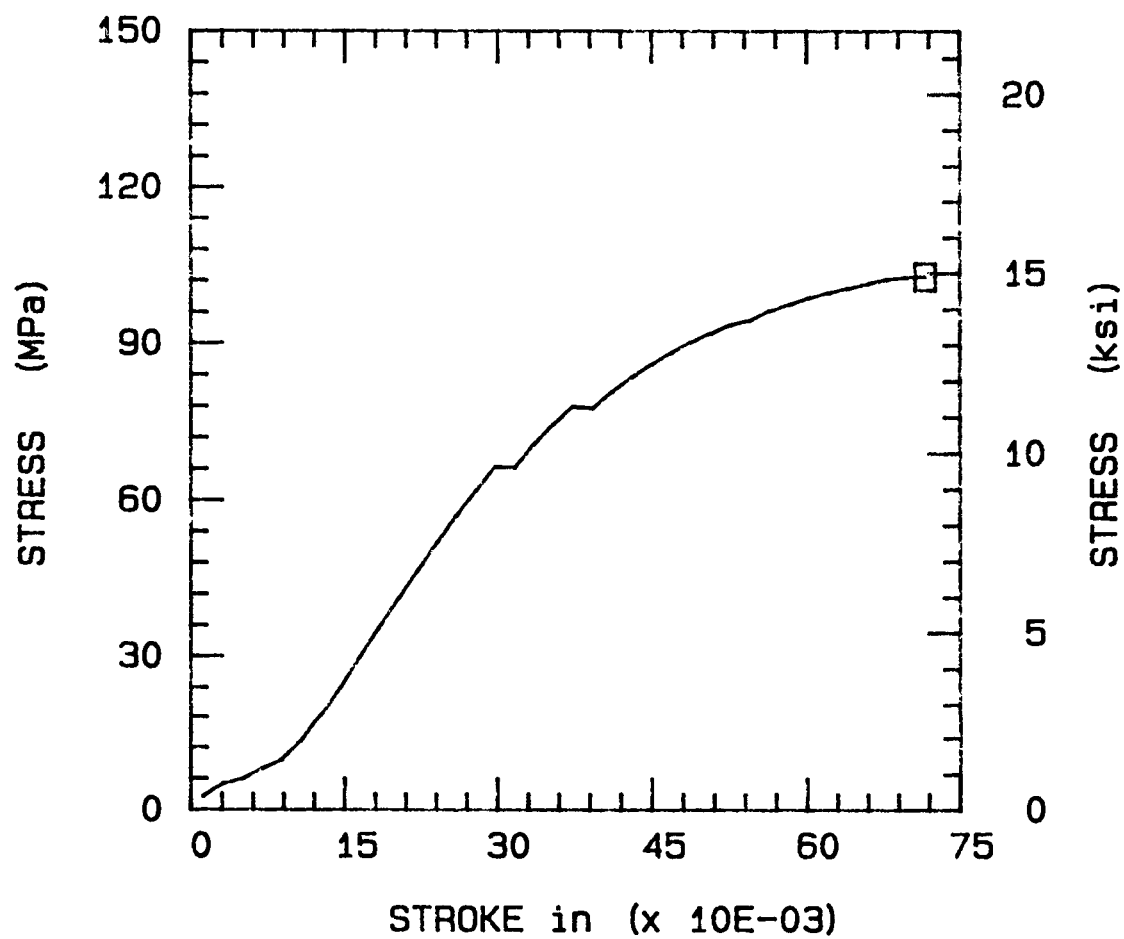


NFIRD2.IOS

ULT. STRESS = 14.910 ksi
TEMP = 24.0 DEG. C MOD = 0.873 Msi



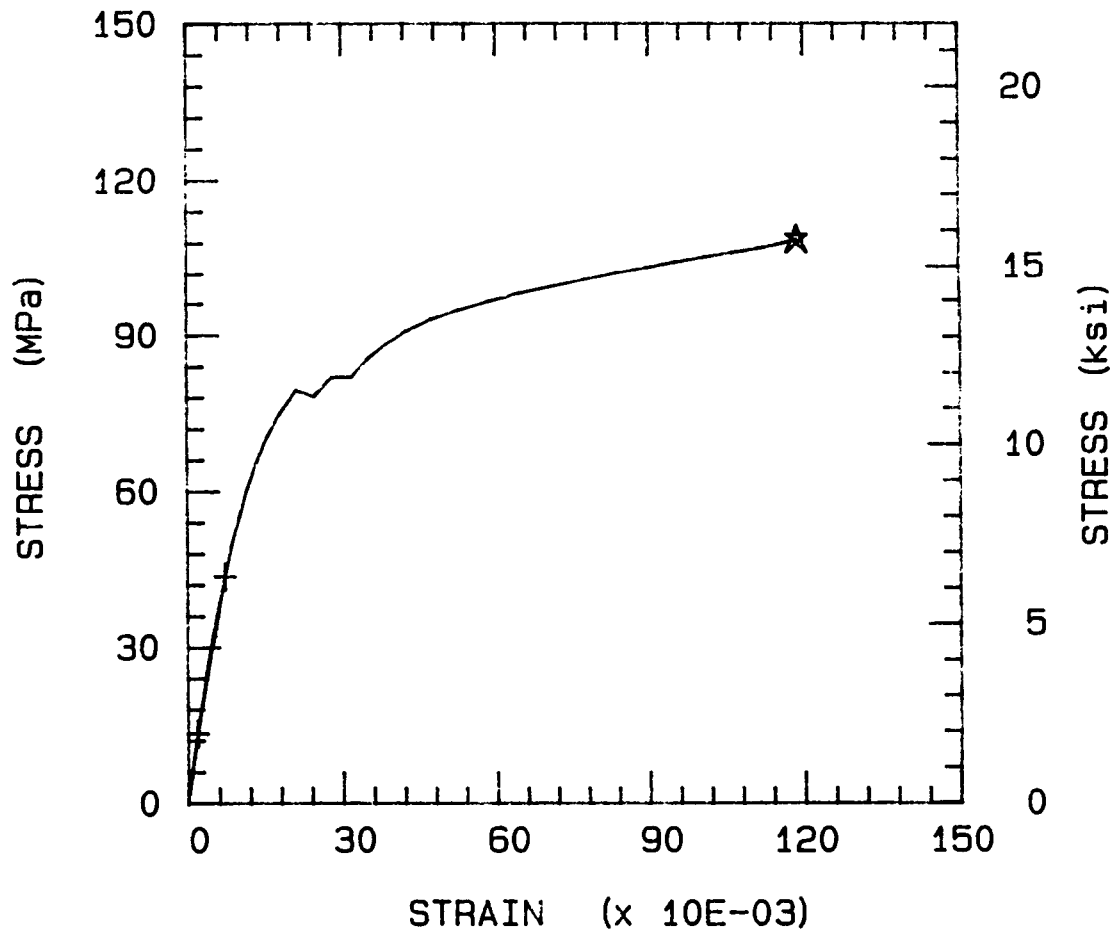
NFIRD2.IOS



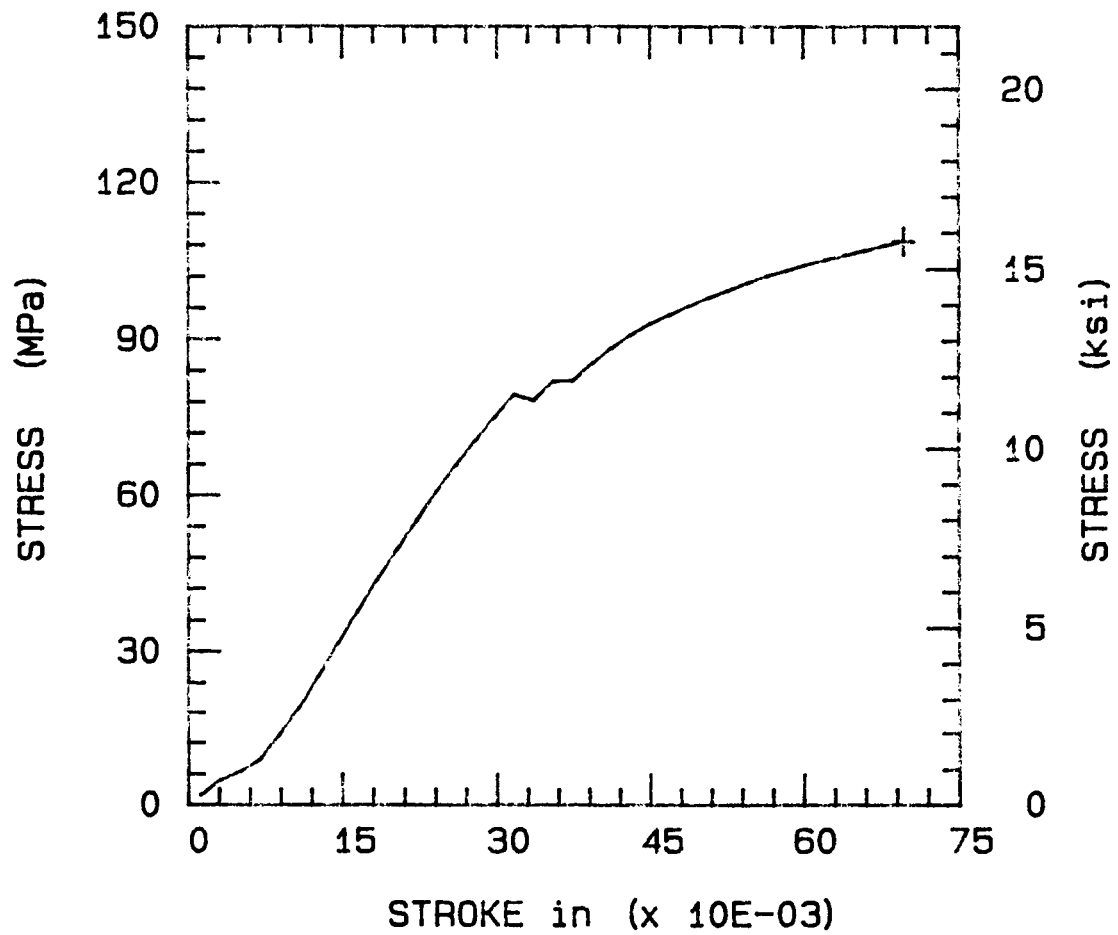
NFIRD3.IOS

ULT. STRESS = 15.770 ksi

TEMP = 24.0 DEG. C MOD = 0.828 Msi



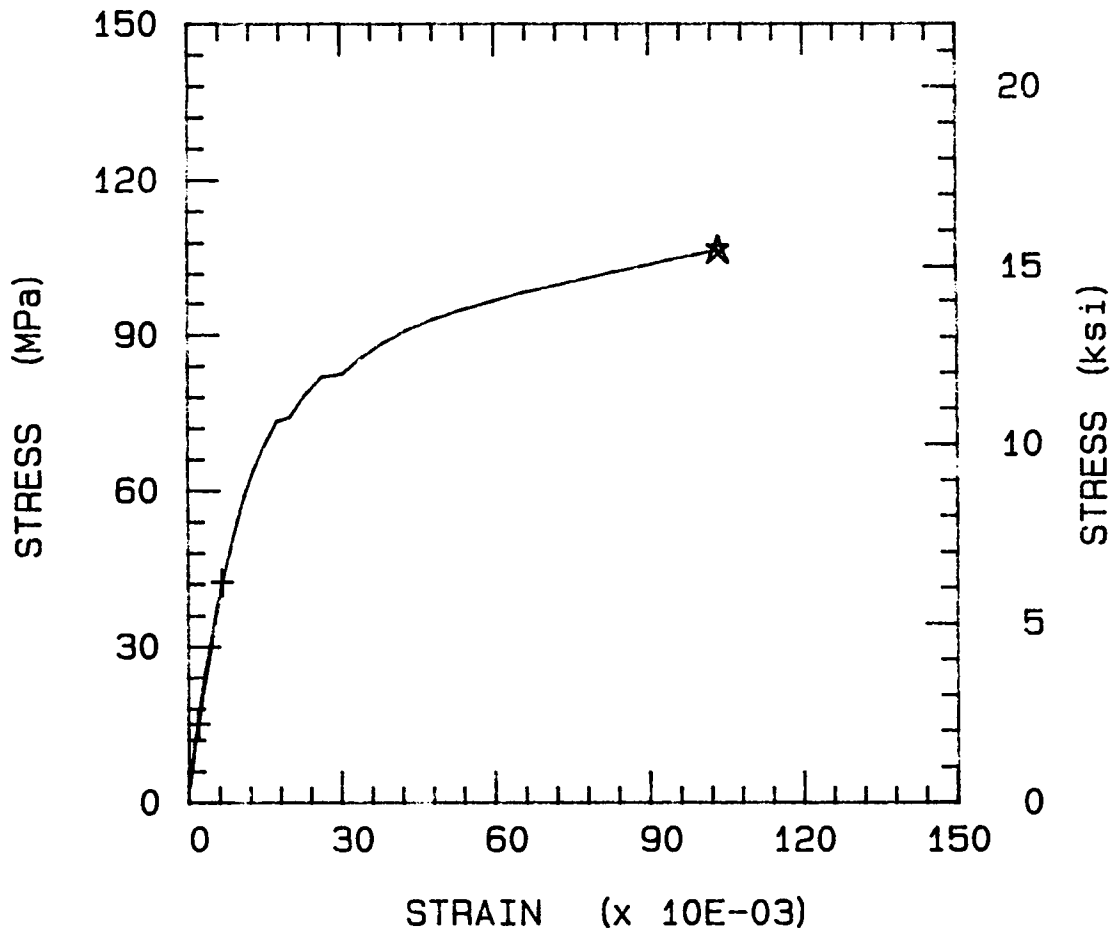
NFIRD3.IOS



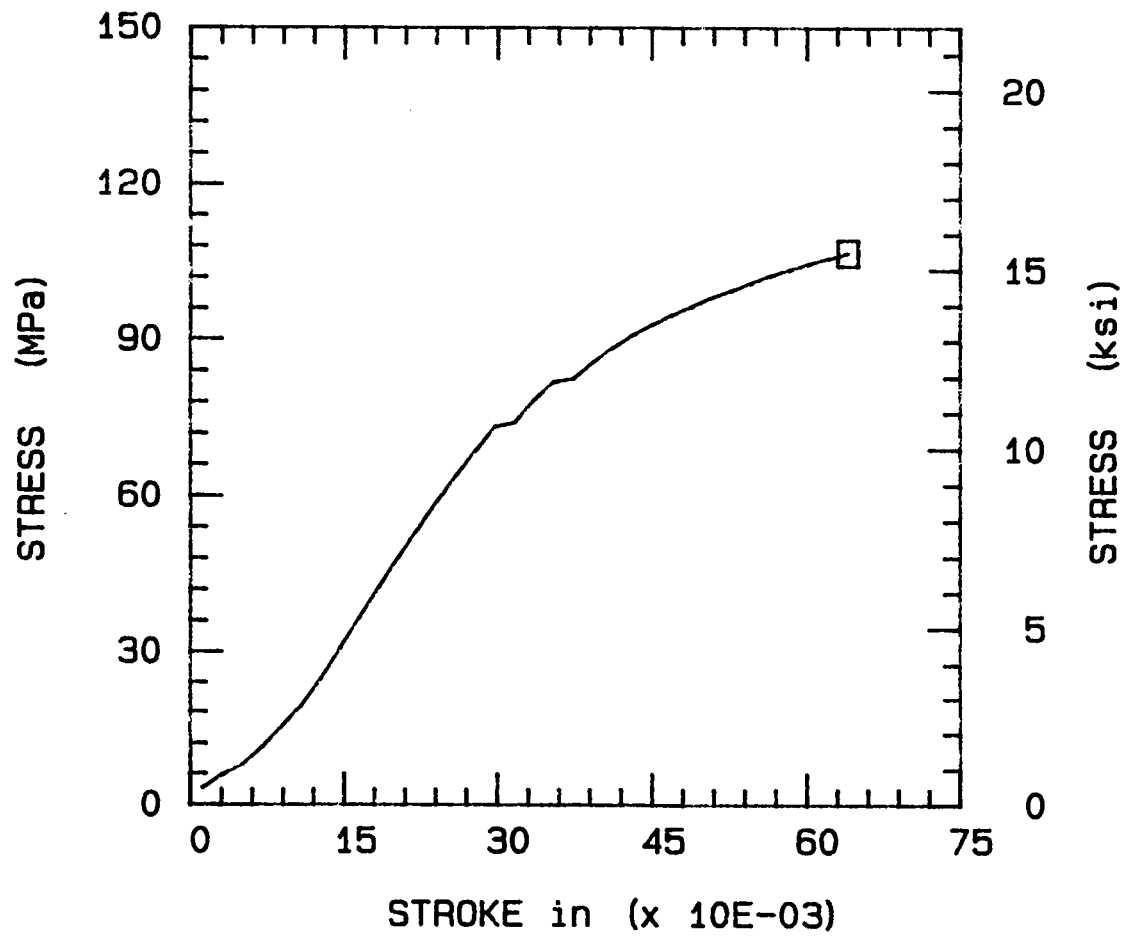
NFIRD4.IOS

ULT. STRESS = 15.480 ksi

TEMP = 24.0 DEG. C MOD = 0.831 Msi



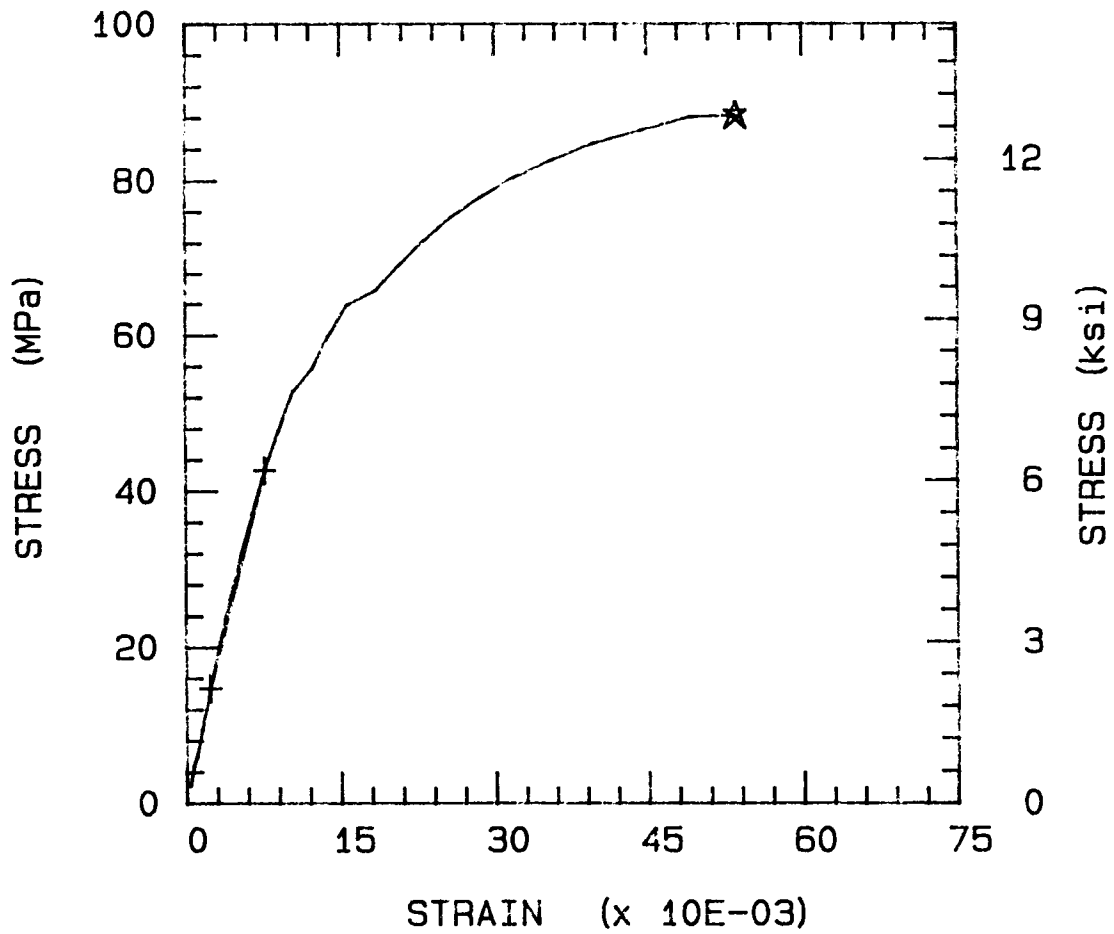
NFIRD4.IOS



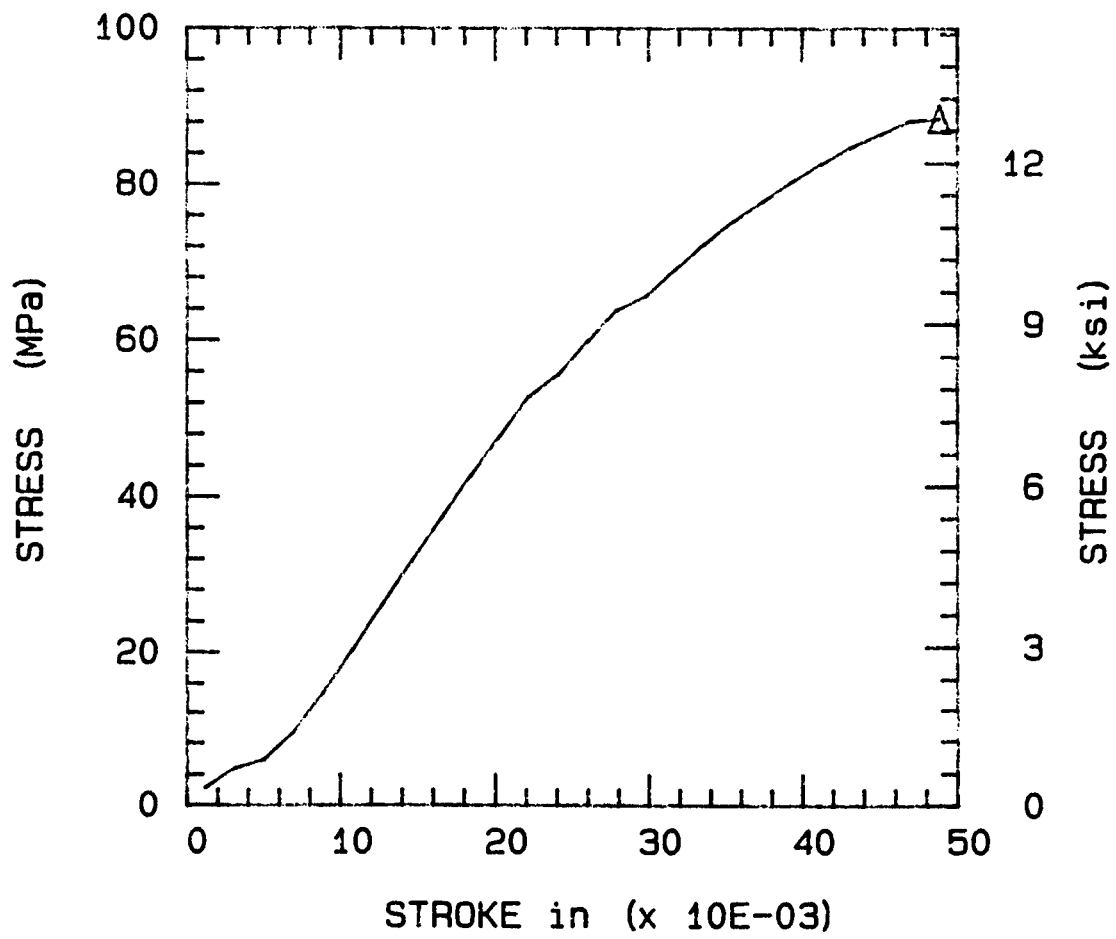
NFIRD5.IOS

ULT. STRESS = 12.820 ksi

TEMP = 24.0 DEG. C MOD = 0.756 Msi



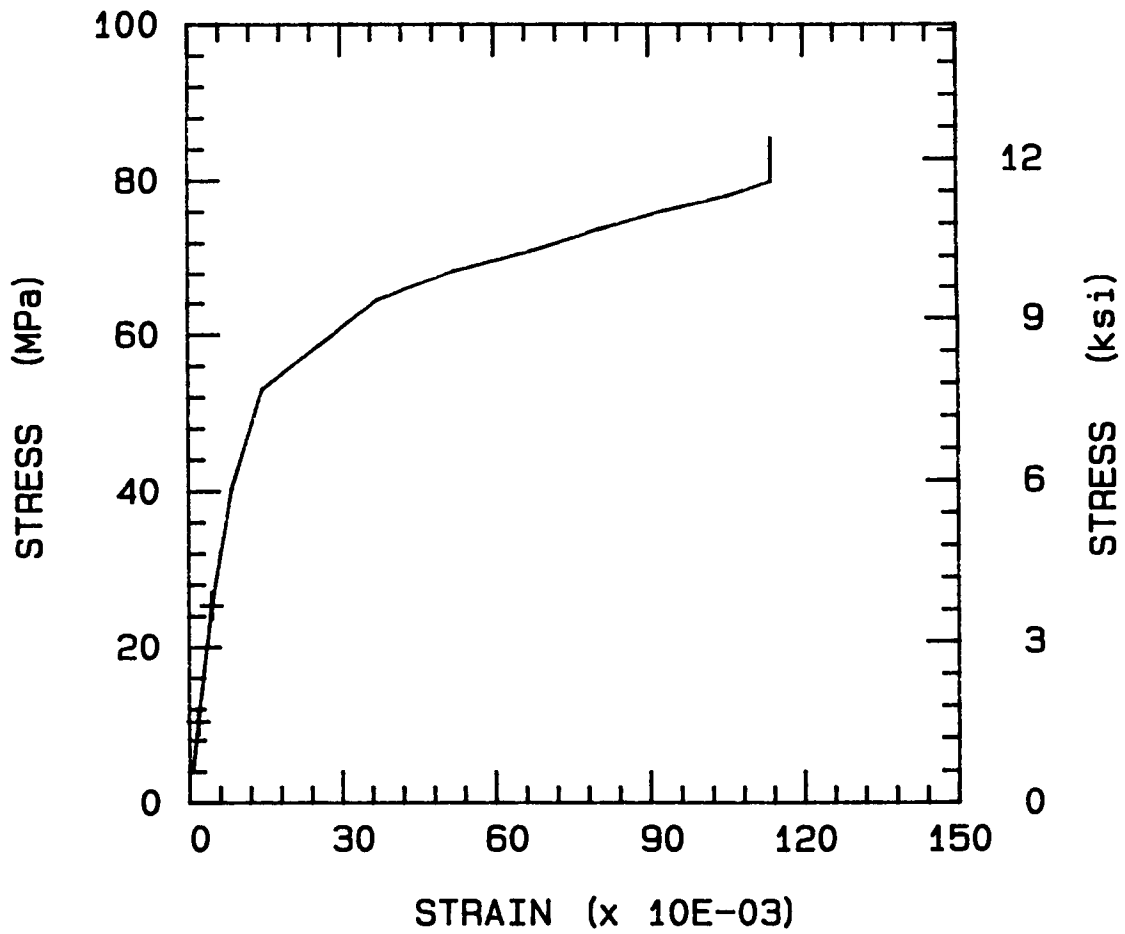
NFIRD5.IOS



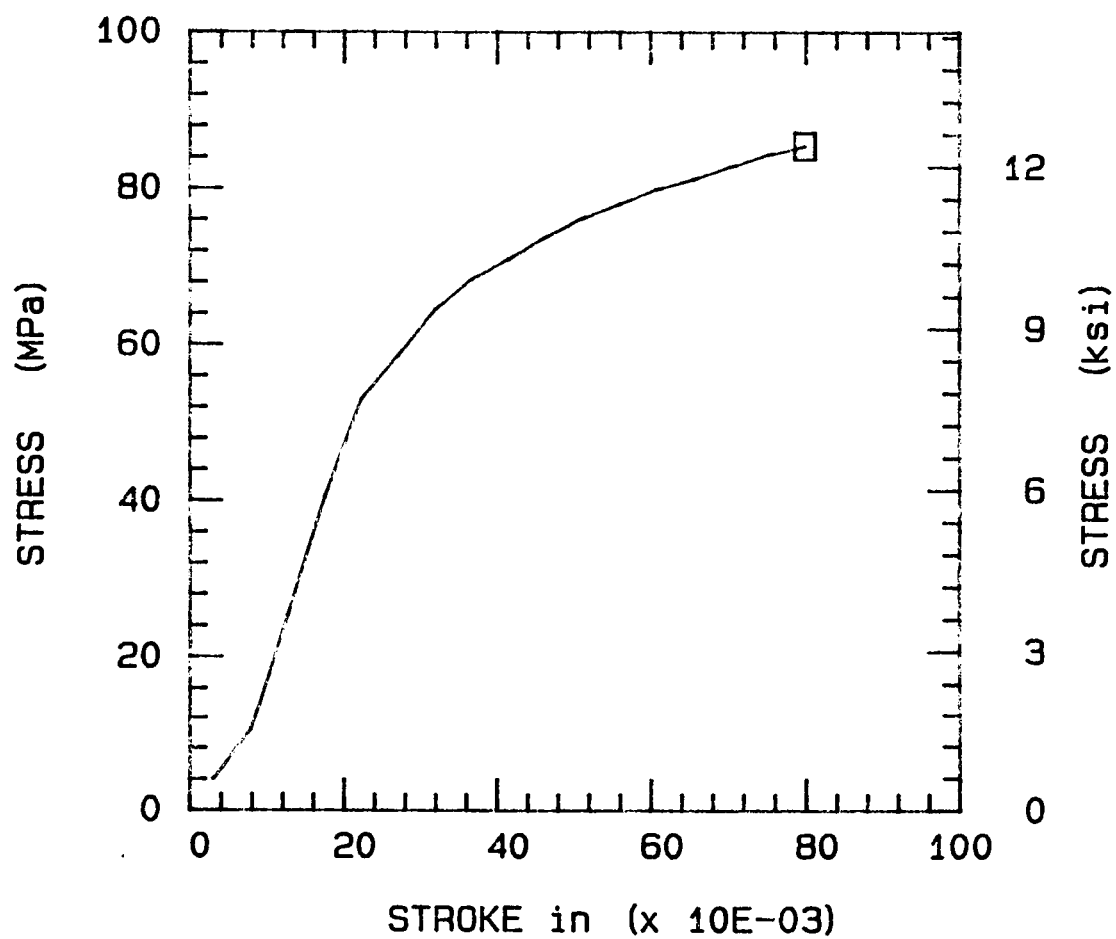
NFIHD1.IOS

ULT. STRESS = 12.390 ksi

TEMP = 82.0 DEG. C MOD = 0.811 Msi



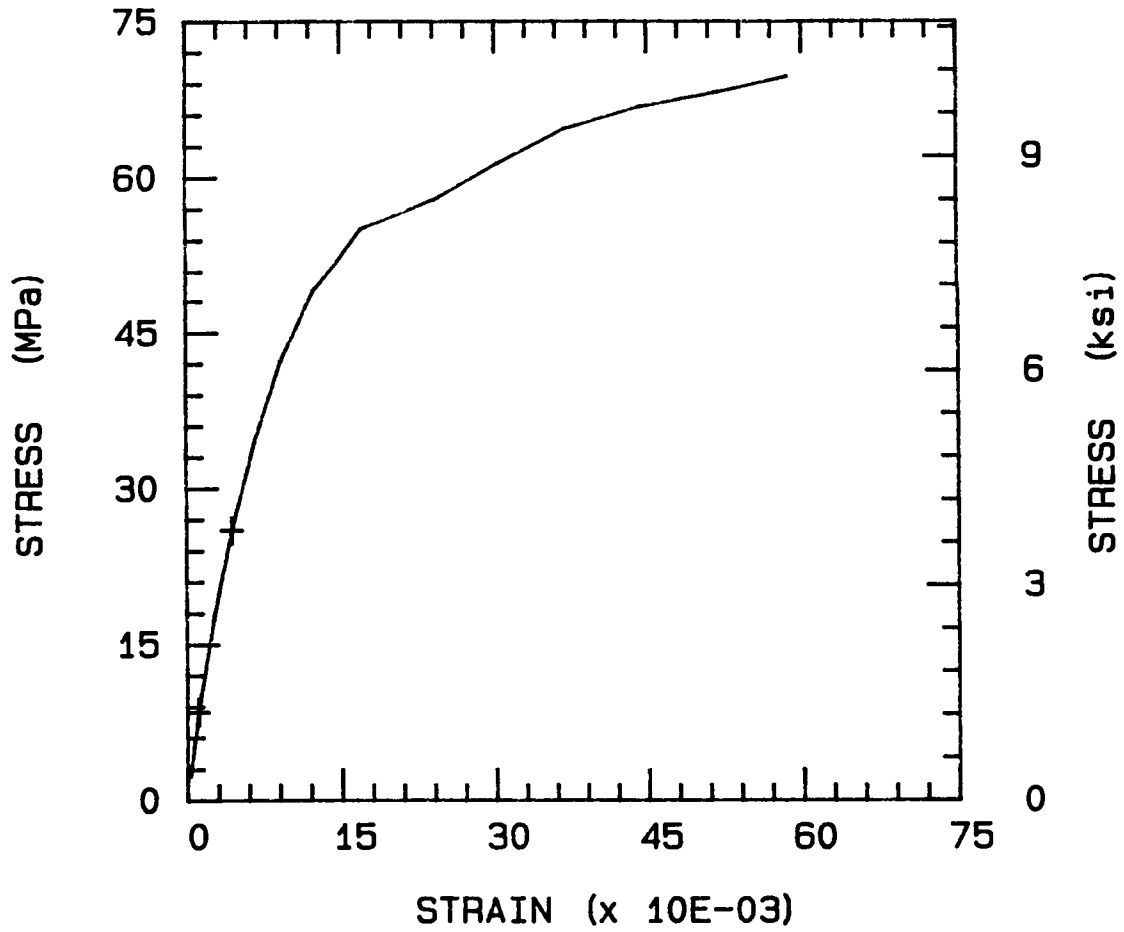
NFIHD1.IOS



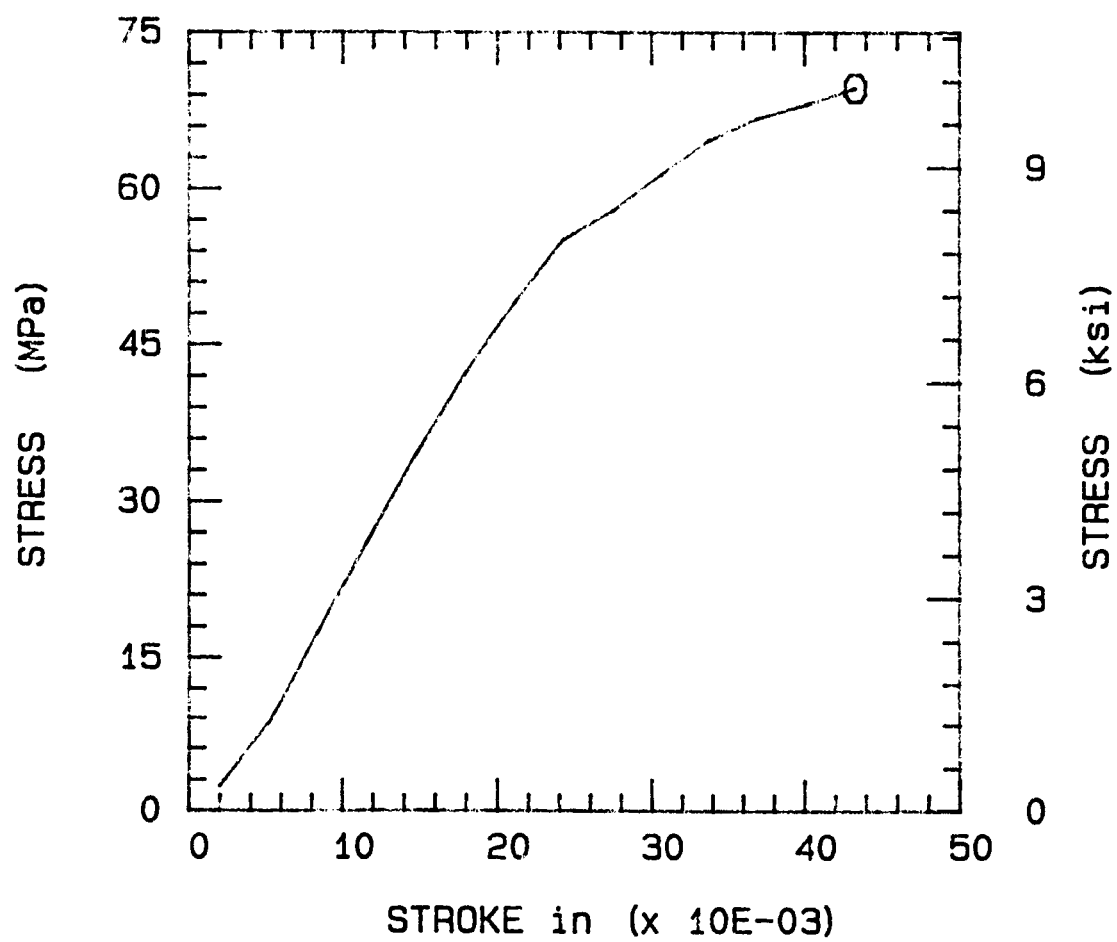
NFIHD2.IOS

ULT. STRESS = 10.110 ksi

TEMP = 82.0 DEG. C MOD = 0.772 Msi



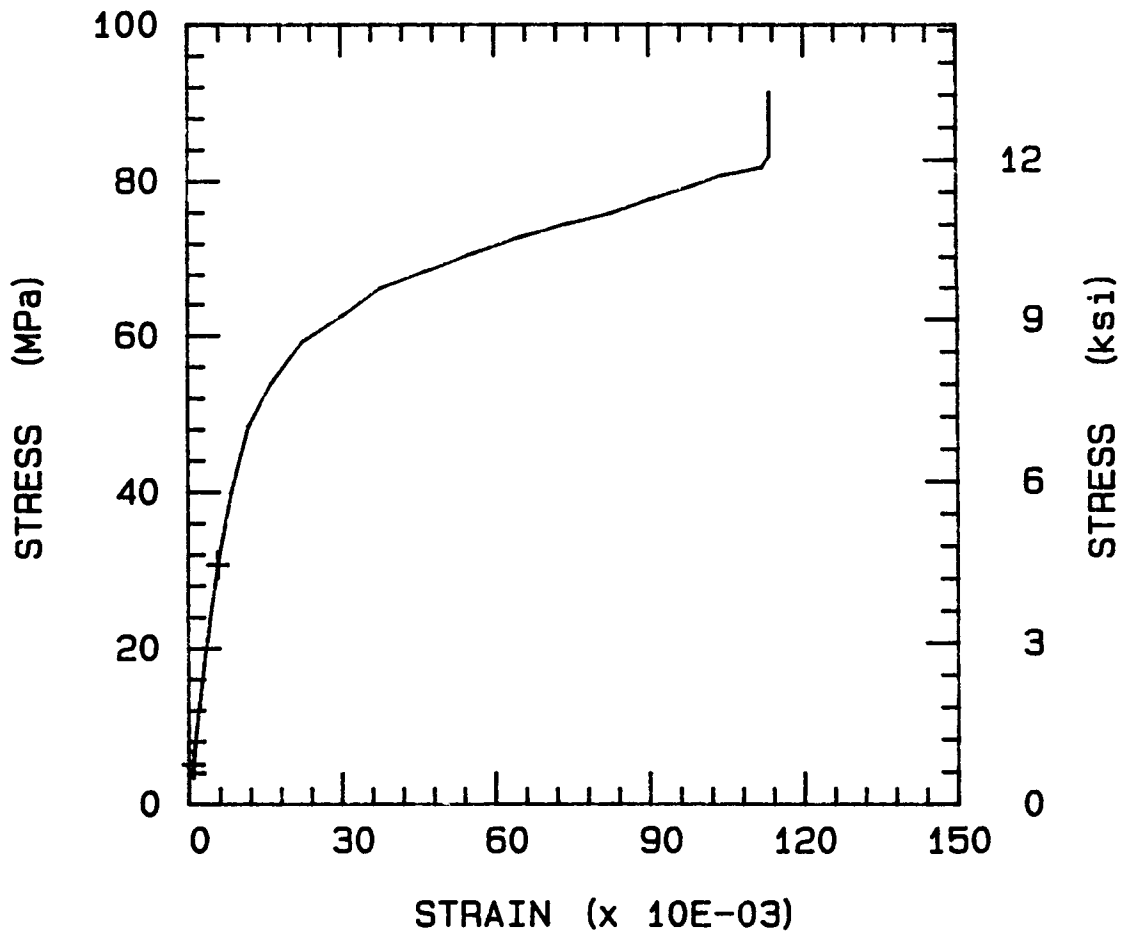
NFIHD2.IOS



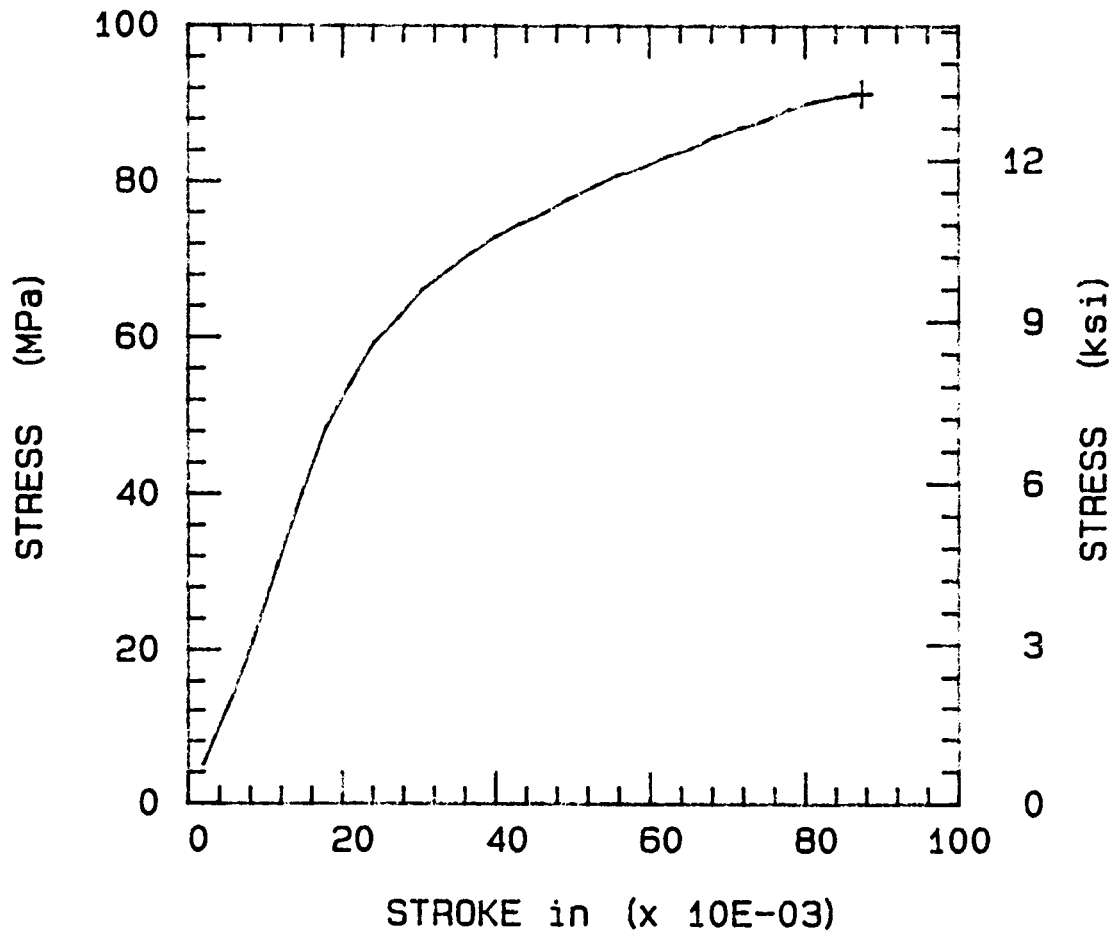
NFIHD3.IOS

ULT. STRESS = 13.250 ksi

TEMP = 82.0 DEG. C MOD = 0.764 Msi



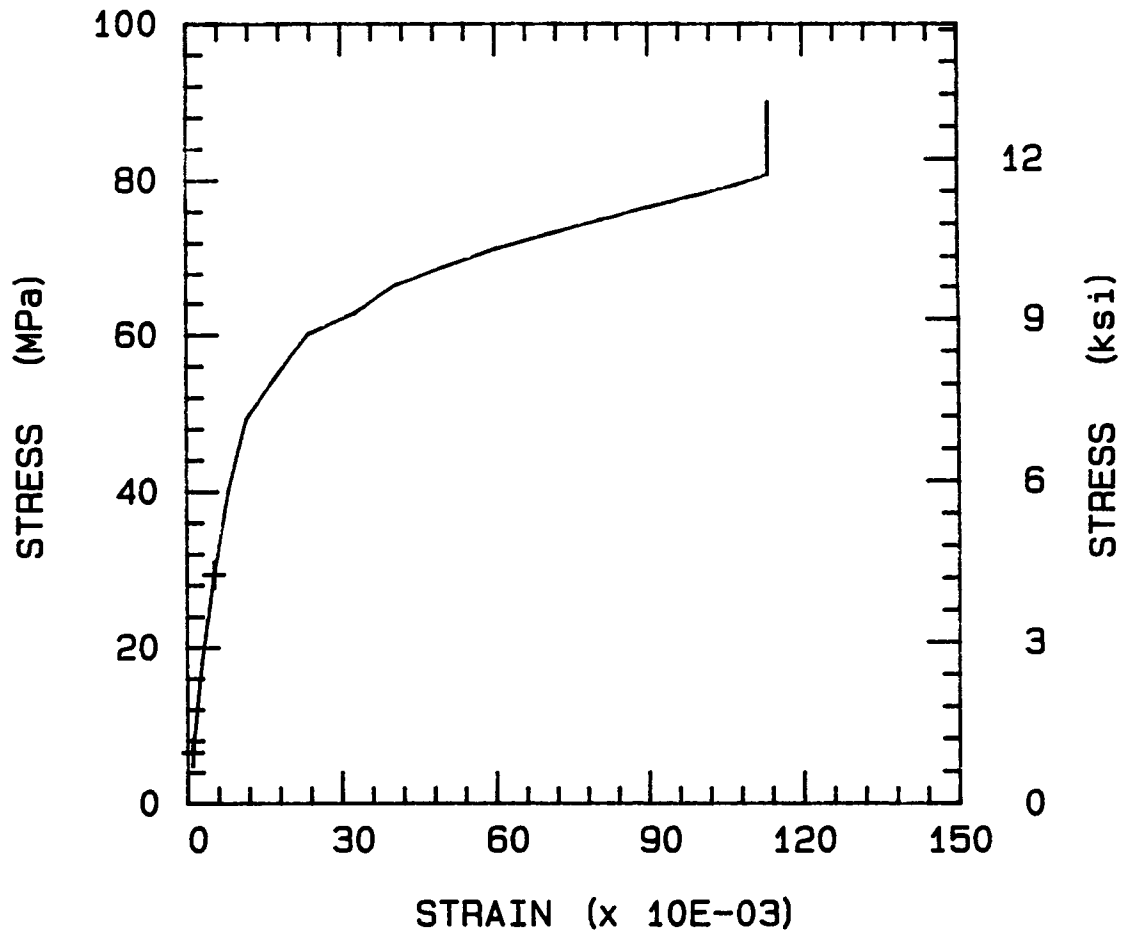
NFIHD3.IOS



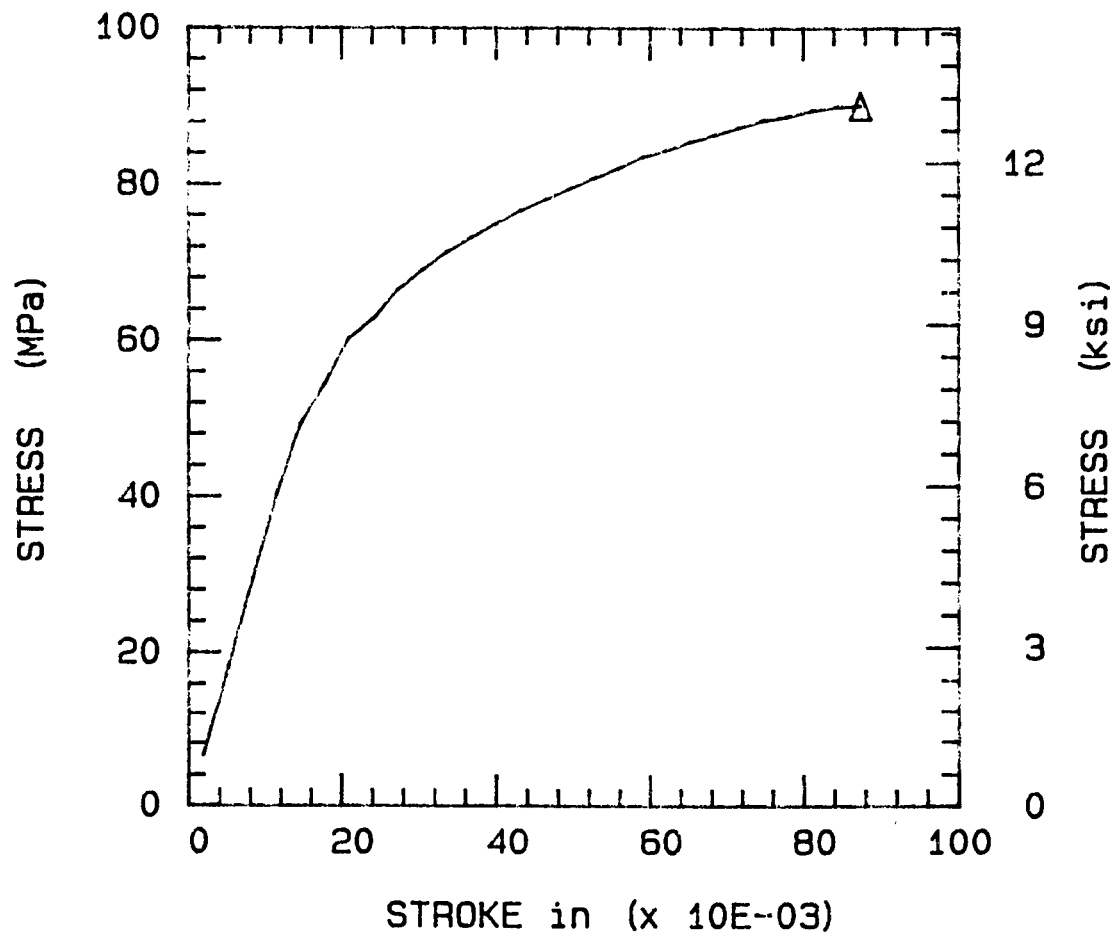
NFIHD4.IOS

ULT. STRESS = 13.060 ksi

TEMP = 82.0 DEG. C MOD = 0.780 Msi



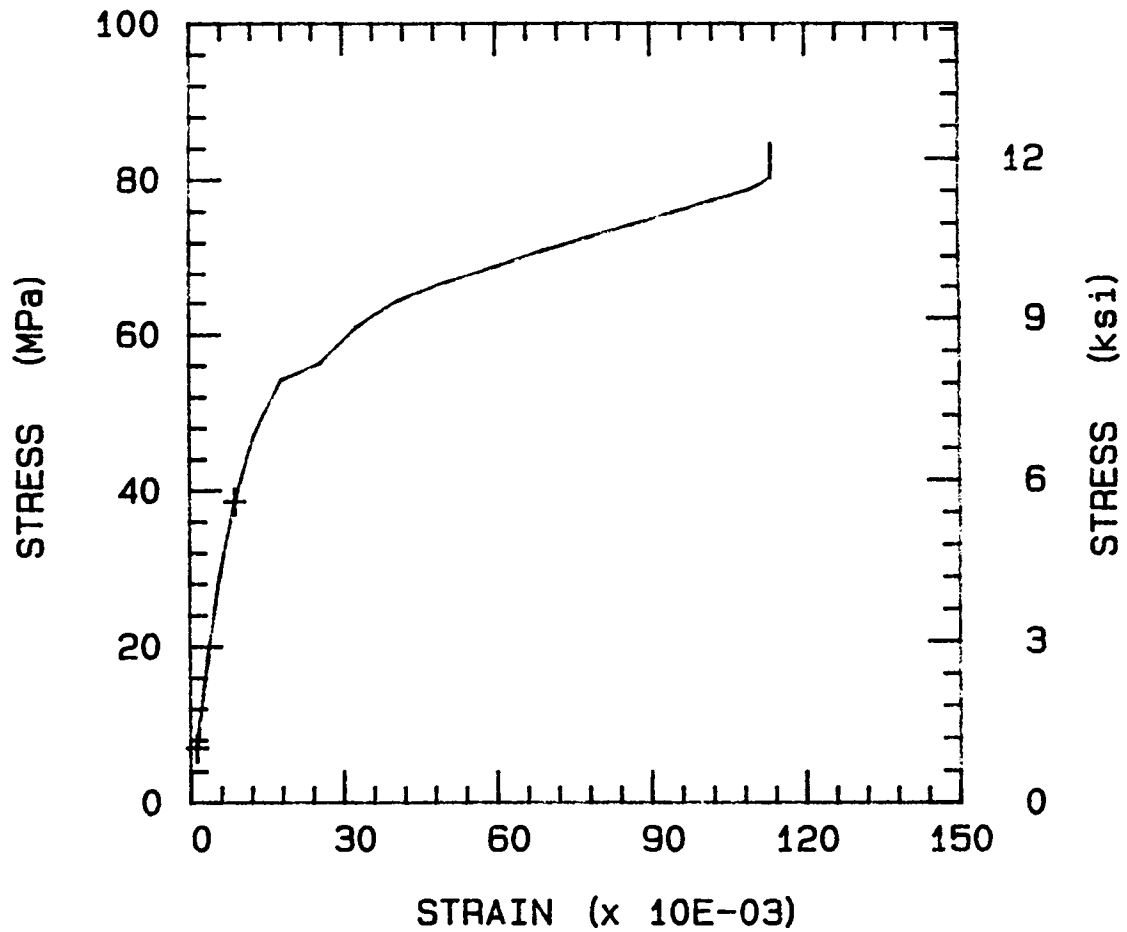
NFIHD4.IOS



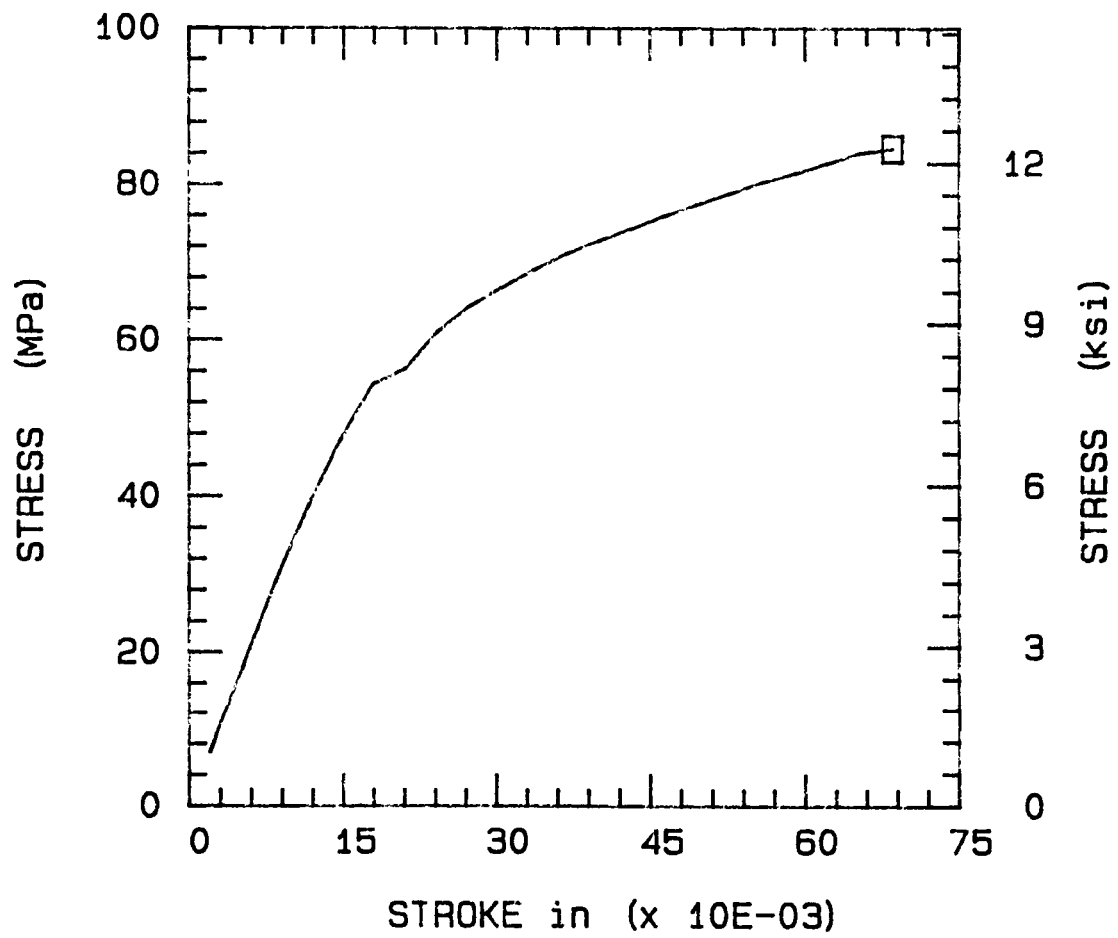
NFIHD5.IOS

ULT. STRESS = 12.270 ksi

TEMP = 82.0 DEG. C MOD = 0.615 Msi



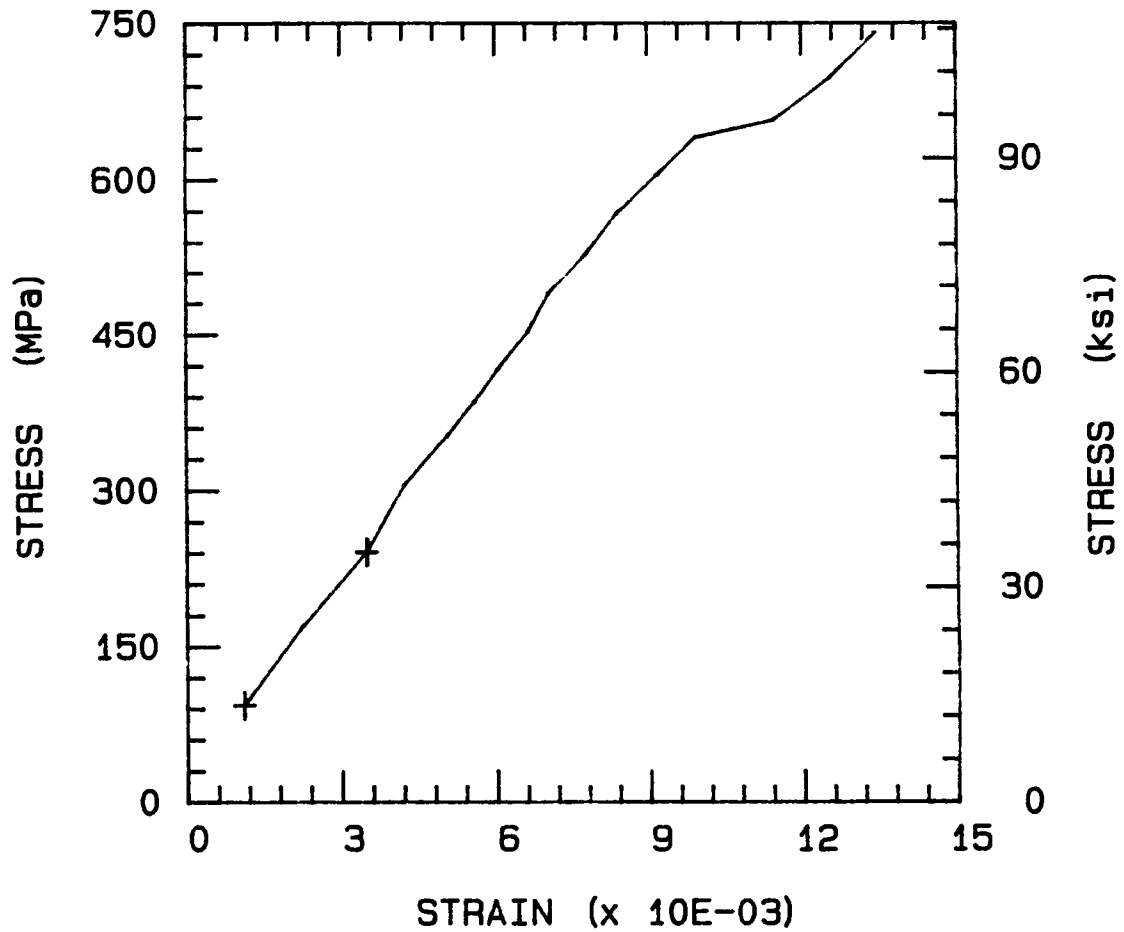
NFIHD5.IOS



NLDTD1.EDT

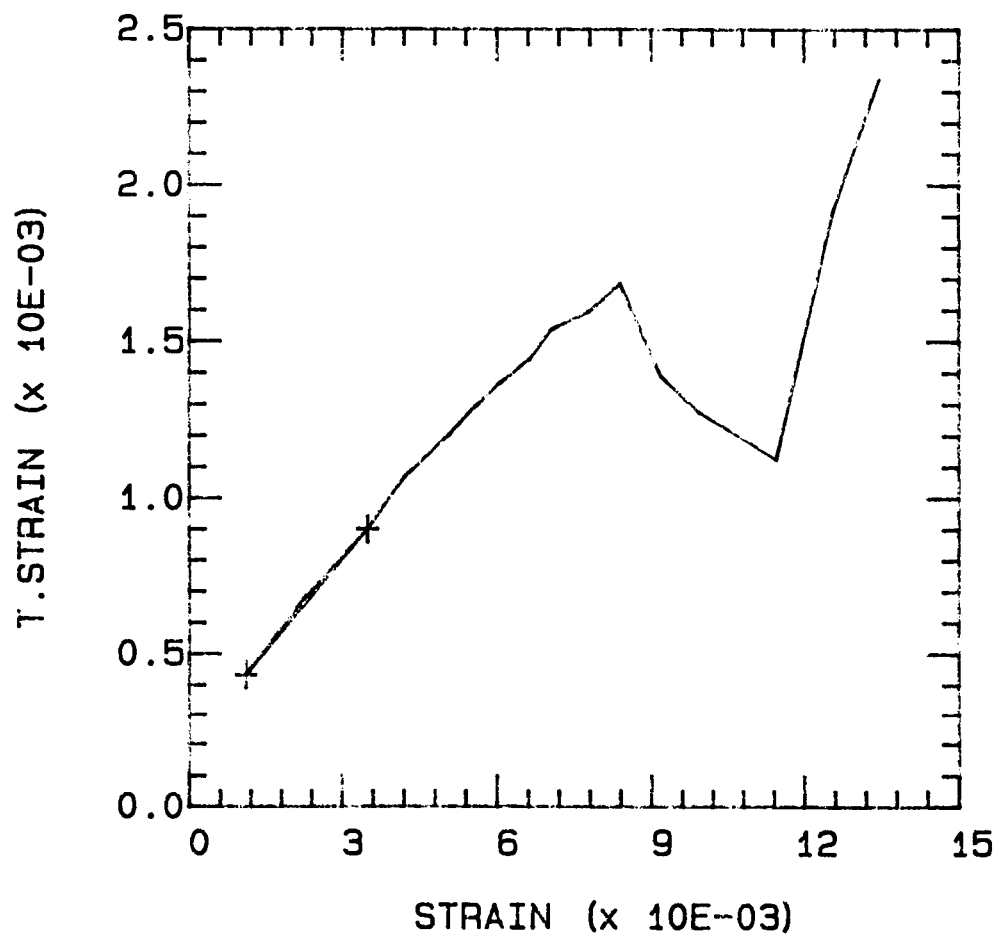
ULT. STRESS = 107.500 ksi

TEMP = 23.0 DEG. C MOD = 8.969 Msi



NLDTD1.EDT

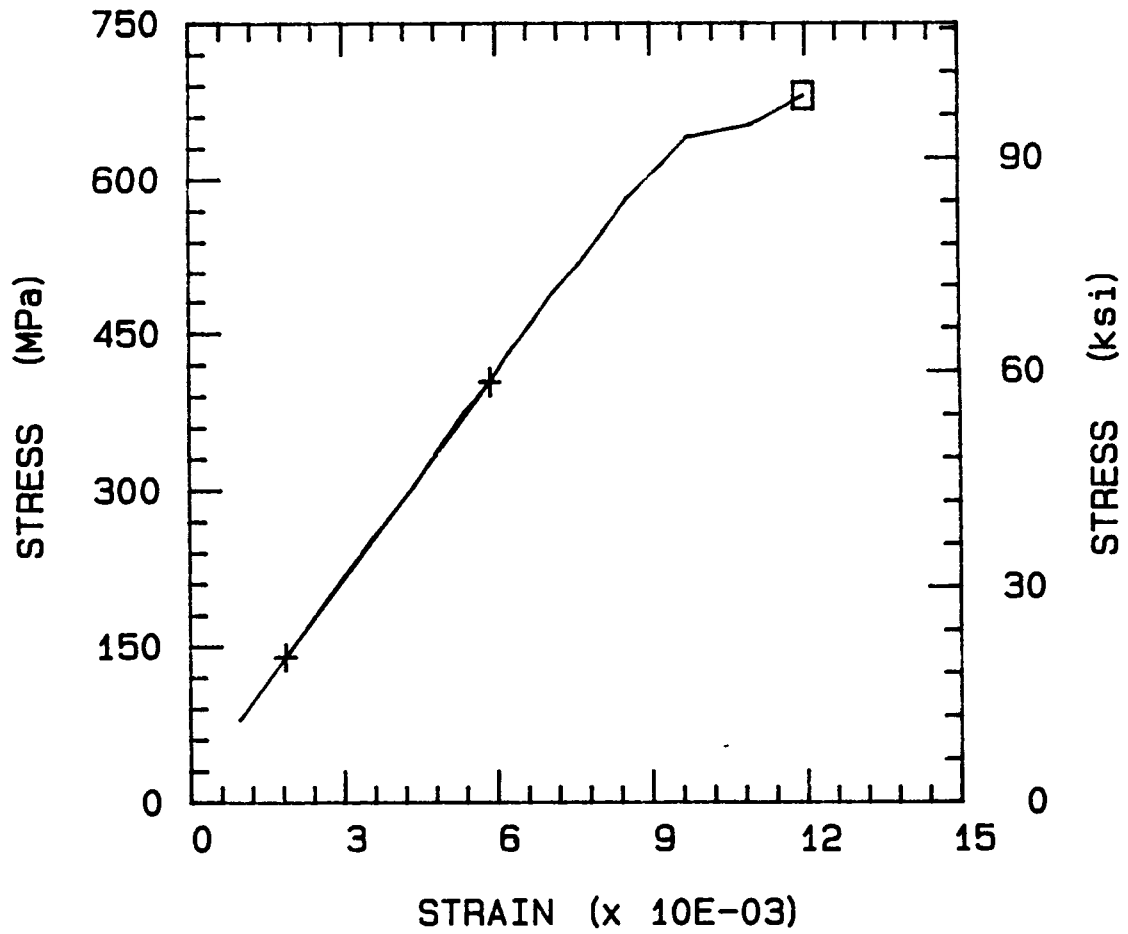
ULT. STRESS = 107.500 ksi
TEMP = 23.0 DEG. C NU = 0.196



NLDTD2.EDT

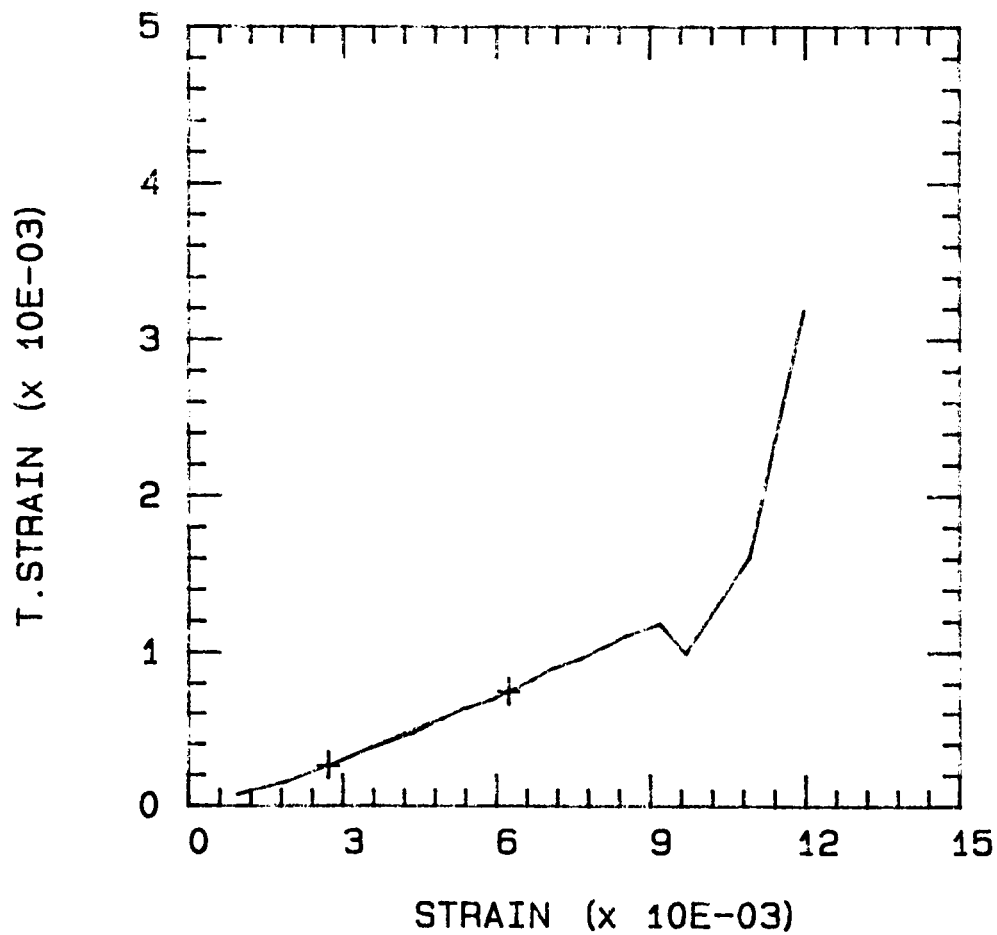
ULT. STRESS = 98.660 ksi

TEMP = 23.0 DEG. C MOD = 9.573 Msi



NLDTD2.EDT

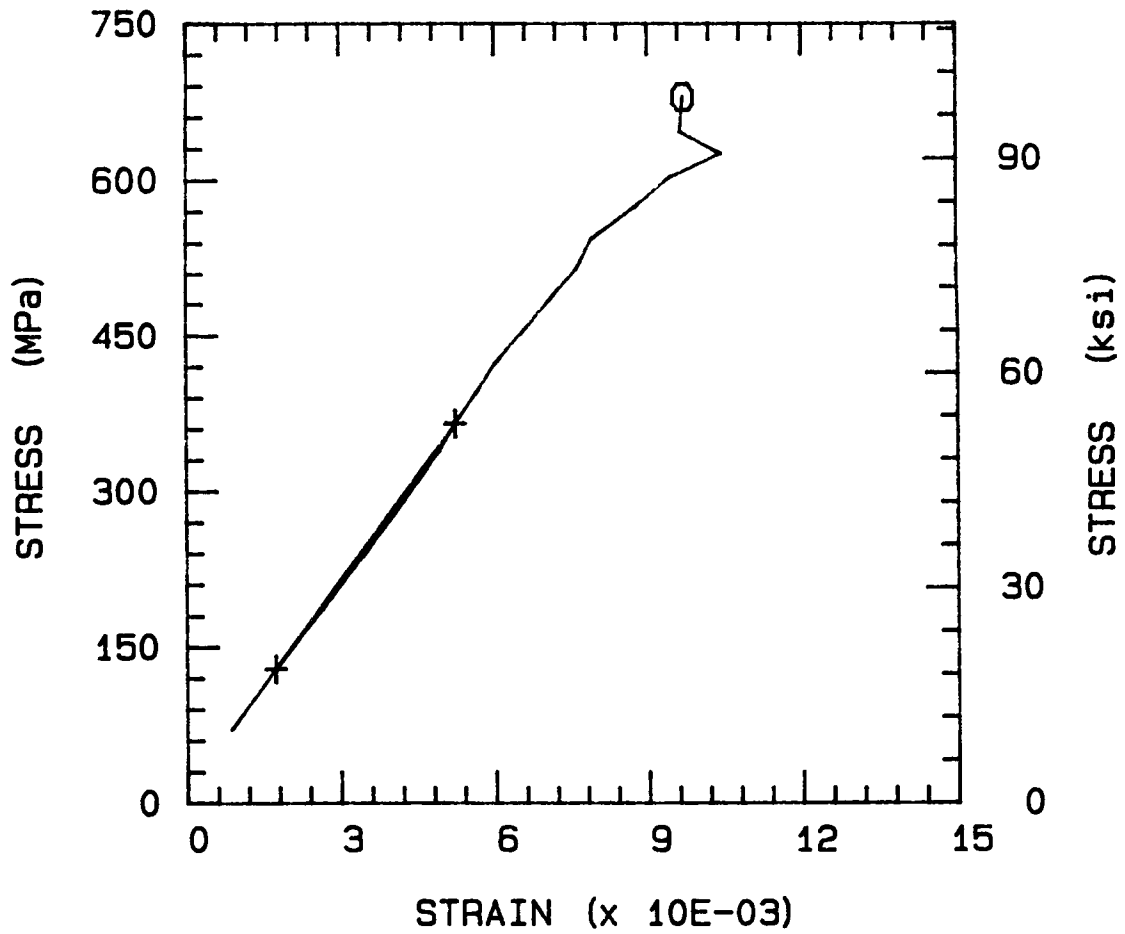
ULT. STRESS = 98.660 ksi
TEMP = 23.0 DEG. C NU = 0.138



NLDTD3.EDT

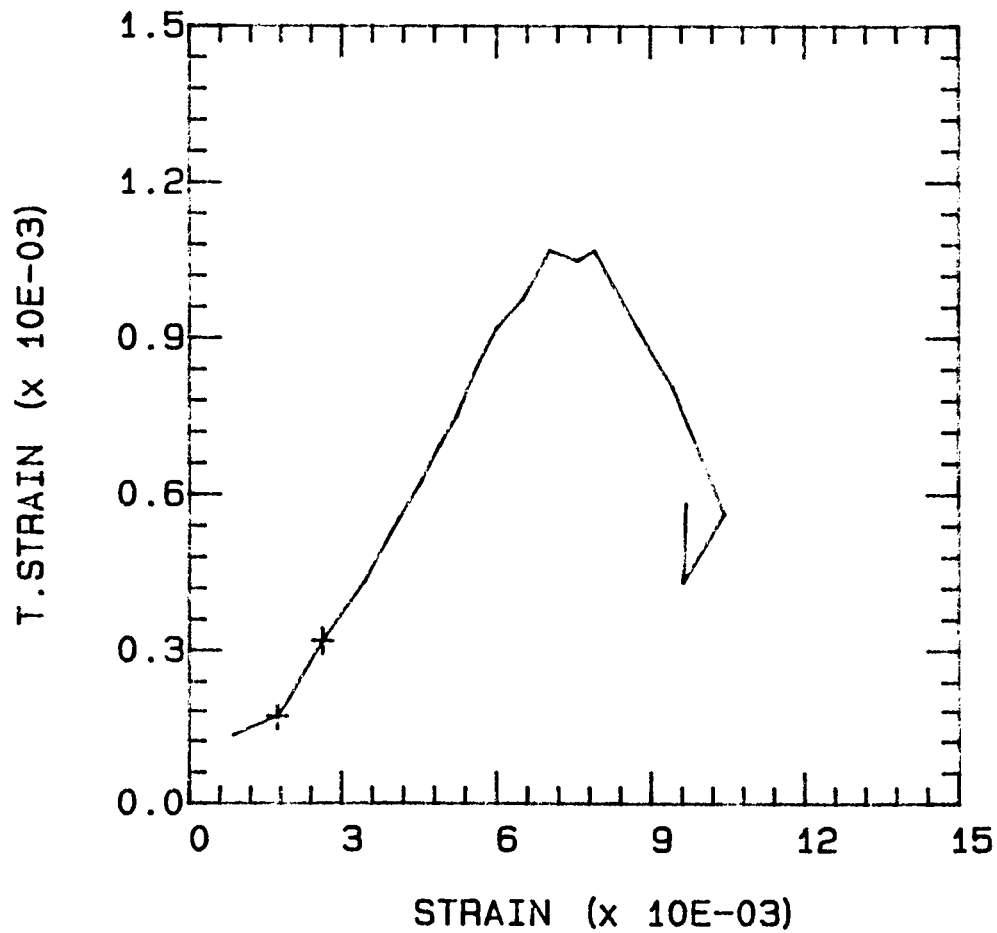
ULT. STRESS = 98.510 ksi

TEMP = 23.0 DEG. C MOD = 9.735 Msi



NLDTD3.EDT

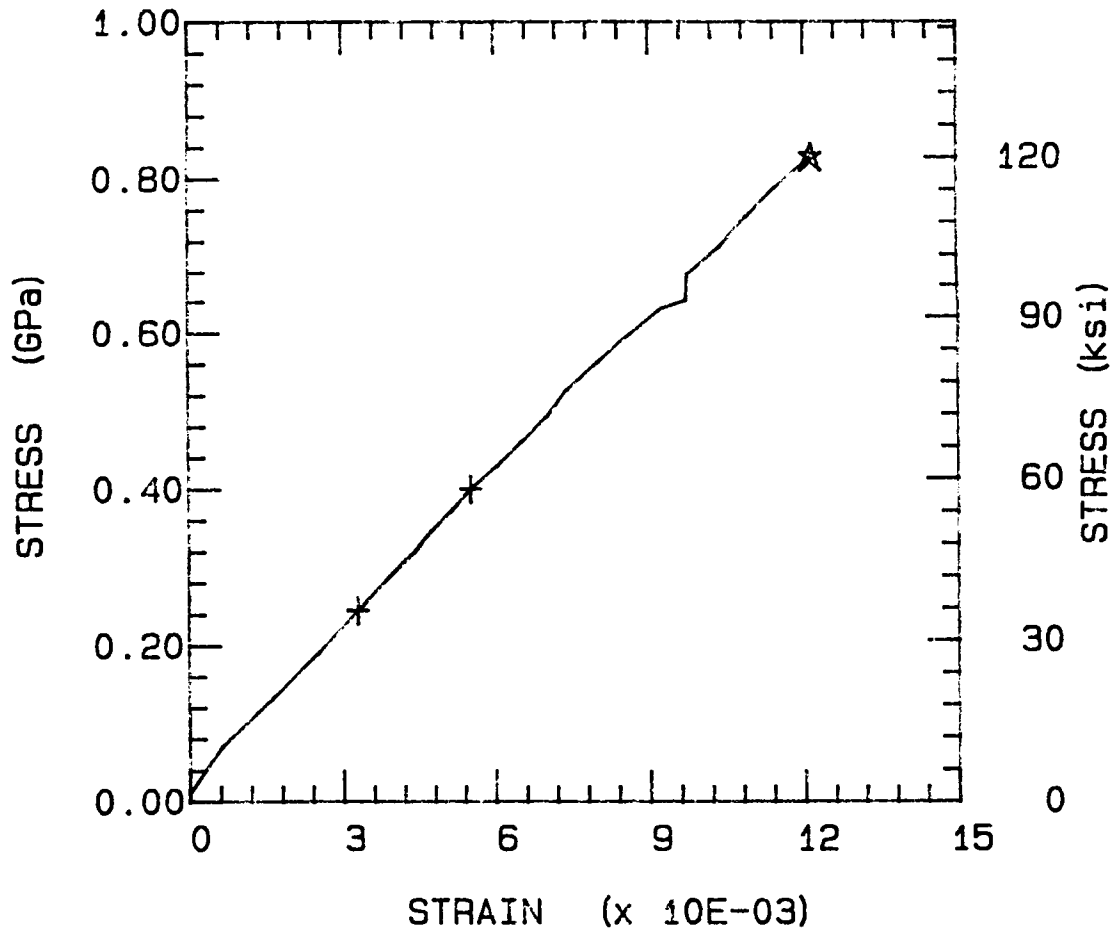
ULT. STRESS = 98.510 ksi
TEMP = 23.0 DEG. C NU = 0.168



NLDTD4.EDT

ULT. STRESS = 120.000 ksi

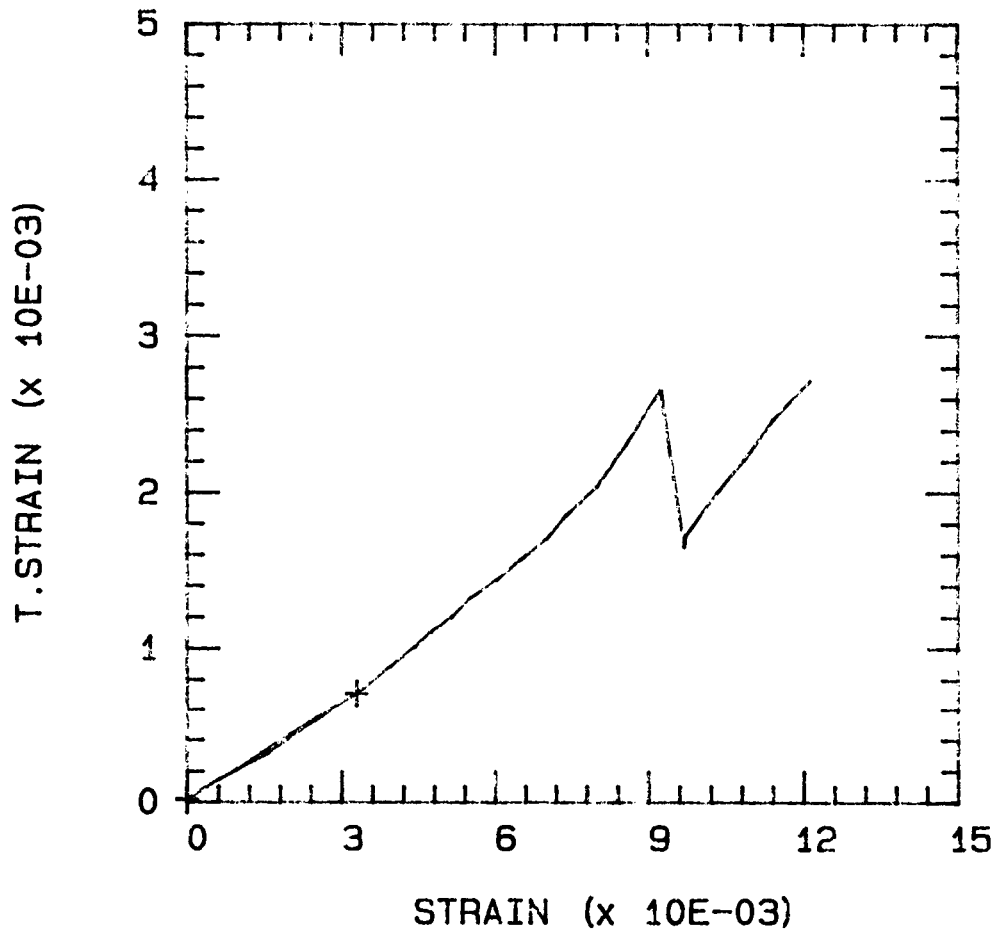
TEMP = 23.0 DEG. C MOD = 10.061 Msi



NLDTD4.EDT

ULT. STRESS = 120.000 ksi

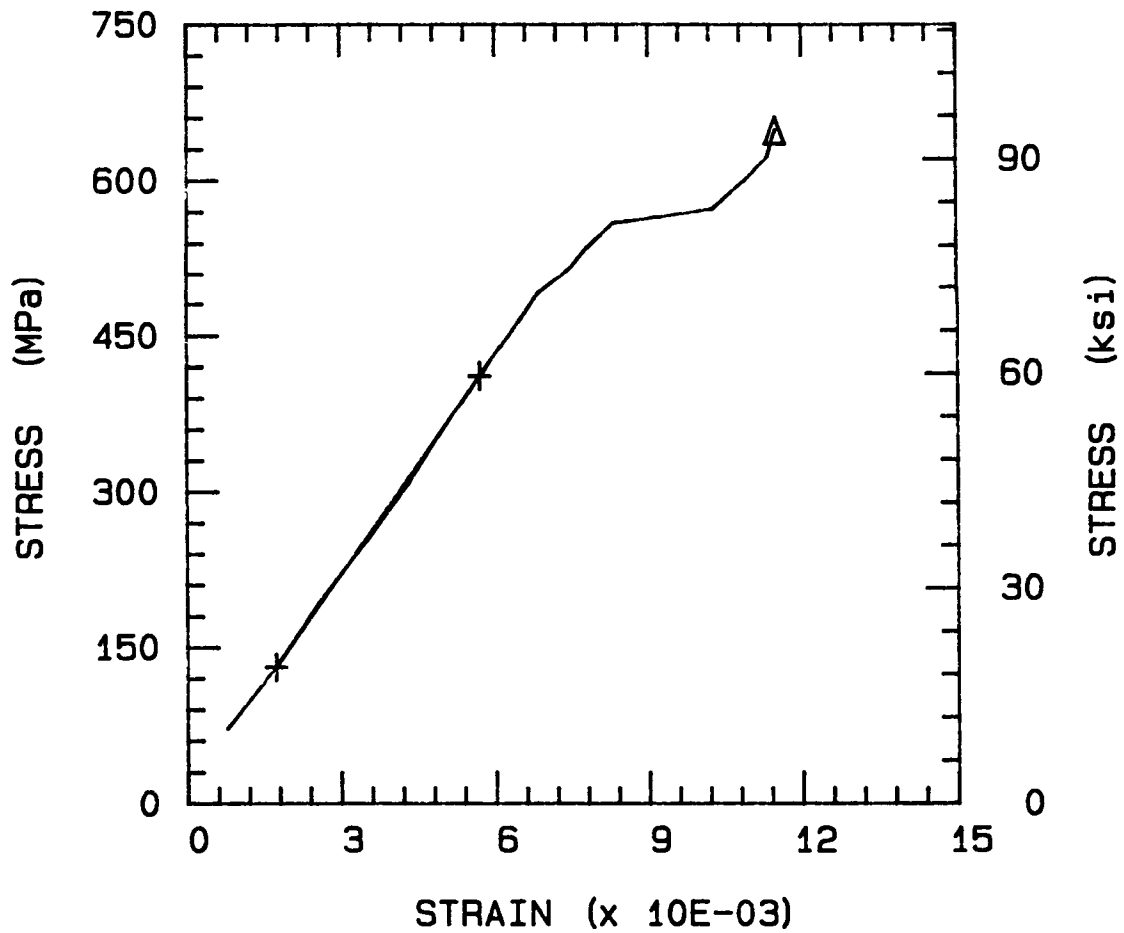
TEMP = 23.0 DEG. C NU = 0.211



NLDTD5.EDT

ULT. STRESS = 93.990 ksi

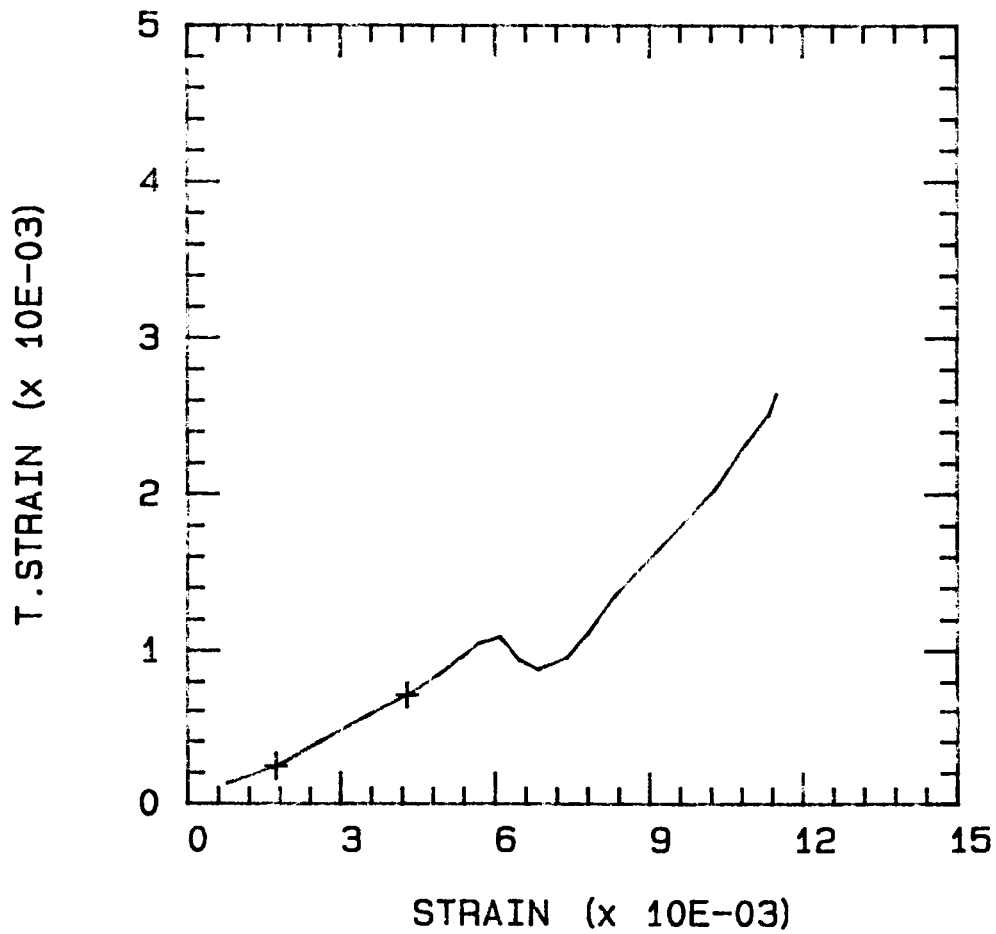
TEMP = 23.0 DEG. C MOD = 10.191 Msi



NLDTD5.EDT

ULT. STRESS = 93.990 ksi

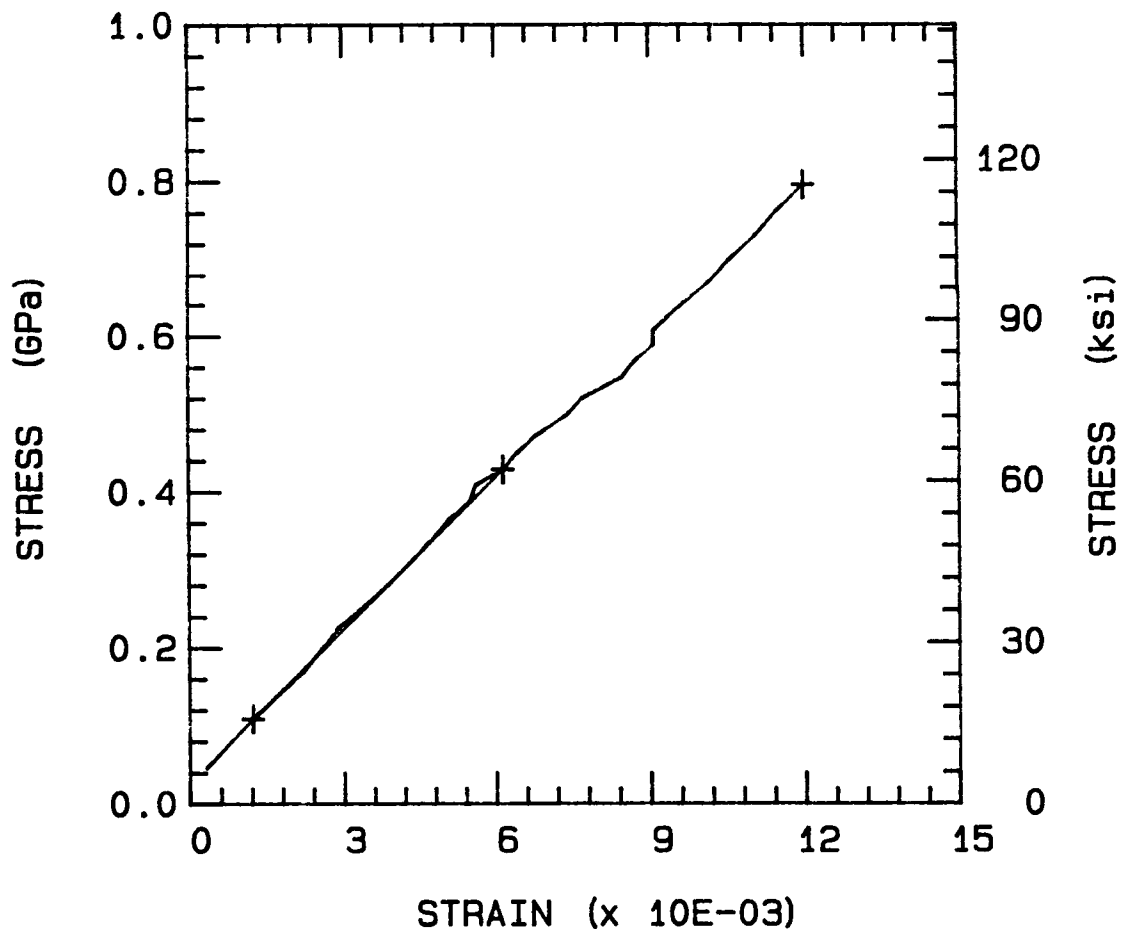
TEMP = 23.0 DEG. C NU = 0.183



NLDTD6.EDT

ULT. STRESS = 115.400 ksi

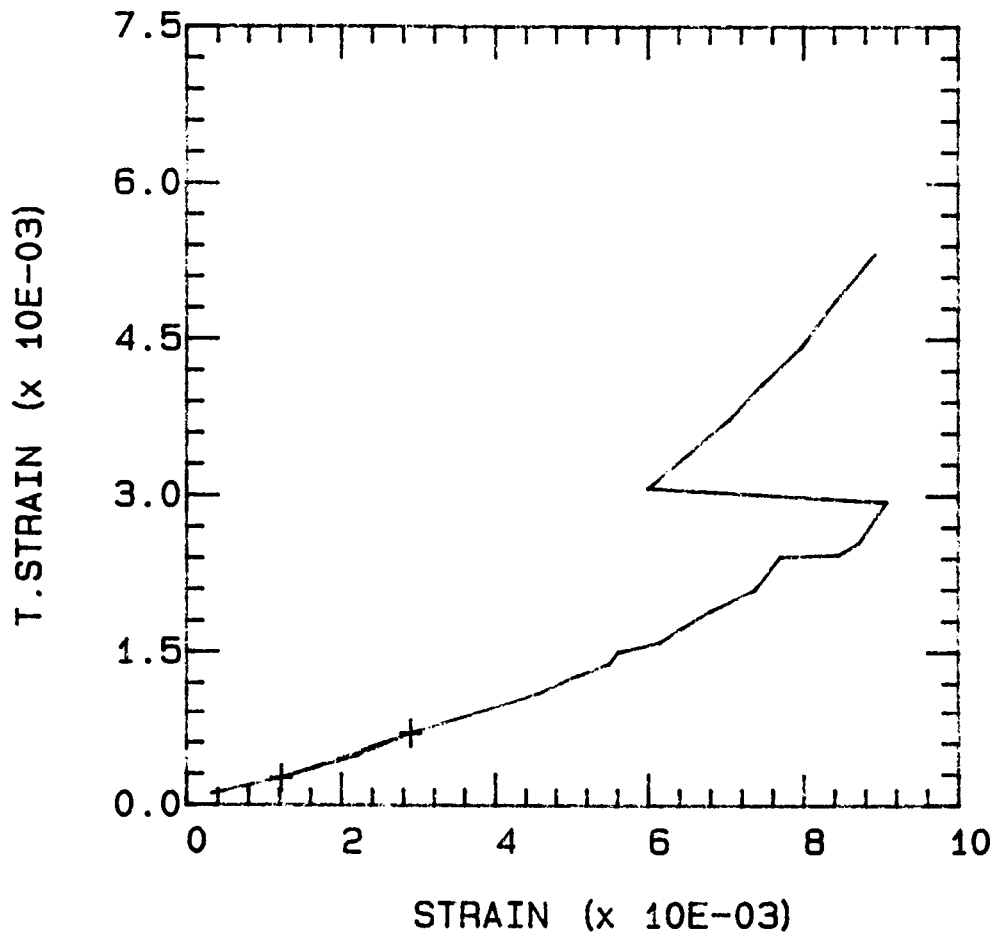
TEMP = 23.0 DEG. C MOD = 9.577 Msi



NLDTD6.EDT

ULT. STRESS = 115.400 ksi

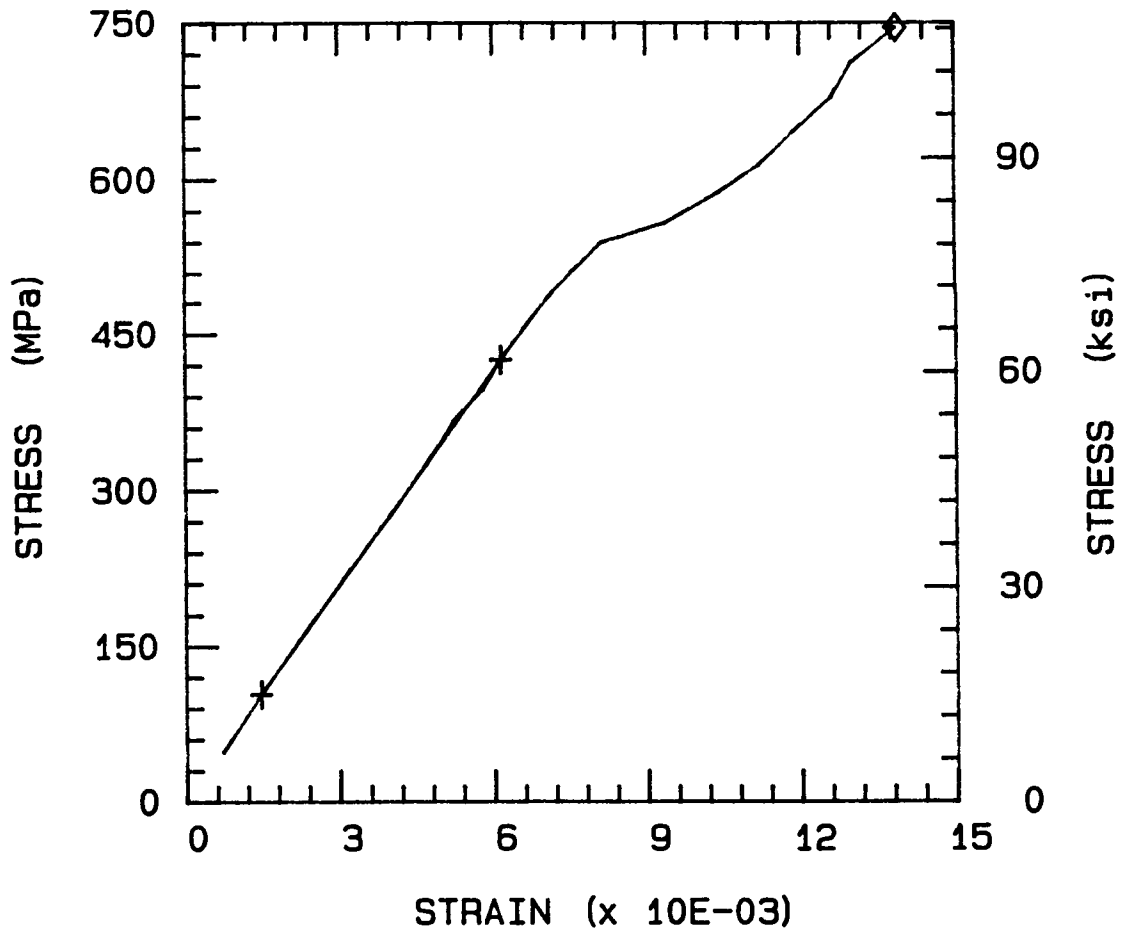
TEMP = 23.0 DEG. C NU = 0.258



NLDTD7.EDT

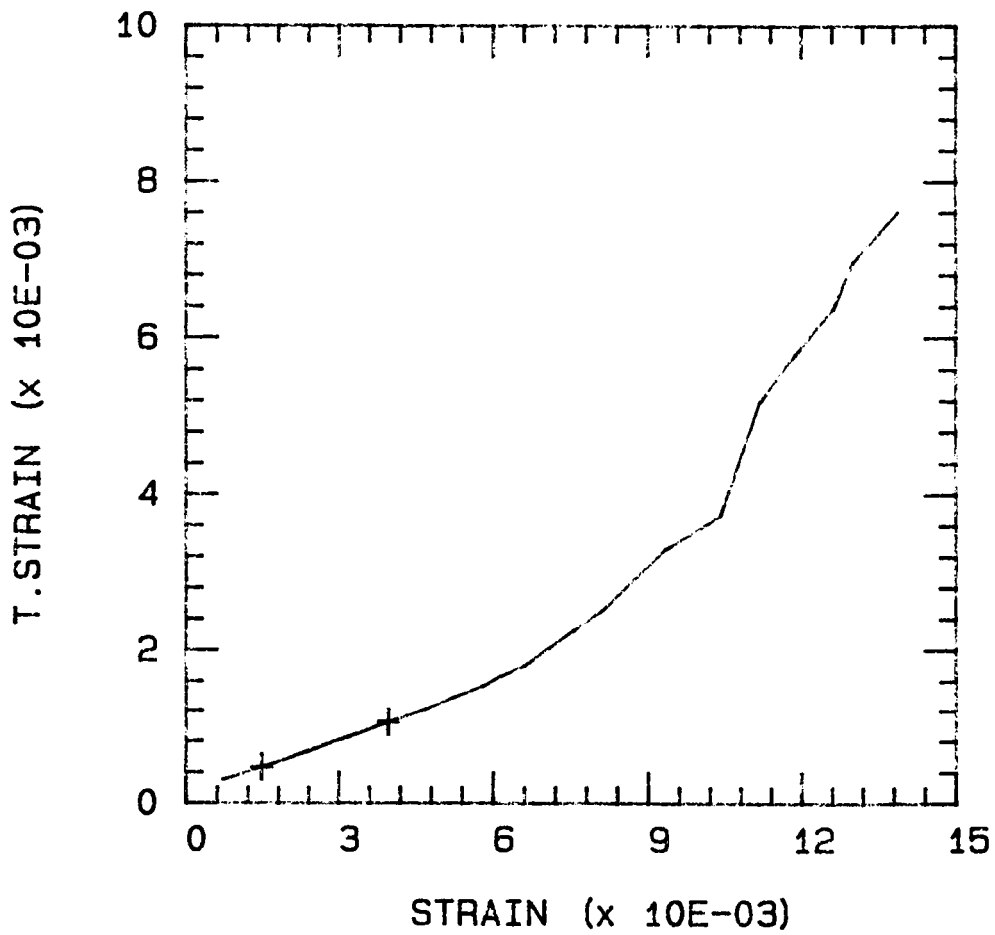
ULT. STRESS = 108.100 ksi

TEMP = 23.0 DEG. C MOD = 9.926 Msi



NLDTD7.EDT

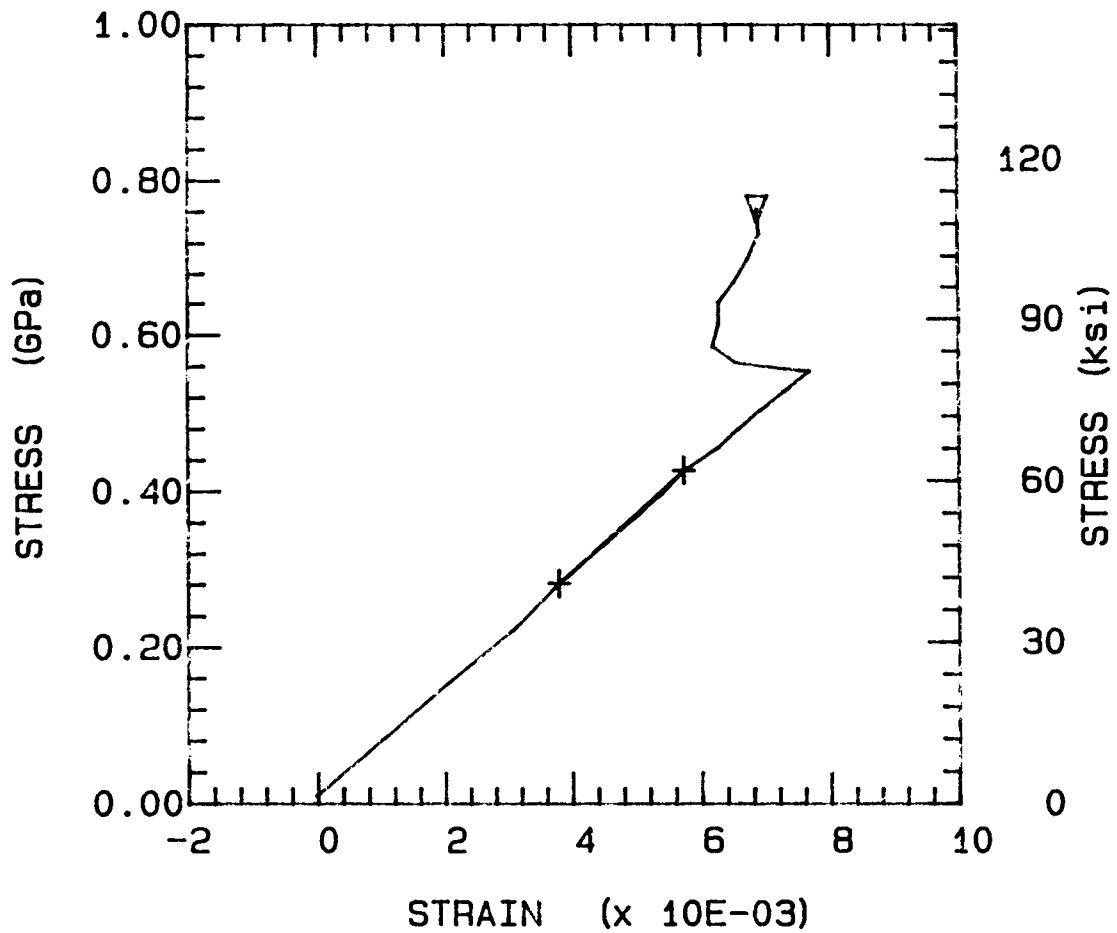
ULT. STRESS = 108.100 ksi
TEMP = 23.0 DEG. C NU = 0.232



NLDTD8.EDT

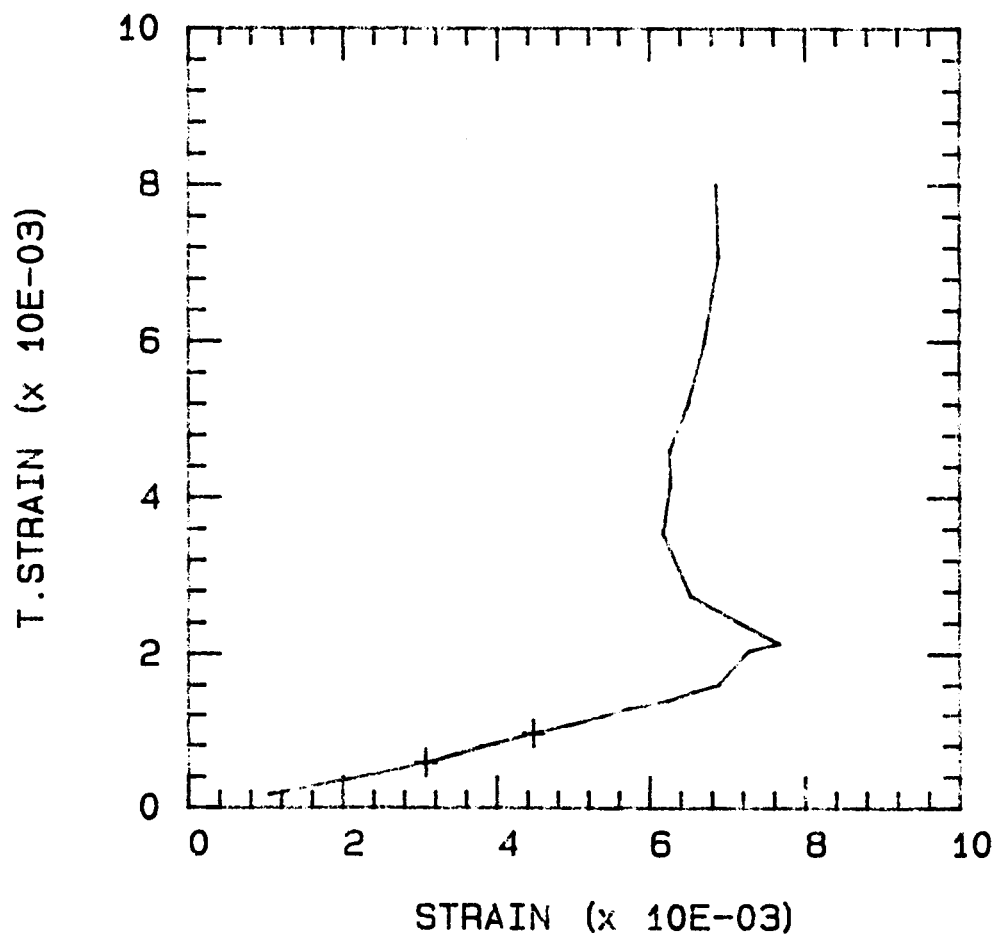
ULT. STRESS = 110.700 ksi

TEMP = 23.0 DEG. C MOD = 10.769 Msi



NLDTD8.EDT

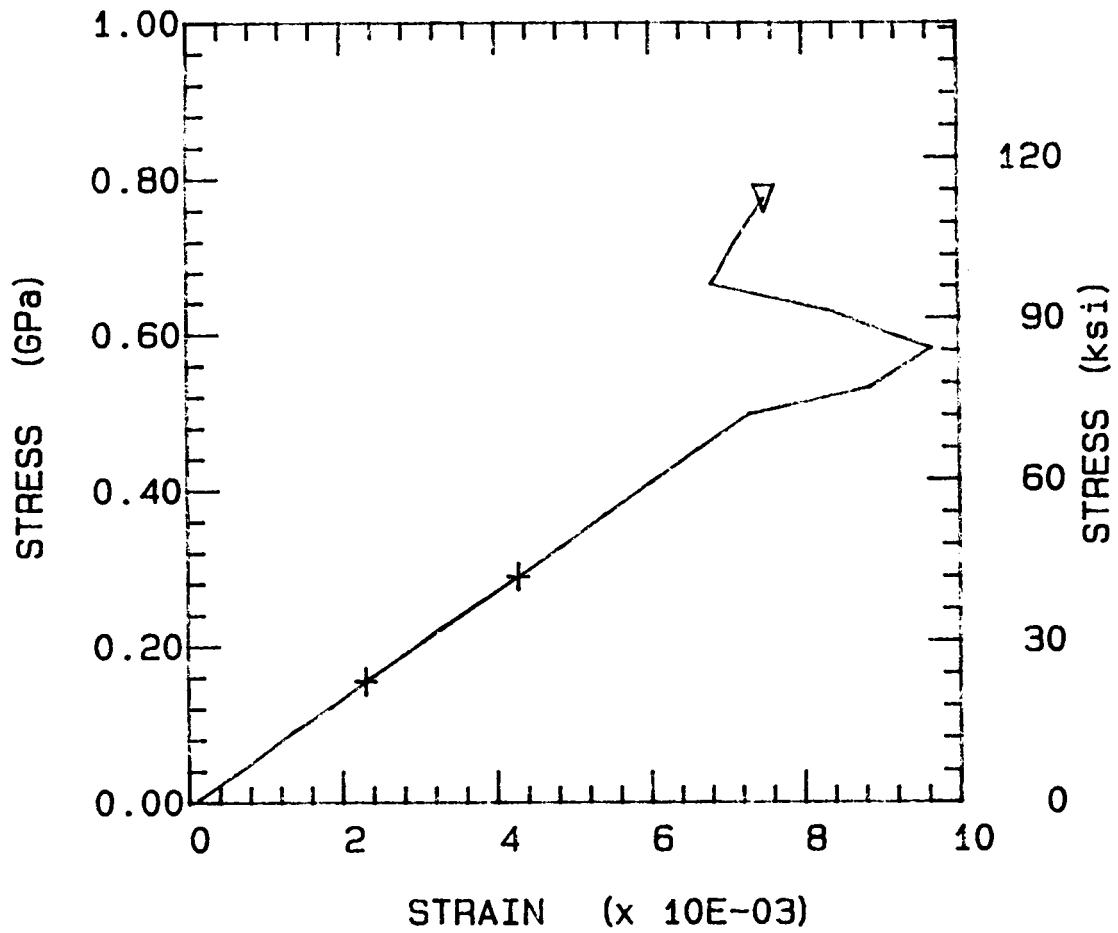
ULT. STRESS = 110.700 ksi
TEMP = 23.0 DEG. C NU = 0.267



NLTD21.EDT

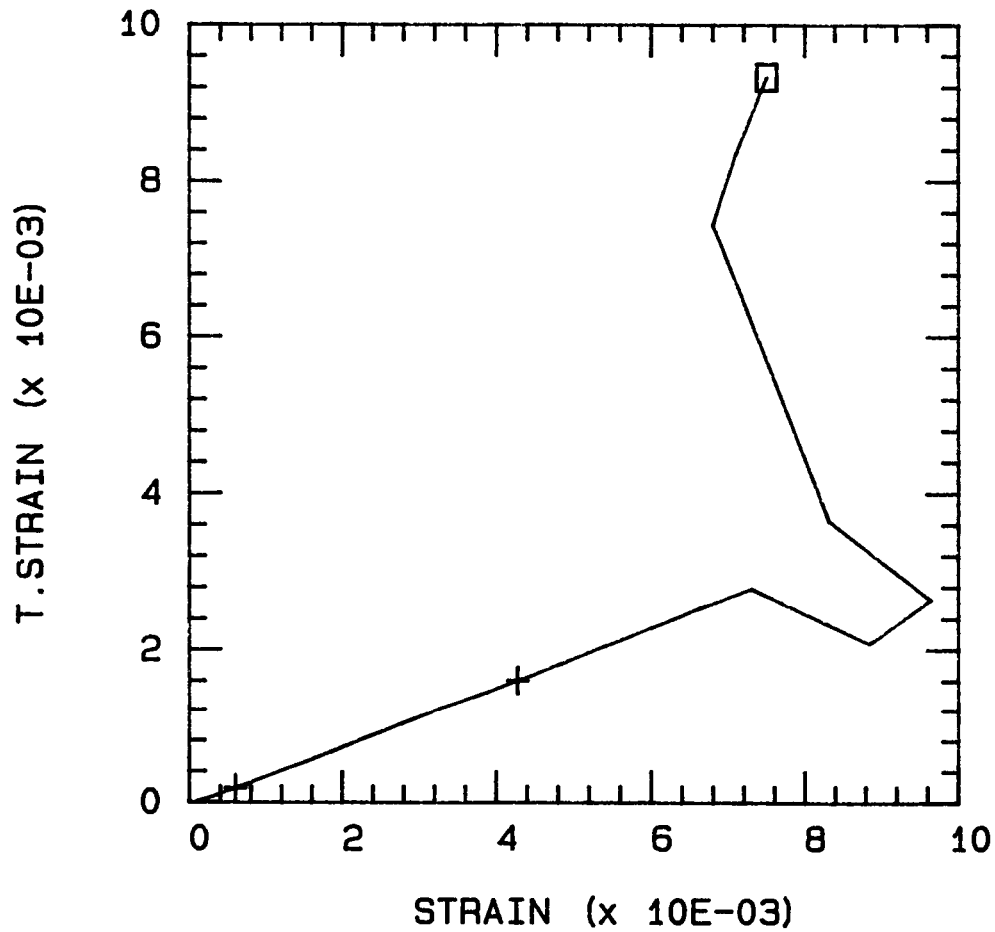
ULT. STRESS = 112.400 ksi

TEMP = 82.0 DEG. C MOD = 9.882 Msi



NLTD21.EDT

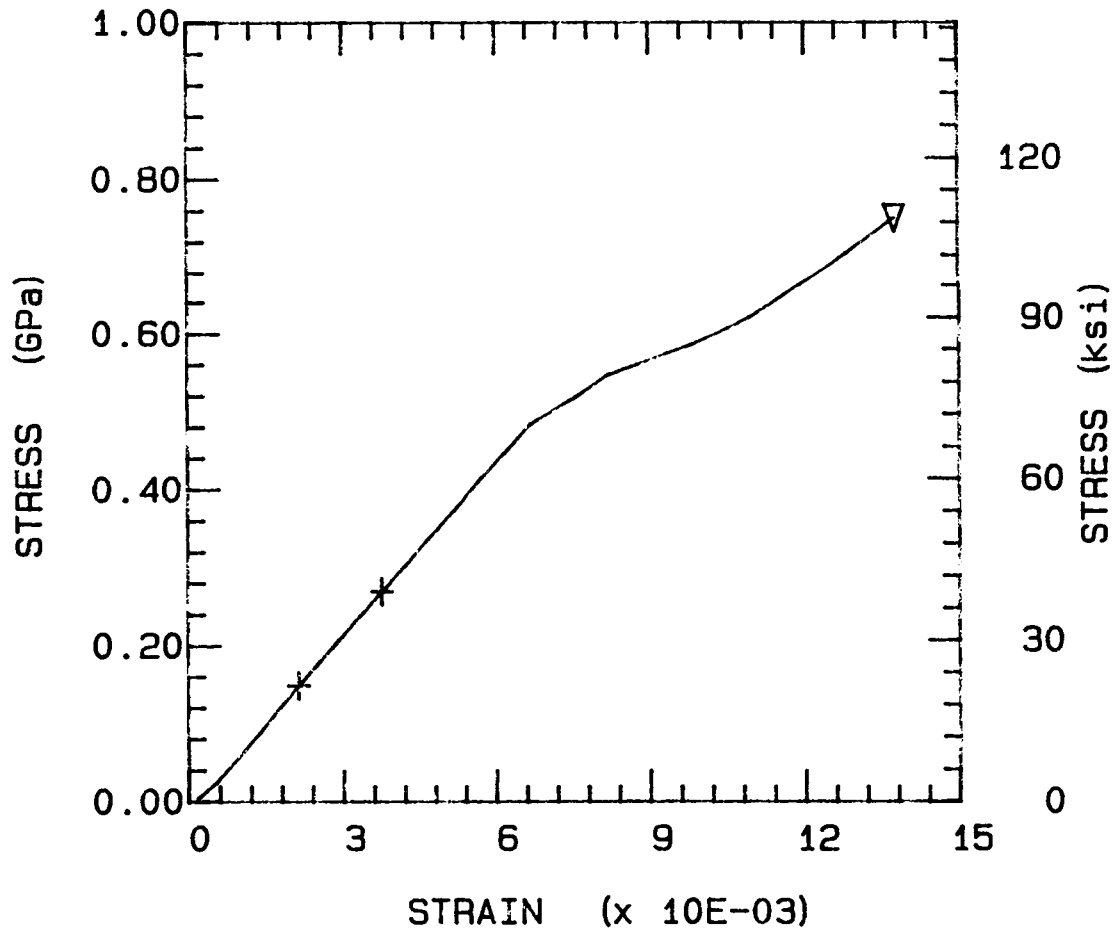
ULT. STRESS = 112.400 ksi
TEMP = 82.0 DEG. C NU = 0.388



NLTD22.EDT

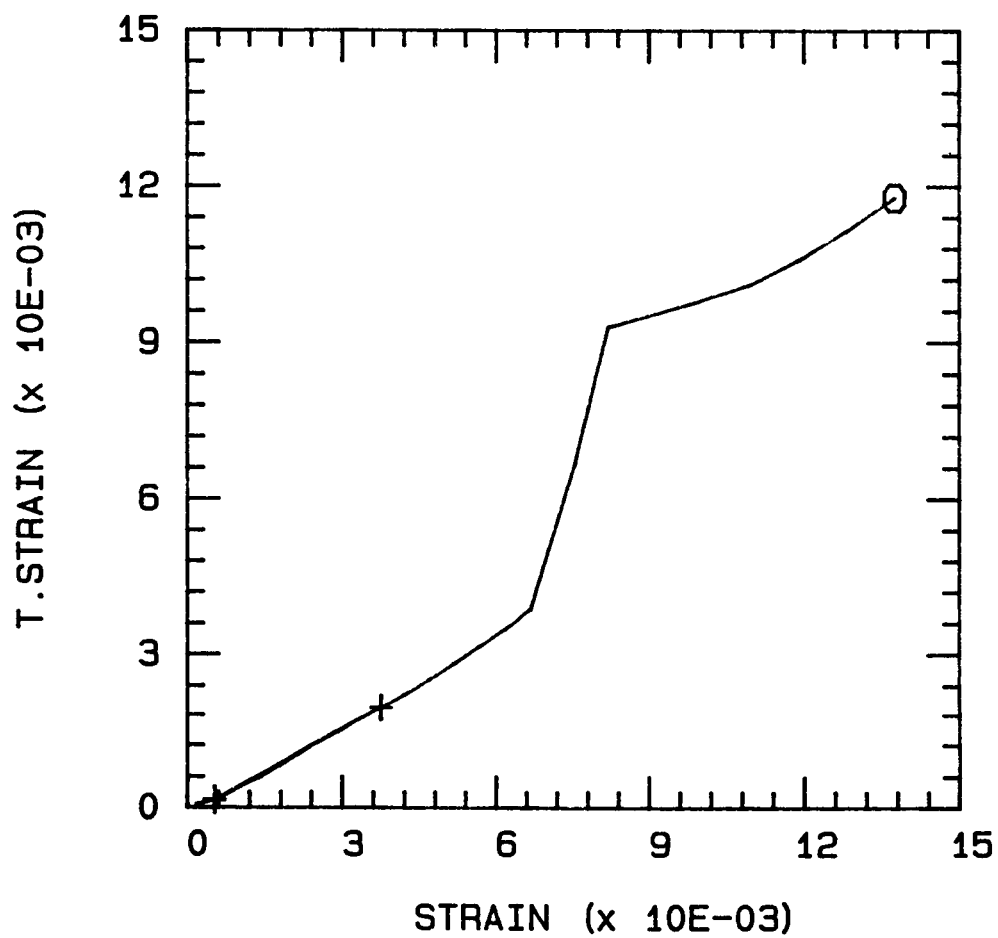
ULT. STRESS = 108.800 ksi

TEMP = 82.0 DEG. C MOD = 10.789 Msi



NLTD22.EDT

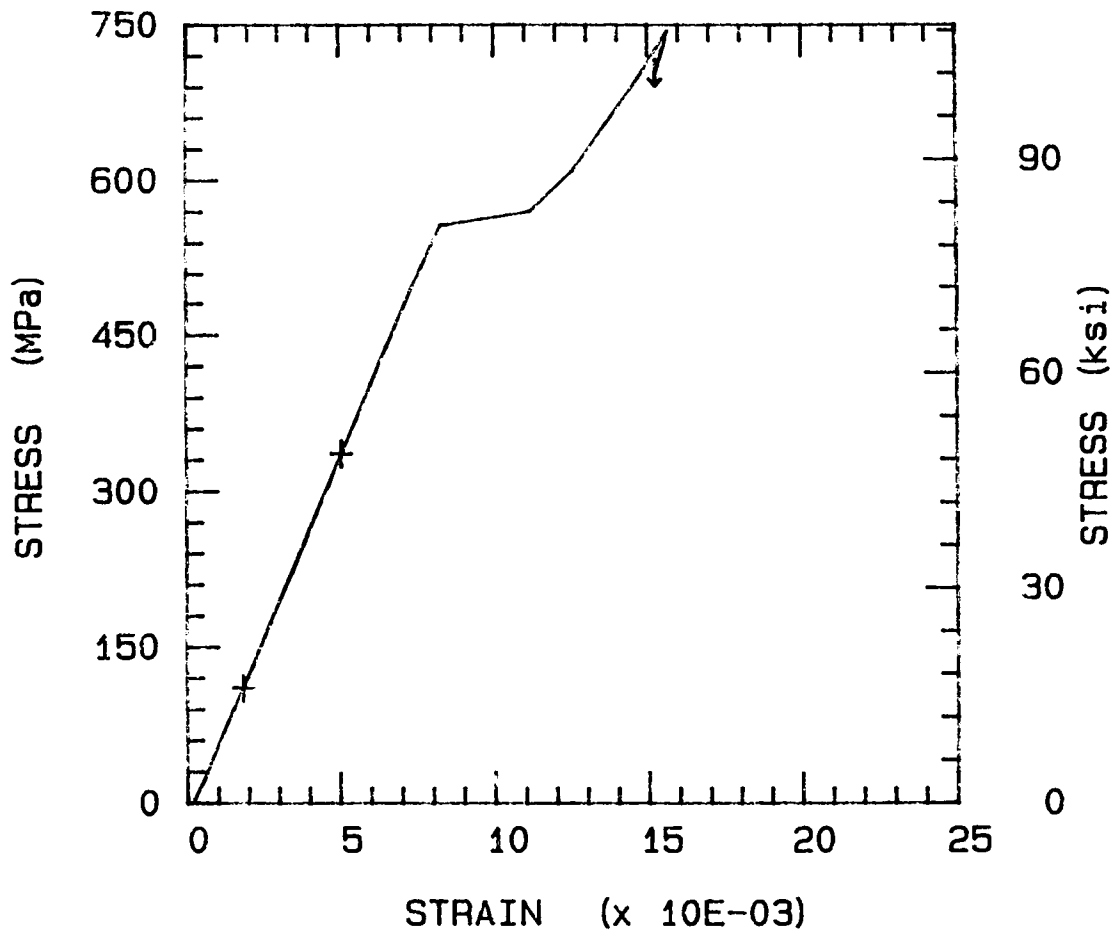
ULT. STRESS = 108.800 ksi
TEMP = 82.0 DEG. C NU = 0.564



NLTD23.EDT

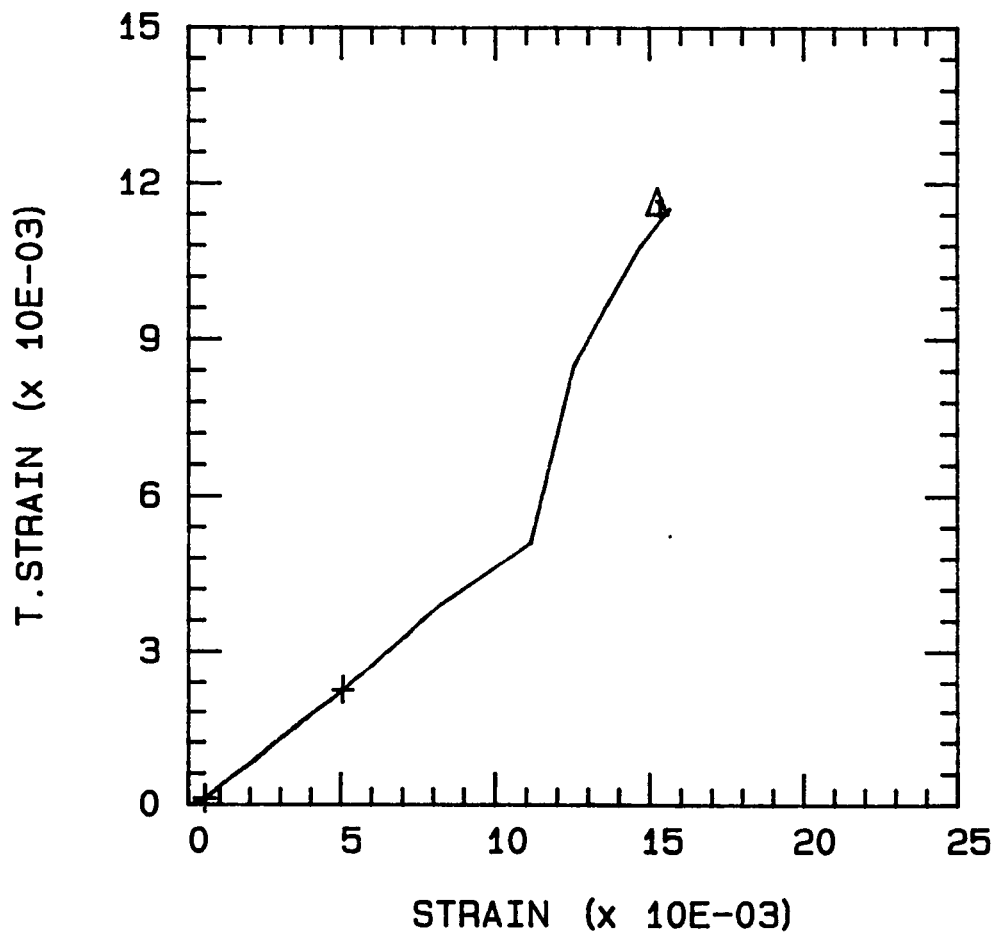
ULT. STRESS = 107.900 ksi

TEMP = 82.0 DEG. C MOD = 10.141 Msi



NLTD23.EDT

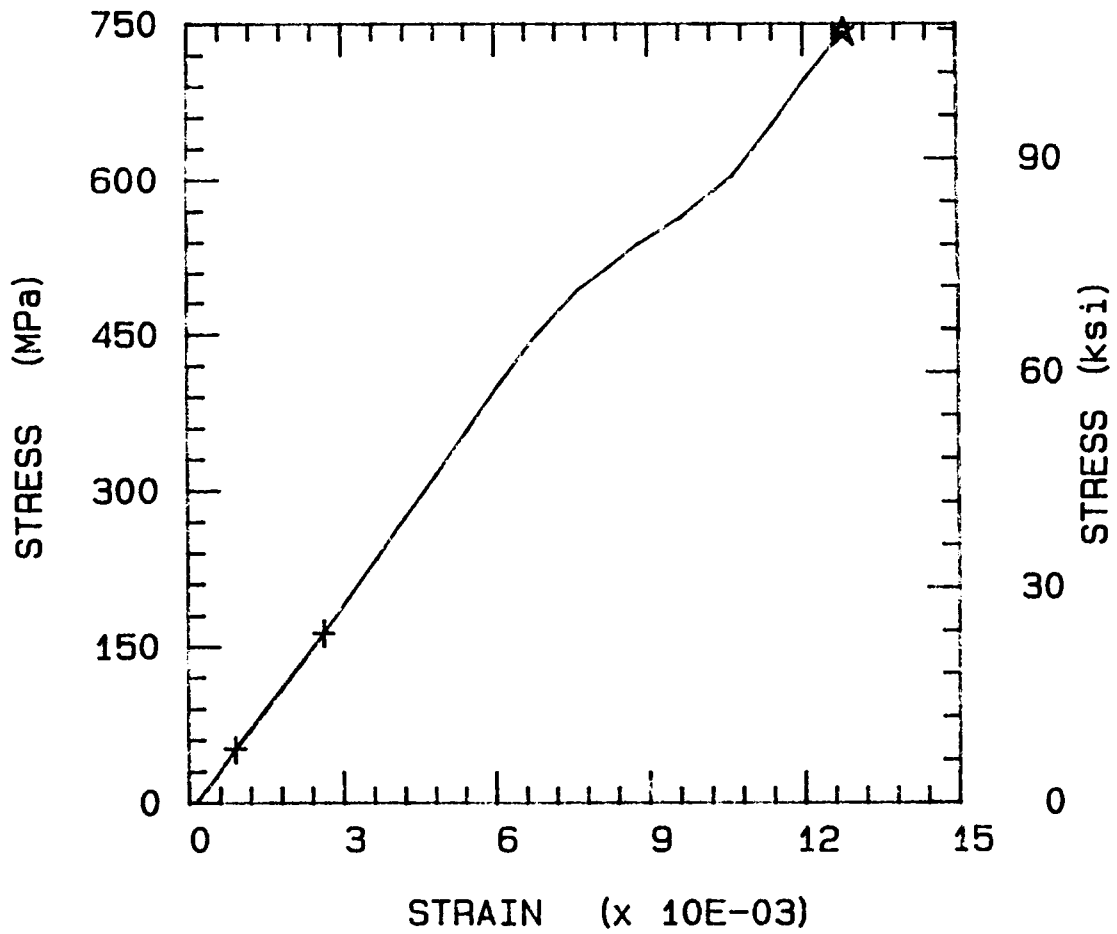
ULT. STRESS = 107.900 ksi
TEMP = 82.0 DEG. C NU = 0.471



NLTD24.EDT

ULT. STRESS = 107.700 ksi

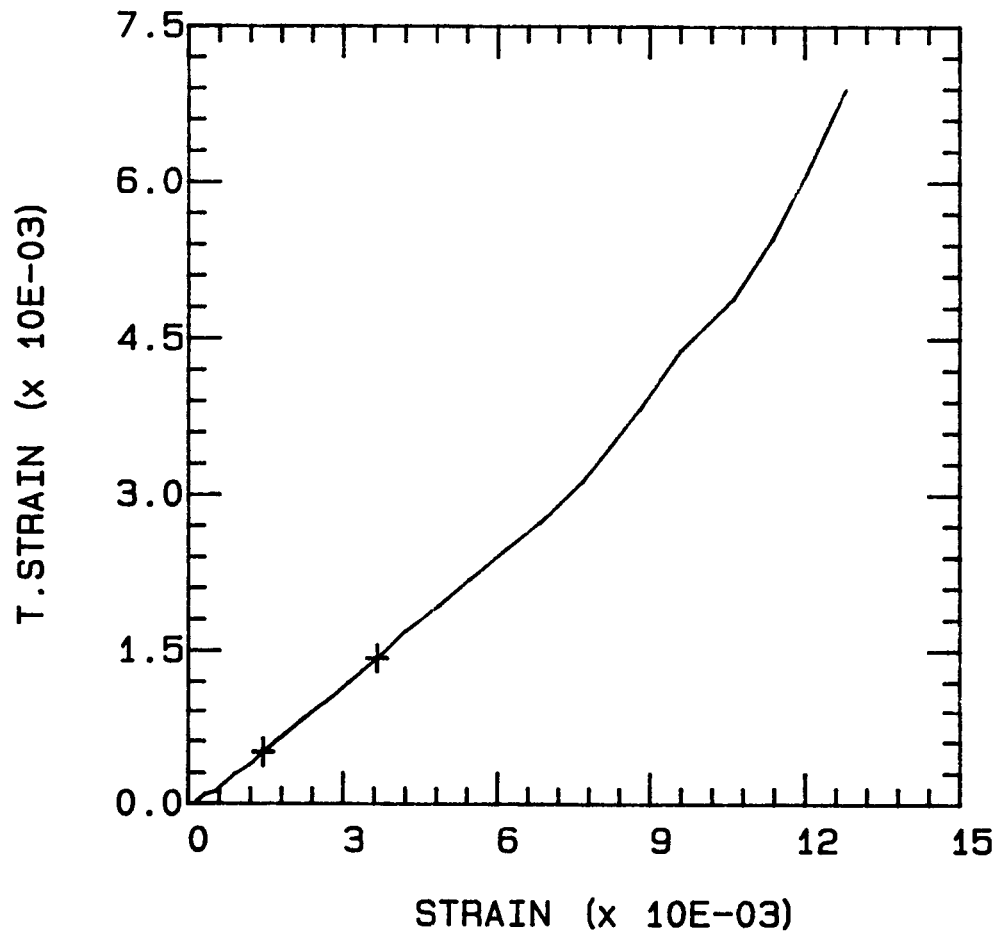
TEMP = 82.0 DEG. C MOD = 9.421 Msi



NLTD24.EDT

ULT. STRESS = 107.700 ksi

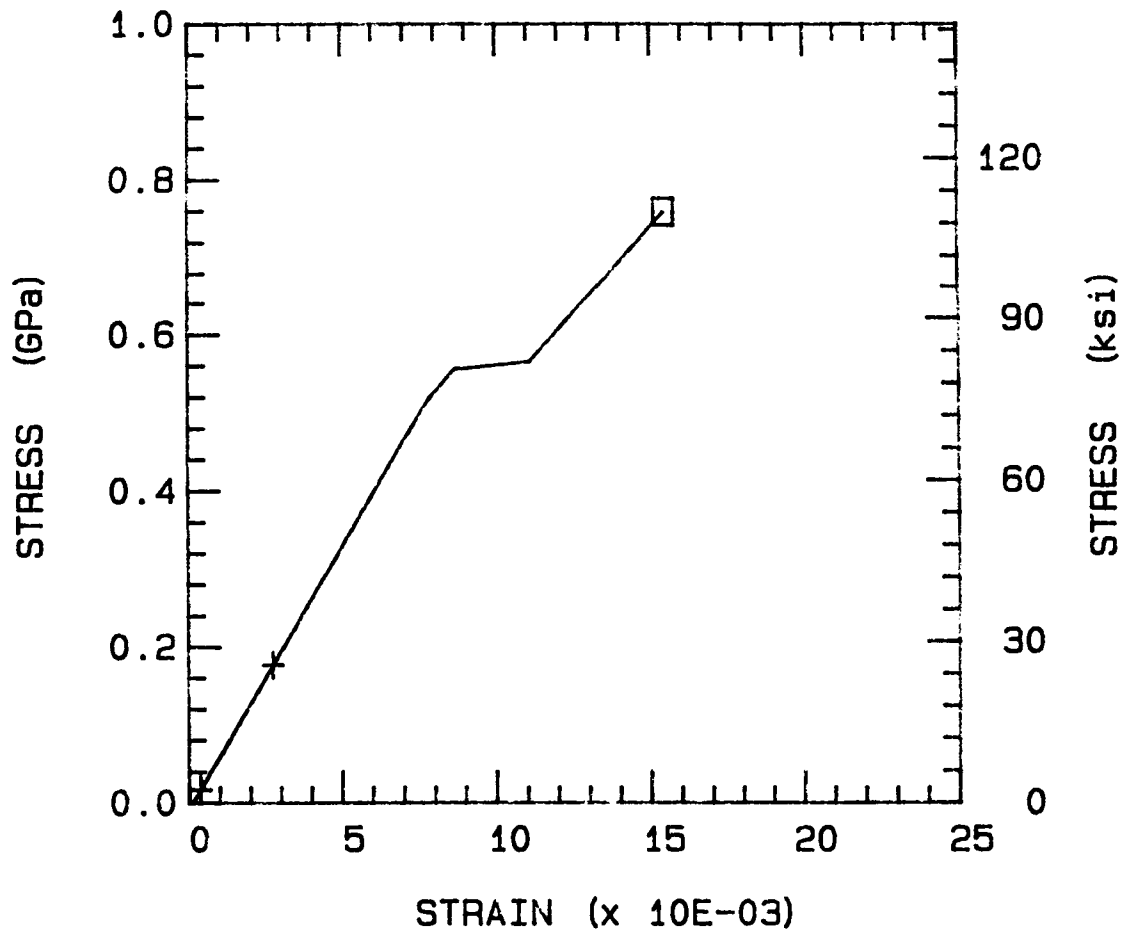
TEMP = 82.0 DEG. C NU = 0.421



NLTD25.EDT

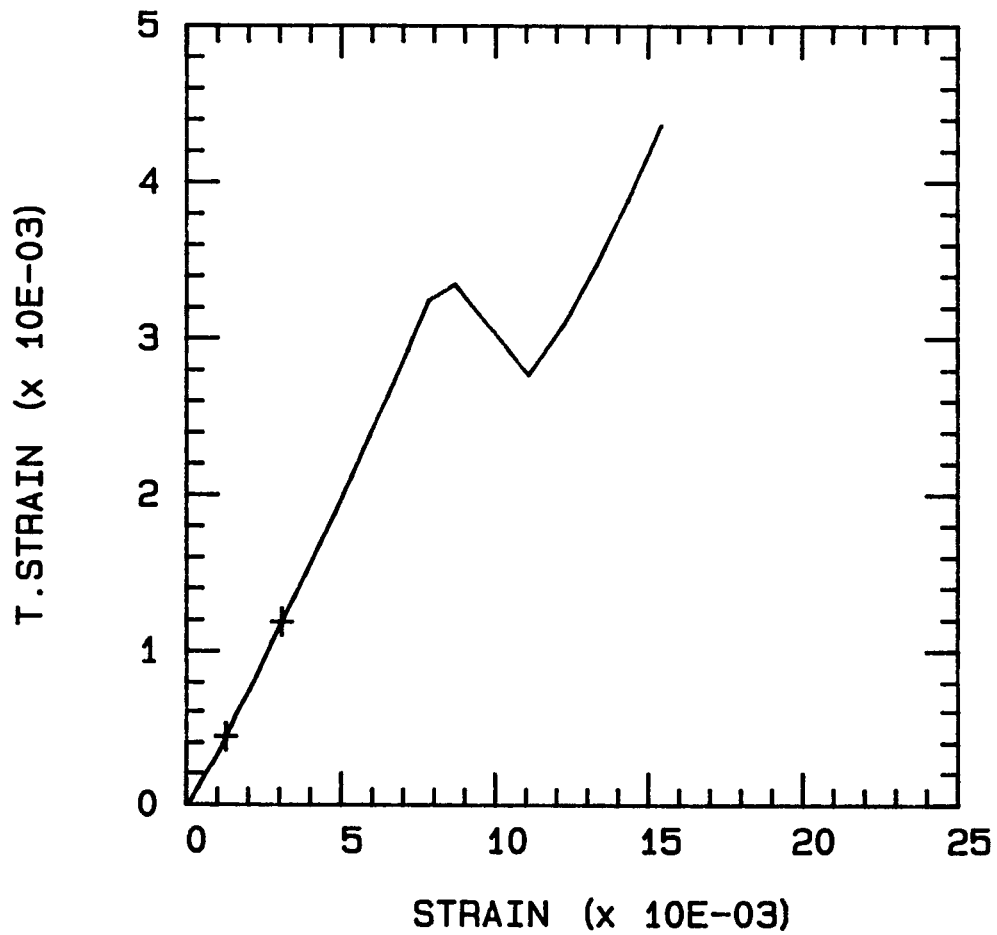
ULT. STRESS = 110.100 ksi

TEMP = 82.0 DEG. C MOD = 9.733 Msi



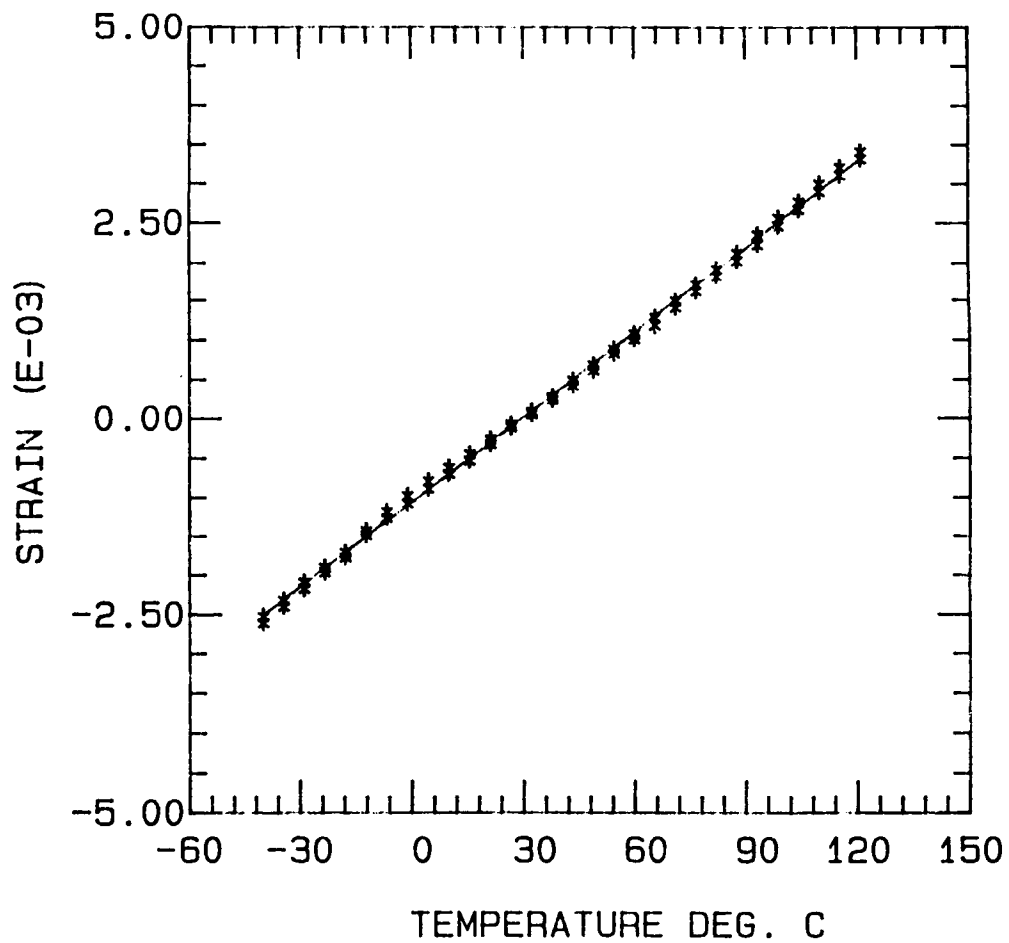
NLTD25.EDT

ULT. STRESS = 110.100 ksi
TEMP = 82.0 DEG. C NU = 0.415



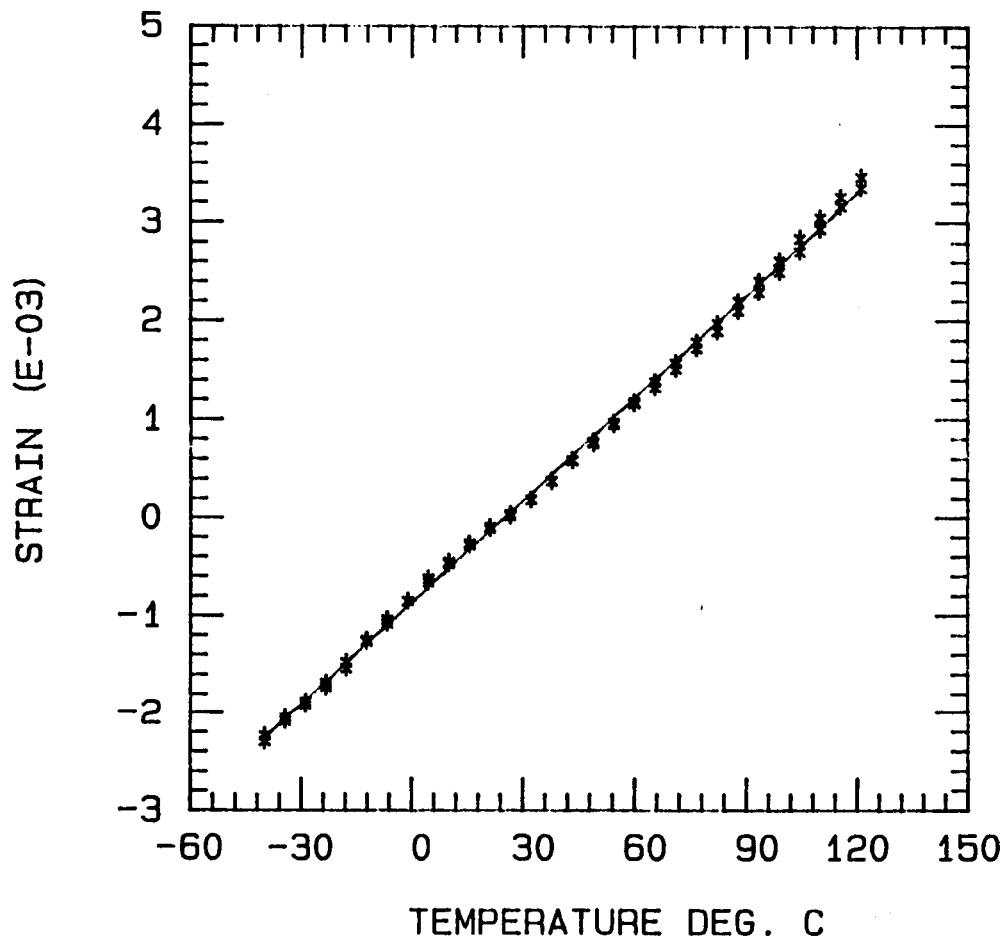
IM7/8551-7 90 DEG NO. 1

$\text{ALPHA} = +3.618\text{E-}05 \text{ / } ^\circ\text{C}$



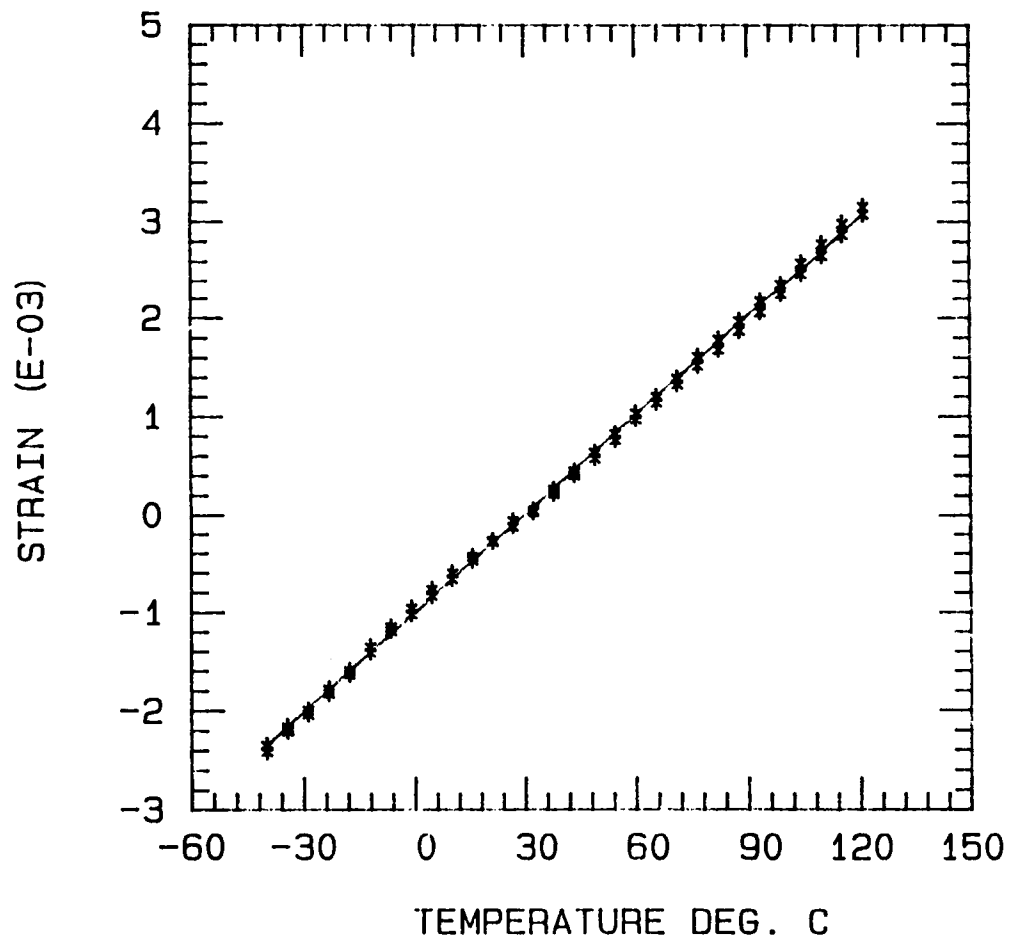
IM7/8551-7 90 DEG NO. 2

ALPHA = +3.471E-05 / C



IM7/8551-7 90 DEG NO. 3

$\text{ALPHA} = +3.365\text{E-}05 / \text{C}$



APPENDIX B

INDIVIDUAL TENSION-TENSION FATIGUE RESULTS

Naming Convention for Edge Delamination
Fatigue Specimens

Specimen name = 123456.FTG - six characters with .FTG extension

Character Meaning:

1. L - NASA-Langley
2. F - Fatigue Specimen
3. L or H - Test Temperature
L = Low 75°F (25°C)
H = High 180°F (82°C)
4. Maximum Load Value where:

A = 95% of Ultimate Load	J = 50% of Ultimate Load
B = 90%	K = 45%
C = 85%	L = 40%
D = 80%	M = 35%
E = 75%	N = 30%
F = 70%	O = 25%
G = 65%	P = 20%
H = 60%	Q = 15%
I = 55%	R = 10%
5. - Precondition Type
S = No precondition (Normal)
M = High Mean Load (1000 cycles)
P = Spike Load (One cycle)
6. - Specimen Number 0-9, A-Z

Example - LFLESA.FTG

Explanation - LF = NASA-Langley Fatigue Program
L = Low temperature 75°F (25°C)
E = 75% of Ultimate Load
S = No Precondition
A = Specimen No. A

PRECEDING PAGE BLANK NOT FILMED

Table B1

Individual Tension-Tension Edge Delamination Fatigue Results for
IM7/8551-7 Composites at Room Temperature No Precondition

Specimen Name	Thickness		Peak Stress	Initial Modulus		Final Modulus		R Ratio	Cycles to 5% Modulus Decay	Cycles to Delamination	Delamination Strain	Gc	Gc	
	(in)	(mm)		(ksi)	(MPa)	(Msi)	(GPa)					($\frac{\text{lb}_f}{\text{in}^2}$)	($\frac{\text{J}}{\text{m}^2}$)	
LFSASA 95%	0.044	1.12	79.1	545	9.34	64.35	8.86	61.05	0.113	66	1	0.87	1.11	193.58
LFLASC 95%	0.044	1.12	81.8	564	9.37	64.56	8.26	56.91	0.151	6	1	0.81	0.970	169.77
LFLCSA 85%	0.044	1.12	73.6	507	10.12	69.73	9.55	65.80	0.139	56	1	0.66	0.642	112.44
LFLDSB 80%	0.044	1.12	70.8	488	9.82	67.66	9.31	64.15	0.119	390	170	0.56	0.454	79.51
LFLESA 75%	0.044	1.12	62.5	431	10.16	70.00	9.65	66.49	0.112	950	36	0.61	0.545	95.42
LFLFSA 70%	0.045	1.14	55.2	380	8.96	61.73	8.51	58.63	0.110	3,700	150	0.64	0.619	108.47
LFLGSA 65%	0.044	1.12	50.8	350	9.30	64.08	8.83	60.84	0.087	37,000	3,900	0.57	0.484	84.75
LFLISC 55%	0.043	1.09	42.6	294	9.27	63.87	8.87	61.11	0.127	240,000	8,200	0.47	0.322	56.44
LFLISH 55%	0.045	1.14	47.4	327	8.82	60.77	8.37	57.67	0.124	31,000	2,400	0.53	0.422	73.88
LFLISK 55%	0.047	1.19	38.5	265	8.23	56.70	7.79	53.67	0.112	240,000	150	0.45	0.317	55.59
LFLJSE 50%	0.044	1.12	39.7	274	9.01	62.08	8.56	58.98	0.087	52,000	4,000	0.44	0.283	49.52
LFLKSA 45%	0.044	1.12	34.3	236	8.93	61.53	8.48	58.43	0.099	300,000	9,600	0.40	0.231	40.48
LFLKSE 45%	0.044	1.12	35.2	243	9.41	64.83	8.88	61.18	0.107	370,000	8,800	0.39	0.220	38.46
LFLLSA 40%	0.044	1.12	33.7	232	9.52	65.59	8.99	61.94	0.112	8,600	1,900	0.36	0.190	33.27
LFLLSB 40%	0.043	1.09	32.9	227	9.68	66.70	9.17	63.18	0.096	39,000	37,000	0.34	0.166	28.99
LFLUSD 40%	0.045	1.14	30.2	208	9.10	62.70	8.63	59.46	0.126	480,000	7,500	0.38	0.212	37.12
LFLMSA 35%	0.045	1.14	30.2	208	9.03	62.22	8.65	59.60	0.116	9,500,000	4,300,000	0.34	0.179	31.42

Table B2
Individual Tension-Tension Edge Delamination Fatigue Results for
IM7/8551-7 Composites at High Temperature No Precondition

Specimen Name	Thickness		Peak Stress	Initial Modulus		Final Modulus	R Ratio	Cycles to 5% Modulus Decay	Cycles to Delamination	Delamination Strain (percent)	Gc $\left(\frac{\text{lb}_f \text{ in}}{\text{in}^2}\right)$	Gc (J/m ²)		
	(in)	(mm)		(ksi)	(MPa)								(Msi)	(GPa)
LFLBPA 90%	0.044	1.12	74.2	511	9.14	62.97	8.68	59.81	0.138	330	11	0.82	1.00	175.69
LFLBPB 90%	0.045	1.14	73.9	509	9.50	65.46	9.01	62.08	0.109	36	1	0.76	0.864	151.28
LFLCPA 85%	0.044	1.12	70.6	486	10.22	70.42	9.71	66.90	0.144	86	6	0.68	0.690	120.76
LFLDPA 80%	0.044	1.12	65.6	452	9.04	62.29	8.57	59.05	0.133	490	1	0.70	0.733	128.29
LFLSPA 75%	0.043	1.09	66.0	455	10.23	70.48	9.71	66.90	0.105	320	1	0.61	0.541	94.79
LFLFPA 70%	0.045	1.14	59.1	407	9.07	62.49	8.59	59.19	0.103	490	1	0.64	0.612	107.12
LFLFPB 70%	0.045	1.14	54.7	377	9.13	62.91	8.66	59.67	0.109	3,800	750	0.60	0.546	95.67
LFLGPA 65%	0.045	1.14	53.7	370	8.87	61.11	8.37	57.67	0.118	15,000	9,900	0.57	0.493	86.37
LFLHPA 60%	0.043	1.09	50.9	351	9.16	63.11	8.70	59.94	0.104	5,800	9,400	0.55	0.437	76.59
LFLIPA 55%	0.045	1.14	42.0	289	8.91	61.39	8.45	58.22	0.114	200,000	160,000	0.45	0.301	52.75
LFLIPB 55%	0.044	1.12	46.9	323	10.18	70.14	9.63	66.35	0.099	24,000	3,200	0.45	0.299	52.27
LFLJPA 50%	0.044	1.12	41.7	287	8.97	61.80	8.52	58.70	0.106	140,000	6,700	0.45	0.299	52.27
LFLKPA 45%	0.044	1.12	36.2	249	8.88	61.18	8.42	58.01	0.118	41,000	5,500	0.41	0.247	43.18
LFLLLPA 40%	0.044	1.12	31.8	219	9.90	68.21	9.40	64.77	0.104	7,900	1	0.31	0.145	25.45
LFLLLPC 40%	0.045	1.14	32.8	226	8.96	61.73	8.51	58.63	0.118	960,000	5,800	0.37	0.208	36.34
LFLNPB 30%	0.044	1.12	24.5	169	8.86	61.05	8.40	57.88	0.110	19,000	1,000	0.24	0.088	15.49
LFLQPB 15%	0.044	1.12	12.9	89	9.55	65.80	9.45	65.11	0.119	*11,700,000	10,788,200	0.11	0.018	3.18

Table B3

Individual Tension-Tension Edge Delamination Fatigue Results for
IM7/8551-7 Composites at Room Temperature High Spike

Specimen Name	Thickness		Peak Stress	Initial Modulus	Final Modulus	R Ratio	Cycles to 5% Modulus Decay	Cycles to Delami- nation	Delami- nation Strain	Gc $(\frac{\text{lb}_f \text{ in}}{\text{in}^2})$	Gc (J/m^2)			
	(in)	(mm)												
LFLAMB 95%	0.043	1.09	80.1	552	9.40	64.77	8.91	61.39	0.102	170	1	0.83	0.985	172.53
LFLAMC 95%	0.044	1.12	77.1	531	9.14	62.97	8.65	59.60	0.122	190	1	0.80	0.953	166.86
LFLBMA 90%	0.043	1.09	77.0	531	9.80	67.52	9.25	63.73	1.177	11	1	0.80	0.917	160.64
LFLBMC 90%	0.044	1.12	75.3	519	10.22	70.42	9.65	66.49	0.091	31	1	0.70	0.716	125.40
LFLDMA 90%	0.045	1.14	73.4	506	9.76	67.25	9.26	63.80	0.114	6	1	0.72	0.775	135.71
LFLDMA 80%	0.043	1.09	68.1	469	9.78	67.38	9.29	64.01	0.111	250	1	0.67	0.649	113.58
LFLDMB 80%	0.044	1.12	66.3	457	9.73	67.04	9.23	63.59	0.119	460	66	0.69	0.700	122.54
LFLFMA 70%	0.045	1.14	57.9	399	9.66	66.56	9.16	63.11	0.099	4,800	510	0.62	0.585	102.46
LFLFMB 70%	0.045	1.14	58.6	404	9.48	65.32	8.99	61.94	0.101	900	100	0.60	0.534	93.46
LFLHMA 60%	0.045	1.12	50.2	346	9.60	66.14	9.10	62.70	0.102	27,000	320	0.53	0.428	75.00
LFLHMB 60%	0.044	1.14	51.0	351	9.62	66.28	9.13	62.91	0.101	8,400	960	0.51	0.382	66.88
LFLJMB 50%	0.045	1.12	43.5	300	8.49	58.50	8.06	55.53	0.089	74,000	540	0.50	0.378	66.26
LFLKMA 45%	0.044	1.12	37.3	257	9.40	64.77	8.92	61.46	0.107	20,000	3,300	0.40	0.230	40.27
LFLKMB 45%	0.044	1.14	37.5	258	9.85	67.87	9.32	64.21	0.092	25,000	1,100	0.38	0.213	37.27
LFLKMC 45%	0.045	1.12	37.2	256	9.44	65.04	8.94	61.60	0.097	98,000	3,400	0.39	0.229	40.15
LFLLMA 40%	0.044	1.09	33.0	227	8.81	60.70	8.35	57.53	0.132	36,000	3,300	0.37	0.197	34.58
LFLNMA	0.043	1.09	29.6	204	9.02	62.15	8.55	58.91	0.090	290,000	860	0.31	0.138	24.24
LFLQMA	0.043	1.09	21.4	147	9.71	66.90	9.21	63.46	0.096	13,000	3,400	0.20	0.058	10.19
LFLQMA	0.044	1.12	12.6	87	9.57	65.94	9.12	62.84	0.102	2,000,000	8,800	0.13	0.025	4.30

ORIGINAL PAGE IS
OF POOR QUALITY

Table B4
Individual Tension-Tension Edge Delamination Fatigue Results for
IM7/8551-7 Composites at High Temperature High Spike

Specimen Name	Thickness (in)	Thickness (mm)	Peak Stress (ksi)	Peak Stress (MPa)	Initial Modulus (Msi)	Initial Modulus (GPa)	Final Modulus (Msi)	Final Modulus (GPa)	R Ratio	Cycles to 5% Modulus Decay	Cycles to Delami- nation	Delami- nation Strain (percent)	Gc $\left(\frac{\text{lb}_f \text{ in}}{\text{in}^2}\right)$	Gc (J/m ²)
LFHASC 95%	0.049	1.24	77.8	535	7.60	52.36	7.21	49.68	0.102	320	1	0.98	3.74	655.03
LFHASD 95%	0.044	1.12	78.8	543	8.97	61.80	7.94	54.71	0.113	6	1	0.87	2.64	462.85
LFHCSA 85%	0.044	1.12	71.5	493	8.82	60.77	8.23	56.70	0.123	16	1	0.82	2.31	404.32
LFHCSB 85%	0.045	1.14	71.4	492	9.80	67.52	9.30	64.08	0.103	26	1	0.72	1.83	320.04
LFHDSA 80%	0.049	1.24	67.5	465	8.18	56.36	7.73	53.26	0.125	31	1	0.83	2.69	471.50
LFHESA 75%	0.044	1.12	64.4	444	9.15	63.04	8.66	59.67	0.106	590	51	0.72	1.78	312.06
LFHFSA 70%	0.051	1.30	59.0	407	8.09	55.74	7.66	52.78	0.116	220	1	0.71	2.03	354.67
LFHFBSB 70%	0.043	1.09	59.1	407	10.37	71.45	9.84	67.80	0.101	690	86	0.58	1.12	196.68
LFHGSA 65%	0.043	1.09	55.1	380	10.41	71.72	9.87	68.00	0.100	1,400	110	0.53	0.954	167.10
LFHBSB 60%	0.042	1.07	50.3	347	9.32	64.21	8.83	60.84	0.107	6,300	390	0.54	0.953	166.93
LFHISA 55%	0.043	1.09	46.8	322	9.25	63.73	8.72	60.08	0.102	6,800	1,300	0.50	0.832	145.76
LFHJSA 50%	0.043	1.09	42.3	291	9.57	65.94	9.08	62.56	0.145	50,000	1,400	0.42	0.611	106.94
LFHJSB 50%	0.044	1.12	42.4	292	8.92	61.46	8.48	58.43	0.125	23,000	2,600	0.48	0.791	138.50
LFHKSA 45%	0.044	1.12	37.8	260	9.73	67.04	9.23	63.59	0.106	48,000	7,300	0.39	0.540	94.49
LFHMSB 35%	0.044	1.12	29.2	201	9.09	62.63	8.36	57.60	0.111	1,150,000	210,000	0.33	0.388	67.91
LFHQSB 15%	0.045	1.14	11.8	81	8.88	61.18	8.81	60.70	0.106	10,000,000	9,700,000	0.08	0.026	4.50

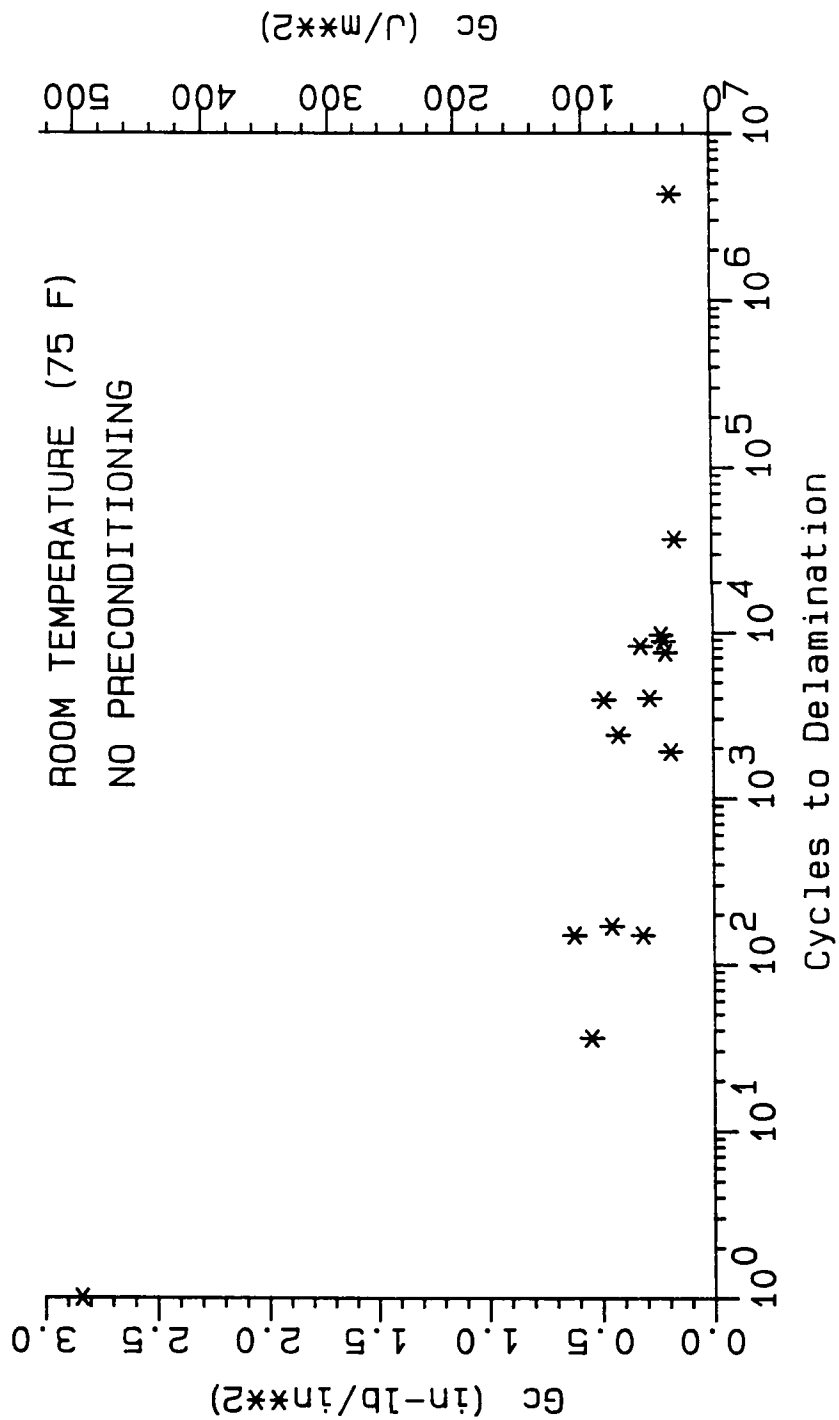
Table B5
Individual Tension-Tension Edge Delamination Fatigue Results for
IM7/8551-7 Composites at Room Temperature High Mean

Specimen Name	Thickness		Peak Stress	Initial Modulus		Final Modulus	R Ratio	Cycles to 5% Modulus Decay		Cycles to Delamination	Delamination Strain		Gc
	(in)	(mm)	(ksi)	(ksi)	(MPa)	(Msi)	(GPa)	(Msi)	(GPa)	(percent)	(lb _f /in ²)	(J/m ²)	
LFHAPB 95%	0.044	1.12	79.5	9.15	63.04	8.64	59.53	0.143	140	21	0.86	2.60	455.45
LFHHPA 90%	0.043	1.09	75.6	10.28	70.83	9.73	67.04	0.128	11	1	0.70	1.67	292.32
LFHCPA 85%	0.045	1.14	72.8	8.91	61.39	8.39	57.81	0.091	16	1	0.76	2.03	355.81
LFHDPA 80%	0.043	1.09	67.7	10.33	71.17	9.79	67.45	0.119	170	1	0.61	1.25	219.18
LFHEPA 75%	0.043	1.09	64.6	10.46	72.07	9.94	68.49	0.115	520	1	0.59	1.18	206.37
LFHEPA 70%	0.044	1.12	60.7	9.87	68.00	9.34	64.35	0.090	500	1	0.59	1.22	213.33
LFHCPA 65%	0.043	1.09	54.3	10.21	70.35	9.70	66.83	0.125	2,600	41	0.51	0.891	155.94
LFHHPA 60%	0.044	1.12	52.6	9.91	68.28	9.37	64.56	0.111	480	1	0.51	0.908	158.95
LFHHPB 60%	0.043	1.09	52.1	9.40	64.77	8.92	61.46	0.106	9,900	1,200	0.55	1.04	181.26
LFHHPA 55%	0.044	1.12	47.9	9.45	65.11	8.96	61.73	0.097	7,500	1,200	0.50	0.859	150.36
LFHHPA 50%	0.045	1.14	42.8	9.69	66.76	9.17	63.18	0.090	41,000	61,400	0.43	0.660	115.64
LFHHPA 45%	0.043	1.09	39.4	8.90	61.32	8.40	57.88	0.097	130,000	19,000	0.45	0.688	120.46
LFHHPA 40%	0.044	1.12	33.6	8.86	61.04	8.37	57.67	0.107	150,000	34,000	0.40	0.548	95.94
LFHHPA 35%	0.044	1.12	30.0	9.55	65.80	9.05	62.35	0.099	370,000	70,000	0.32	0.347	60.78
LFHHPB 15%	0.043	1.09	11.9	10.11	69.66	10.48	72.21	0.093	*11,000,000	11,000,000	0.10	0.035	6.19

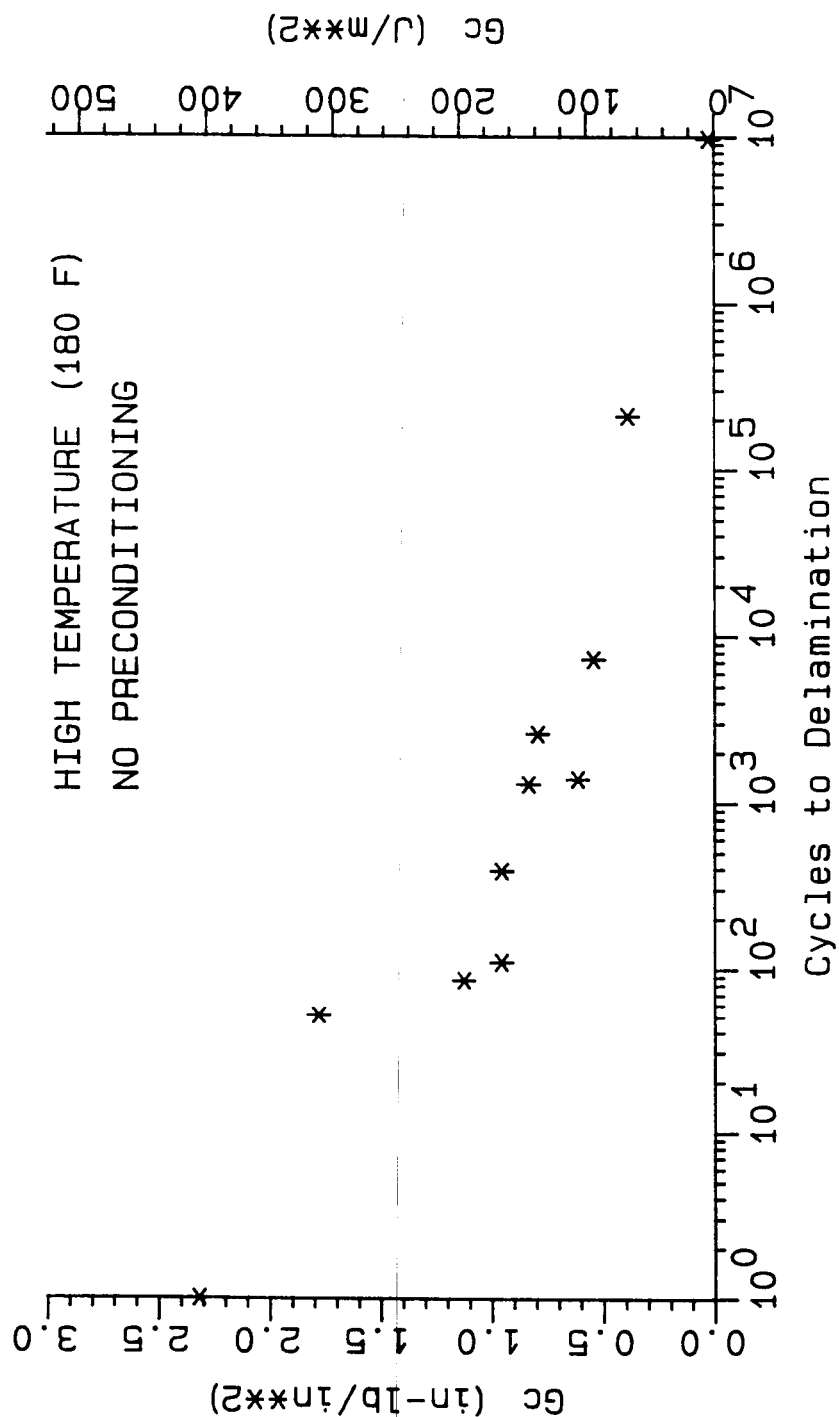
Table B6
Individual Tension-Tension Edge Delamination Fatigue Results for
IM7/8551-7 Composites at High Temperature High Mean

Specimen Name	Thickness (in)	Thickness (mm)	Peak Stress (ksi)	Peak Stress (MPa)	Initial Modulus (Msi)	Initial Modulus (GPa)	Final Modulus (Msi)	Final Modulus (GPa)	R Ratio	Cycles to 5% Modulus Decay	Cycles to Delami- nation	Delami- nation Strain (Percent)	Gc (lb _f in)	Gc (J/m ²)
LFHAMB 95%	0.045	1.14	81.7	563	9.02	62.15	8.50	58.57	0.089	41	1	0.84	2.51	439.27
LFHBMA 90%	0.044	1.12	76.2	525	9.31	64.21	8.66	59.67	0.089	16	1	0.76	1.99	348.82
LFHCMA 85%	0.044	1.12	72.7	501	9.07	62.49	8.60	59.25	0.093	140	1	0.74	1.92	336.94
LFHDMA 80%	0.044	1.12	69.5	479	9.07	62.49	8.61	59.32	0.081	130	21	0.76	2.03	355.30
LFHEMA 75%	0.042	1.07	63.1	435	9.77	67.32	9.28	63.94	0.134	390	21	0.64	1.36	237.25
LFHFMA 70%	0.044	1.12	58.7	404	10.01	68.97	9.50	65.46	0.117	340	1	0.54	1.00	175.53
LFHFMB 70%	0.044	1.12	58.9	406	9.51	65.52	9.01	62.08	0.130	790	36	0.63	1.37	239.30
LFHGMA 65%	0.045	1.14	54.4	375	9.30	64.08	8.81	60.70	0.120	1,700	1	0.53	0.991	173.56
LFHHMA 60%	0.045	1.14	50.9	351	9.52	65.59	9.03	62.22	0.144	2,700	11	0.51	0.925	161.92
LFHIMA 55%	0.045	1.14	47.1	325	9.17	63.18	8.69	59.87	0.134	2,600	150	0.50	0.882	154.39
LFHIMC 55%	0.044	1.12	46.8	322	9.83	67.73	9.27	63.87	0.127	9,800	1,300	0.44	0.667	116.78
LFHJMA 50%	0.044	1.12	42.5	293	9.80	67.52	9.28	63.94	0.120	17,000	940	0.38	0.507	88.83
LFHJMB 50%	0.042	1.07	41.7	287	9.63	66.35	9.04	62.29	0.111	180,000	2,600	0.44	0.628	109.95
LFHKMA 45%	0.045	1.14	38.2	263	9.28	63.94	8.81	60.70	0.142	44,000	9,100	0.42	0.621	108.77
LFHILMA 40%	0.044	1.12	32.9	227	8.89	61.25	8.45	58.22	0.139	160,000	4,500	0.36	0.446	78.01
LFHMMMA 35%	0.044	1.12	29.5	203	9.15	63.04	8.87	61.11	0.119	2,370,000	890,000	0.33	0.369	64.69
LFHMMC 35%	0.042	1.07	27.5	189	8.88	61.18	8.34	57.46	0.142	7,400,000	2,000,000	0.31	0.321	56.20

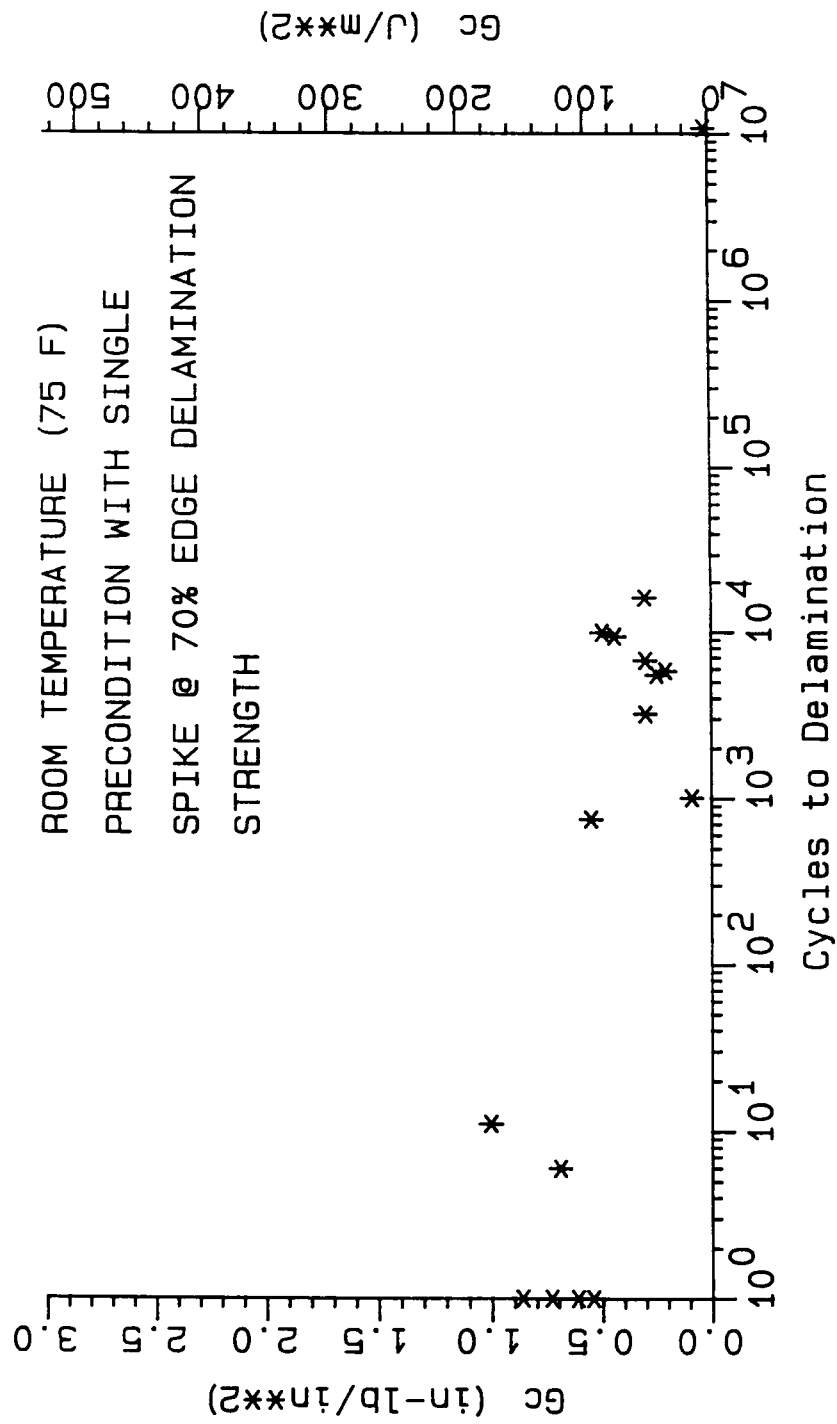
STRAIN ENERGY RELEASE RATE AT ONSET OF DELAMINATION



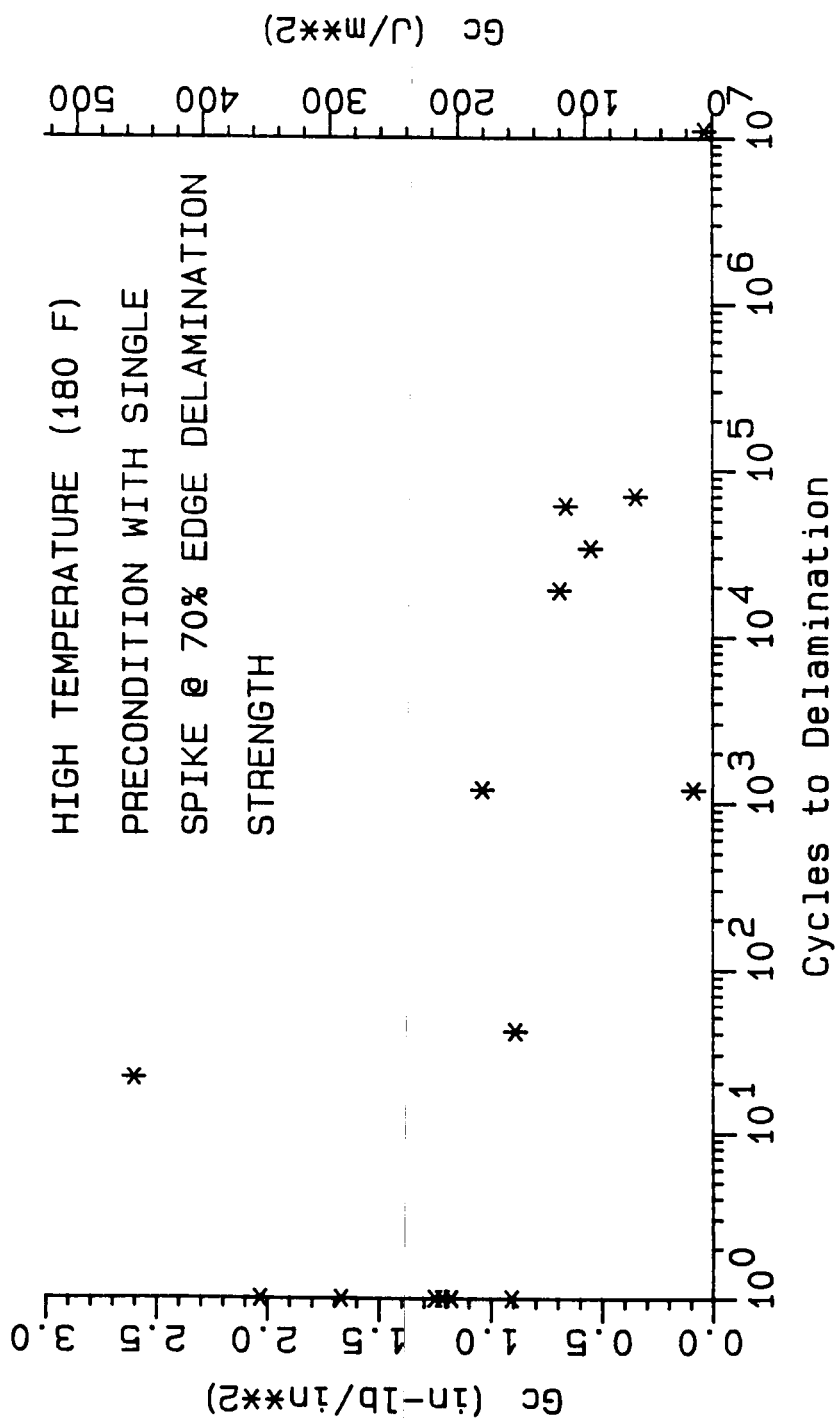
STRAIN ENERGY RELEASE RATE AT ONSET OF DELAMINATION



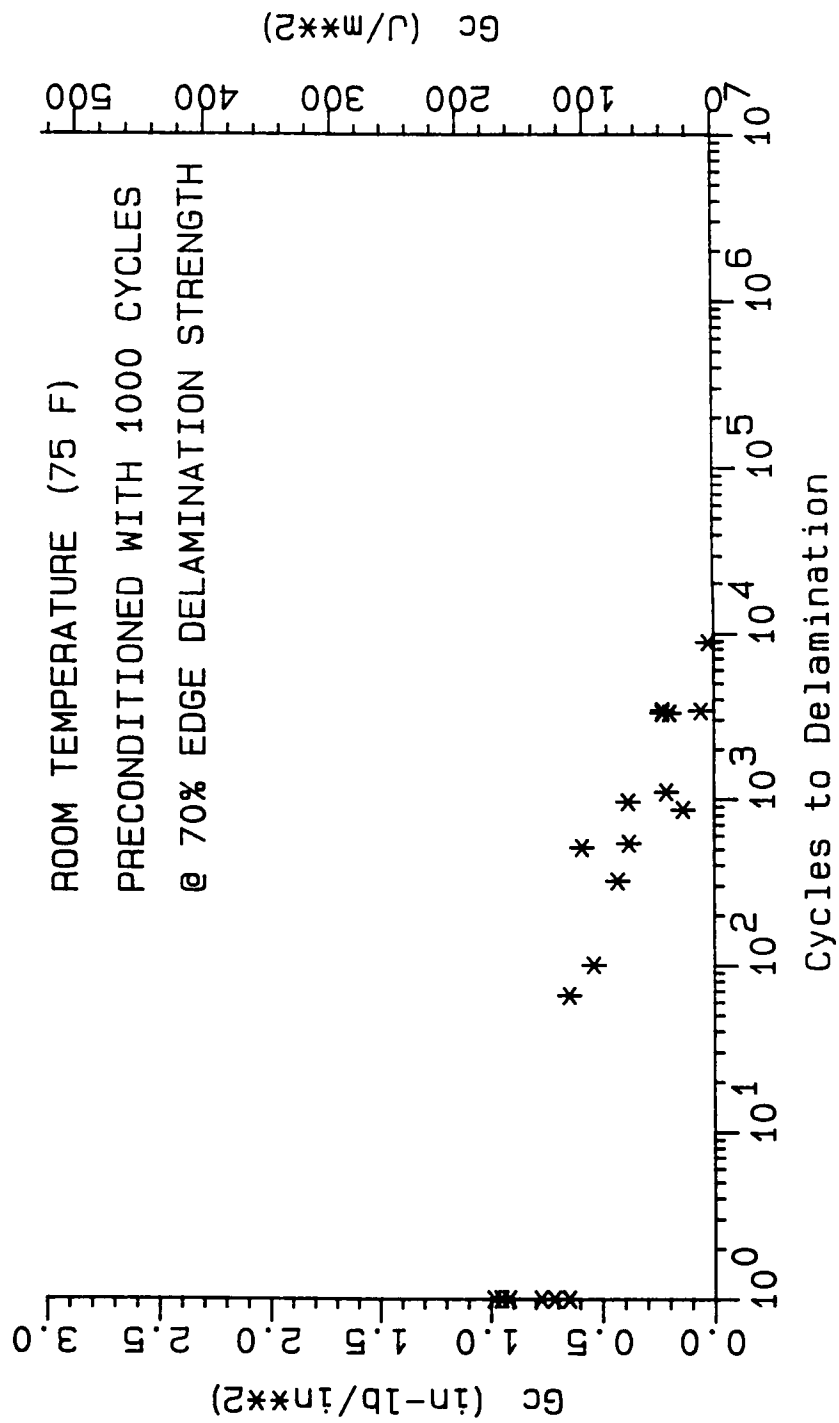
STRAIN ENERGY RELEASE RATE AT ONSET OF DELAMINATION



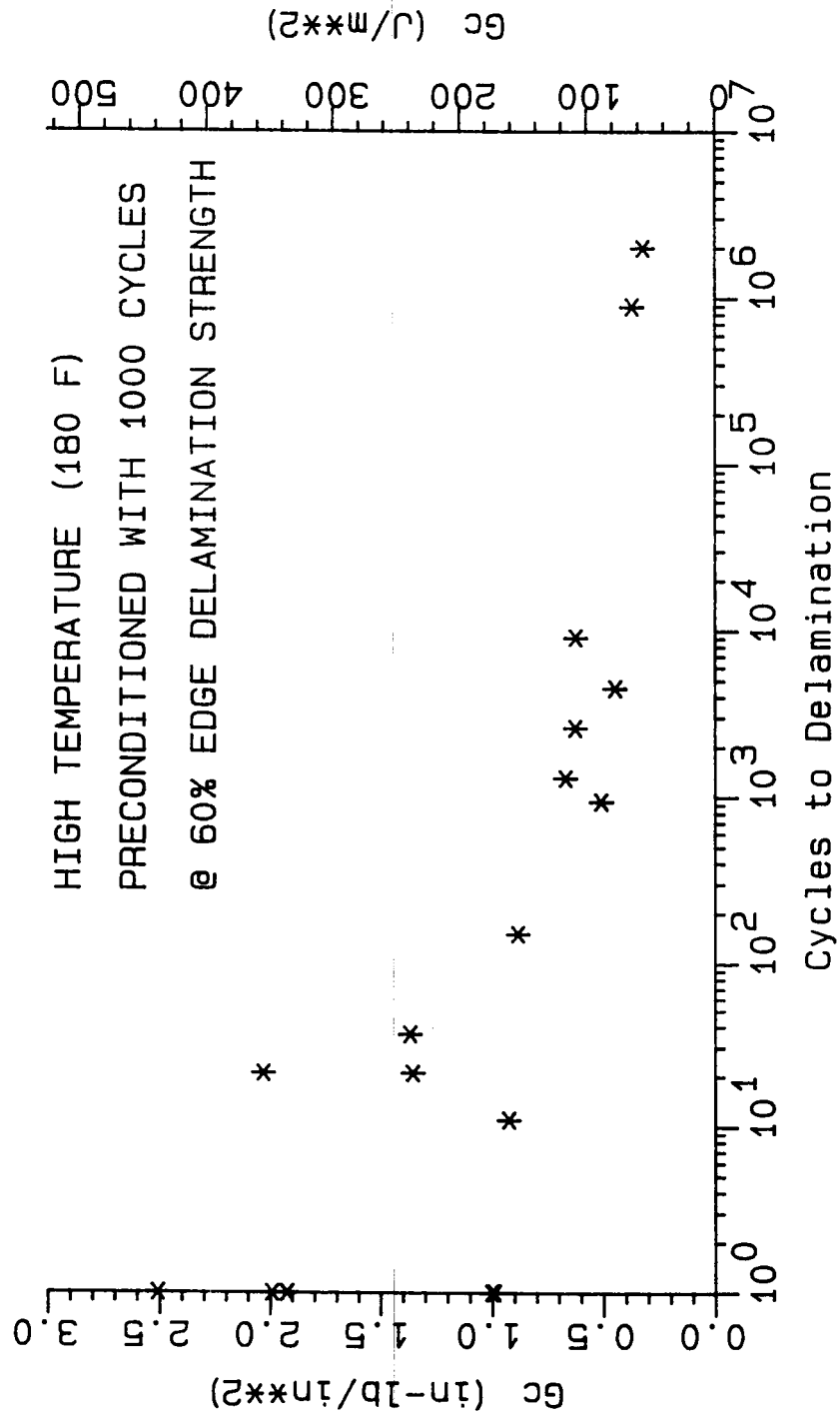
STRAIN ENERGY RELEASE RATE AT ONSET OF DELAMINATION



STRAIN ENERGY RELEASE RATE AT ONSET OF DELAMINATION



STRAIN ENERGY RELEASE RATE AT ONSET OF DELAMINATION

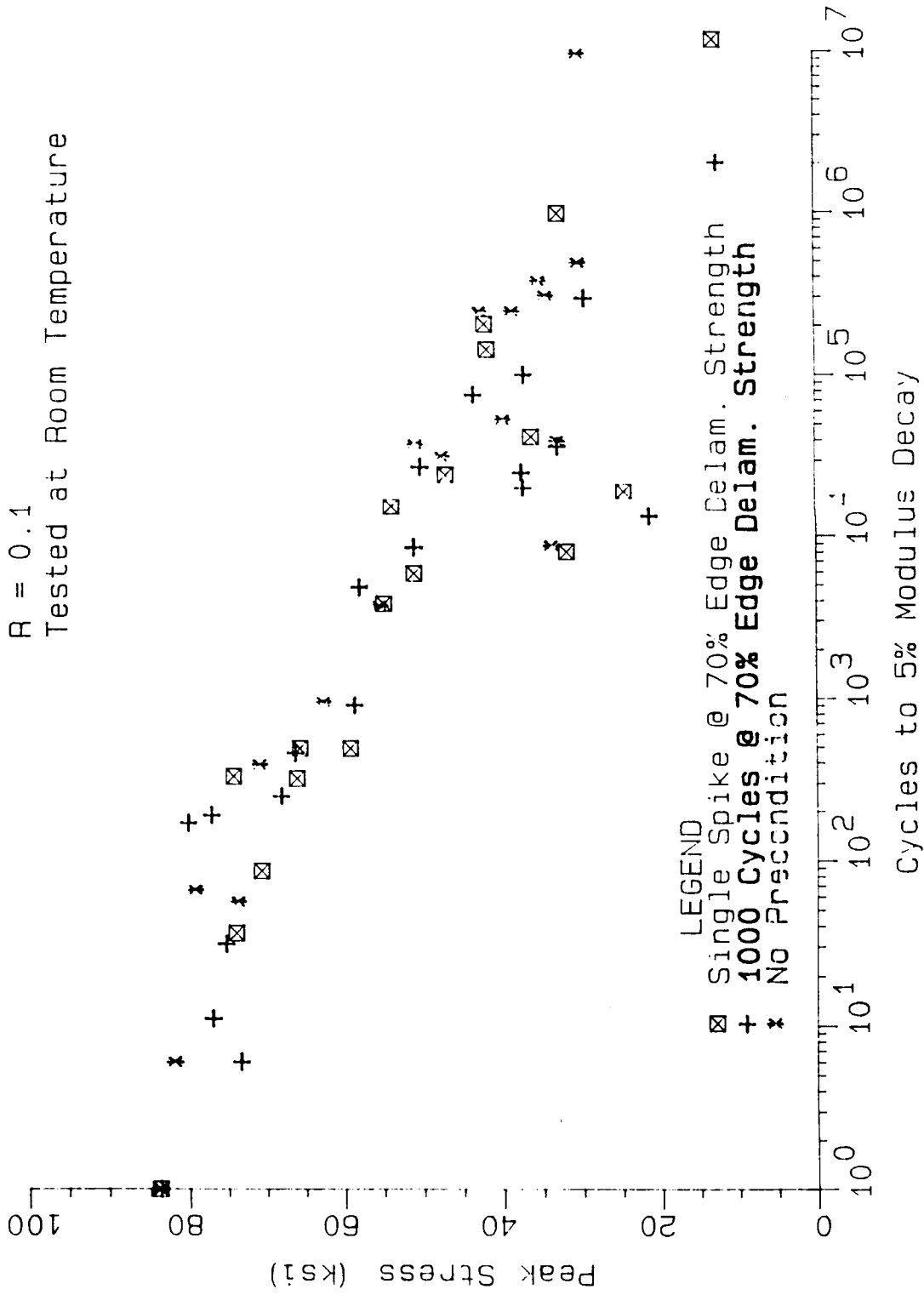


Edge Delam. Tension/Tension Fatigue

IM7/8551-7 [+35, 0, 90]s

R = 0.1

Tested at Room Temperature

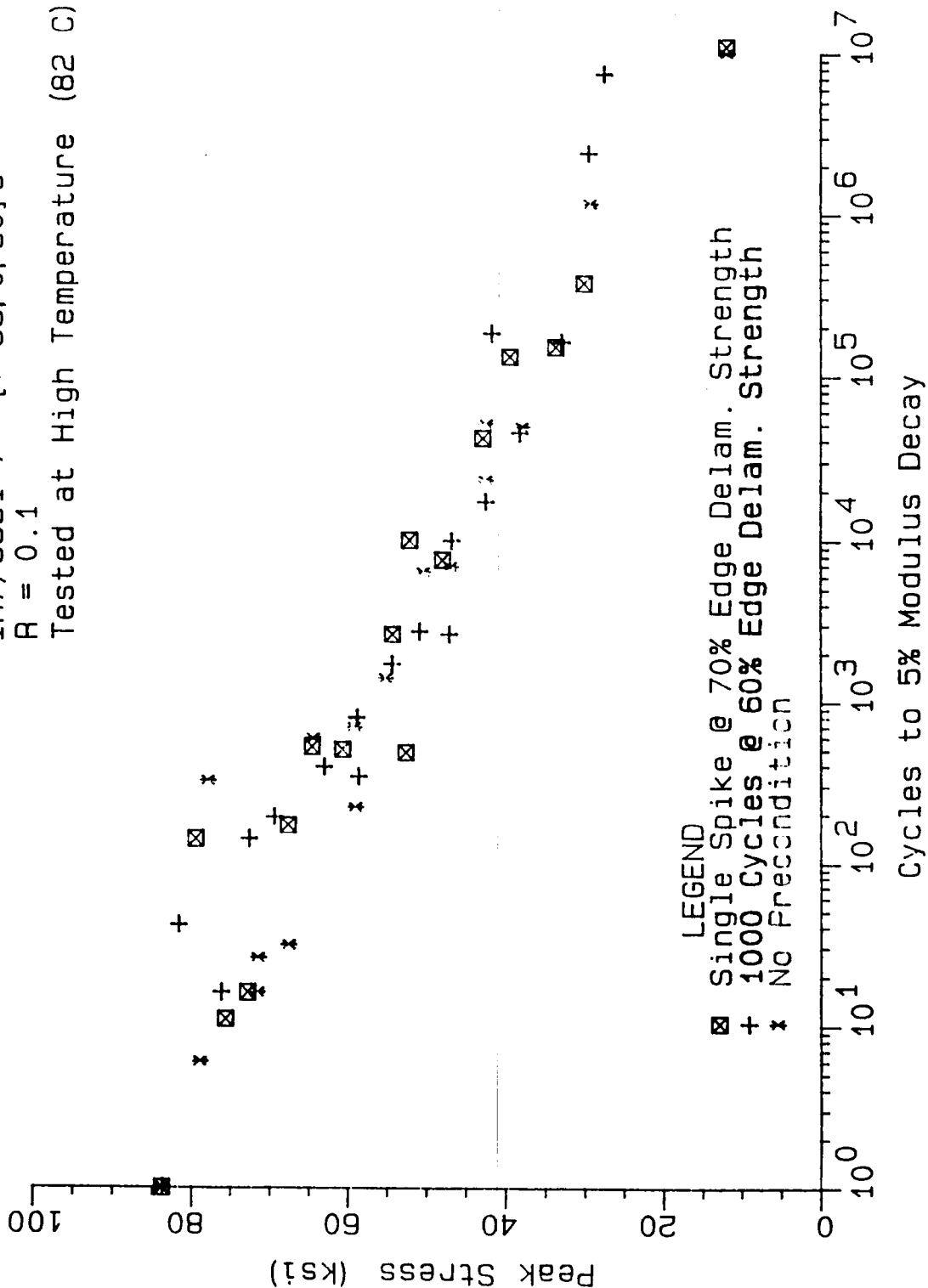


Edge Delam. Tension/Tension Fatigue

IM7/8551-7 [+35, 0, 90]s

R = 0.1

Tested at High Temperature (82 C)

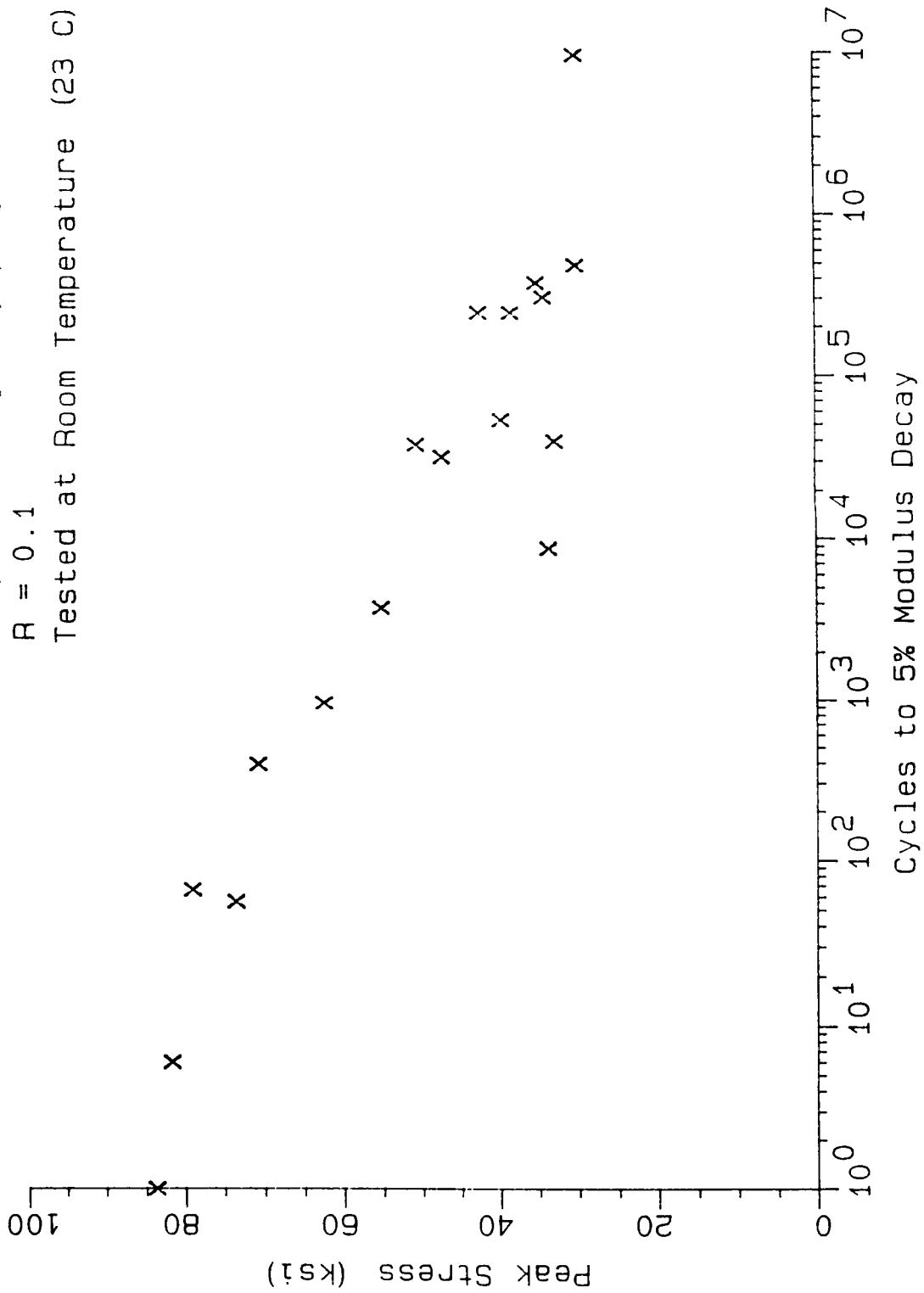


Edge Delam. Tension/Tension Fatigue

IM7/8551-7 [+35, 0, 90]s

R = 0.1

Tested at Room Temperature (23 C)

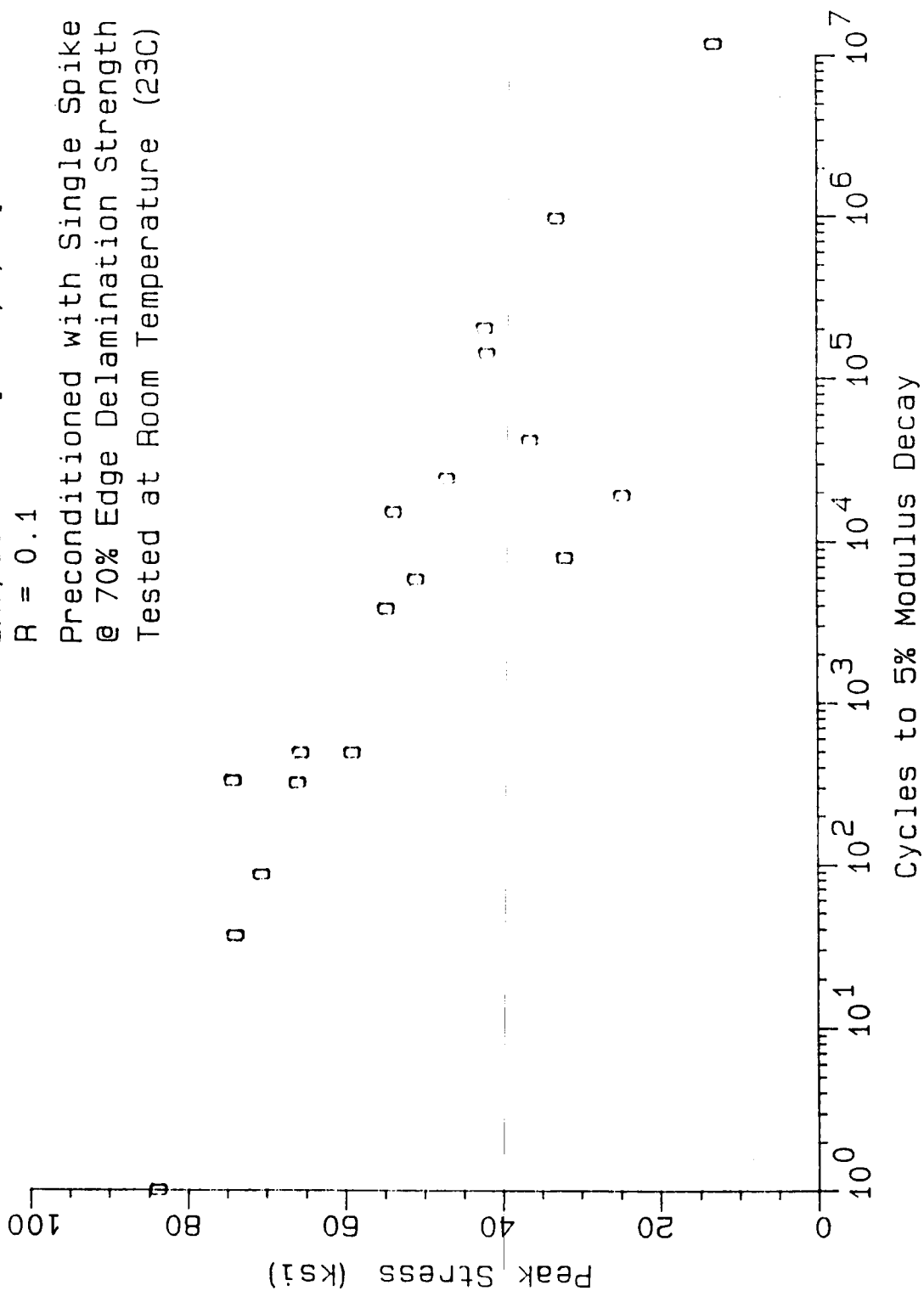


Edge Delam. Tension/Tension Fatigue

IM7/8551-7 [+35, 0, 90]s

R = 0.1

Preconditioned with Single Spike
@ 70% Edge Delamination Strength
Tested at Room Temperature (23C)

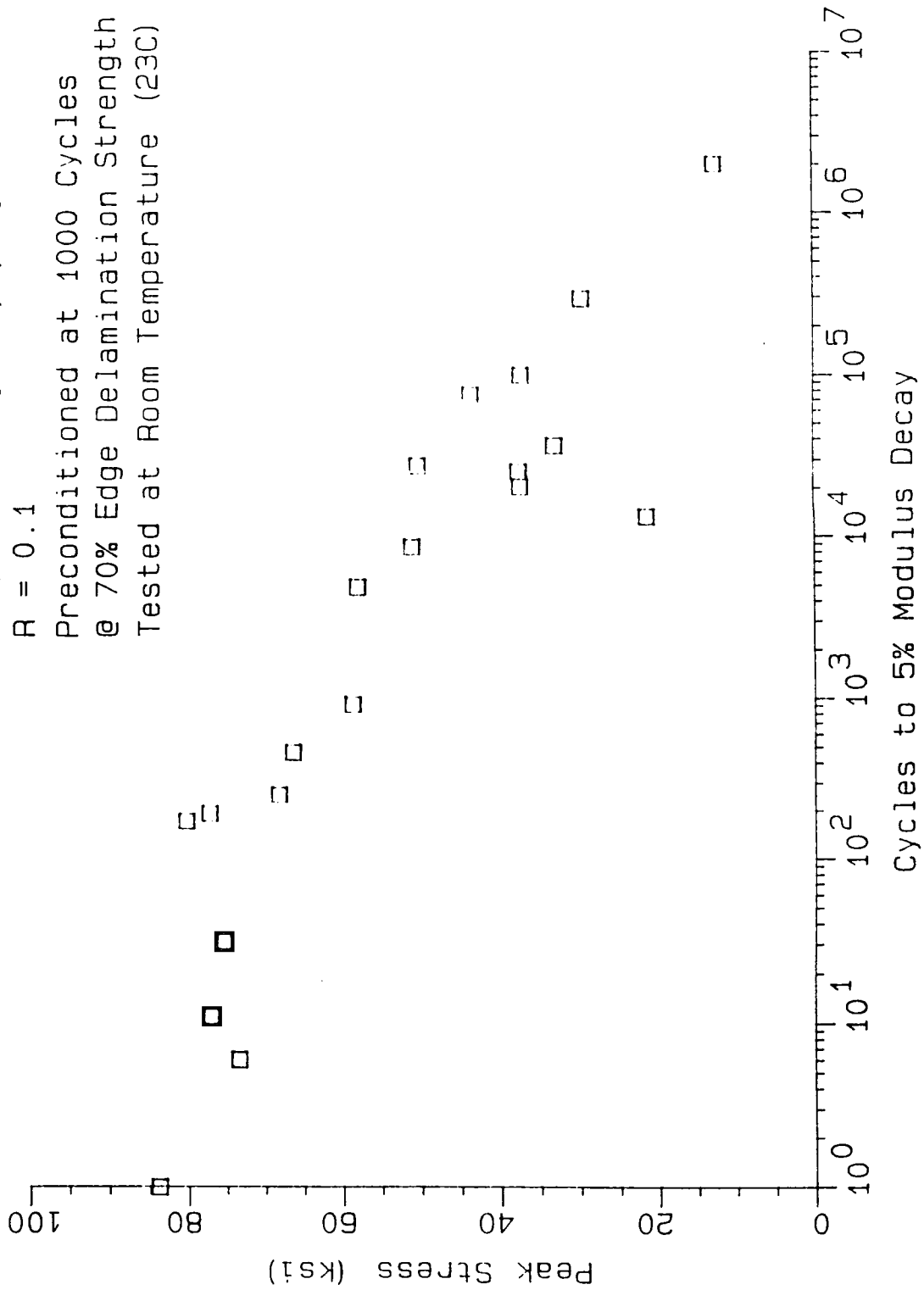


Edge Delam. Tension/Tension Fatigue

IM7/8551-7 [+35, 0, 90]s

R = 0.1

Preconditioned at 1000 Cycles
@ 70% Edge Delamination Strength
Tested at Room Temperature (23C)

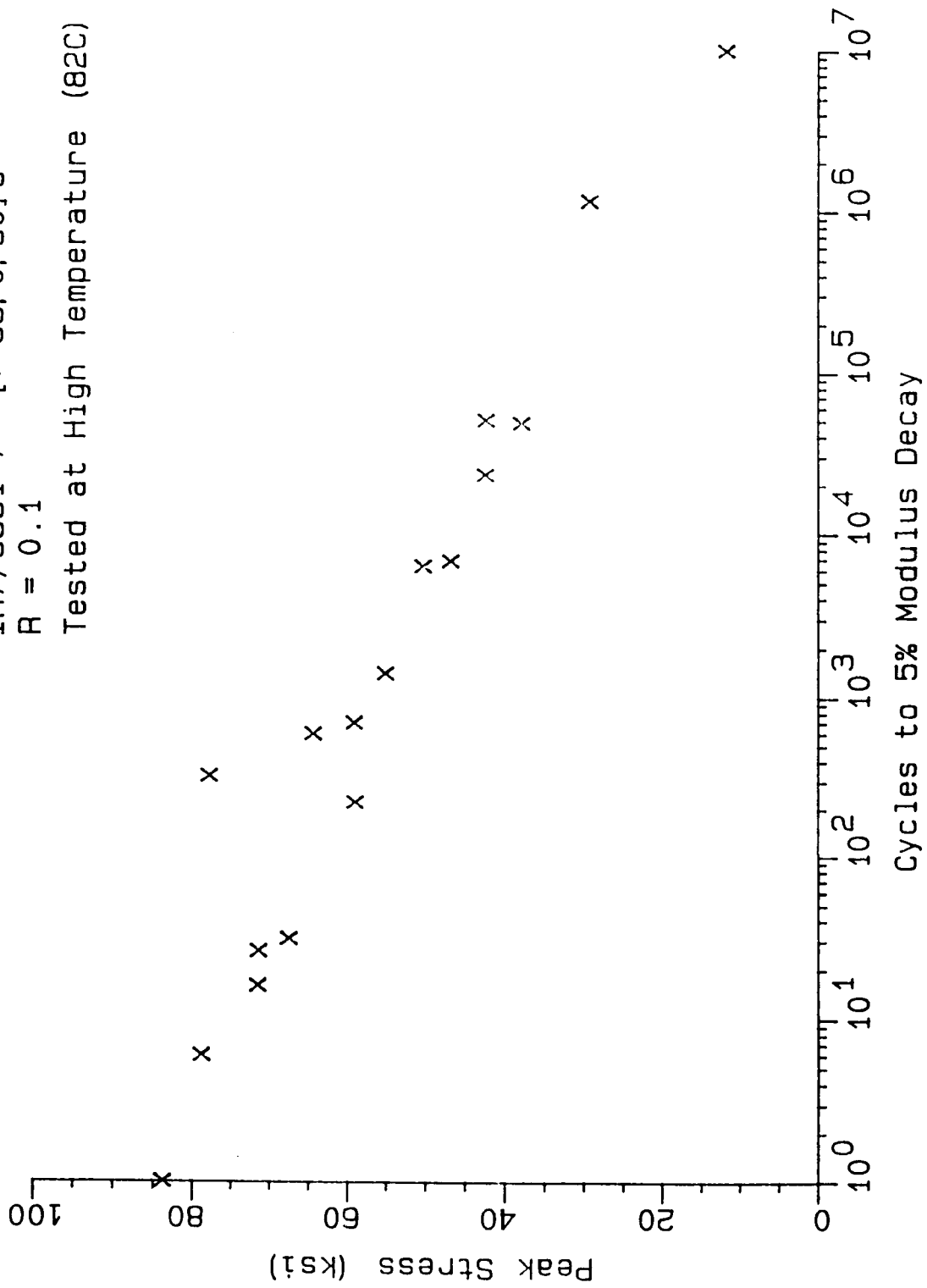


Edge Delam. Tension/Tension Fatigue

IM7/8551-7 [+35, 0, 90] s

R = 0.1

Tested at High Temperature (82C)

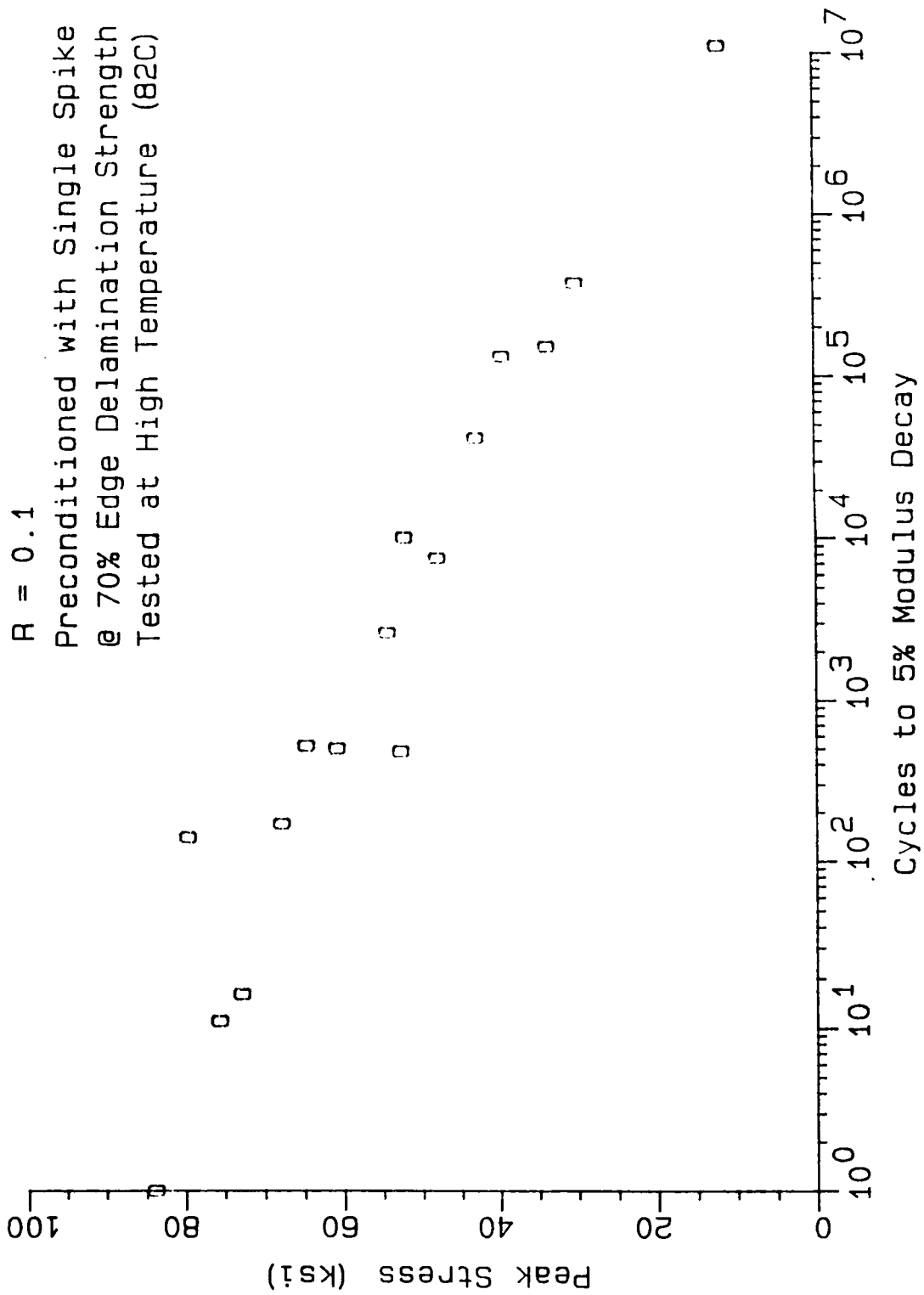


Edge Delam. Tension/Tension Fatigue

IM7/8551-7 [+35, 0, 90]s

R = 0.1

Preconditioned with Single Spike
@ 70% Edge Delamination Strength
Tested at High Temperature (82C)

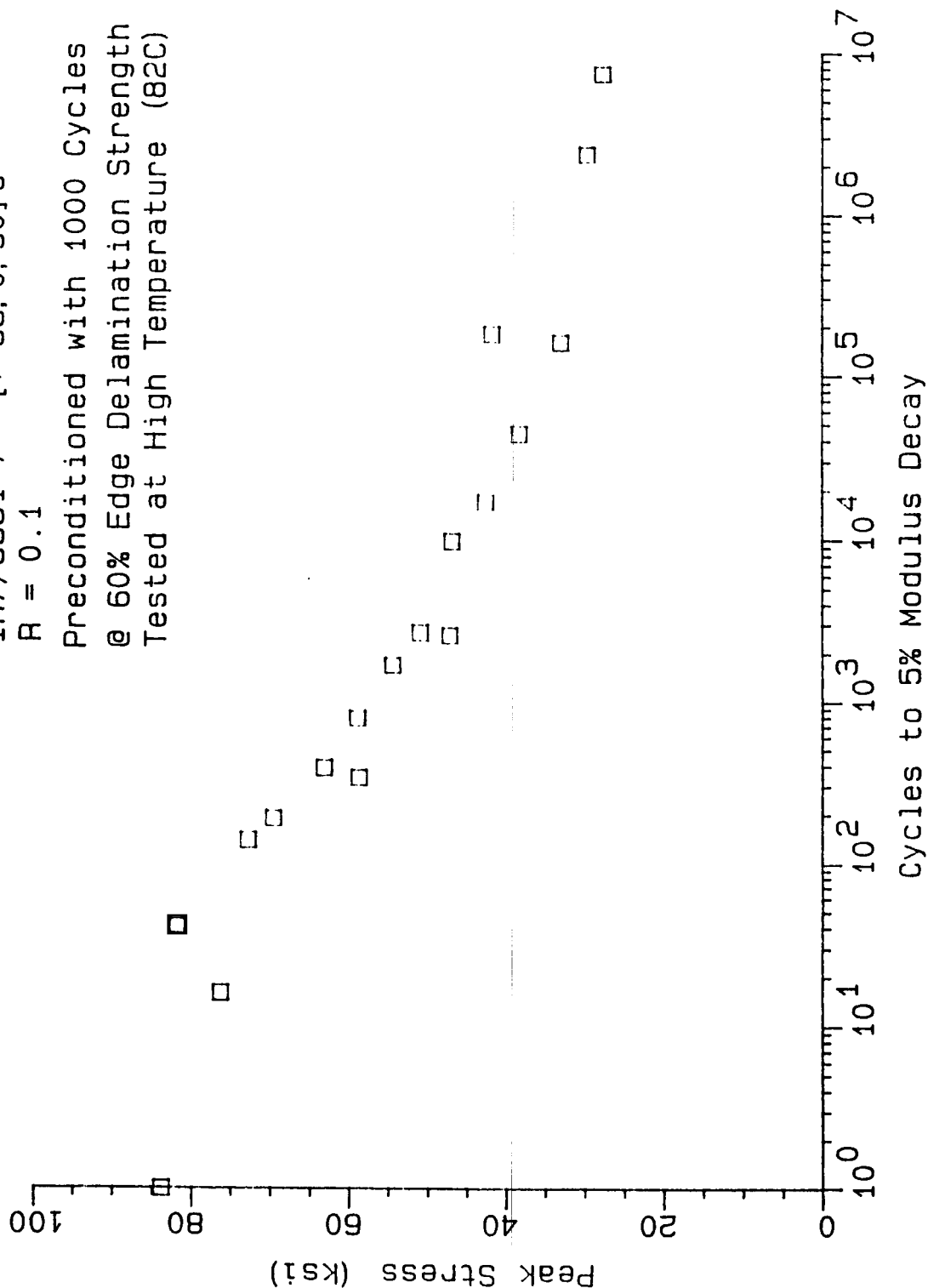


Edge Delam. Tension/Tension Fatigue

IM7/8551-7 [\pm 35, 0, 90]s

R = 0.1

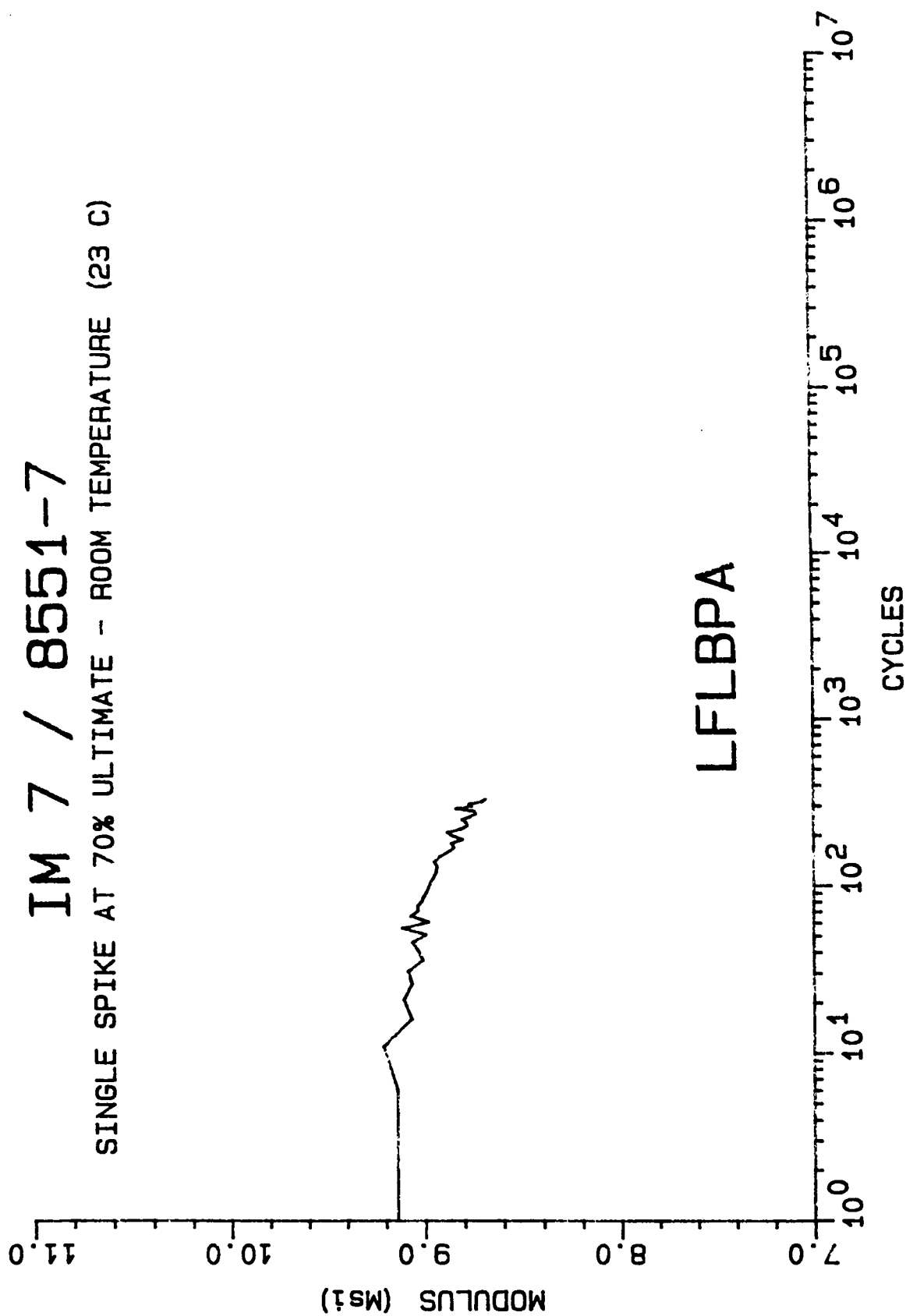
Preconditioned with 1000 Cycles
@ 60% Edge Delamination Strength
Tested at High Temperature (82C)



MODULUS DECAY CURVE

IM 7 / 8551-7

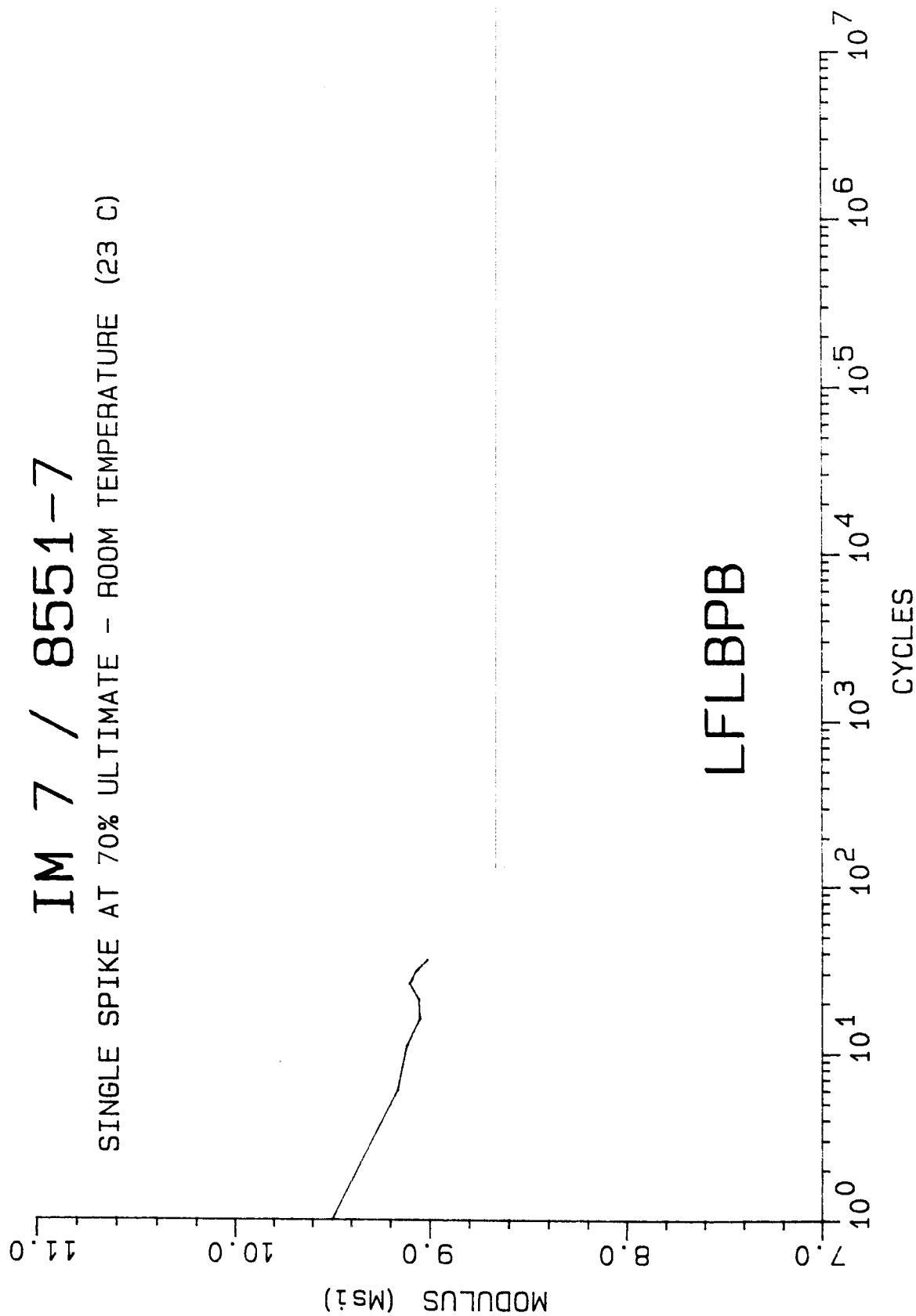
SINGLE SPIKE AT 70% ULTIMATE - ROOM TEMPERATURE (23 C)



MODULUS DECAY CURVE

IM 7 / 8551-7

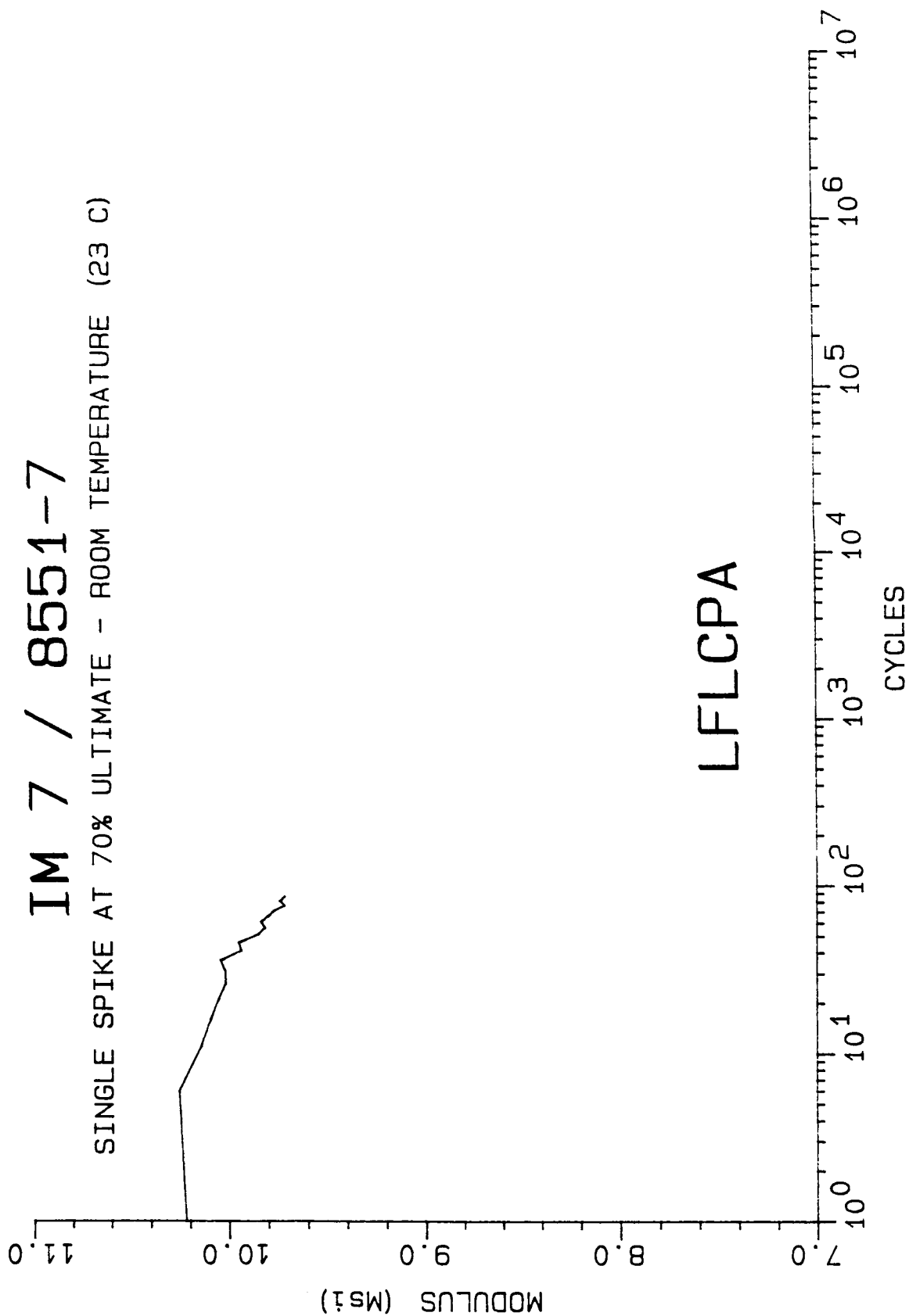
SINGLE SPIKE AT 70% ULTIMATE - ROOM TEMPERATURE (23 C)



MODULUS DECAY CURVE

IM 7 / 8551-7

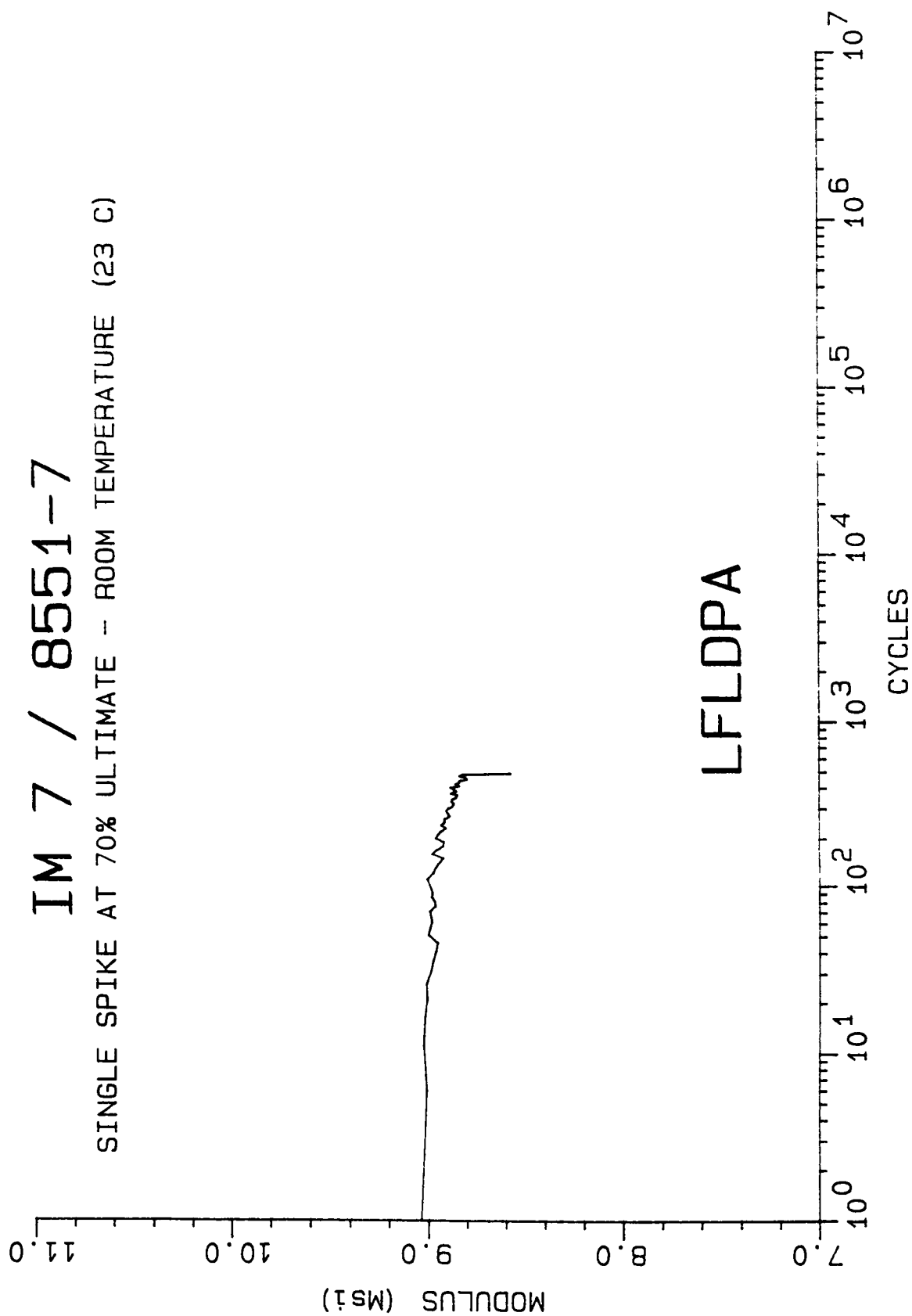
SINGLE SPIKE AT 70% ULTIMATE - ROOM TEMPERATURE (23 C)



MODULUS DECAY CURVE

IM 7 / 8551-7

SINGLE SPIKE AT 70% ULTIMATE - ROOM TEMPERATURE (23 C)

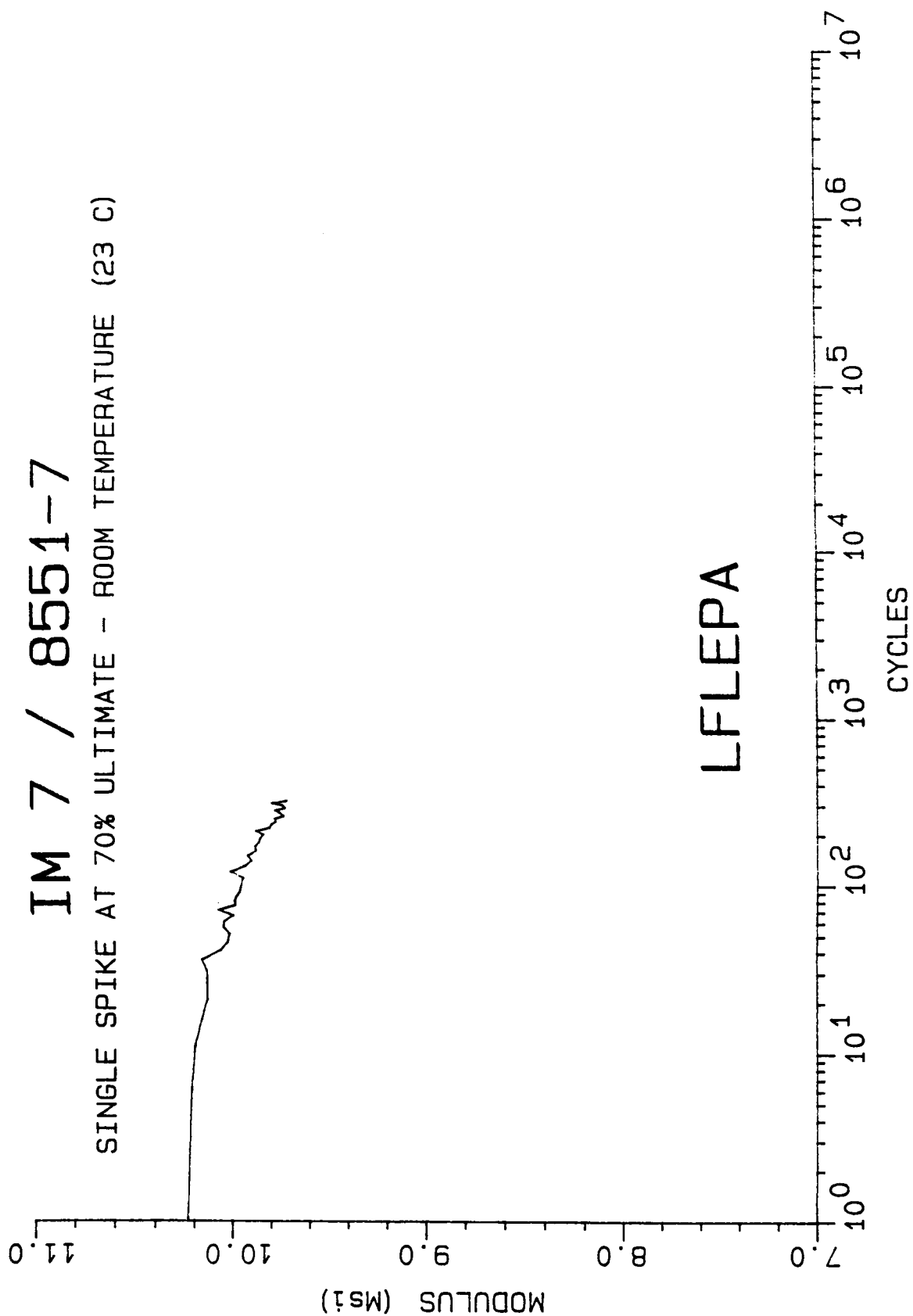


LFLDPA

MODULUS DECAY CURVE

IM 7 / 8551-7

SINGLE SPIKE AT 70% ULTIMATE - ROOM TEMPERATURE (23 C)

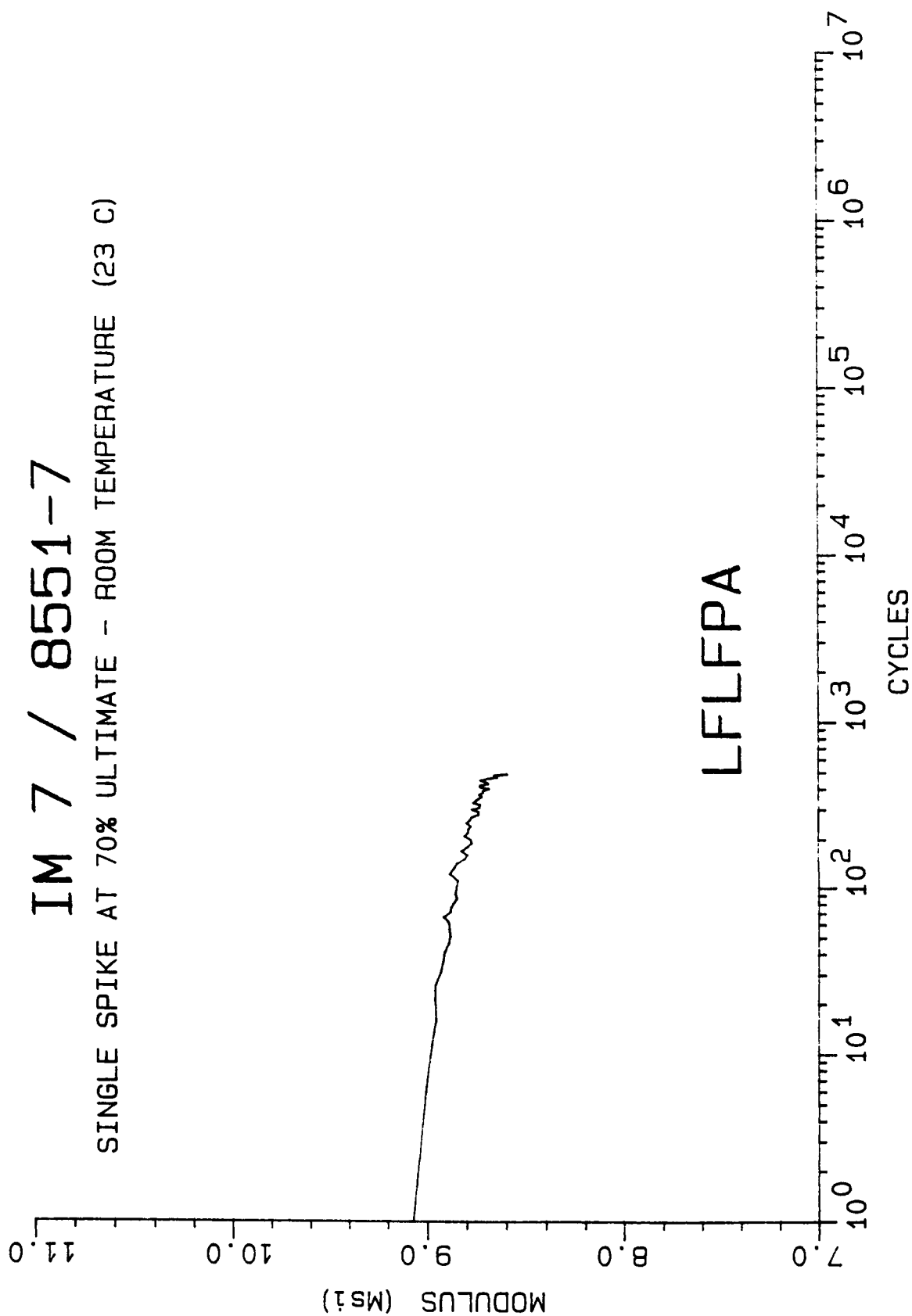


LFLEPA

MODULUS DECAY CURVE

IM 7 / 8551-7

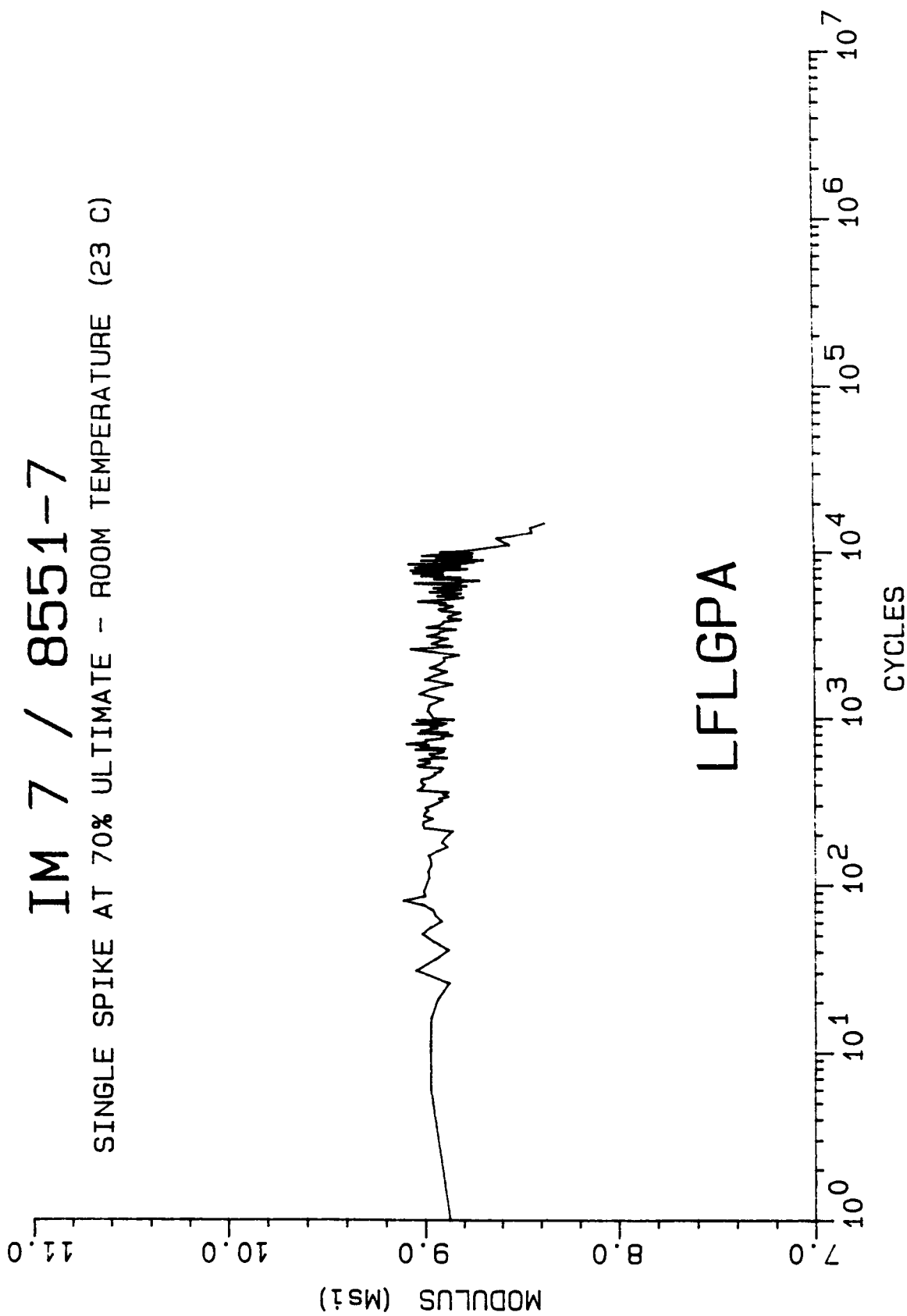
SINGLE SPIKE AT 70% ULTIMATE - ROOM TEMPERATURE (23 C)



MODULUS DECAY CURVE

IM 7 / 8551-7

SINGLE SPIKE AT 70% ULTIMATE - ROOM TEMPERATURE (23 C)

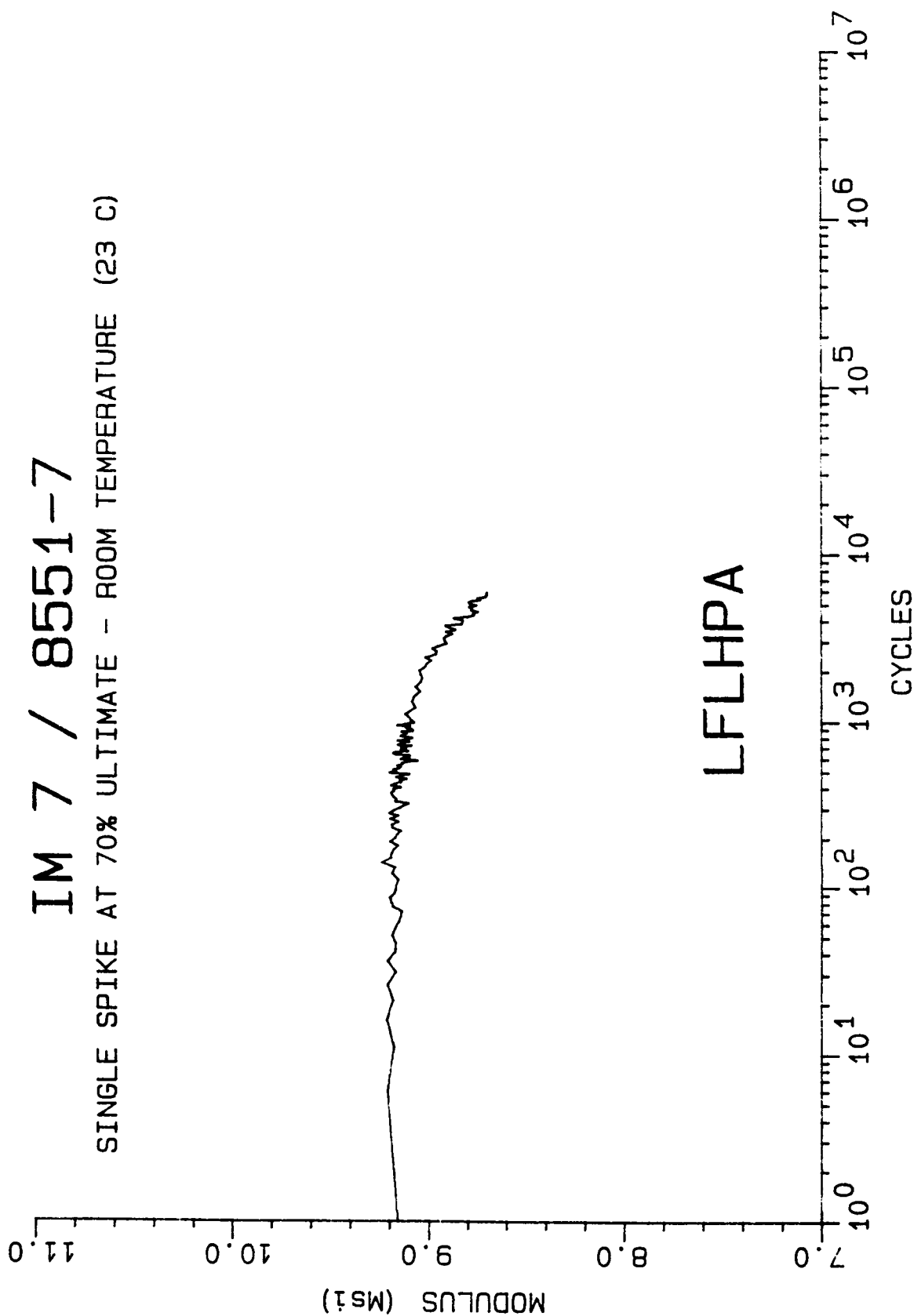


LFLGPA

MODULUS DECAY CURVE

IM 7 / 8551-7

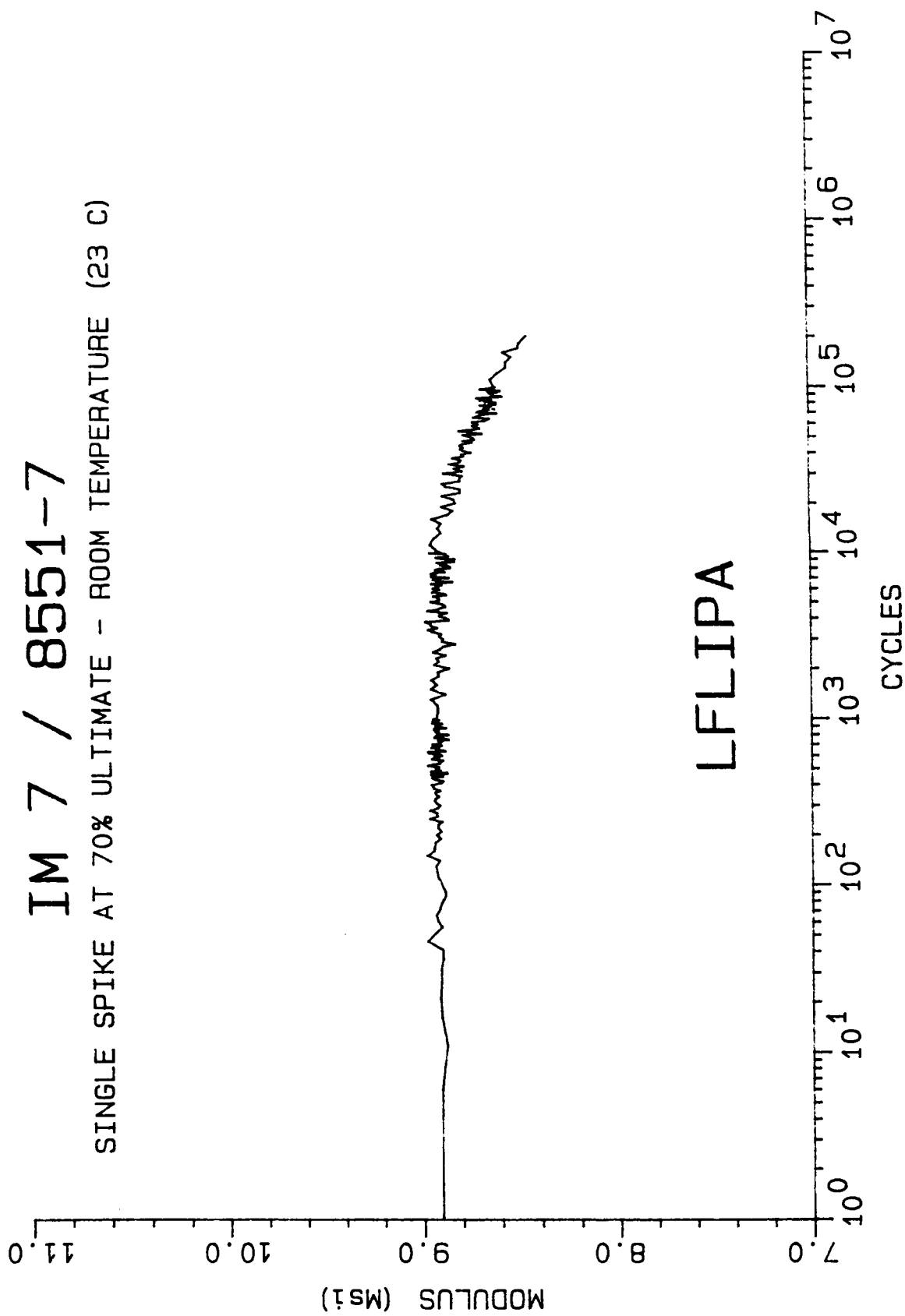
SINGLE SPIKE AT 70% ULTIMATE - ROOM TEMPERATURE (23 C)



MODULUS DECAY CURVE

IM 7 / 8551-7

SINGLE SPIKE AT 70% ULTIMATE - ROOM TEMPERATURE (23 C)

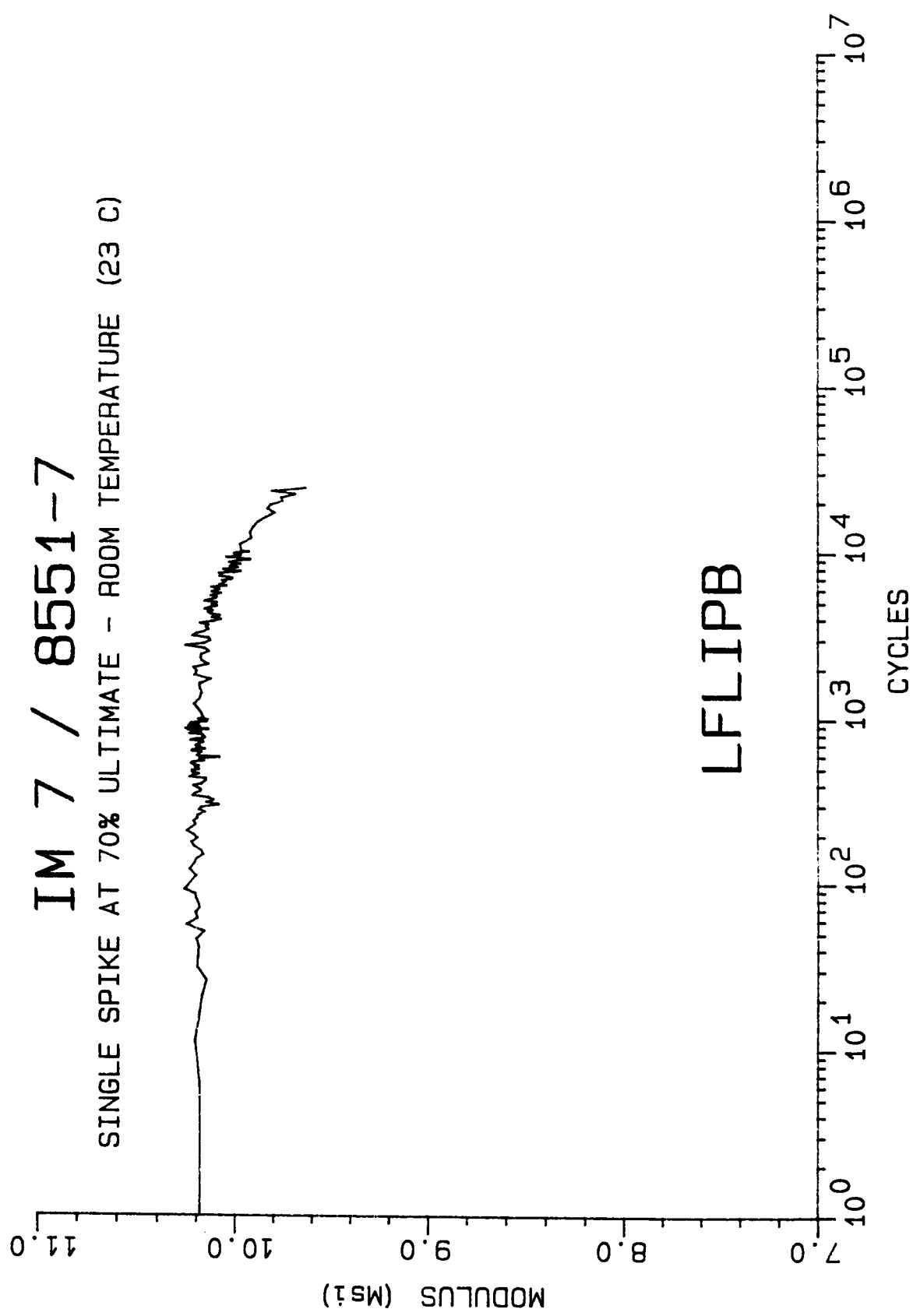


LFLIPA

MODULUS DECAY CURVE

IM 7 / 8551-7

SINGLE SPIKE AT 70% ULTIMATE - ROOM TEMPERATURE (23 C)

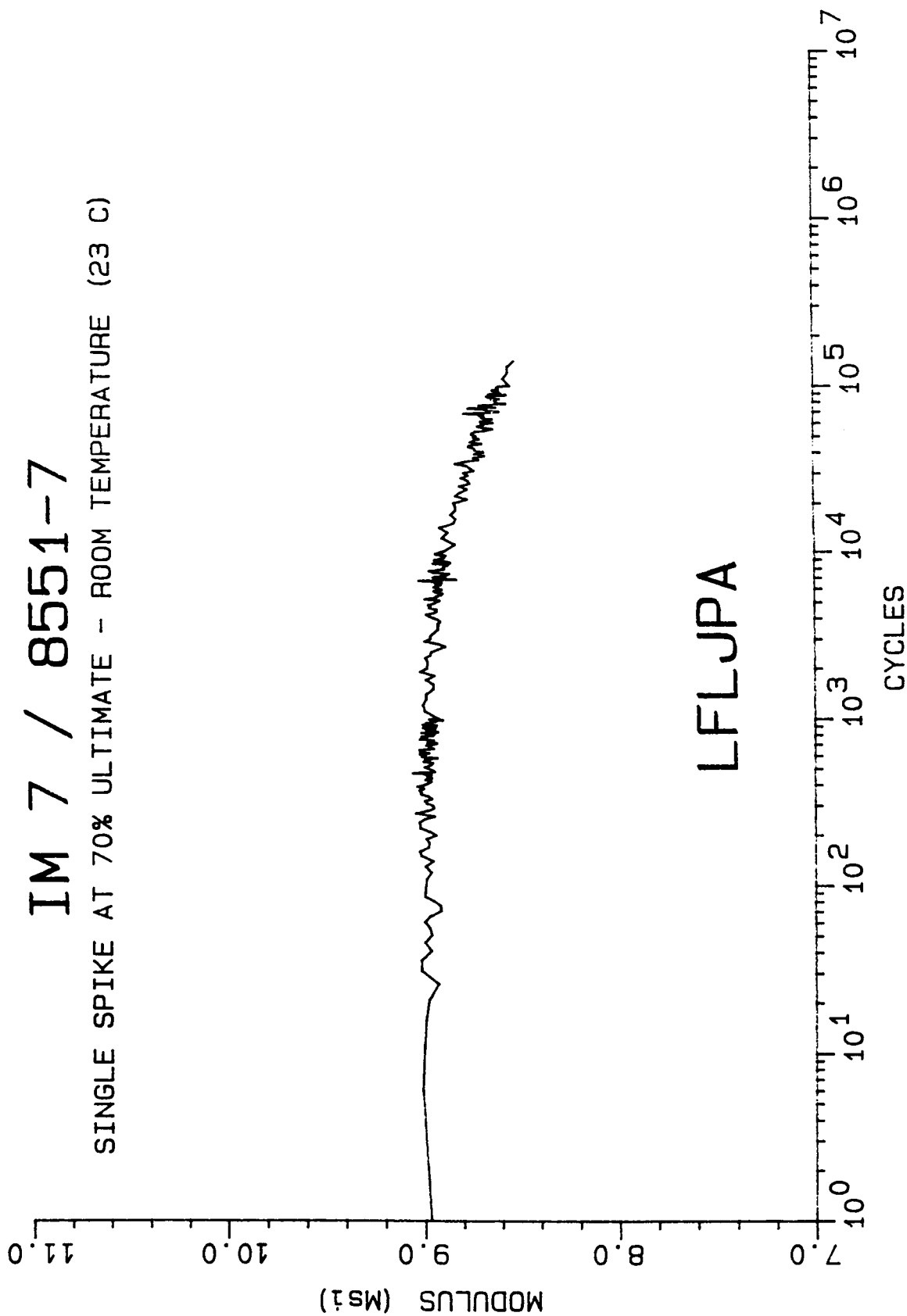


LFLIPB

MODULUS DECAY CURVE

IM 7 / 8551-7

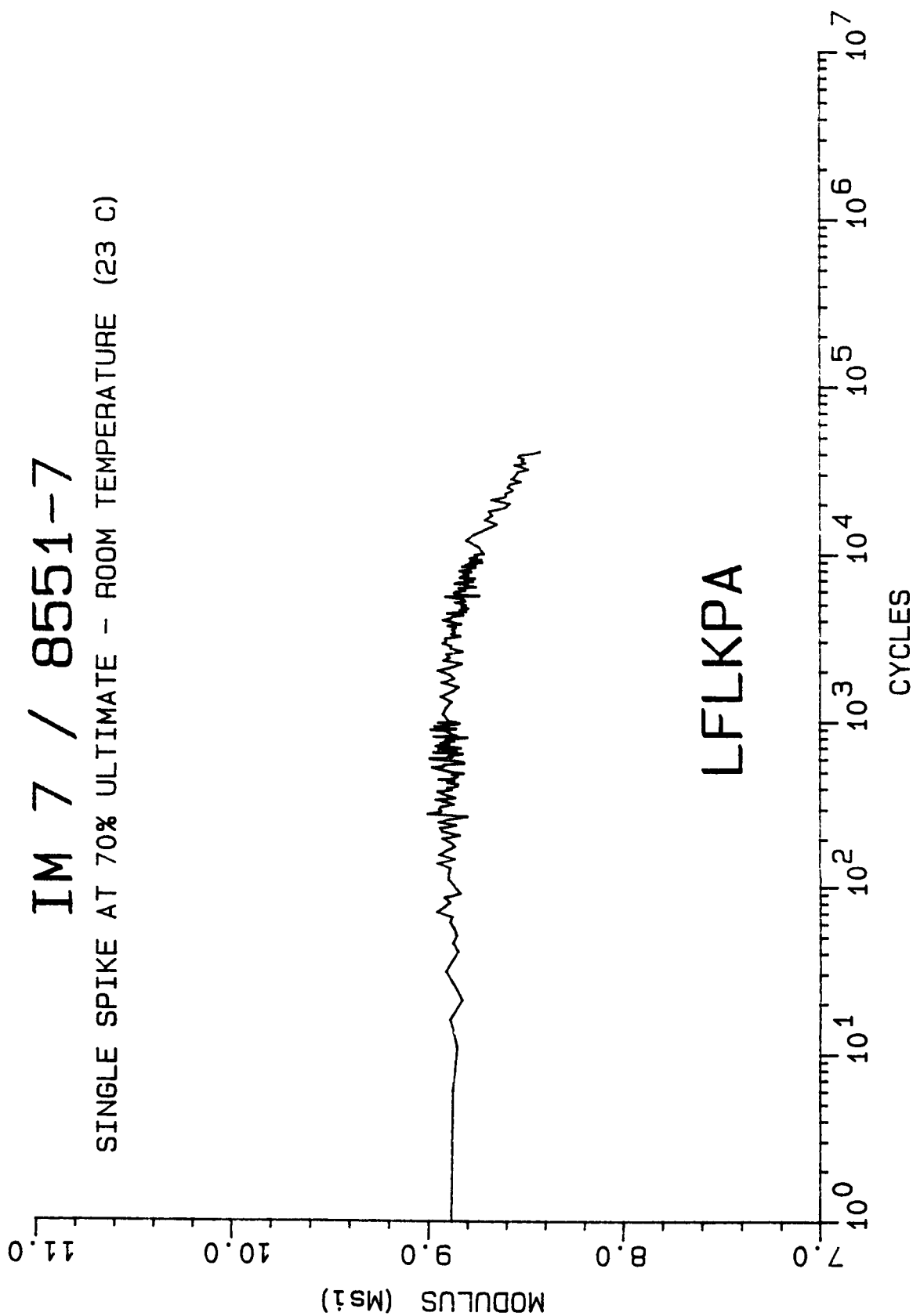
SINGLE SPIKE AT 70% ULTIMATE - ROOM TEMPERATURE (23 C)



MODULUS DECAY CURVE

IM 7 / 8551-7

SINGLE SPIKE AT 70% ULTIMATE - ROOM TEMPERATURE (23 C)

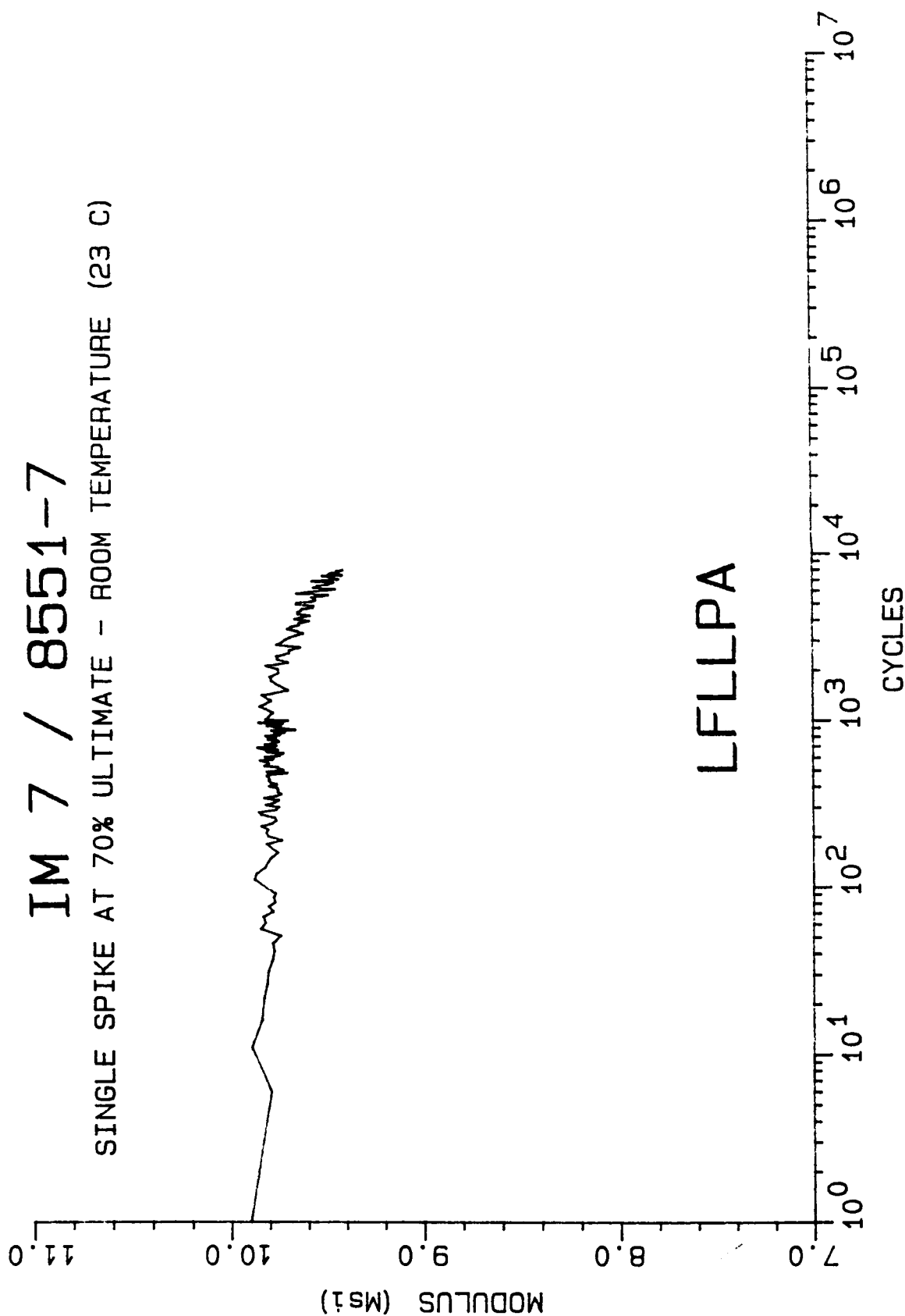


LFLKPA

MODULUS DECAY CURVE

IM 7 / 8551-7

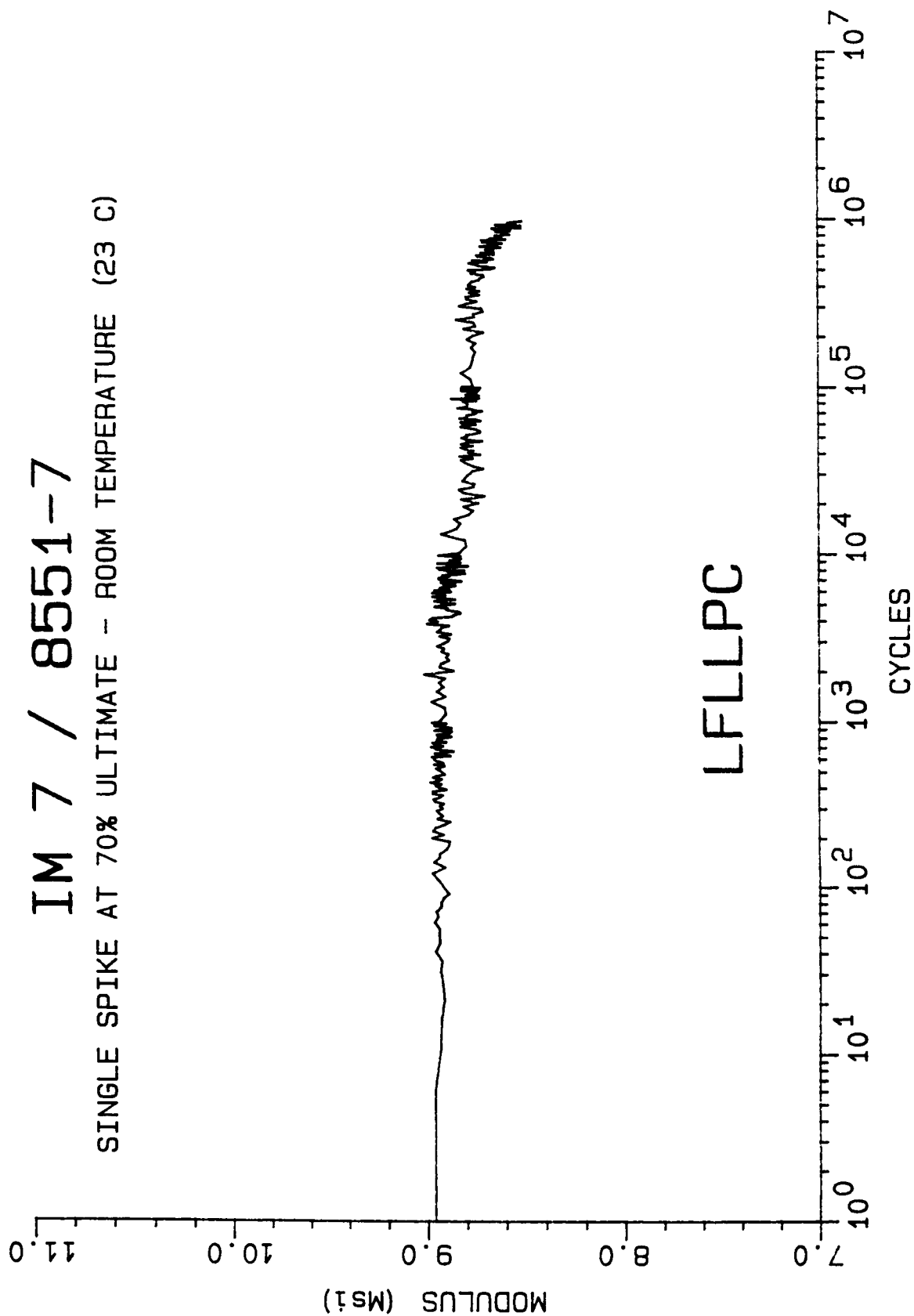
SINGLE SPIKE AT 70% ULTIMATE - ROOM TEMPERATURE (23 C)



MODULUS DECAY CURVE

IM 7 / 8551-7

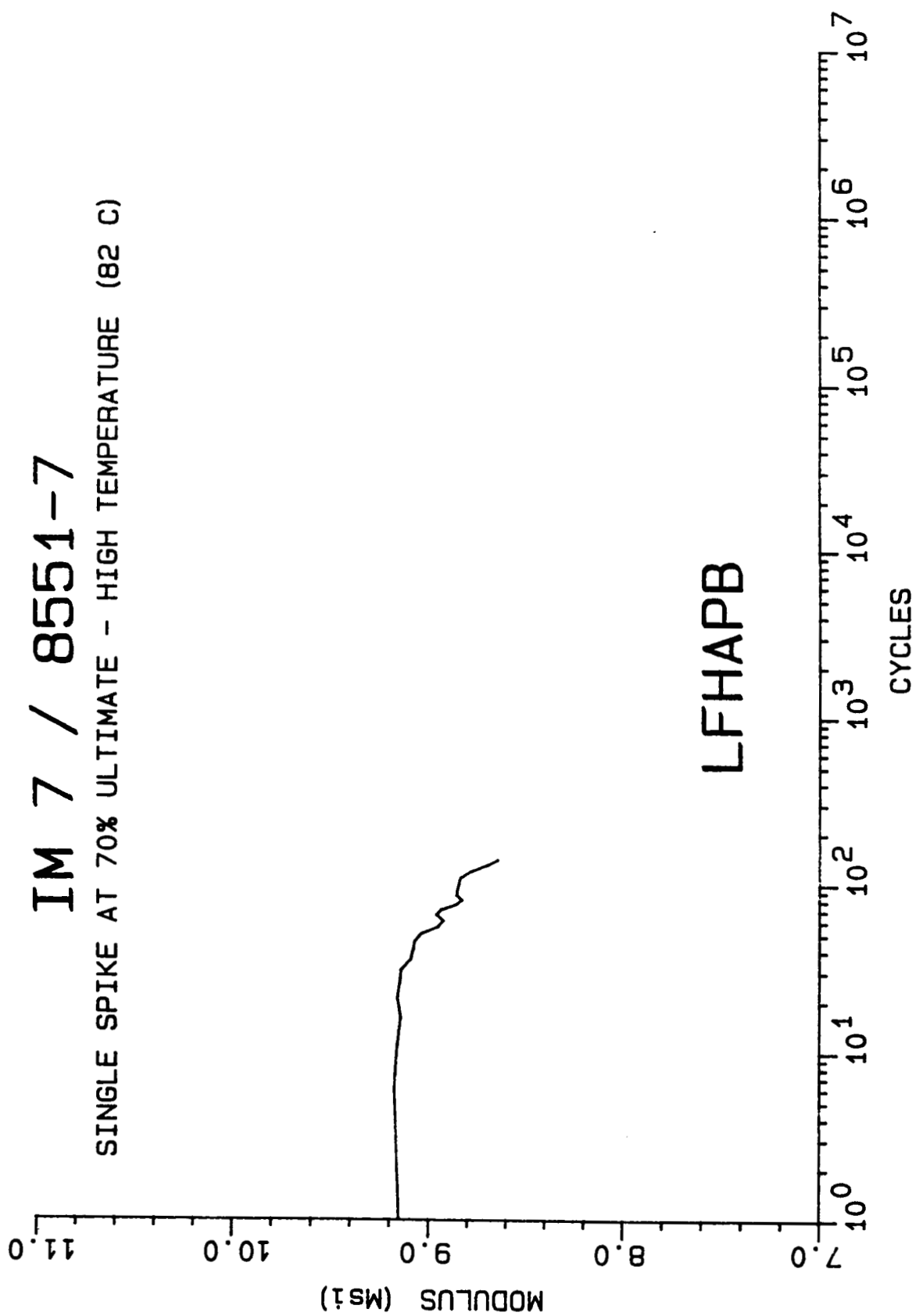
SINGLE SPIKE AT 70% ULTIMATE - ROOM TEMPERATURE (23 C)



MODULUS DECAY CURVE

IM 7 / 8551-7

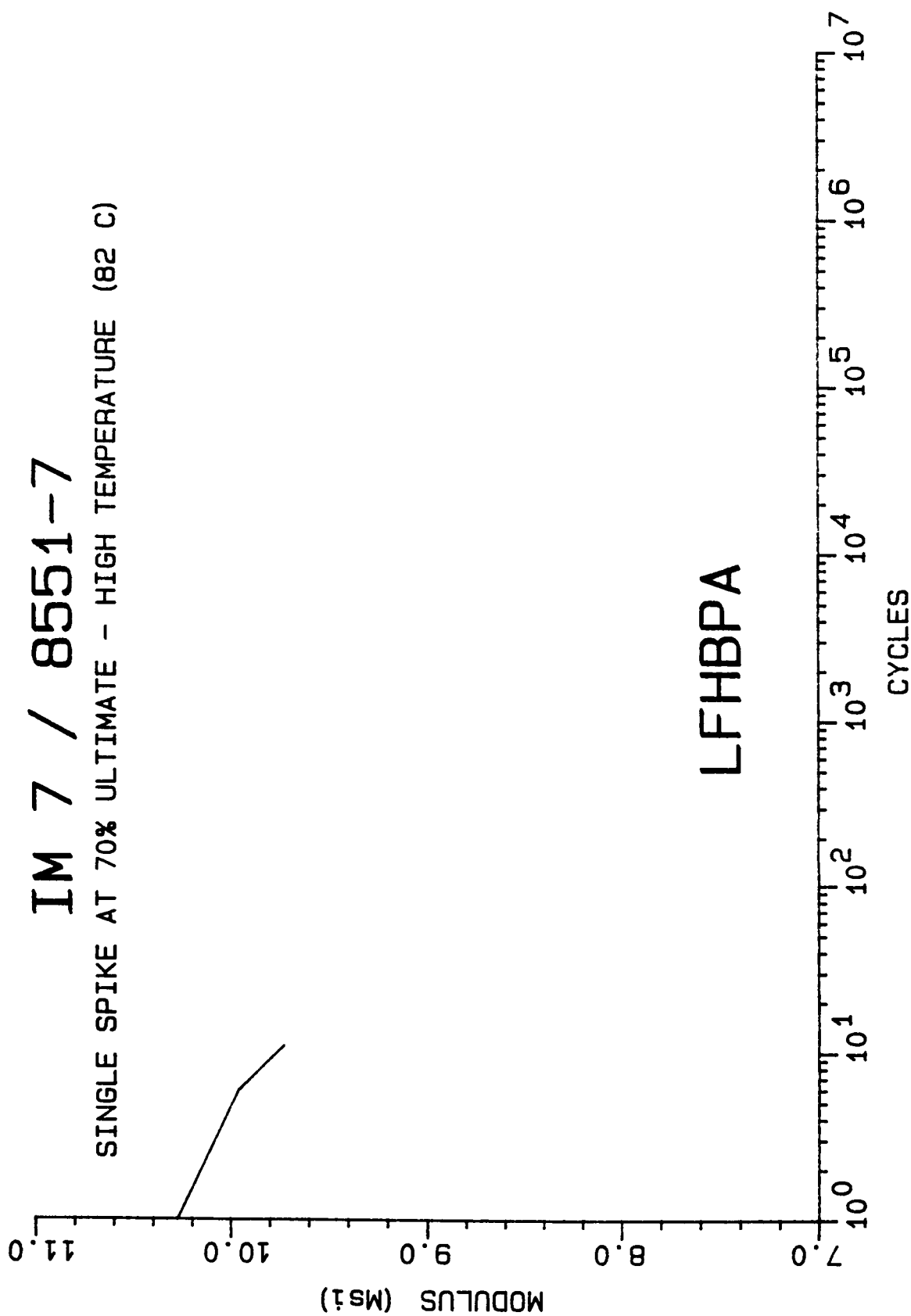
SINGLE SPIKE AT 70% ULTIMATE - HIGH TEMPERATURE (82 C)



MODULUS DECAY CURVE

IM 7 / 8551-7

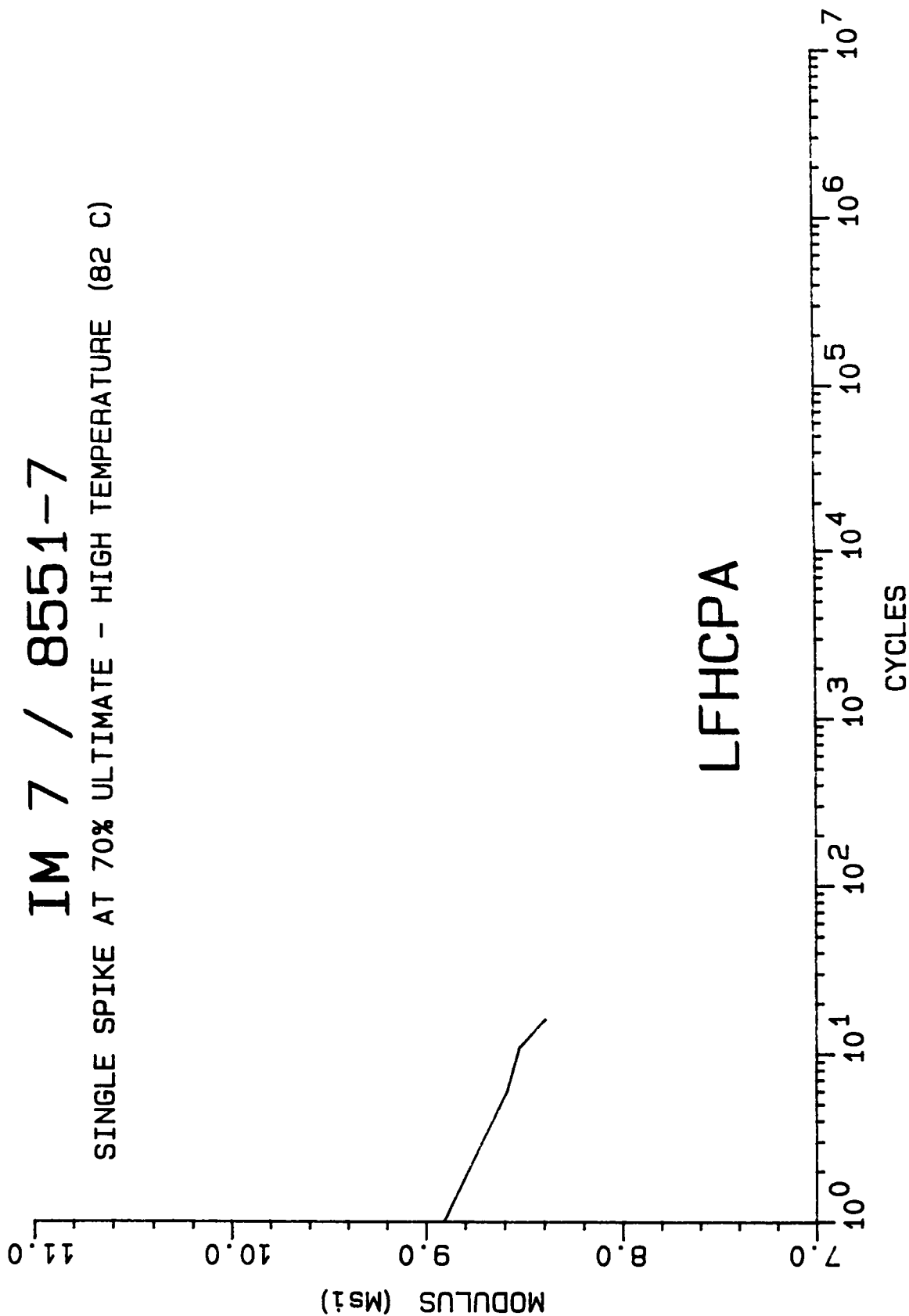
SINGLE SPIKE AT 70% ULTIMATE - HIGH TEMPERATURE (82 C)



MODULUS DECAY CURVE

IM 7 / 8551-7

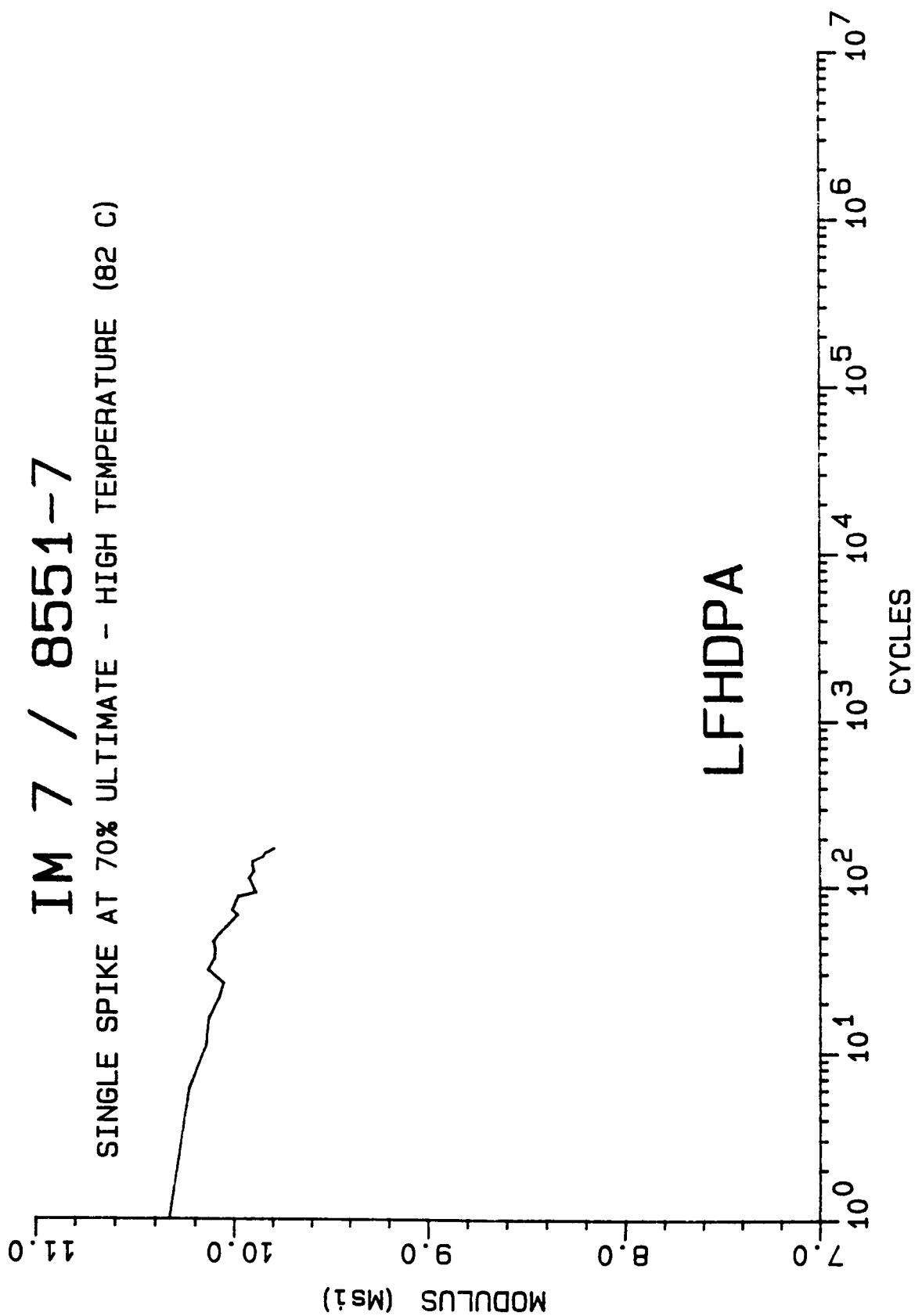
SINGLE SPIKE AT 70% ULTIMATE - HIGH TEMPERATURE (82 C)



MODULUS DECAY CURVE

IM 7 / 8551--7

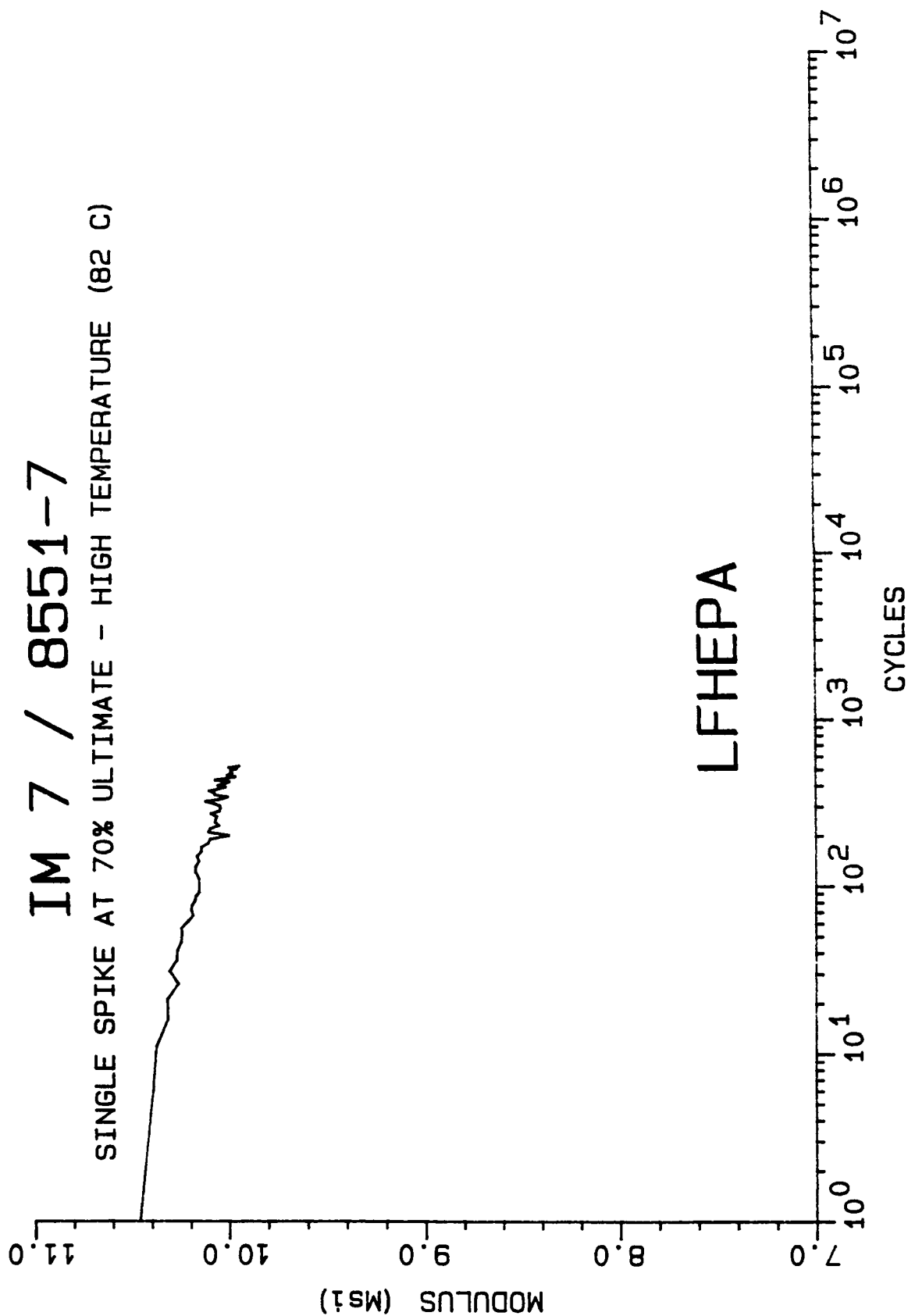
SINGLE SPIKE AT 70% ULTIMATE - HIGH TEMPERATURE (82 C)



MODULUS DECAY CURVE

IM 7 / 8551-7

SINGLE SPIKE AT 70% ULTIMATE - HIGH TEMPERATURE (82 C)

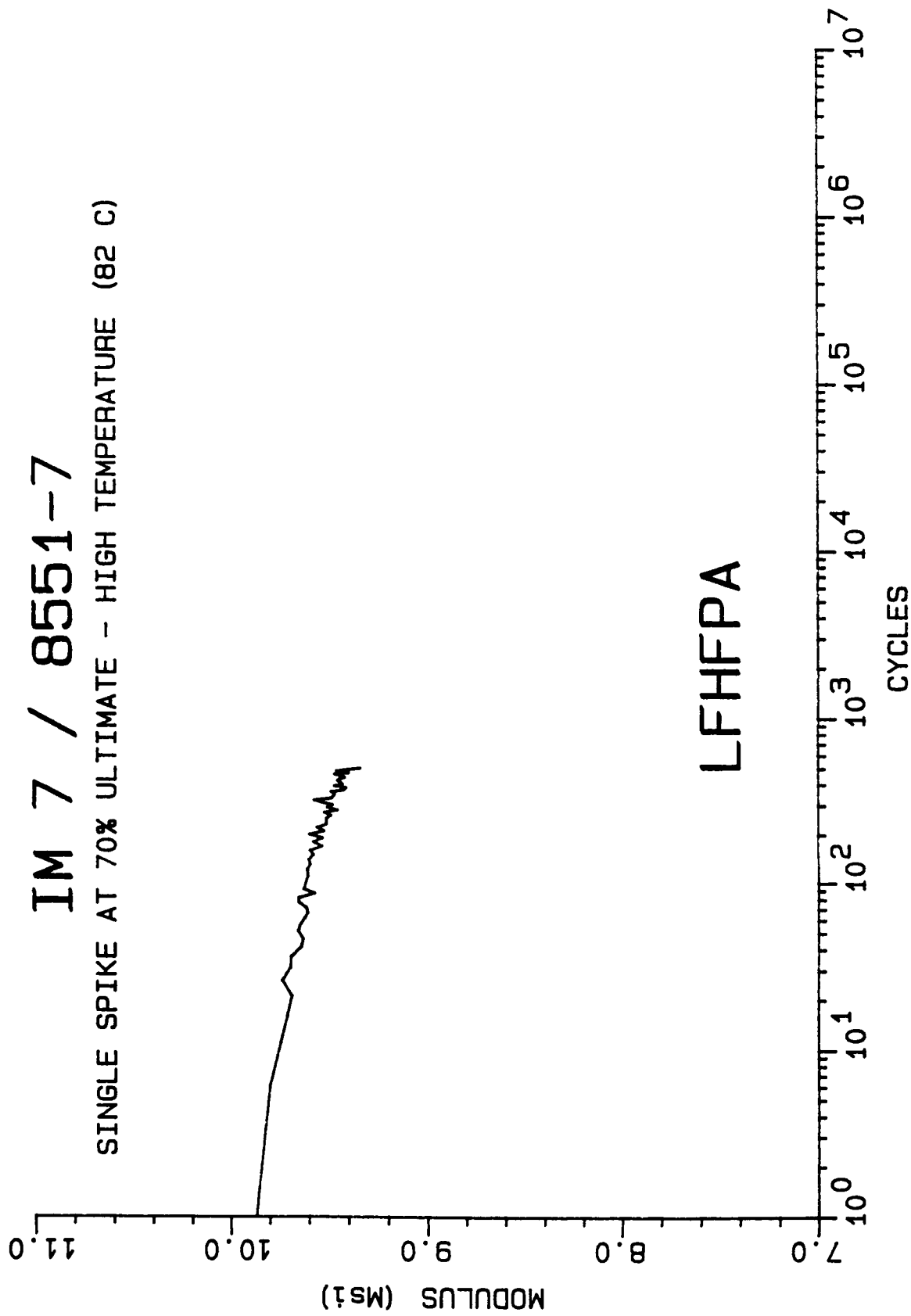


LFHEPA

MODULUS DECAY CURVE

IM 7 / 8551-7

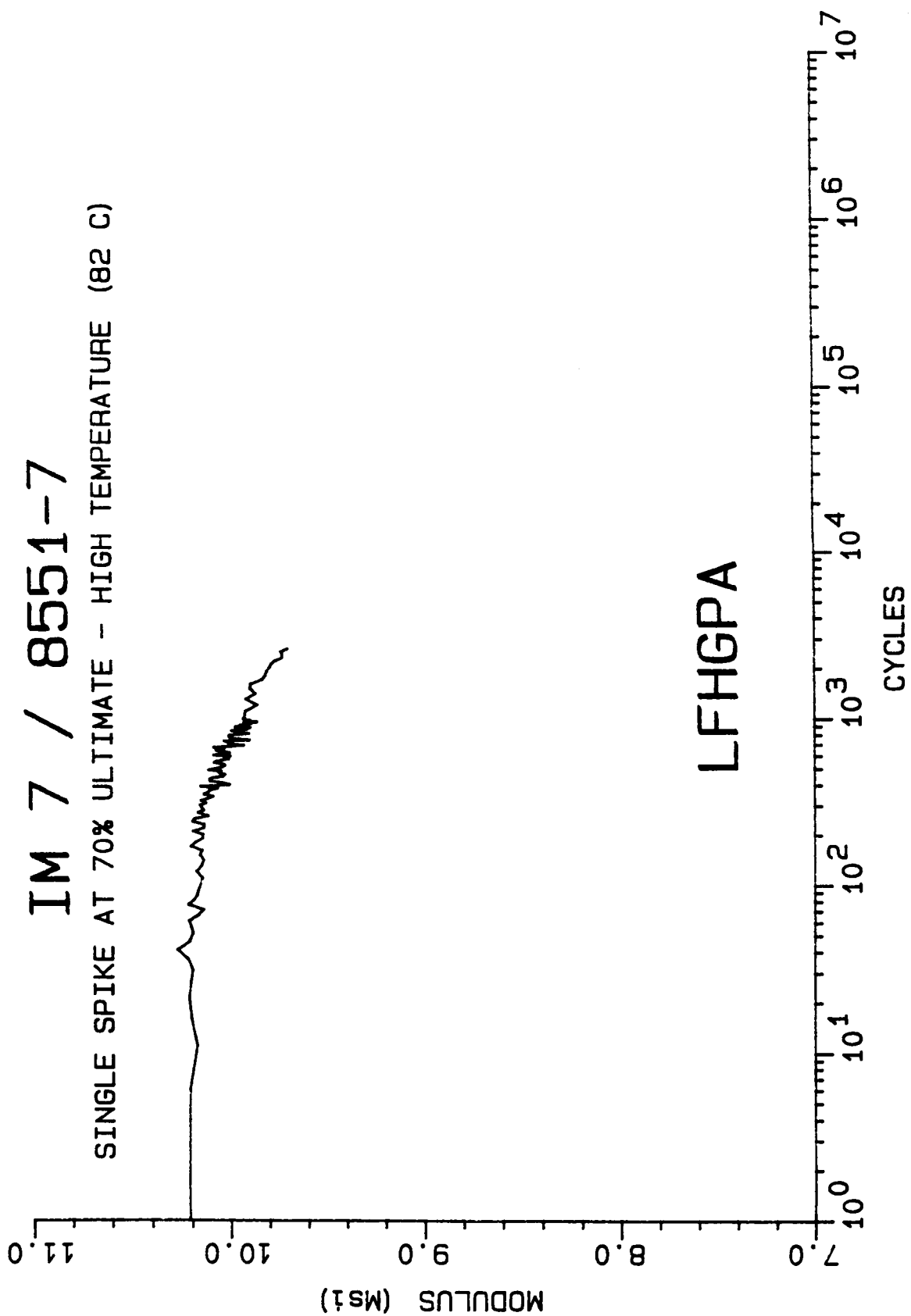
SINGLE SPIKE AT 70% ULTIMATE - HIGH TEMPERATURE (82 C)



MODULUS DECAY CURVE

IM 7 / 8551-7

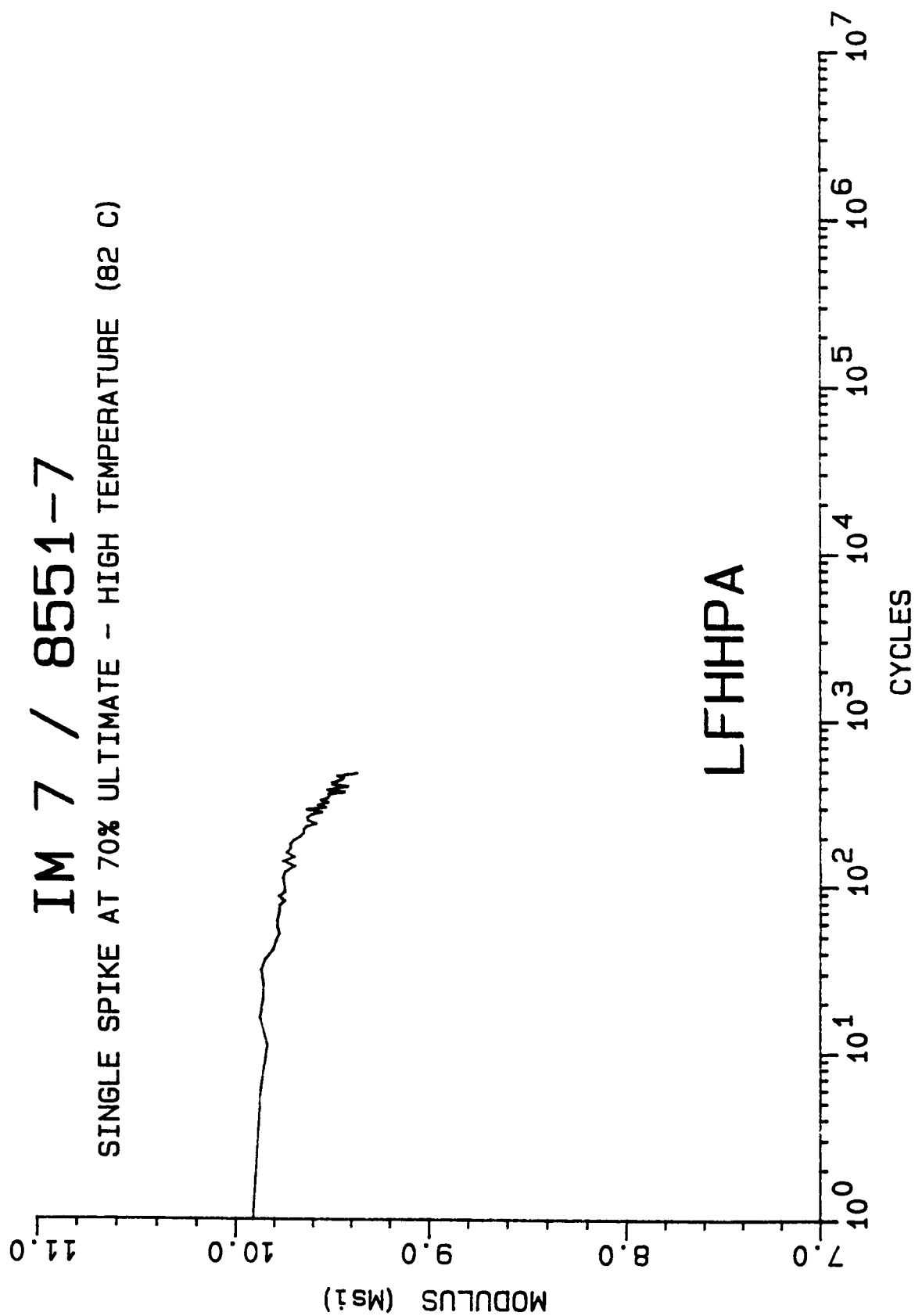
SINGLE SPIKE AT 70% ULTIMATE - HIGH TEMPERATURE (82 C)



MODULUS DECAY CURVE

IM 7 / 8551-7

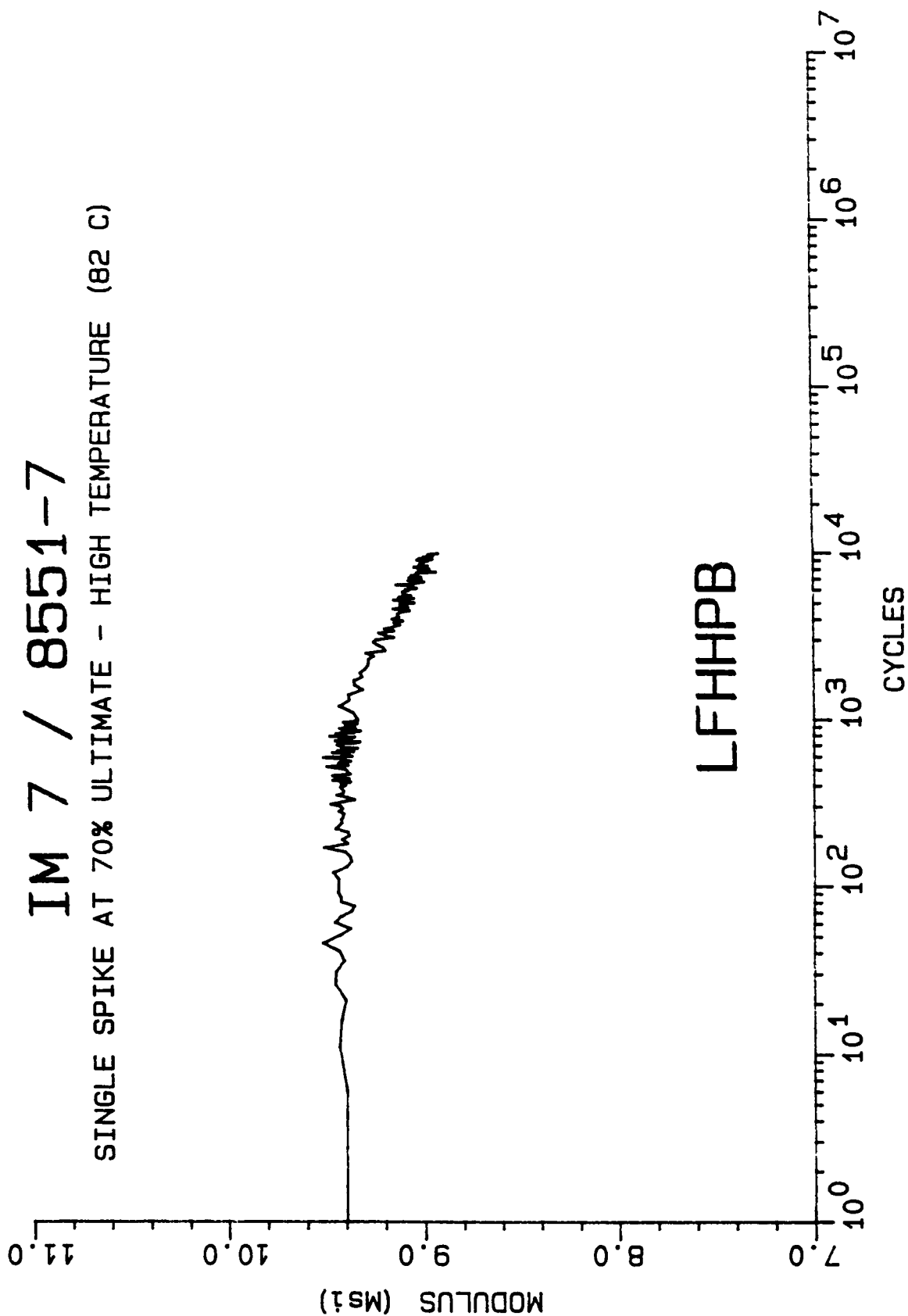
SINGLE SPIKE AT 70% ULTIMATE - HIGH TEMPERATURE (82 C)



MODULUS DECAY CURVE

IM 7 / 8551-7

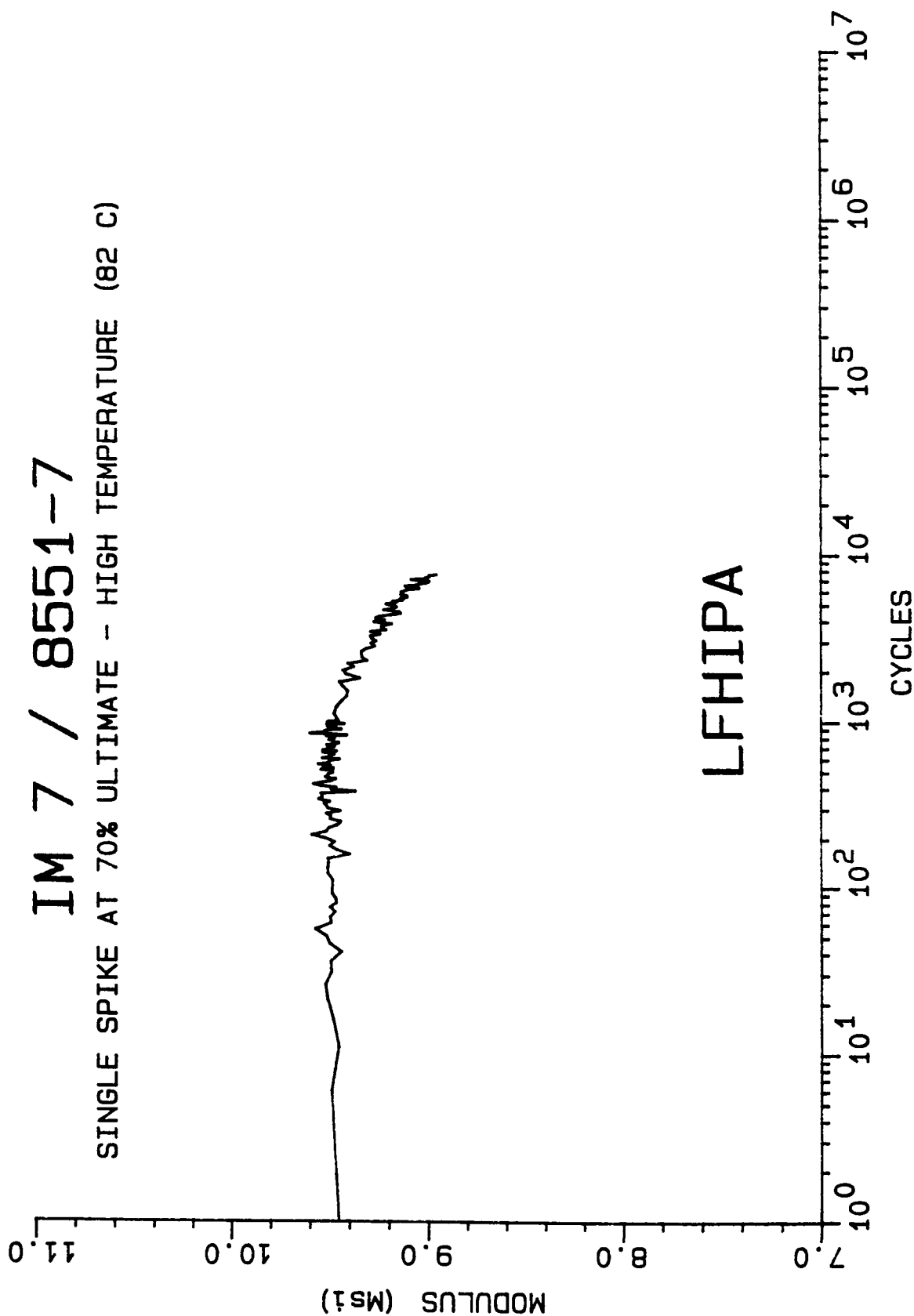
SINGLE SPIKE AT 70% ULTIMATE - HIGH TEMPERATURE (82 C)



MODULUS DECAY CURVE

IM 7 / 8551-7

SINGLE SPIKE AT 70% ULTIMATE - HIGH TEMPERATURE (82 C)

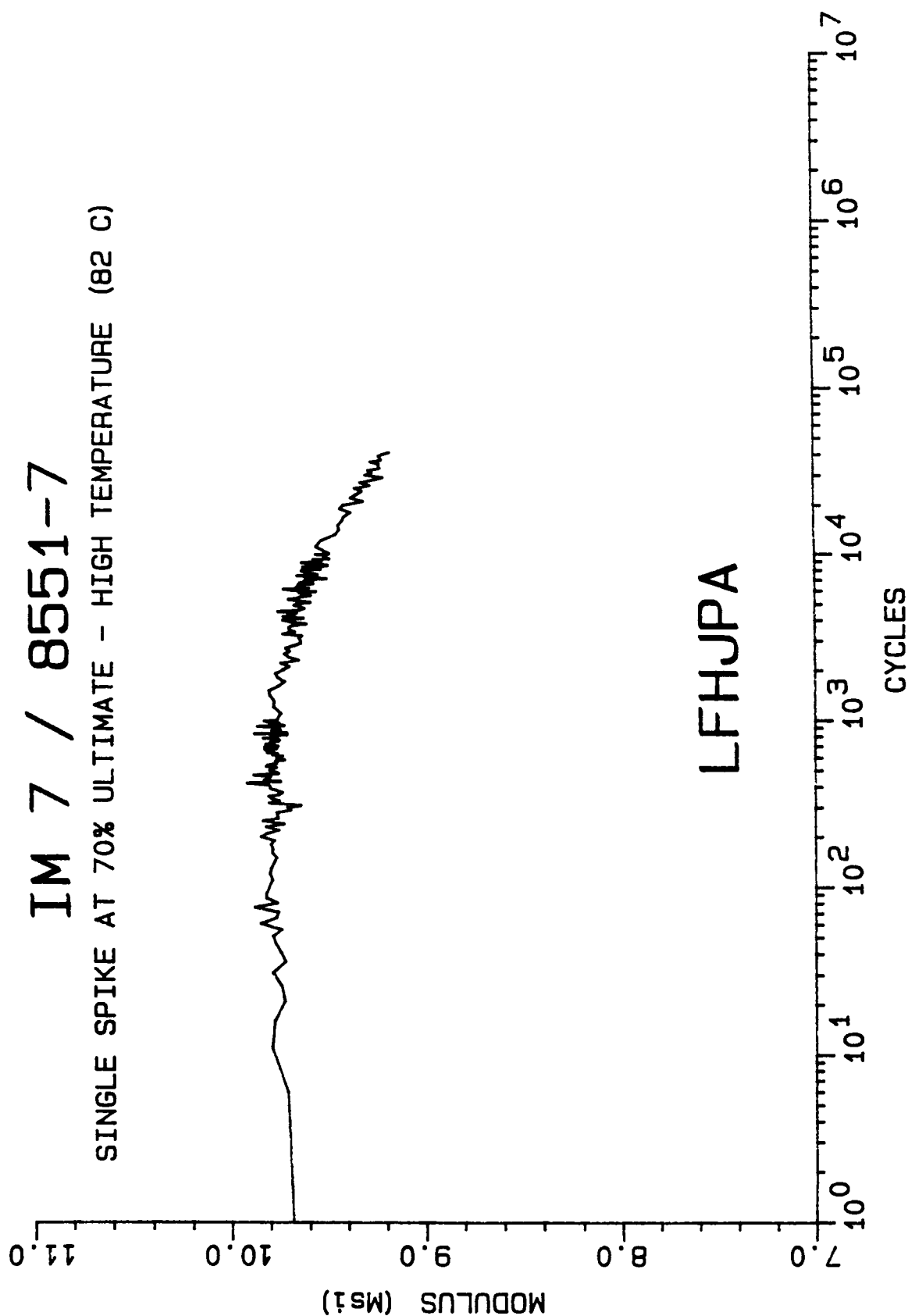


LFHIPA

MODULUS DECAY CURVE

IM 7 / 8551-7

SINGLE SPIKE AT 70% ULTIMATE - HIGH TEMPERATURE (82 C)

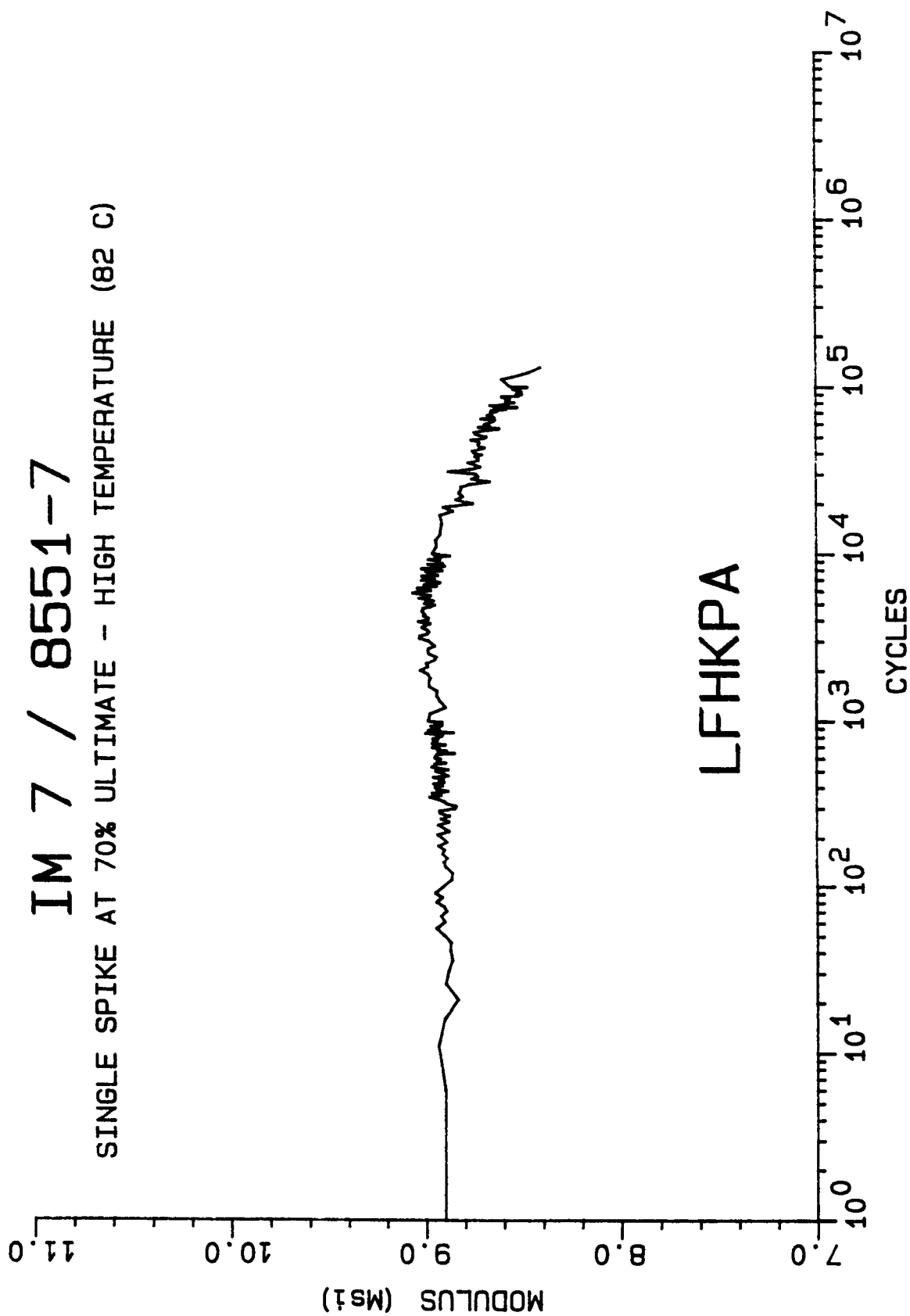


LFHJPA

MODULUS DECAY CURVE

IM 7 / 8551-7

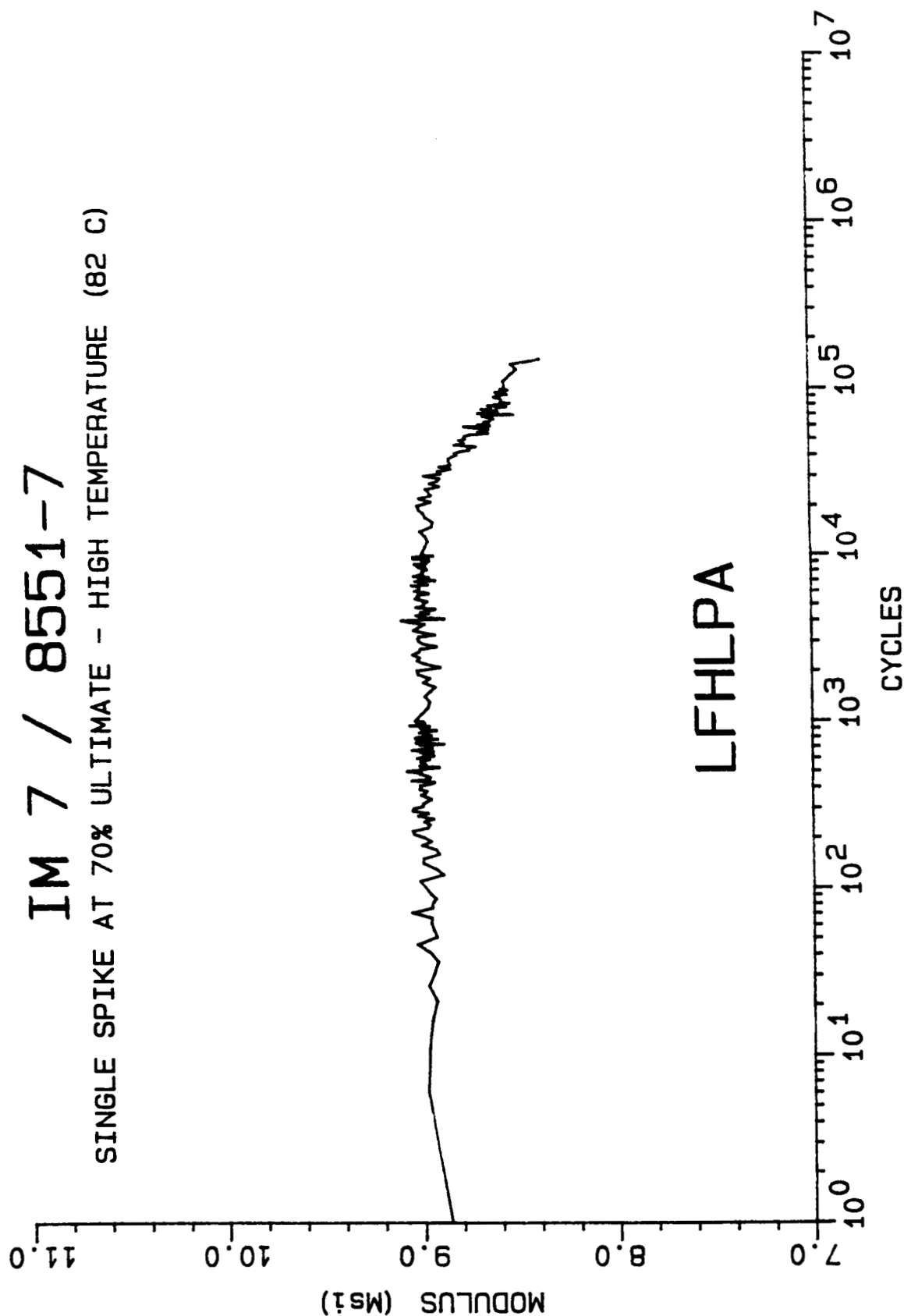
SINGLE SPIKE AT 70% ULTIMATE - HIGH TEMPERATURE (82 C)



MODULUS DECAY CURVE

IM 7 / 8551-7

SINGLE SPIKE AT 70% ULTIMATE - HIGH TEMPERATURE (82 C)

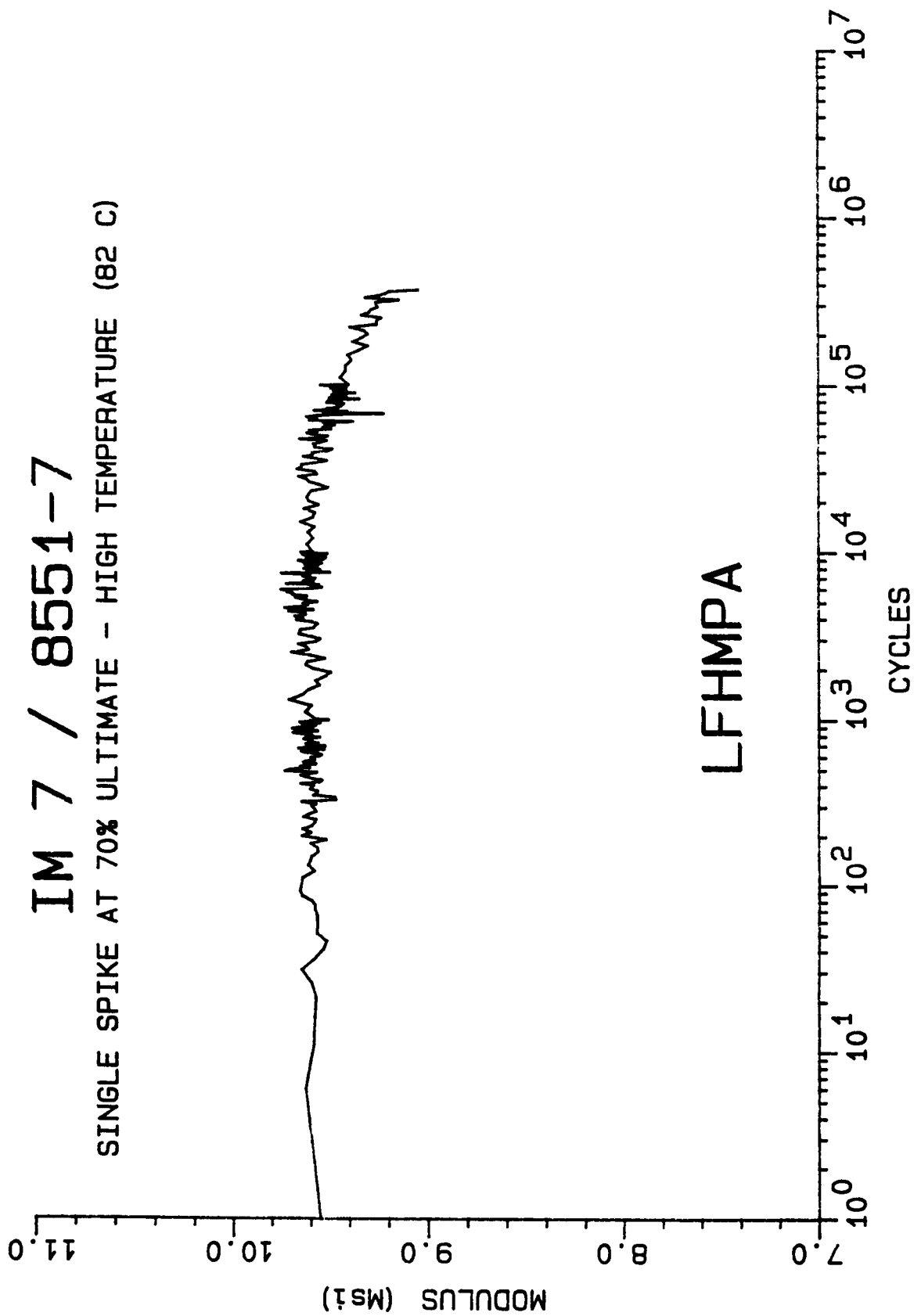


LFHLPA

MODULUS DECAY CURVE

IM 7 / 8551-7

SINGLE SPIKE AT 70% ULTIMATE - HIGH TEMPERATURE (82 C)

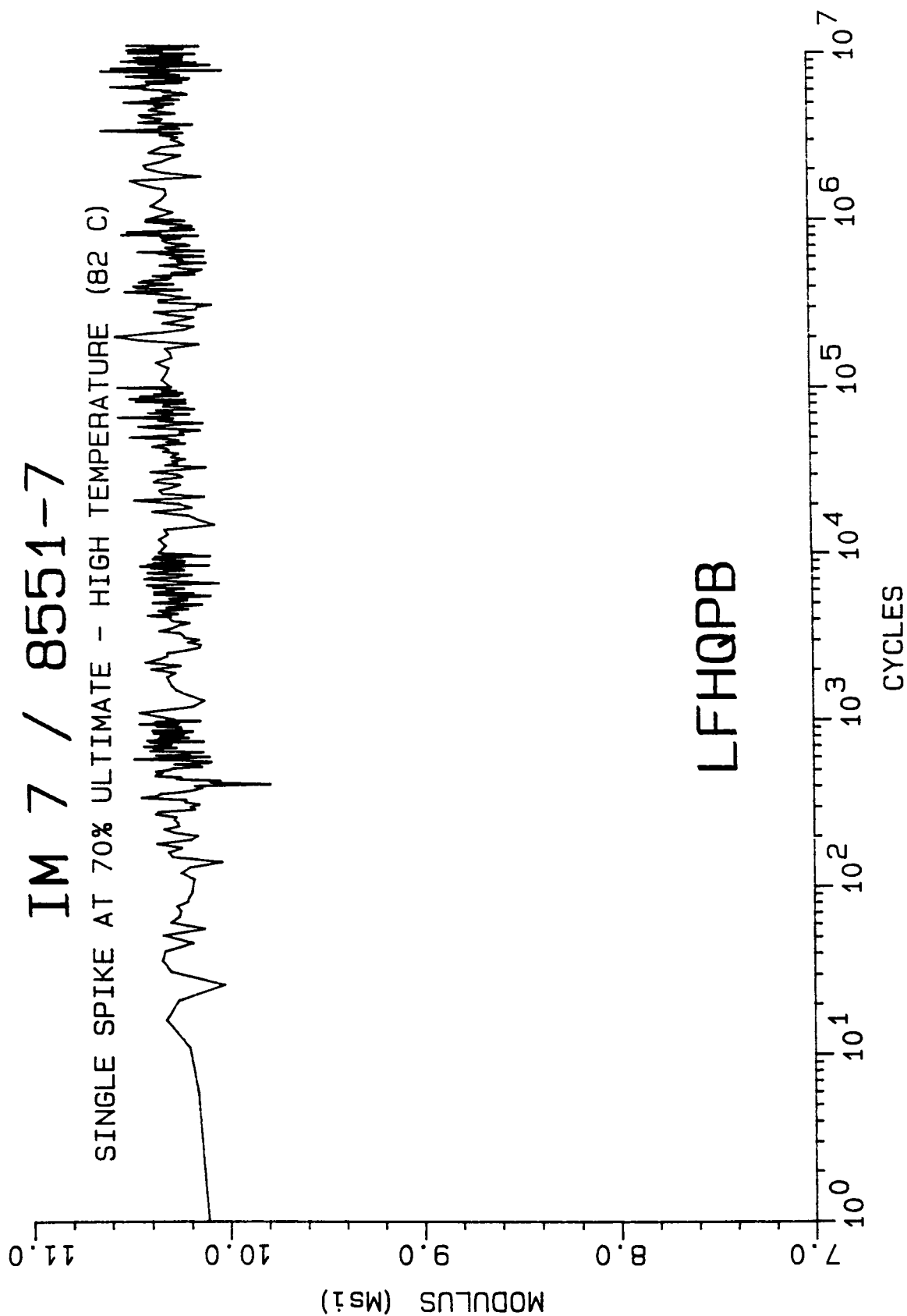


LFHMPA

MODULUS DECAY CURVE

IM 7 / 8551-7

SINGLE SPIKE AT 70% ULTIMATE - HIGH TEMPERATURE (82 C)

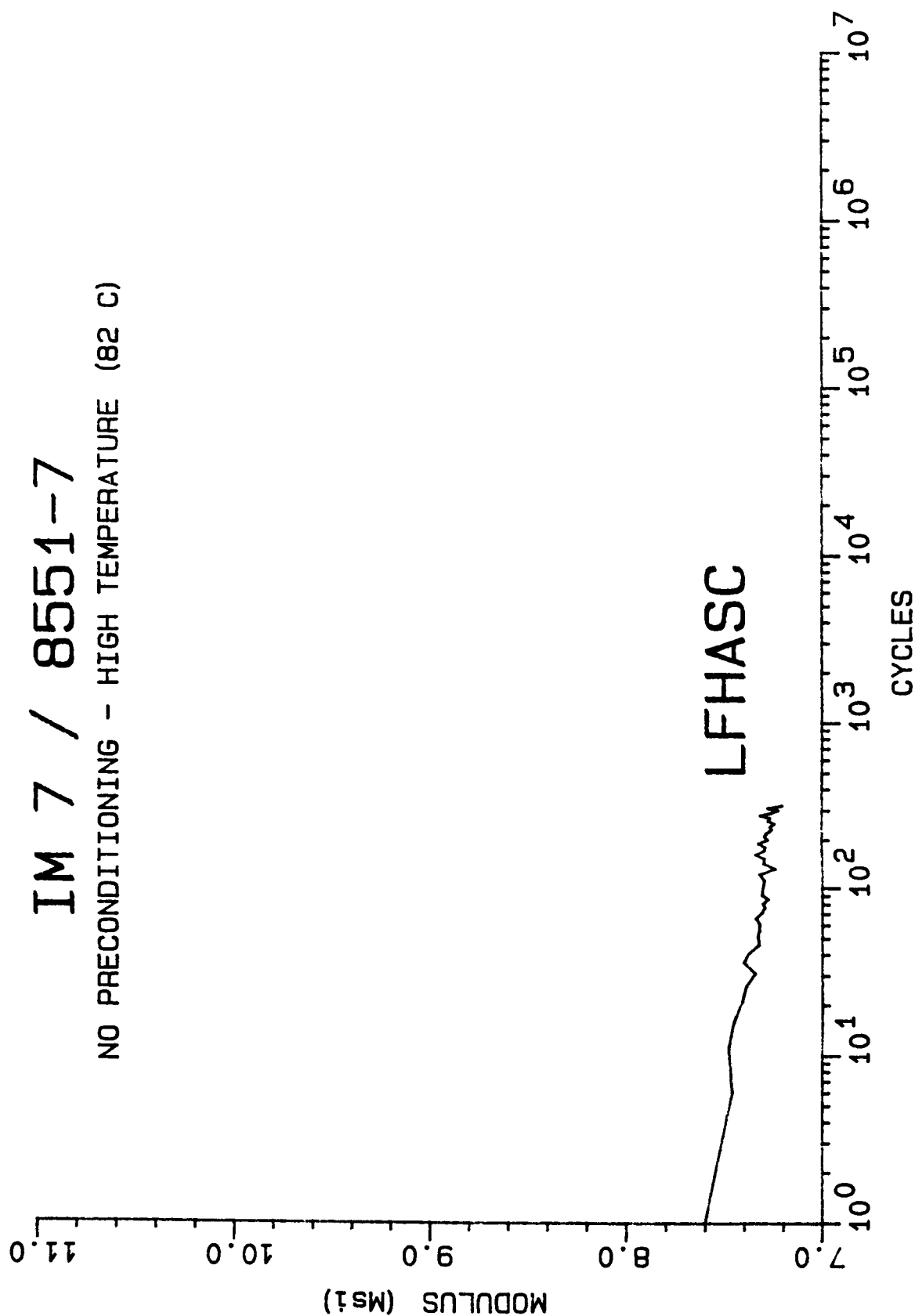


LFHQPB

MODULUS DECAY CURVE

IM 7 / 8551-7

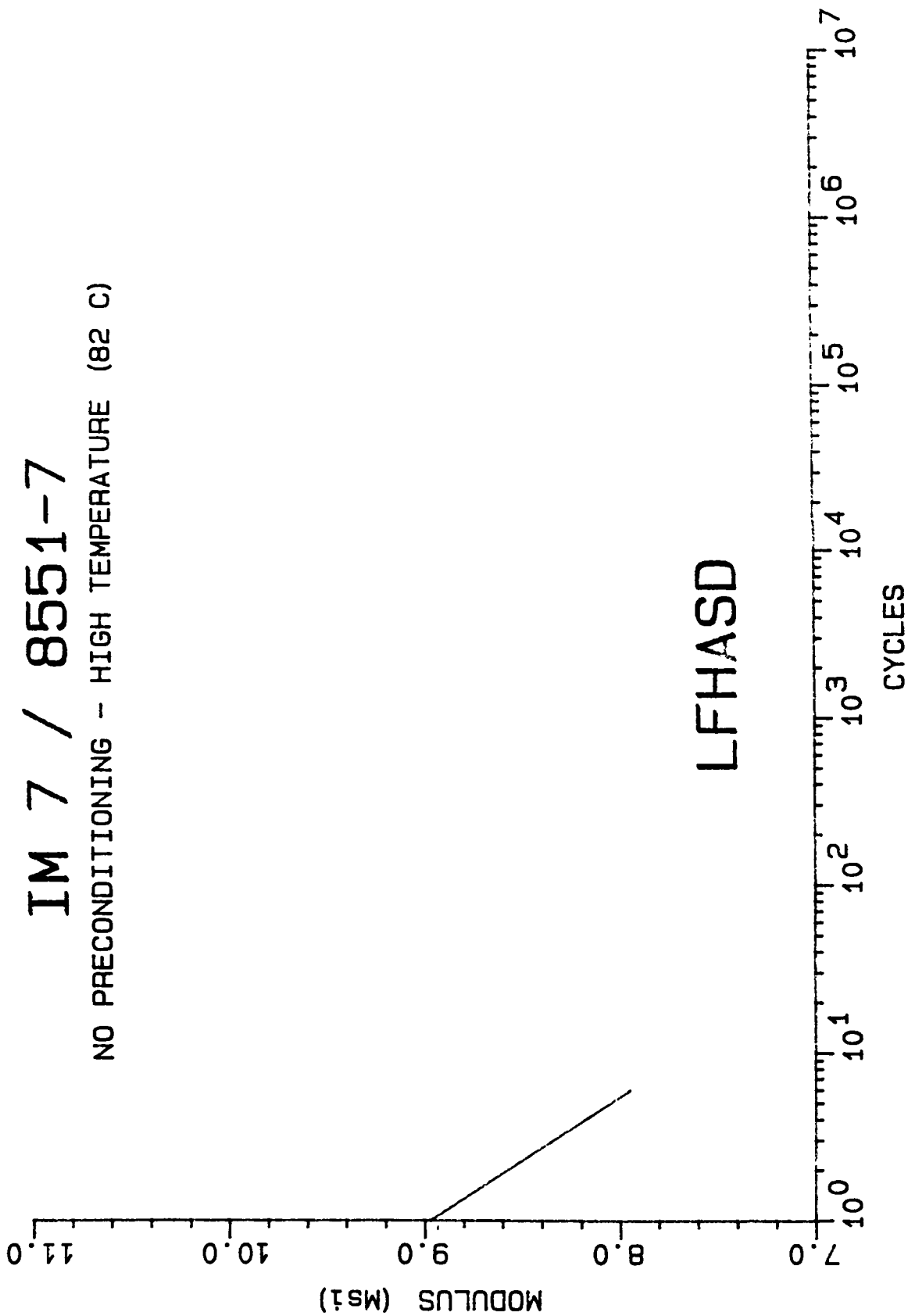
NO PRECONDITIONING - HIGH TEMPERATURE (82 C)



MODULUS DECAY CURVE

IM 7 / 8551-7

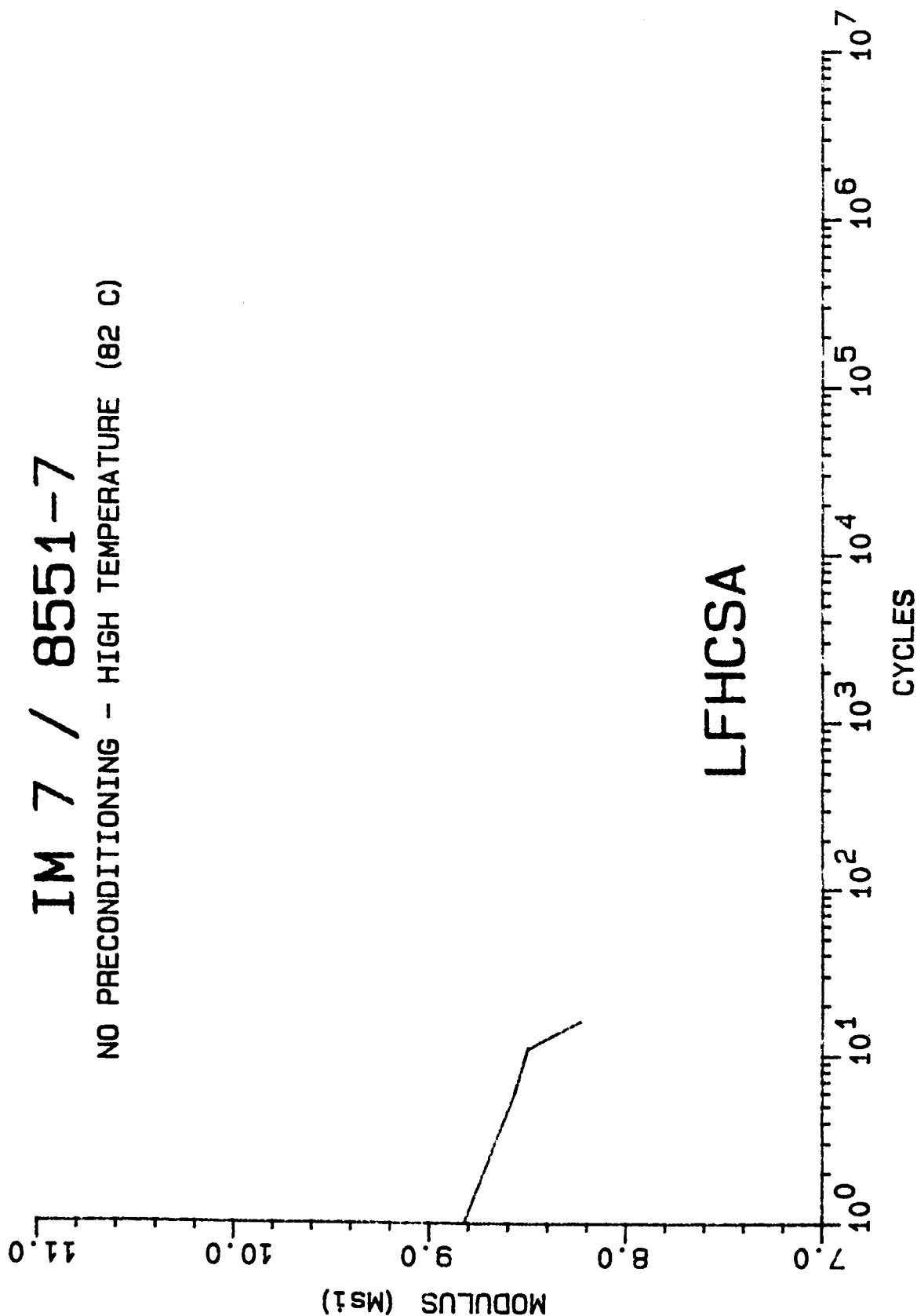
NO PRECONDITIONING - HIGH TEMPERATURE (82 C)



MODULUS DECAY CURVE

IM 7 / 8551-7

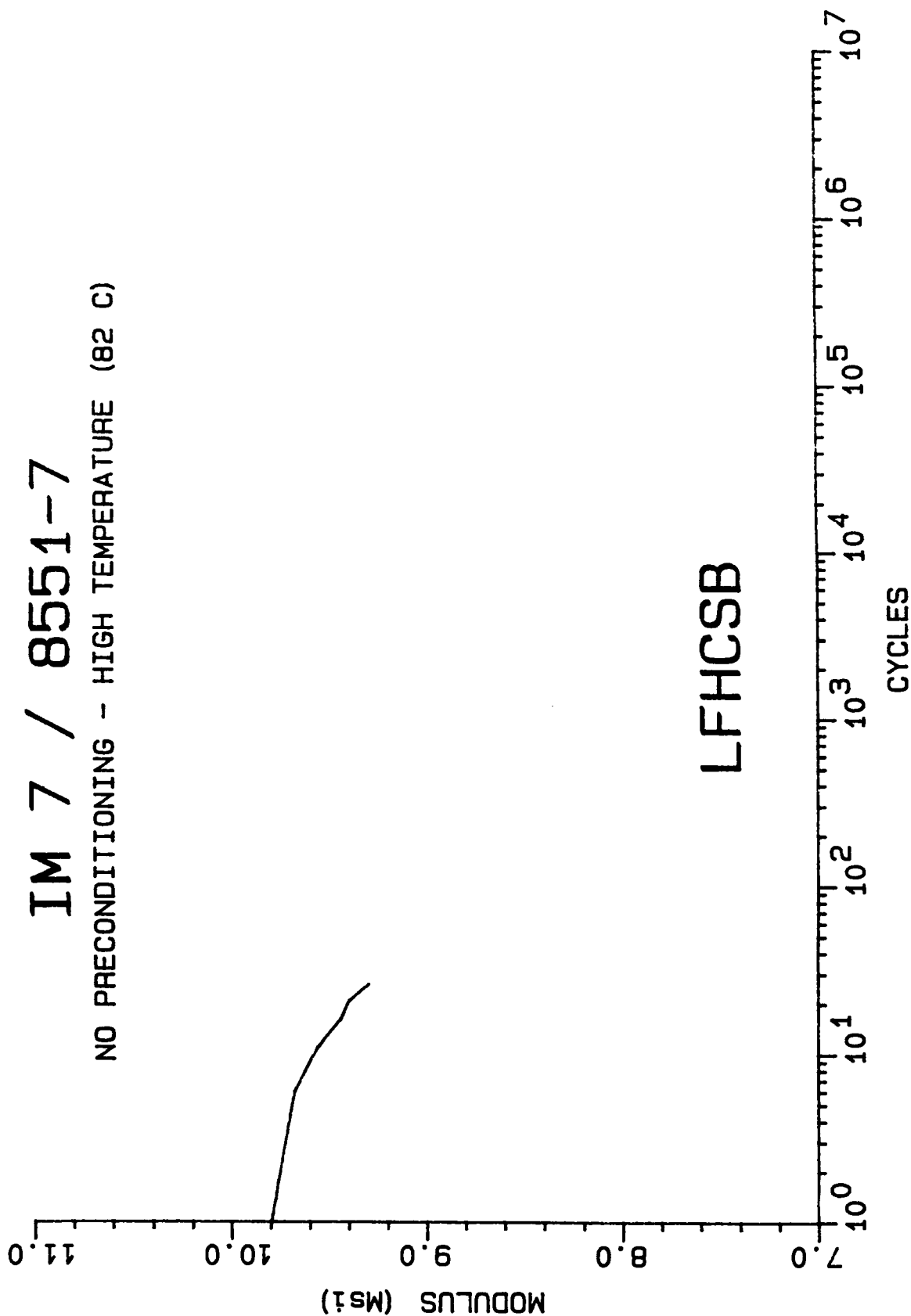
NO PRECONDITIONING - HIGH TEMPERATURE (82 C)



MODULUS DECAY CURVE

IM 7 / 8551-7

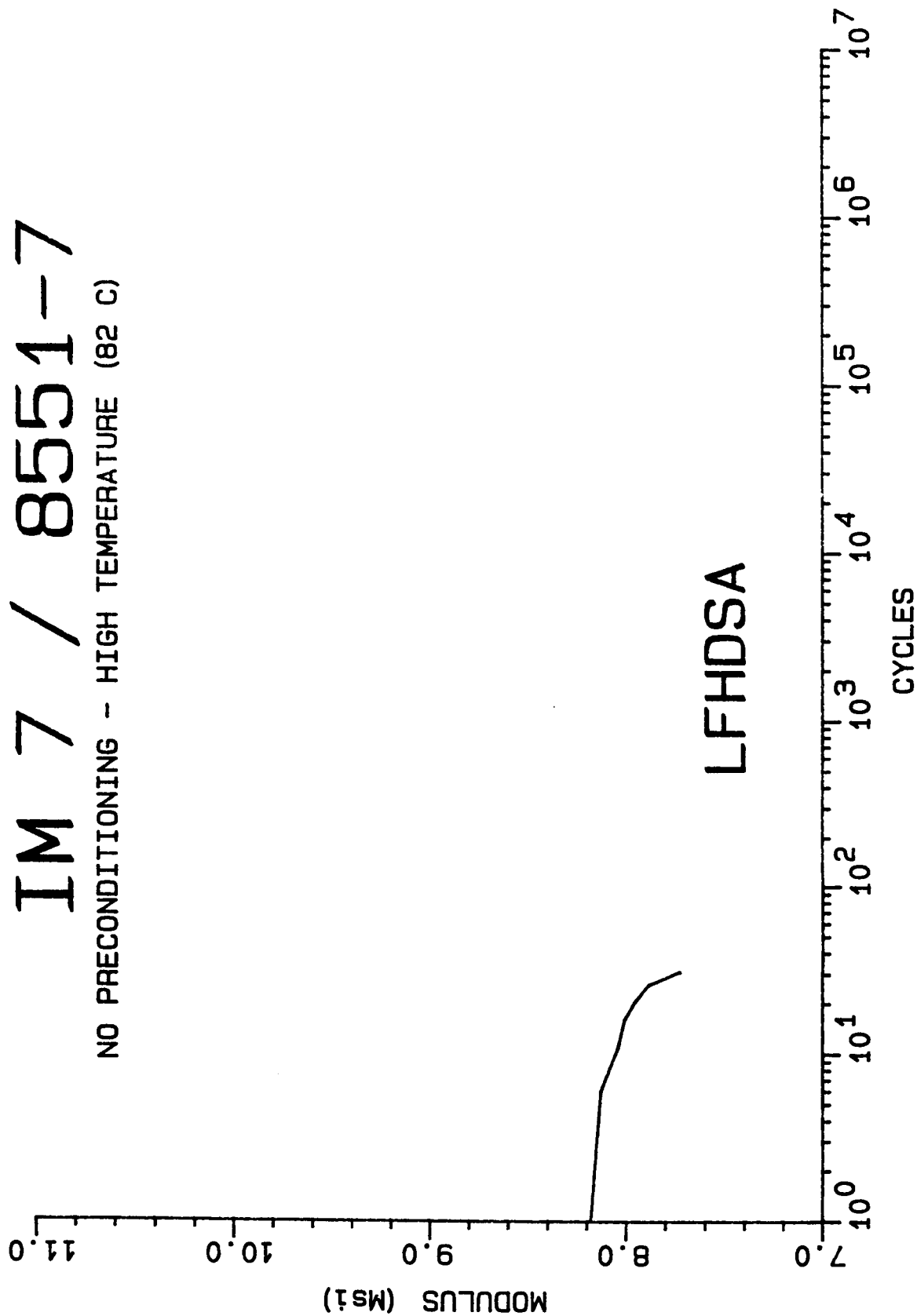
NO PRECONDITIONING - HIGH TEMPERATURE (82 C)



MODULUS DECAY CURVE

IM 7 / 8551-7

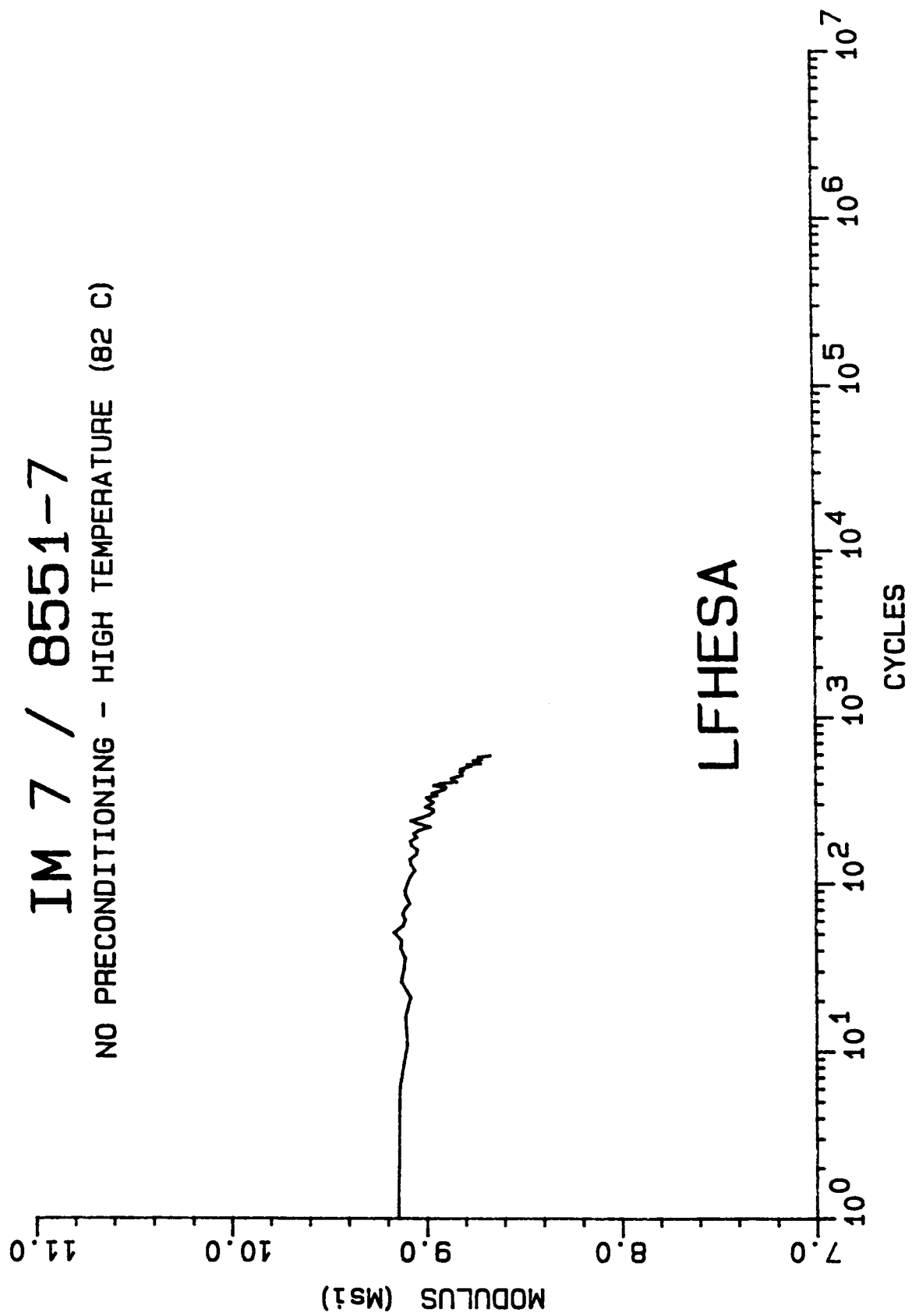
NO PRECONDITIONING - HIGH TEMPERATURE (82 C)



MODULUS DECAY CURVE

IM 7 / 8551-7

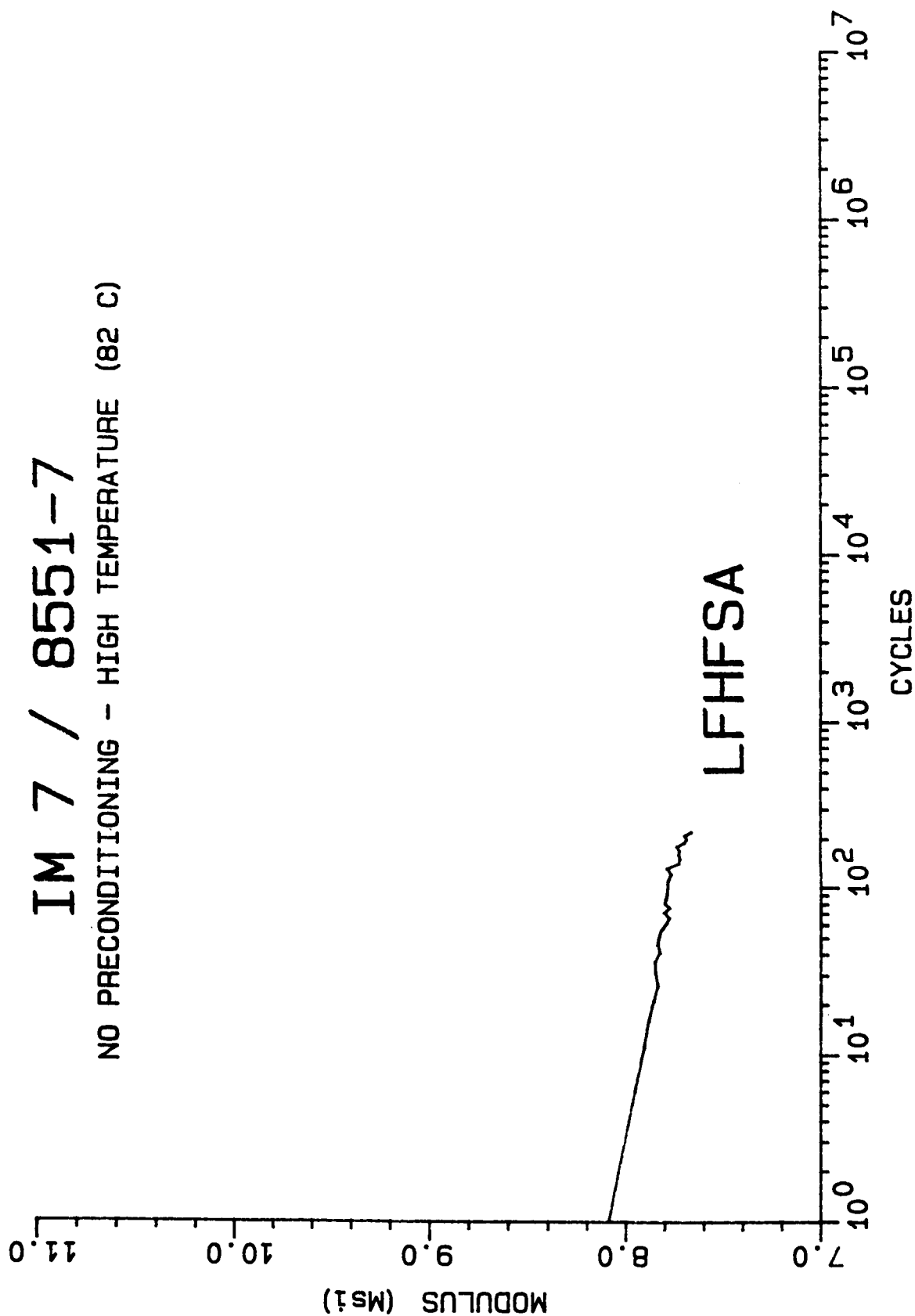
NO PRECONDITIONING - HIGH TEMPERATURE (82 C)



MODULUS DECAY CURVE

IM 7 / 8551-7

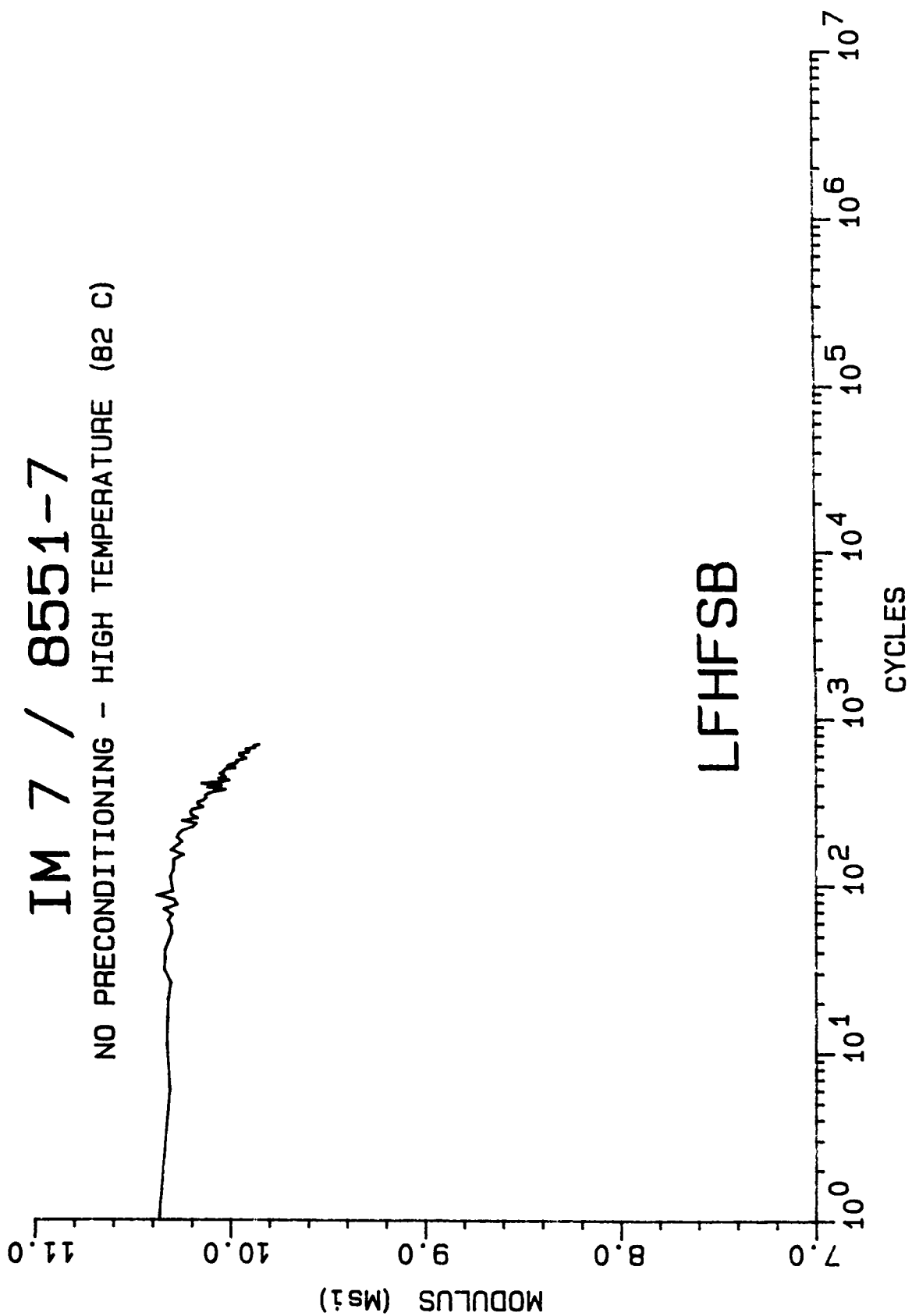
NO PRECONDITIONING - HIGH TEMPERATURE (82 C)



MODULUS DECAY CURVE

IM 7 / 8551-7

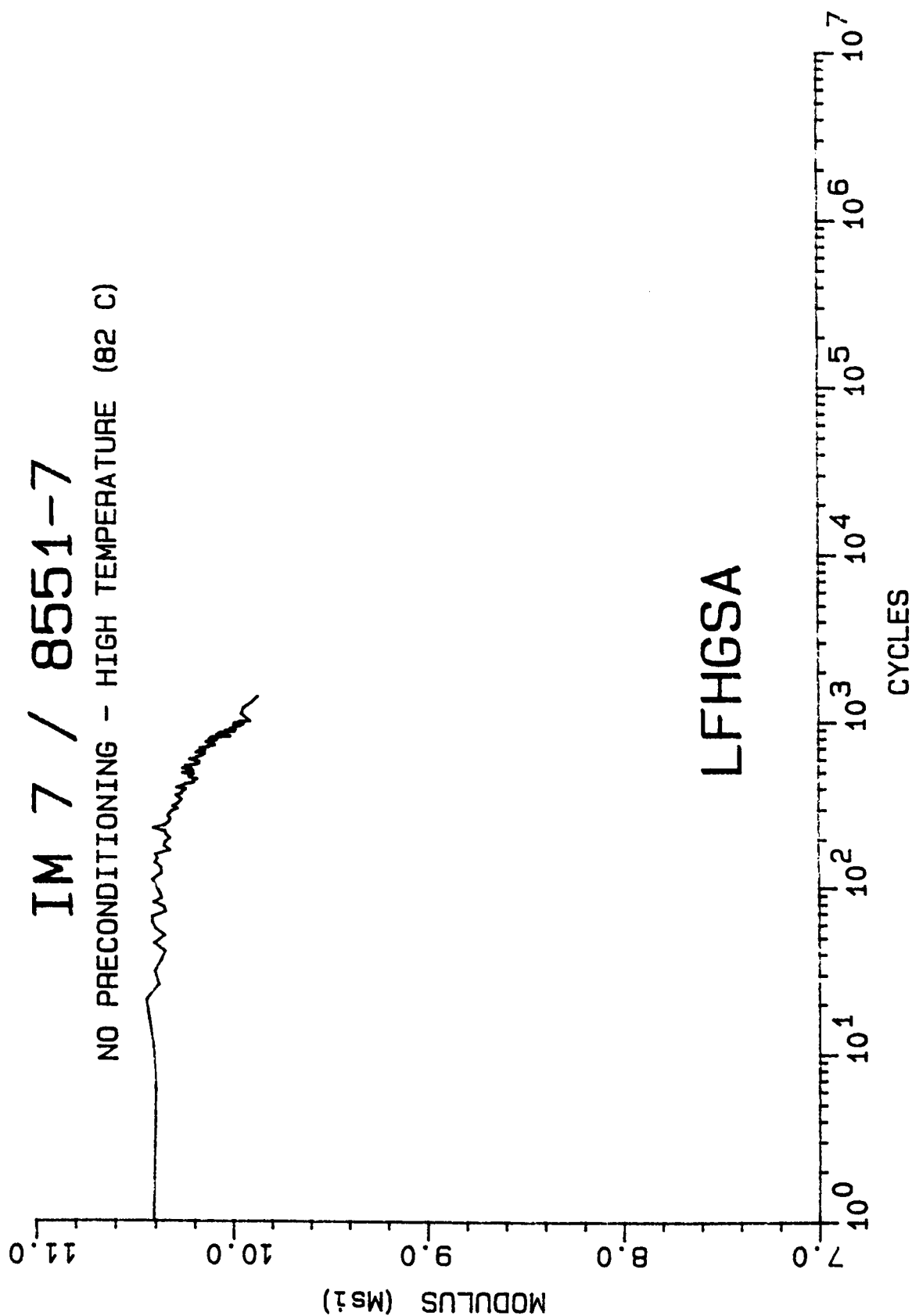
NO PRECONDITIONING - HIGH TEMPERATURE (82 C)



MODULUS DECAY CURVE

IM 7 / 8551-7

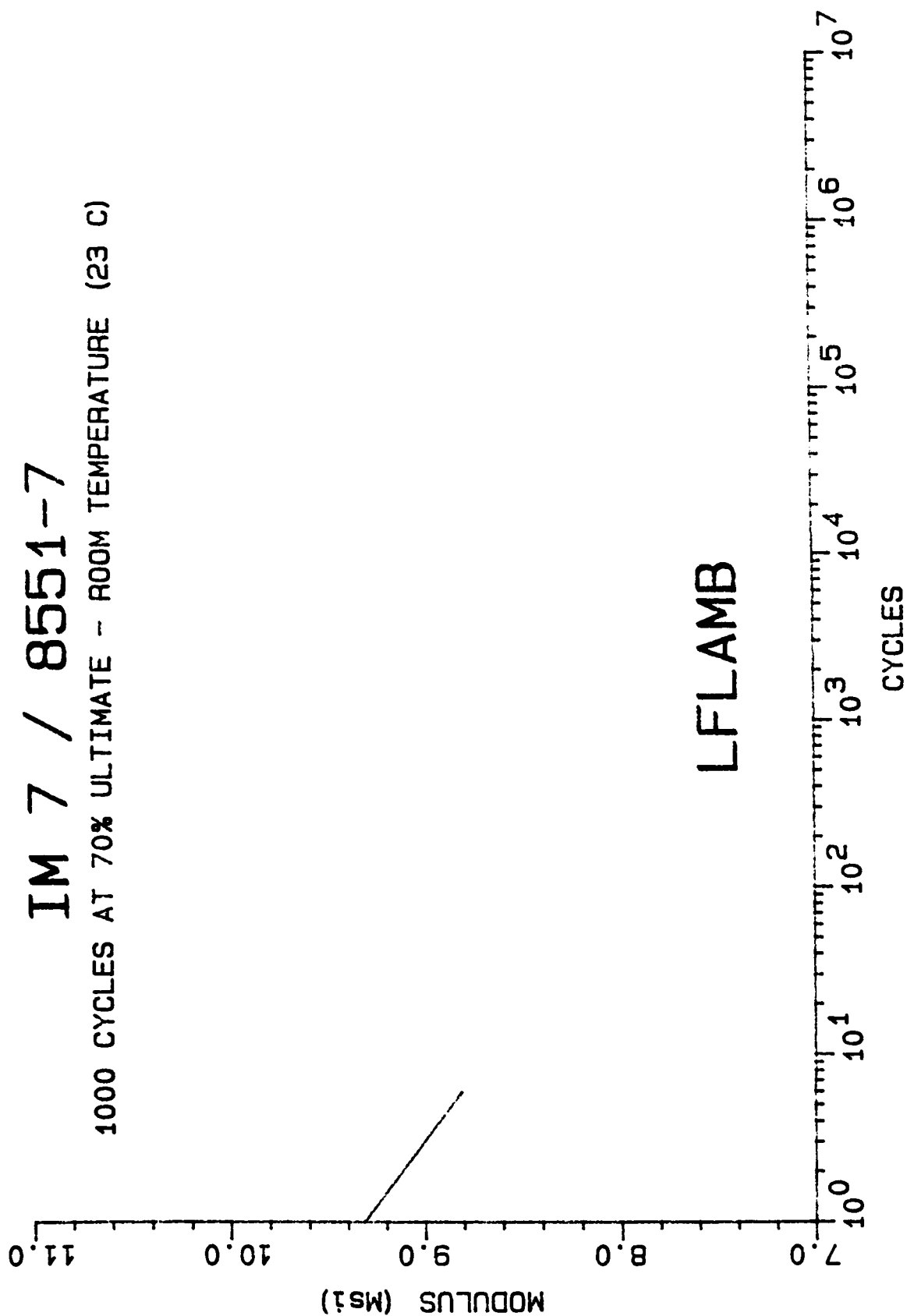
NO PRECONDITIONING - HIGH TEMPERATURE (82 C)



MODULUS DECAY CURVE

IM 7 / 8551-7

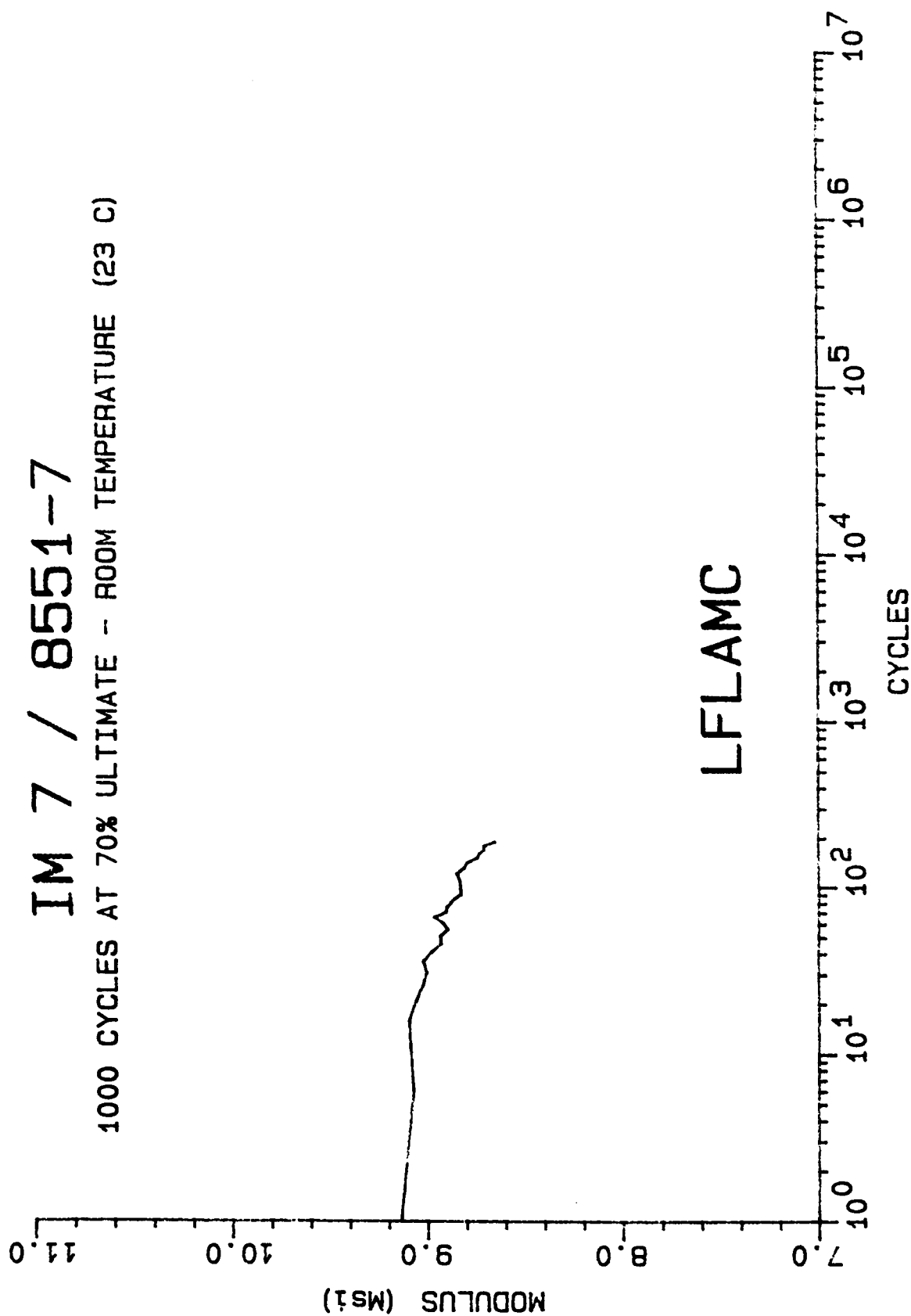
1000 CYCLES AT 70% ULTIMATE - ROOM TEMPERATURE (23 C)



MODULUS DECAY CURVE

IM 7 / 8551-7

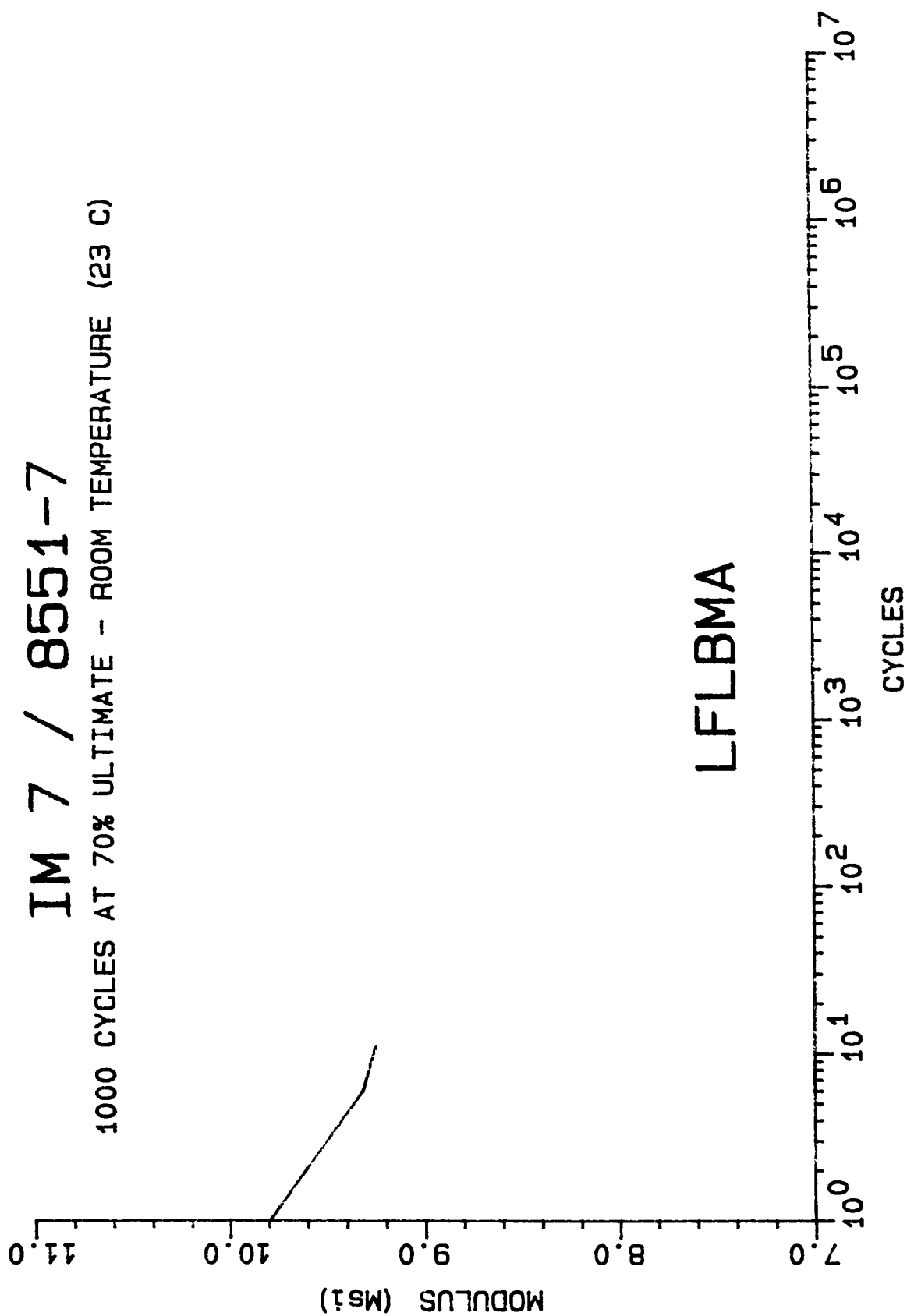
1000 CYCLES AT 70% ULTIMATE - ROOM TEMPERATURE (23 C)



MODULUS DECAY CURVE

IM 7 / 8551-7

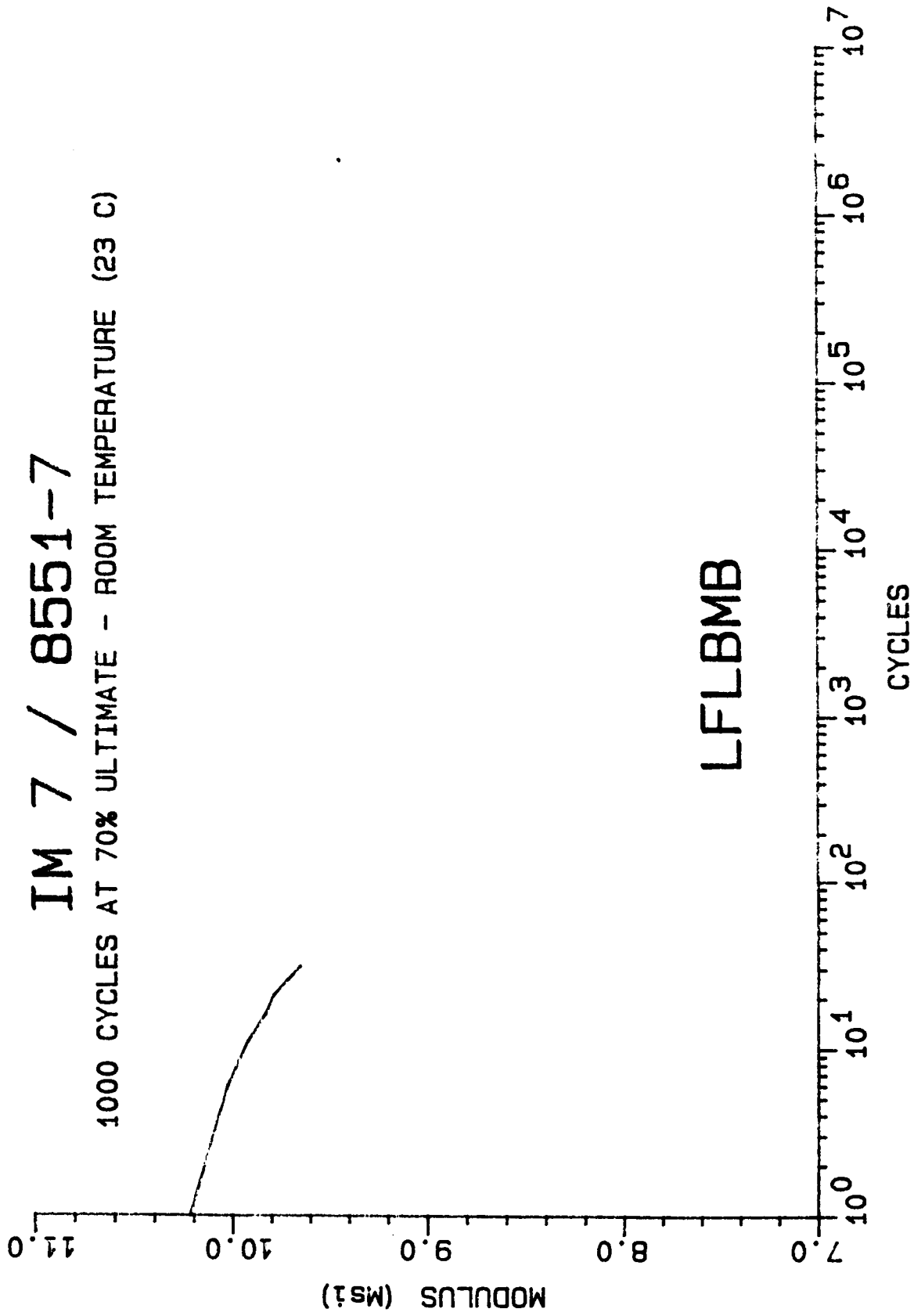
1000 CYCLES AT 70% ULTIMATE - ROOM TEMPERATURE (23 C)



MODULUS DECAY CURVE

IM 7 / 8551-7

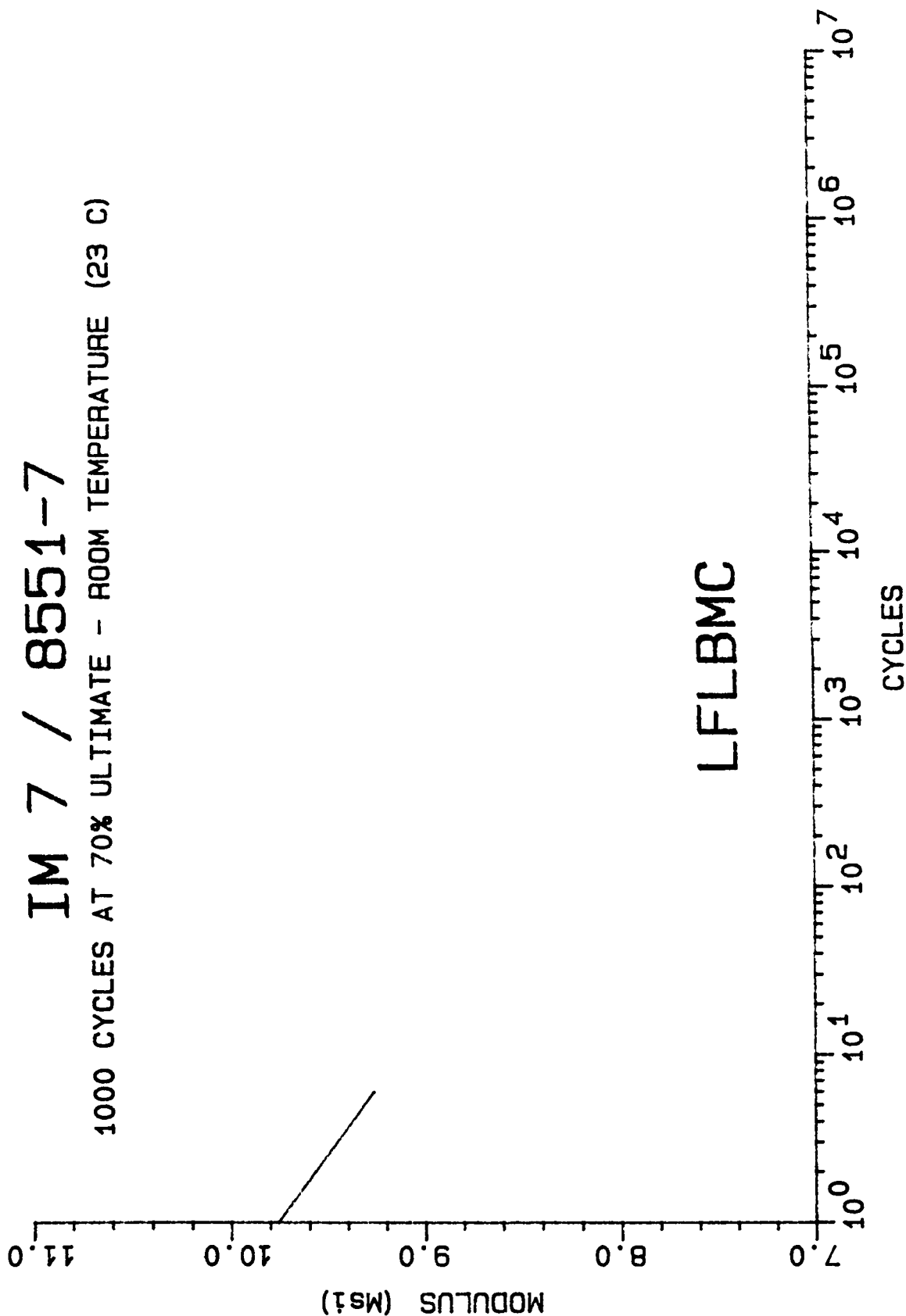
1000 CYCLES AT 70% ULTIMATE - ROOM TEMPERATURE (23 C)



MODULUS DECAY CURVE

IM 7 / 8551-7

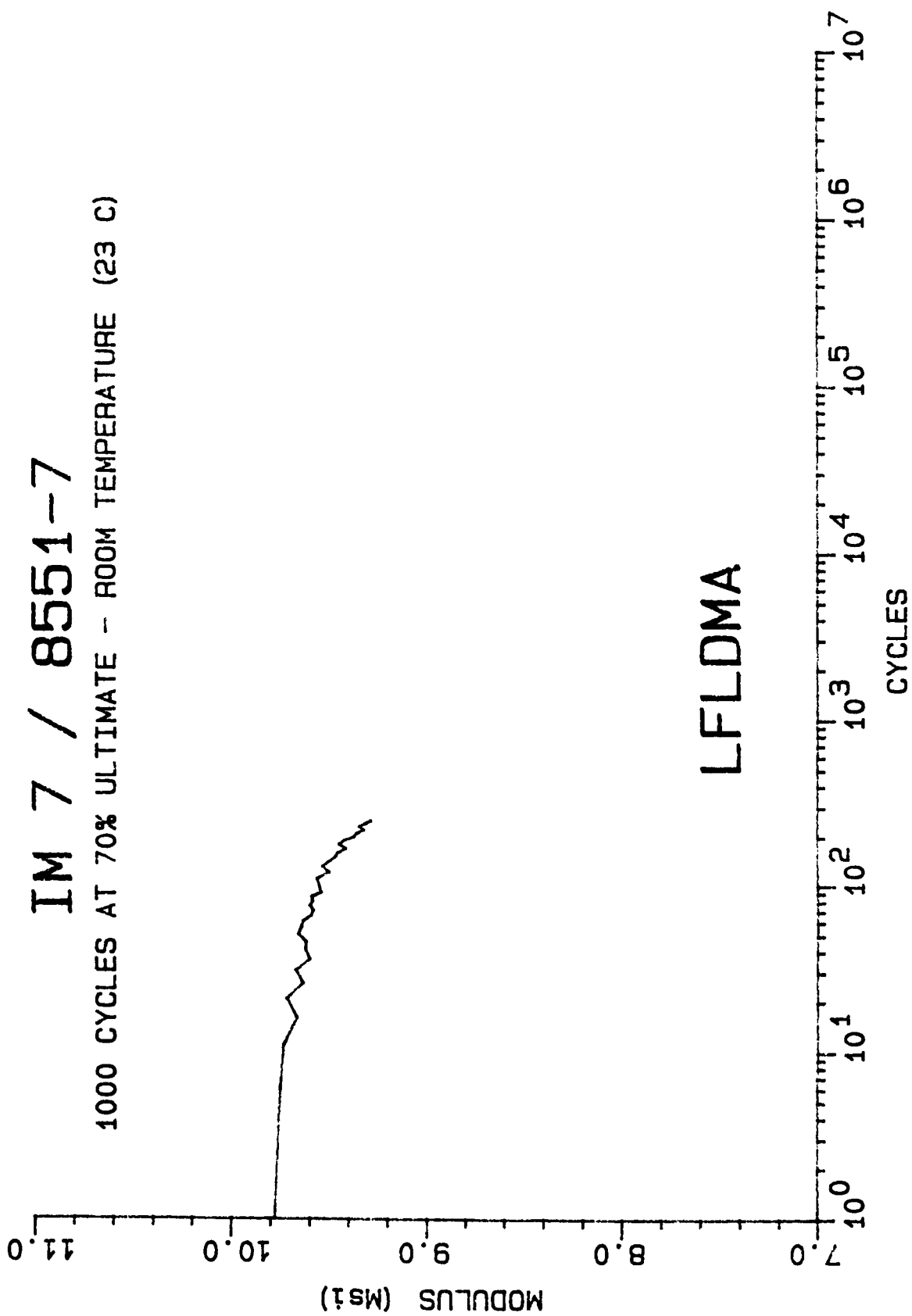
1000 CYCLES AT 70% ULTIMATE - ROOM TEMPERATURE (23 C)



MODULUS DECAY CURVE

IM 7 / 8551-7

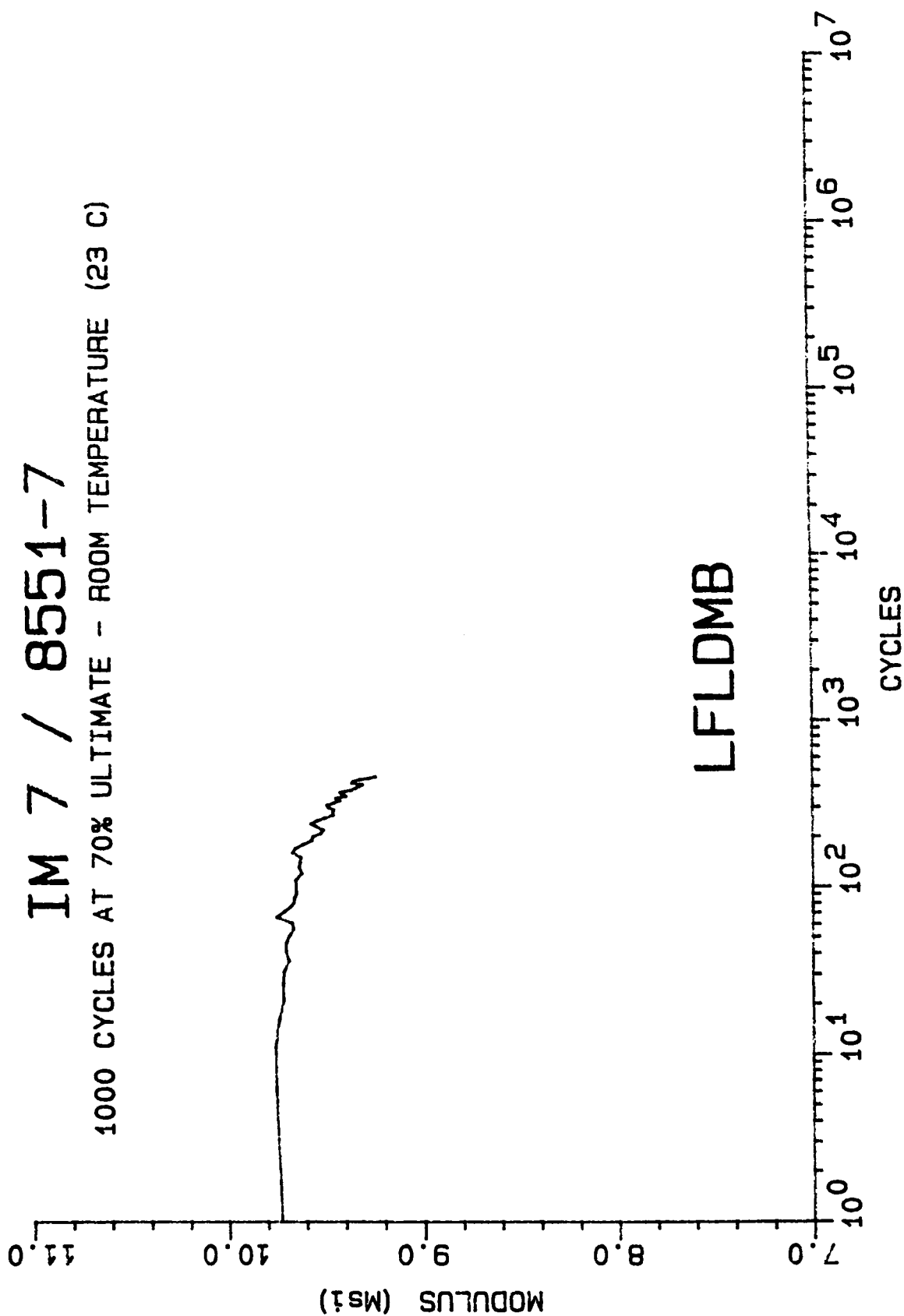
1000 CYCLES AT 70% ULTIMATE - ROOM TEMPERATURE (23 C)



MODULUS DECAY CURVE

IM 7 / 8551-7

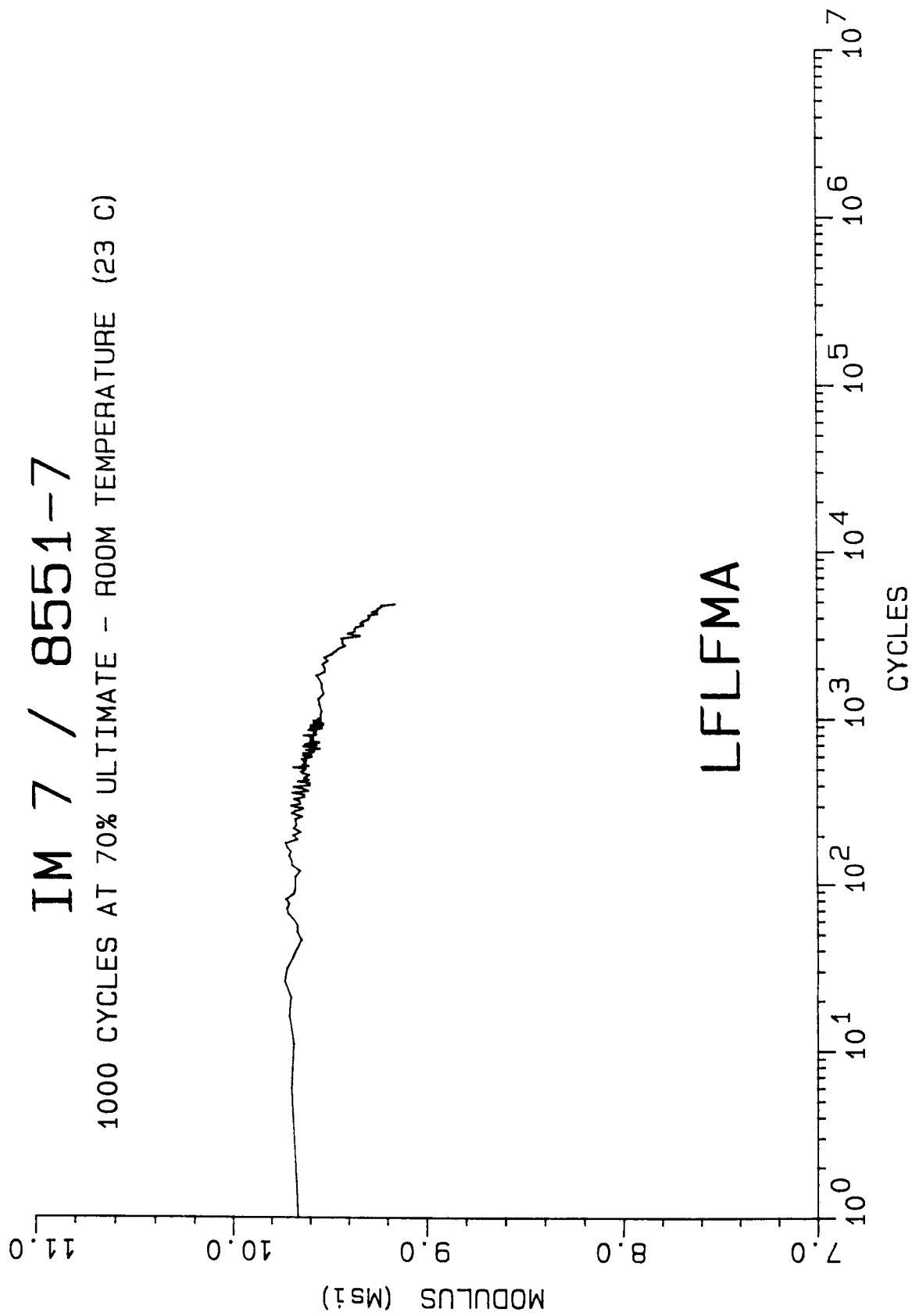
1000 CYCLES AT 70% ULTIMATE - ROOM TEMPERATURE (23 C)



MODULUS DECAY CURVE

IM 7 / 8551-7

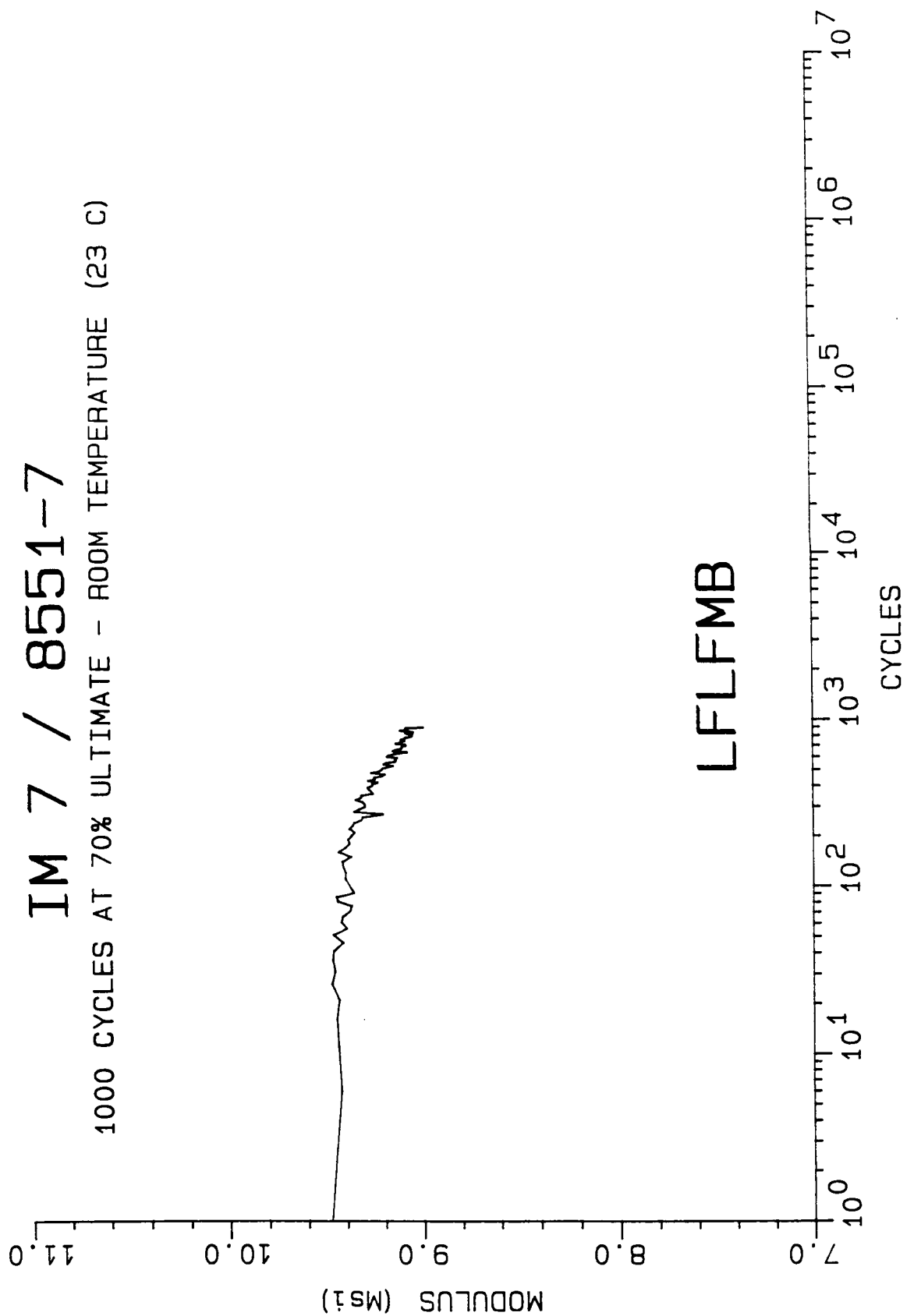
1000 CYCLES AT 70% ULTIMATE - ROOM TEMPERATURE (23 C)



MODULUS DECAY CURVE

IM 7 / 8551-7

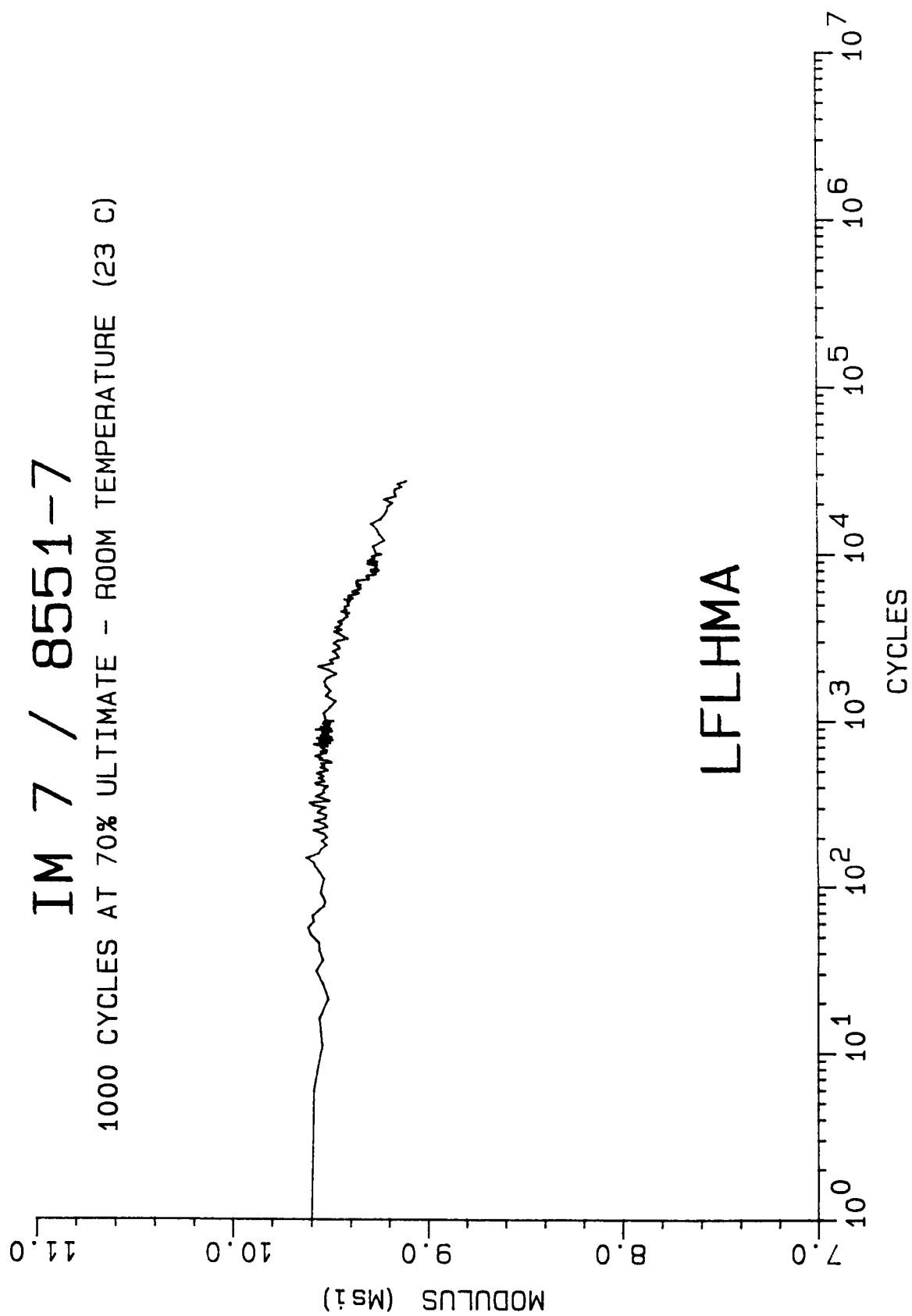
1000 CYCLES AT 70% ULTIMATE - ROOM TEMPERATURE (23 C)



MODULUS DECAY CURVE

IM 7 / 8551-7

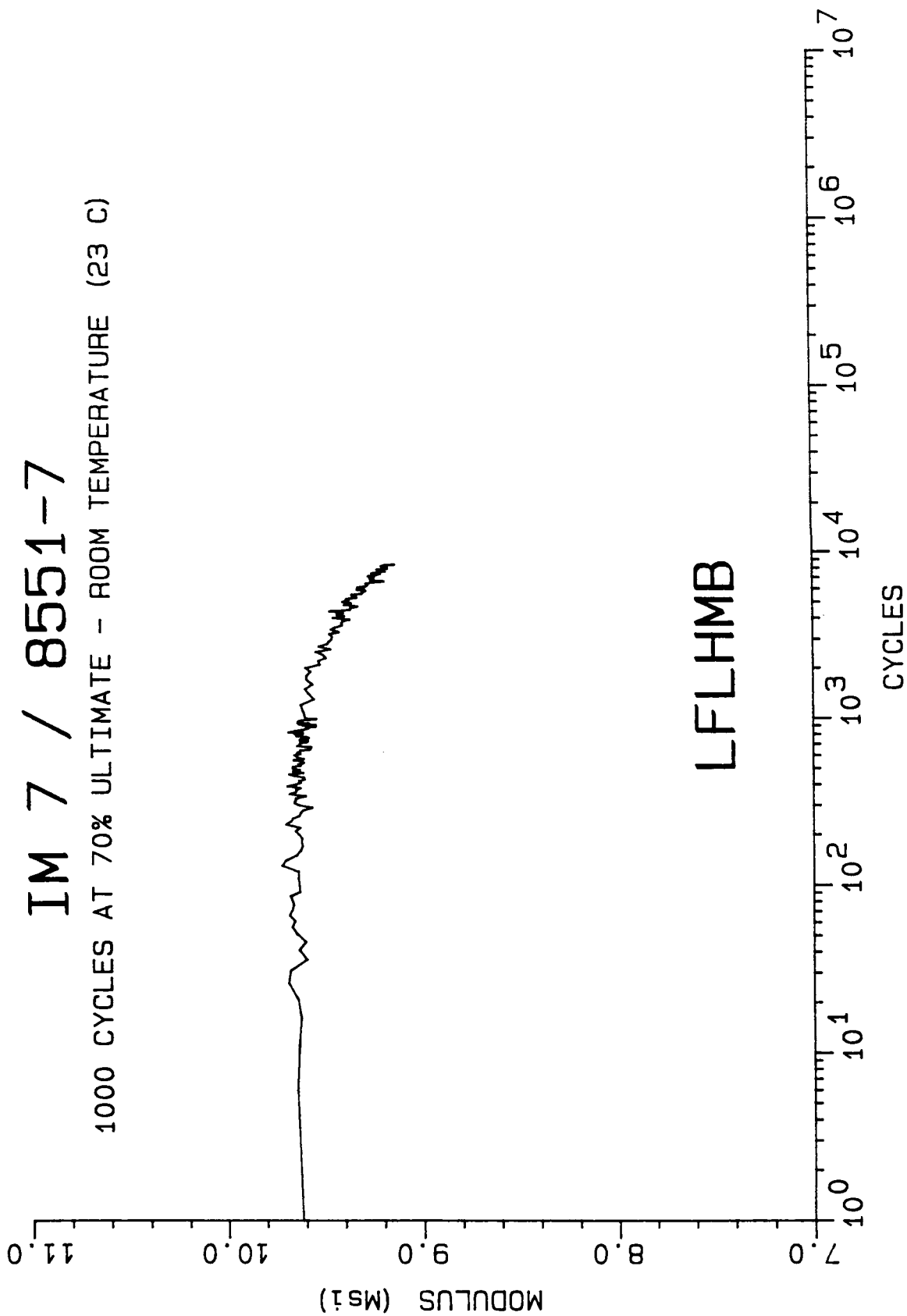
1000 CYCLES AT 70% ULTIMATE - ROOM TEMPERATURE (23 C)



MODULUS DECAY CURVE

IM 7 / 8551-7

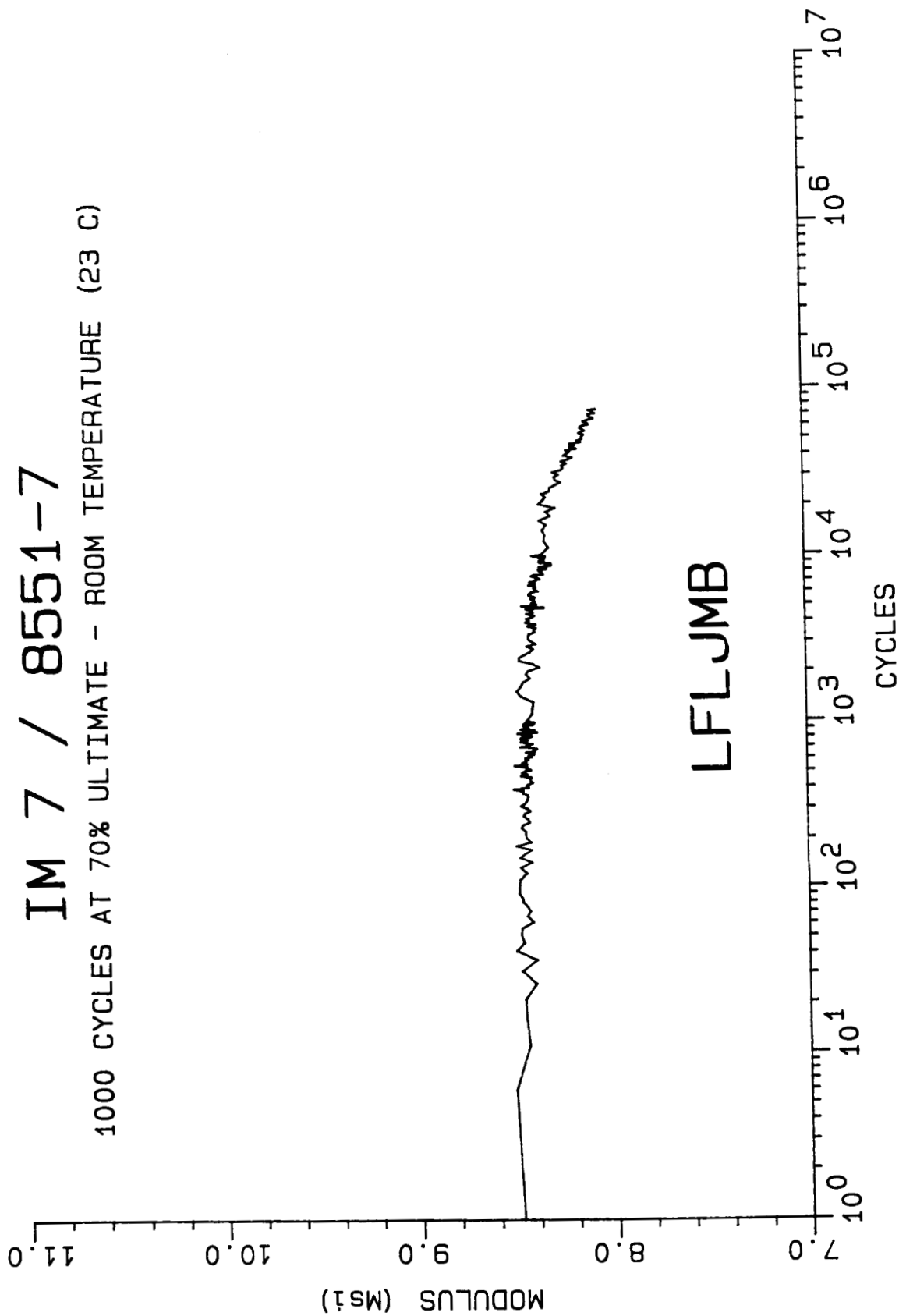
1000 CYCLES AT 70% ULTIMATE - ROOM TEMPERATURE (23 C)



MODULUS DECAY CURVE

IM 7 / 8551-7

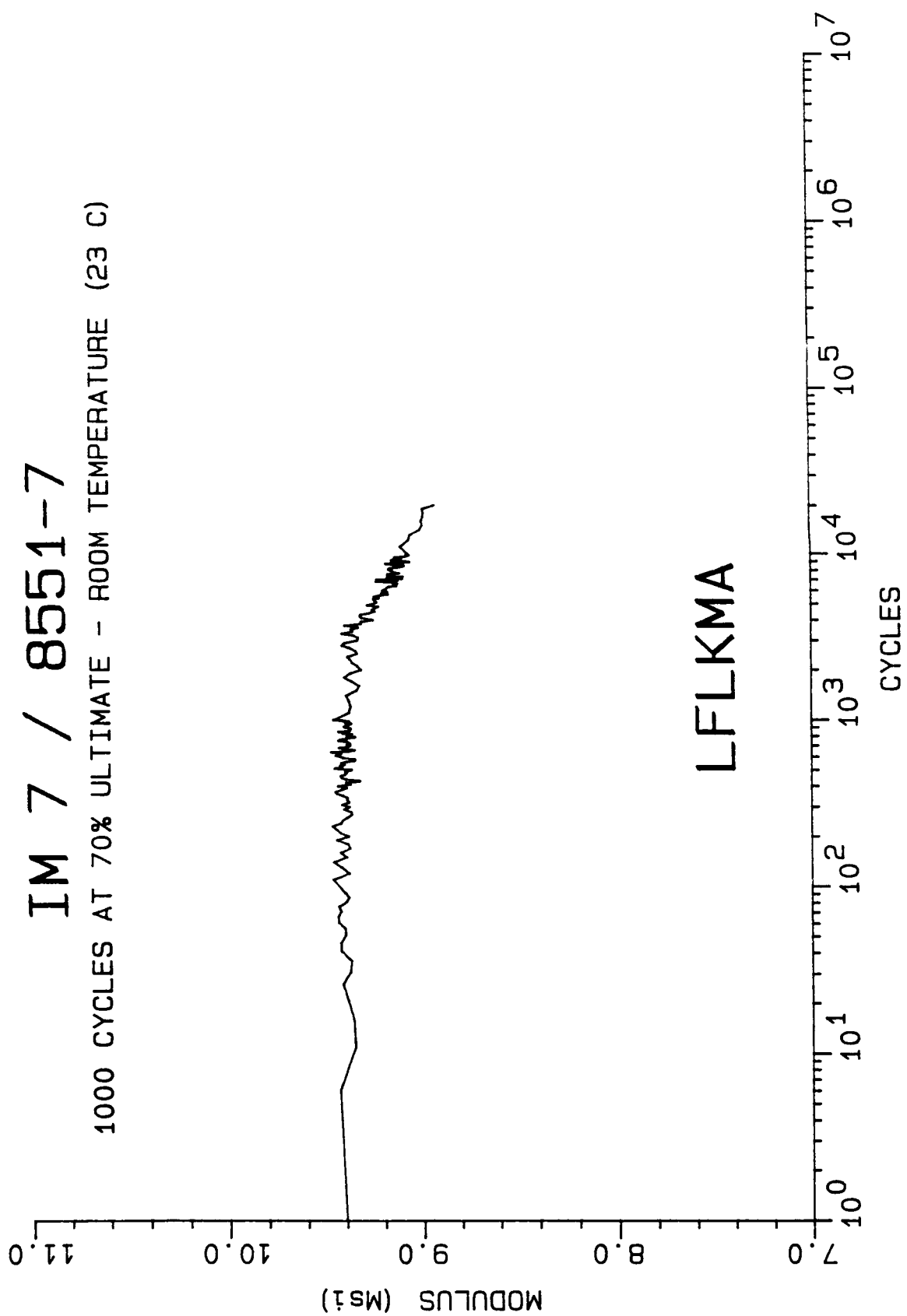
1000 CYCLES AT 70% ULTIMATE - ROOM TEMPERATURE (23 C)



MODULUS DECAY CURVE

IM 7 / 8551-7

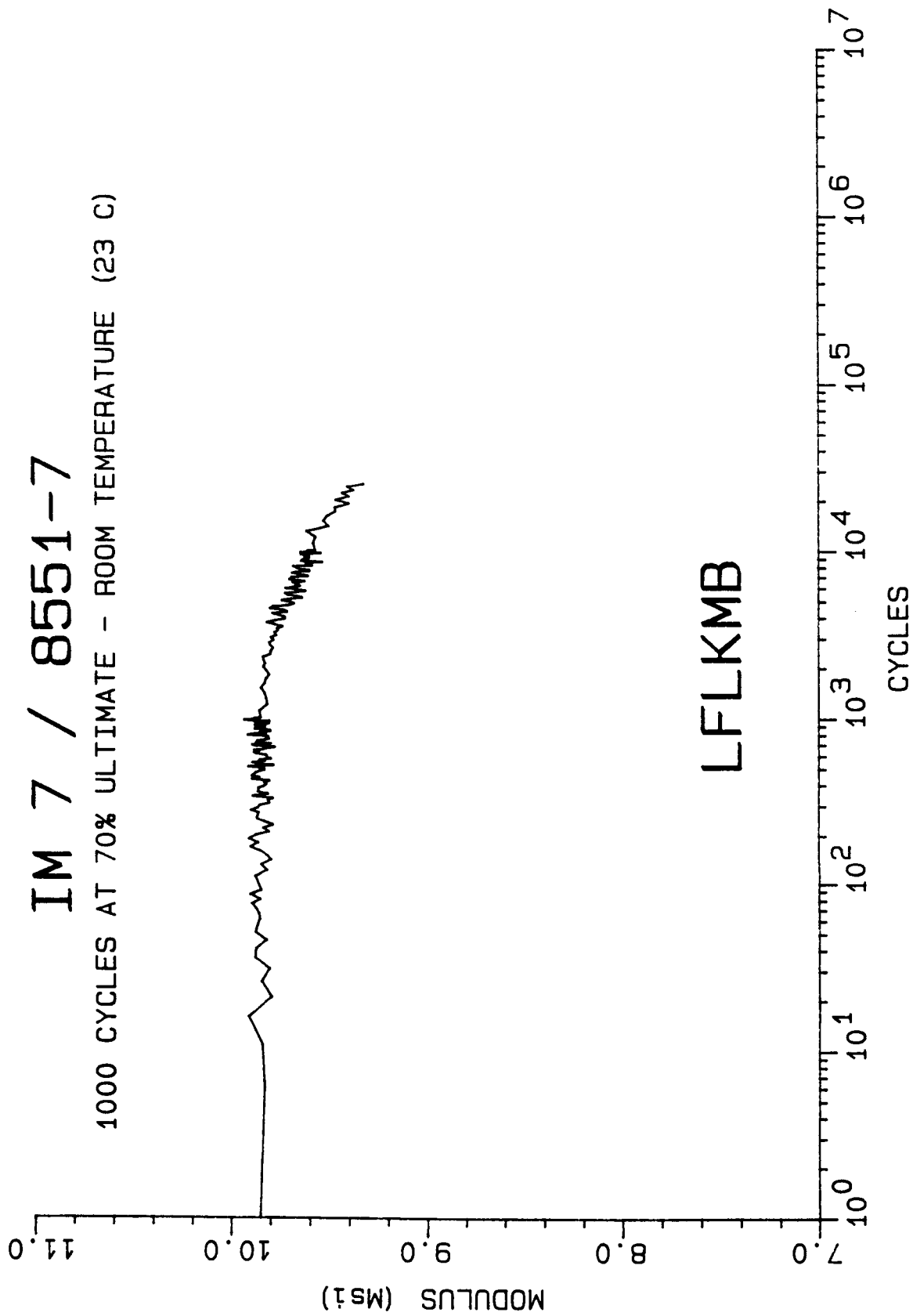
1000 CYCLES AT 70% ULTIMATE - ROOM TEMPERATURE (23 C)



MODULUS DECAY CURVE

IM 7 / 8551-7

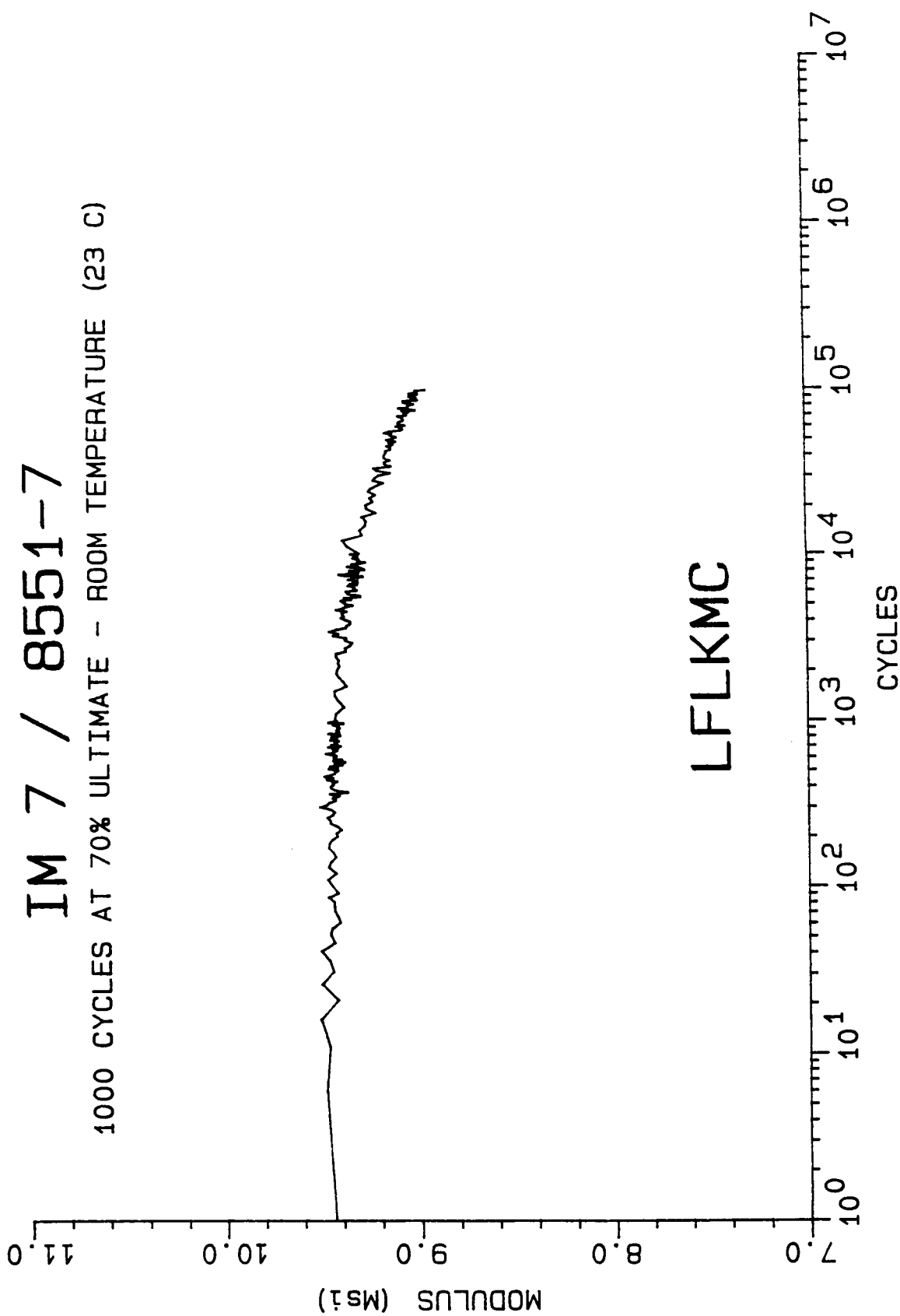
1000 CYCLES AT 70% ULTIMATE - ROOM TEMPERATURE (23 C)



MODULUS DECAY CURVE

IM 7 / 8551-7

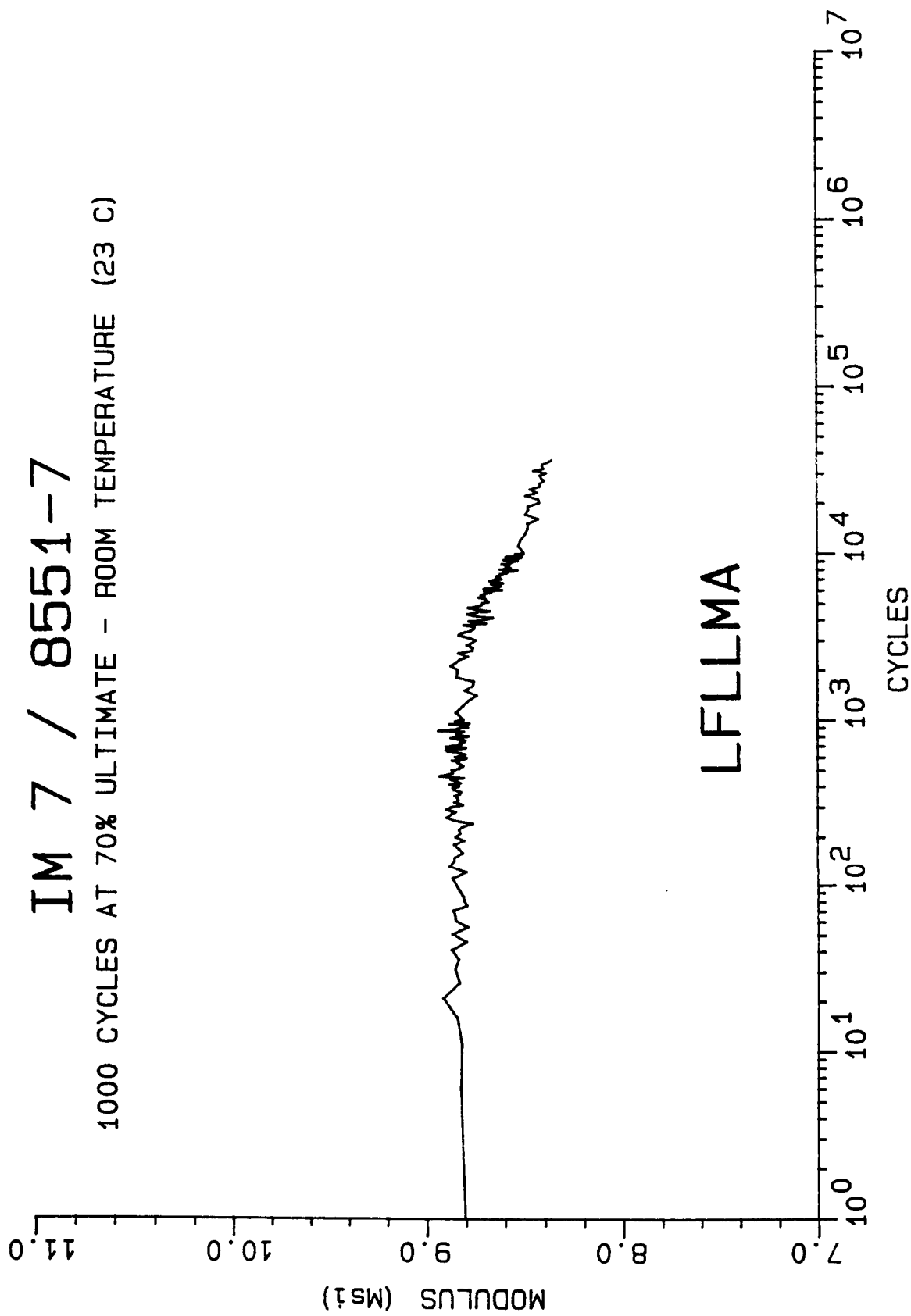
1000 CYCLES AT 70% ULTIMATE - ROOM TEMPERATURE (23 C)



MODULUS DECAY CURVE

IM 7 / 8551-7

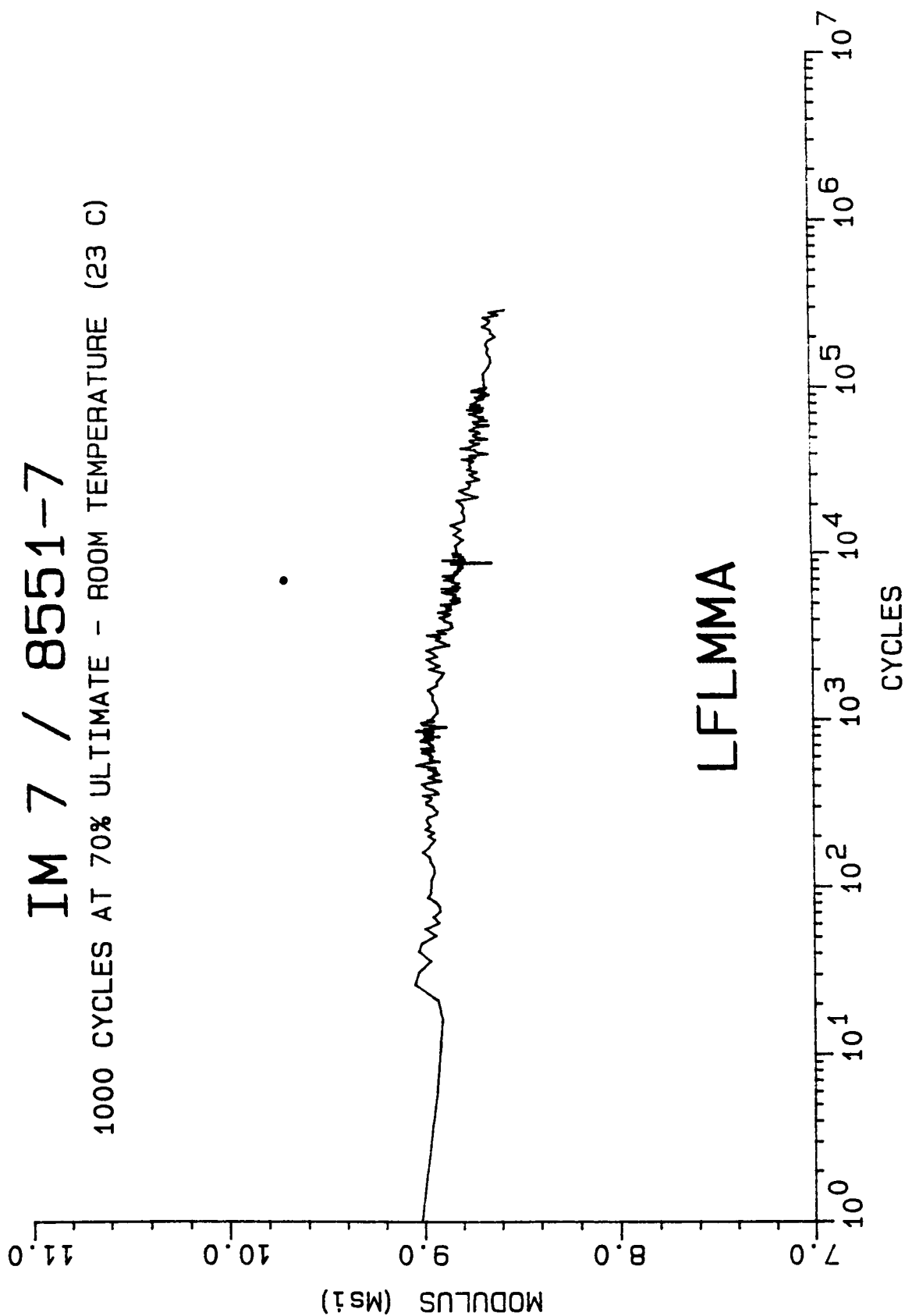
1000 CYCLES AT 70% ULTIMATE - ROOM TEMPERATURE (23 C)



MODULUS DECAY CURVE

IM 7 / 8551-7

1000 CYCLES AT 70% ULTIMATE - ROOM TEMPERATURE (23 C)

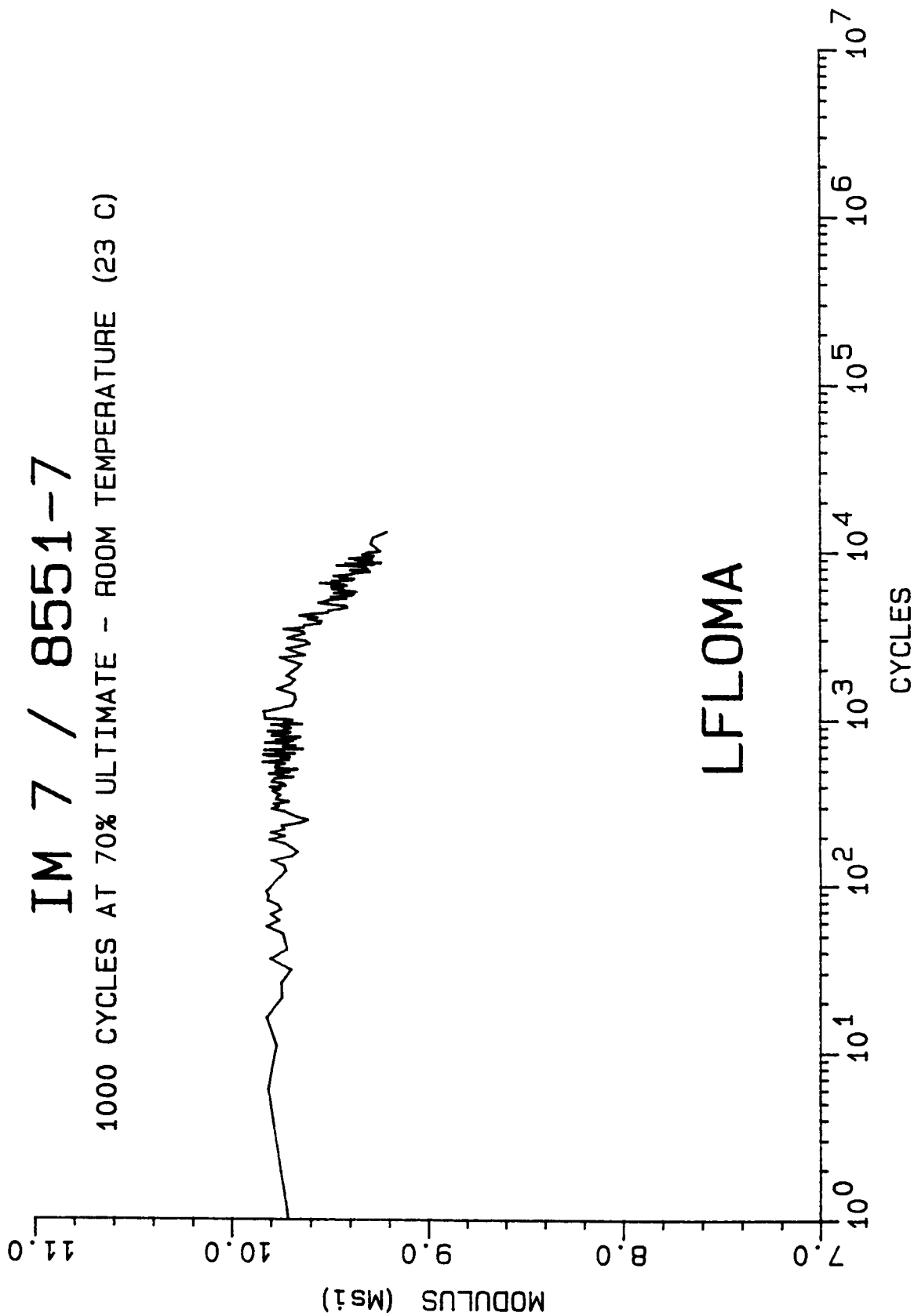


LFLMMA

MODULUS DECAY CURVE

IM 7 / 8551-7

1000 CYCLES AT 70% ULTIMATE - ROOM TEMPERATURE (23 C)

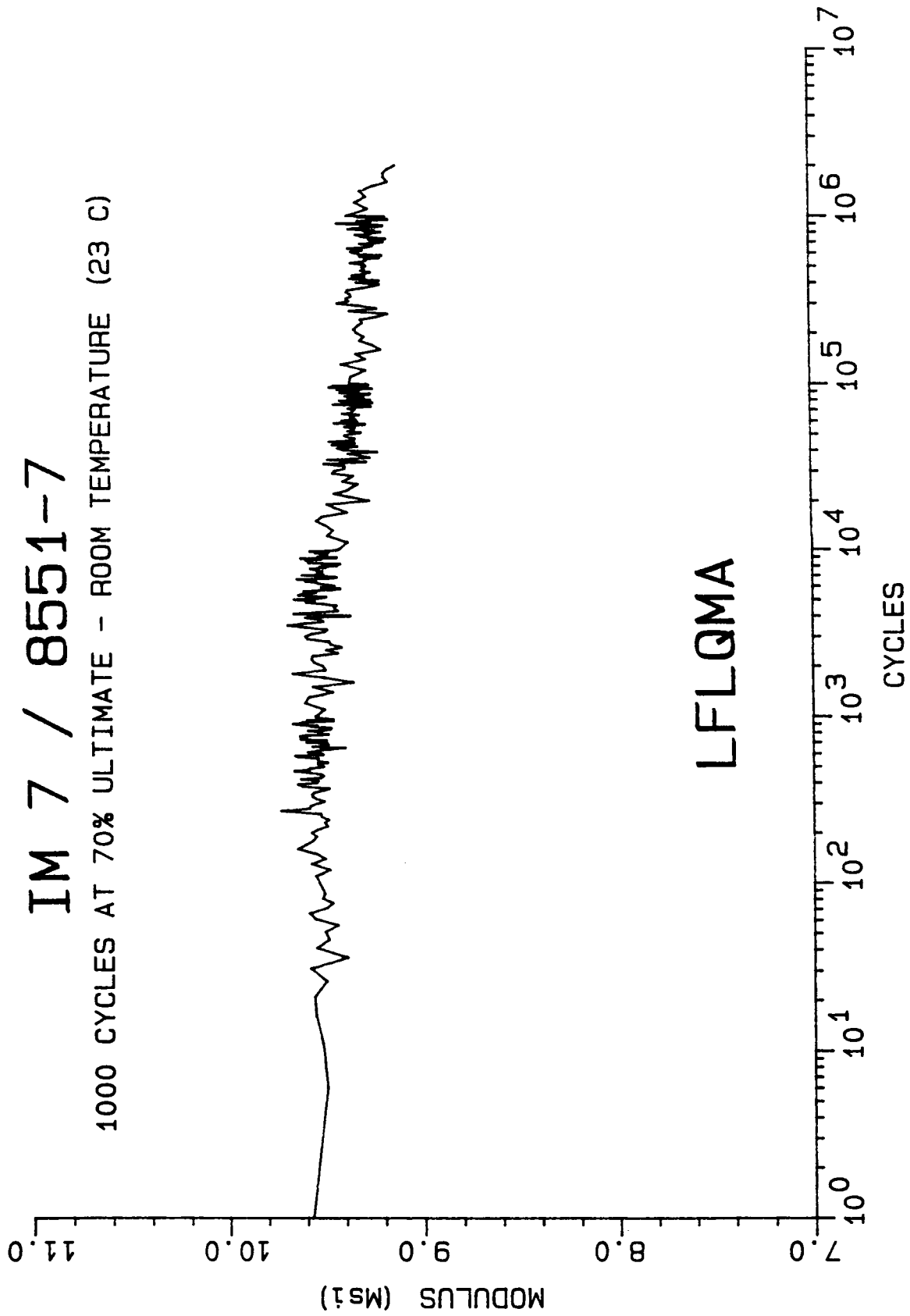


LFLOMA

MODULUS DECAY CURVE

IM 7 / 8551-7

1000 CYCLES AT 70% ULTIMATE - ROOM TEMPERATURE (23 C)

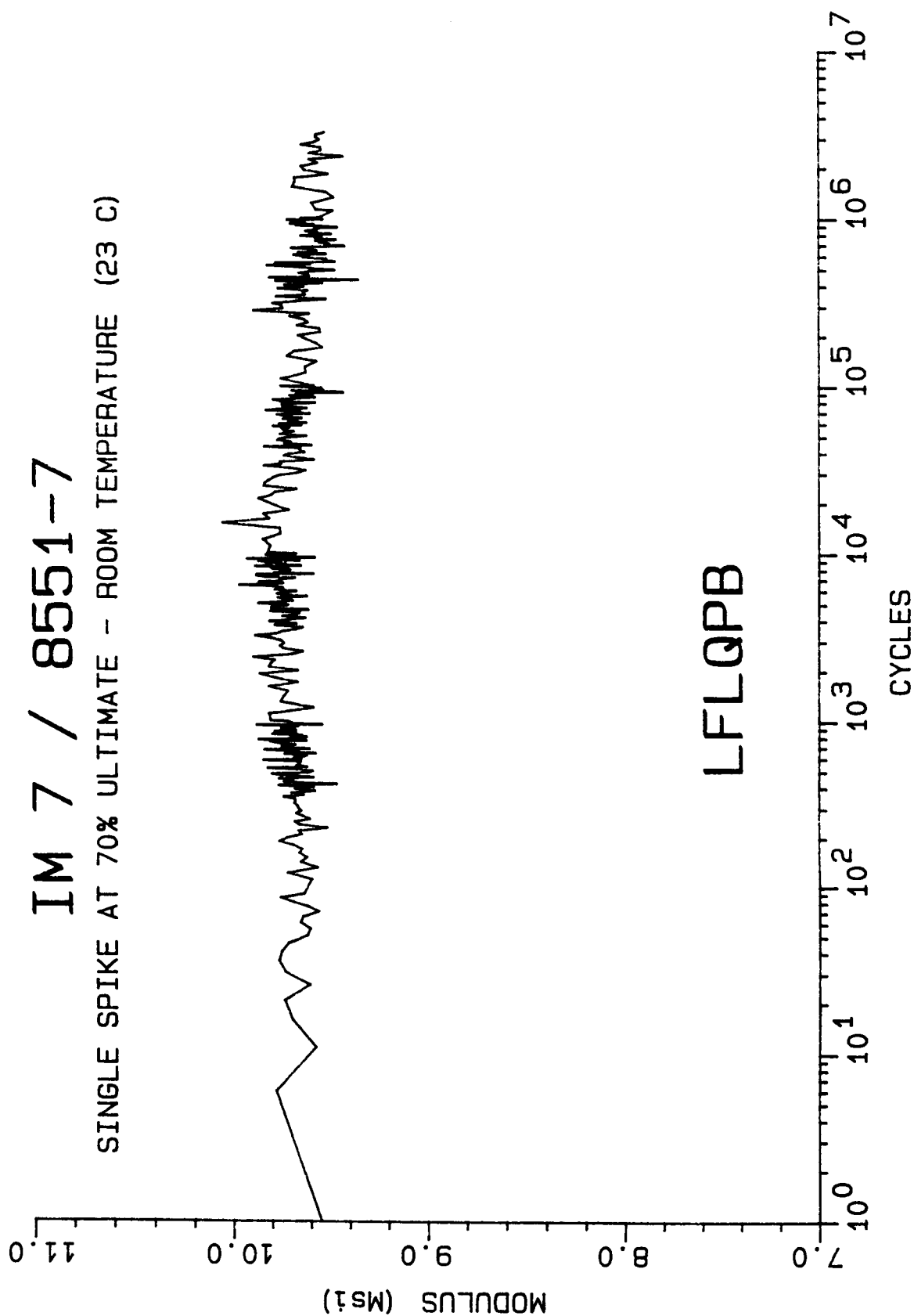


LFLQMA

MODULUS DECAY CURVE

IM 7 / 8551-7

SINGLE SPIKE AT 70% ULTIMATE - ROOM TEMPERATURE (23 C)

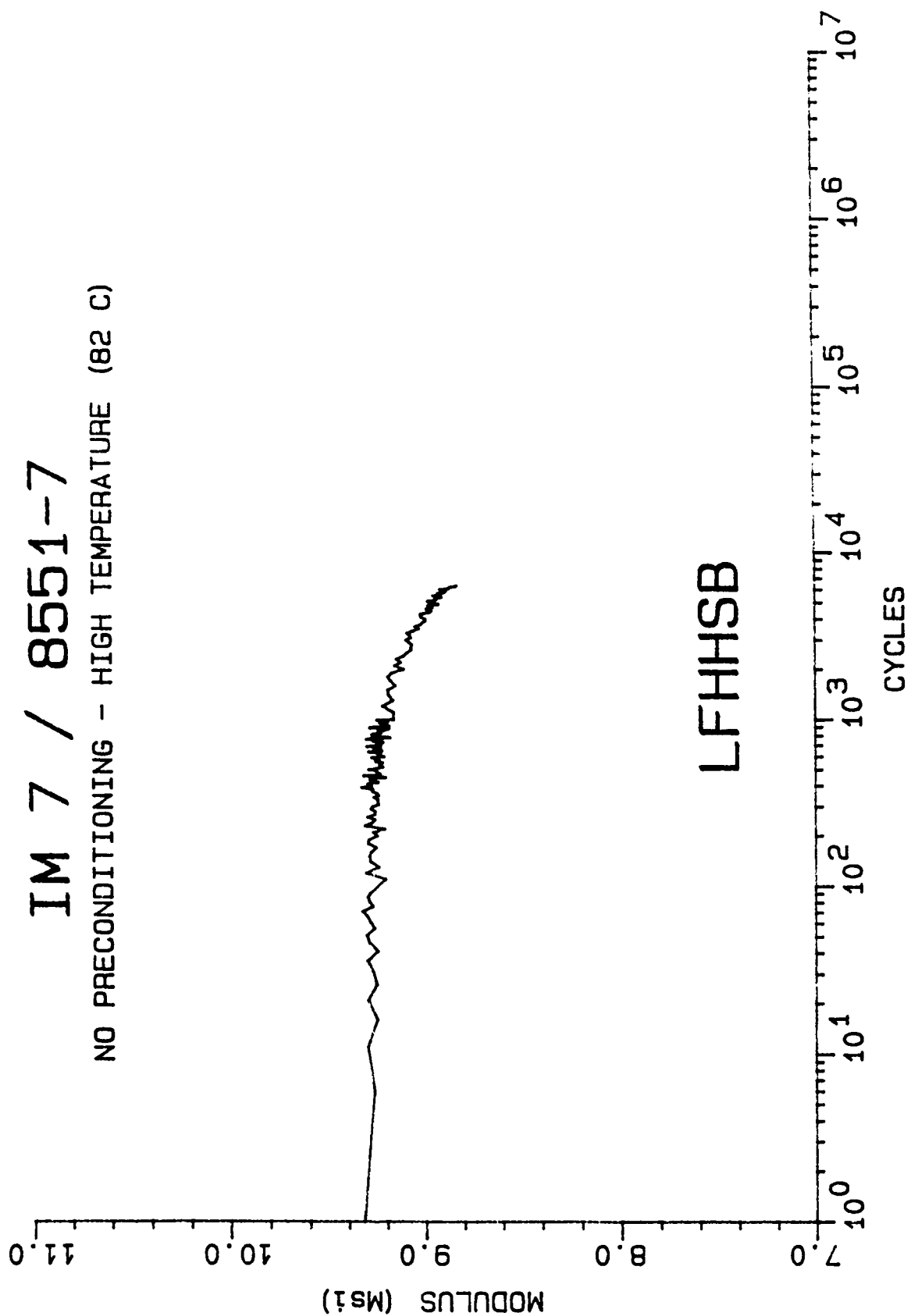


LFLQPB

MODULUS DECAY CURVE

IM 7 / 8551-7

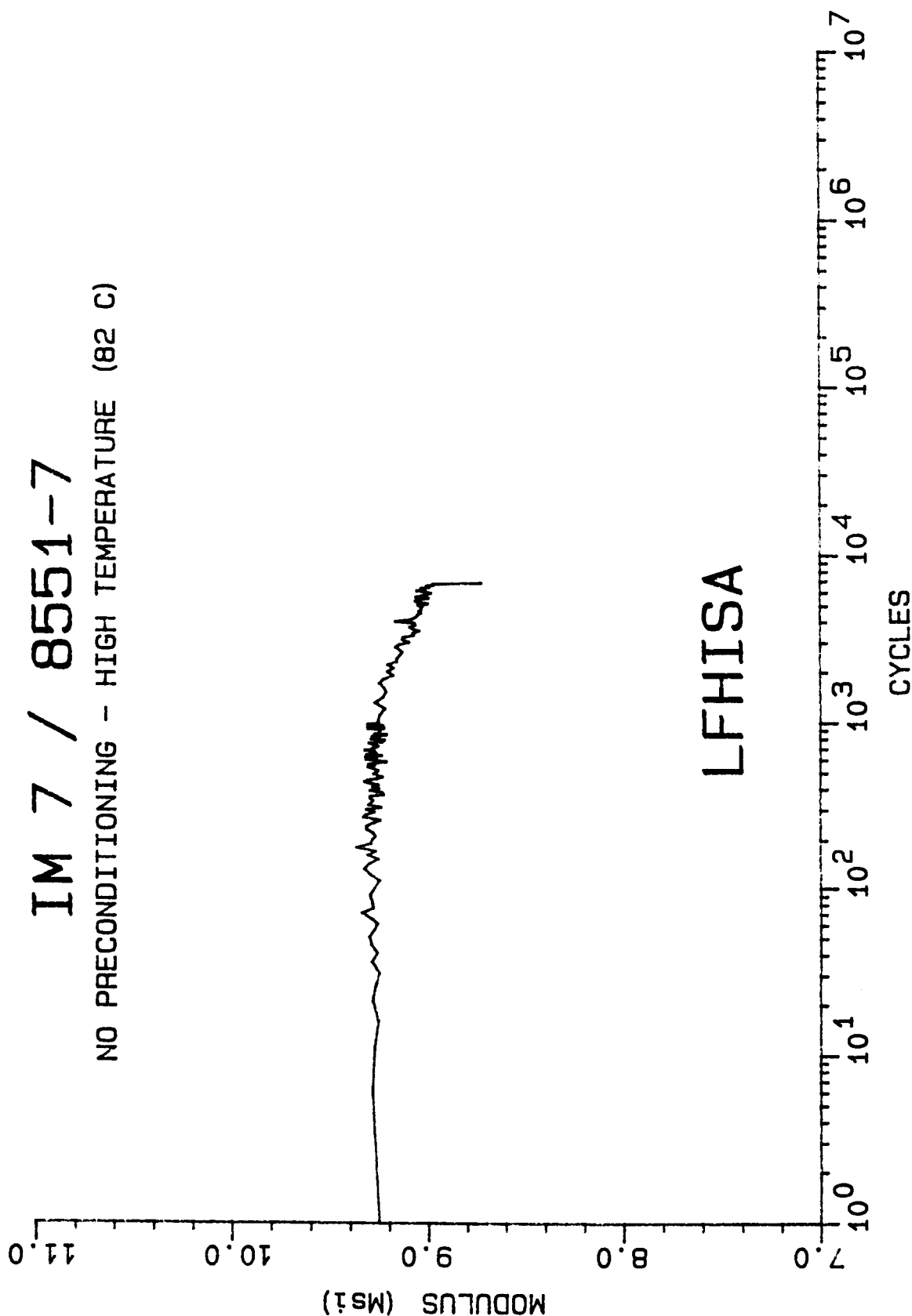
NO PRECONDITIONING - HIGH TEMPERATURE (82 C)



MODULUS DECAY CURVE

IM 7 / 8551-7

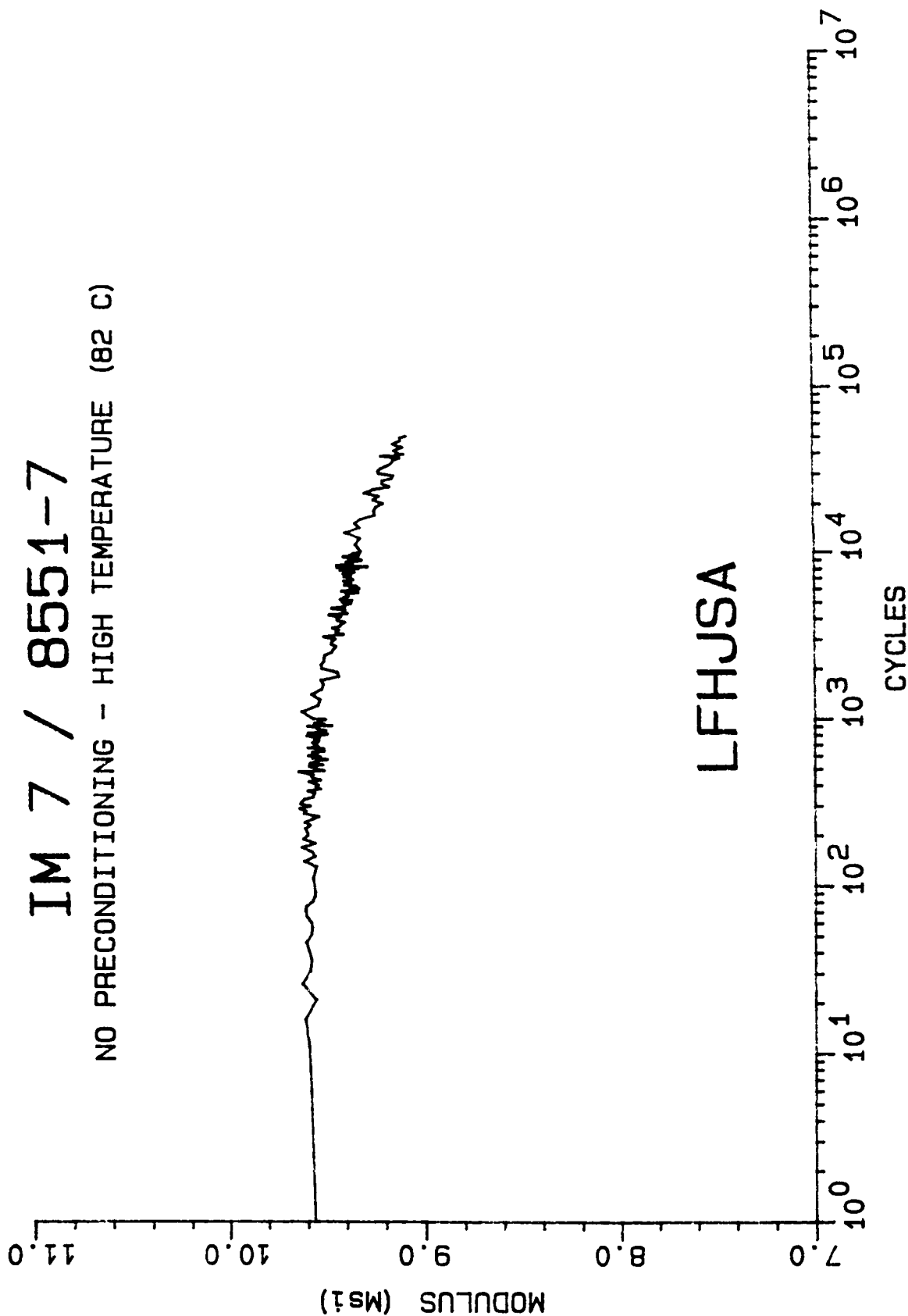
NO PRECONDITIONING - HIGH TEMPERATURE (82 C)



MODULUS DECAY CURVE

IM 7 / 8551-7

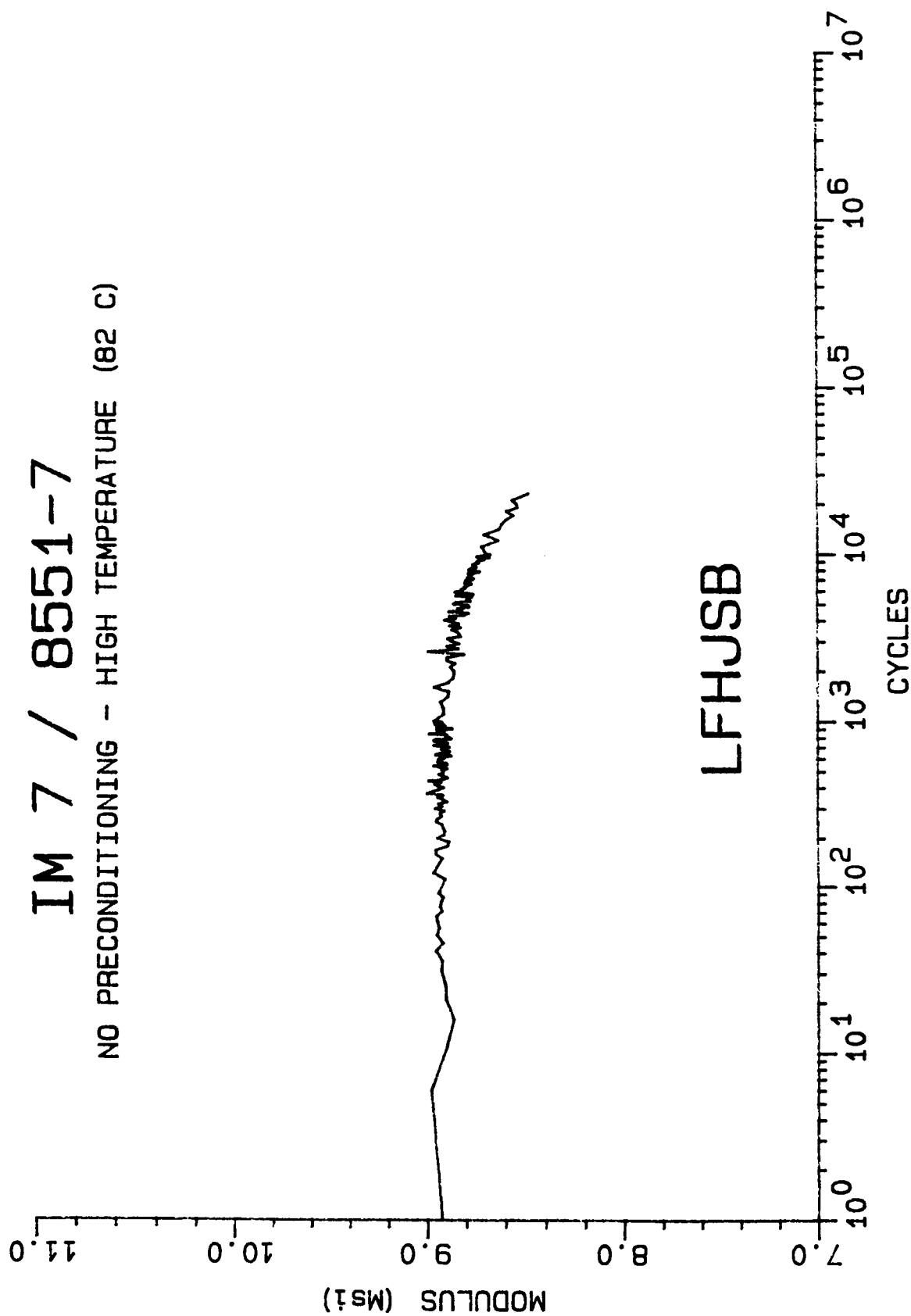
NO PRECONDITIONING - HIGH TEMPERATURE (82 C)



MODULUS DECAY CURVE

IM 7 / 8551-7

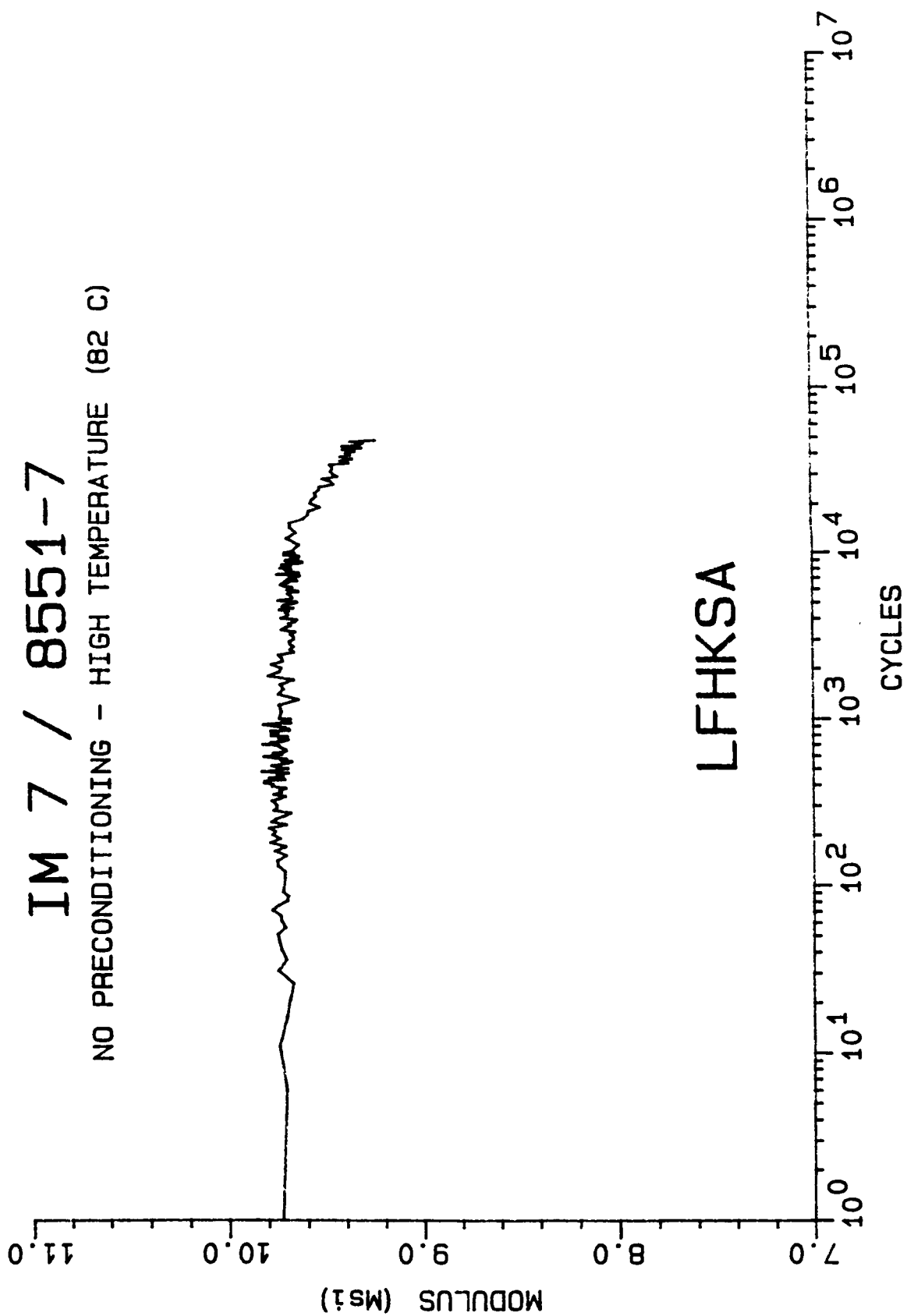
NO PRECONDITIONING - HIGH TEMPERATURE (82 C)



MODULUS DECAY CURVE

IM 7 / 8551-7

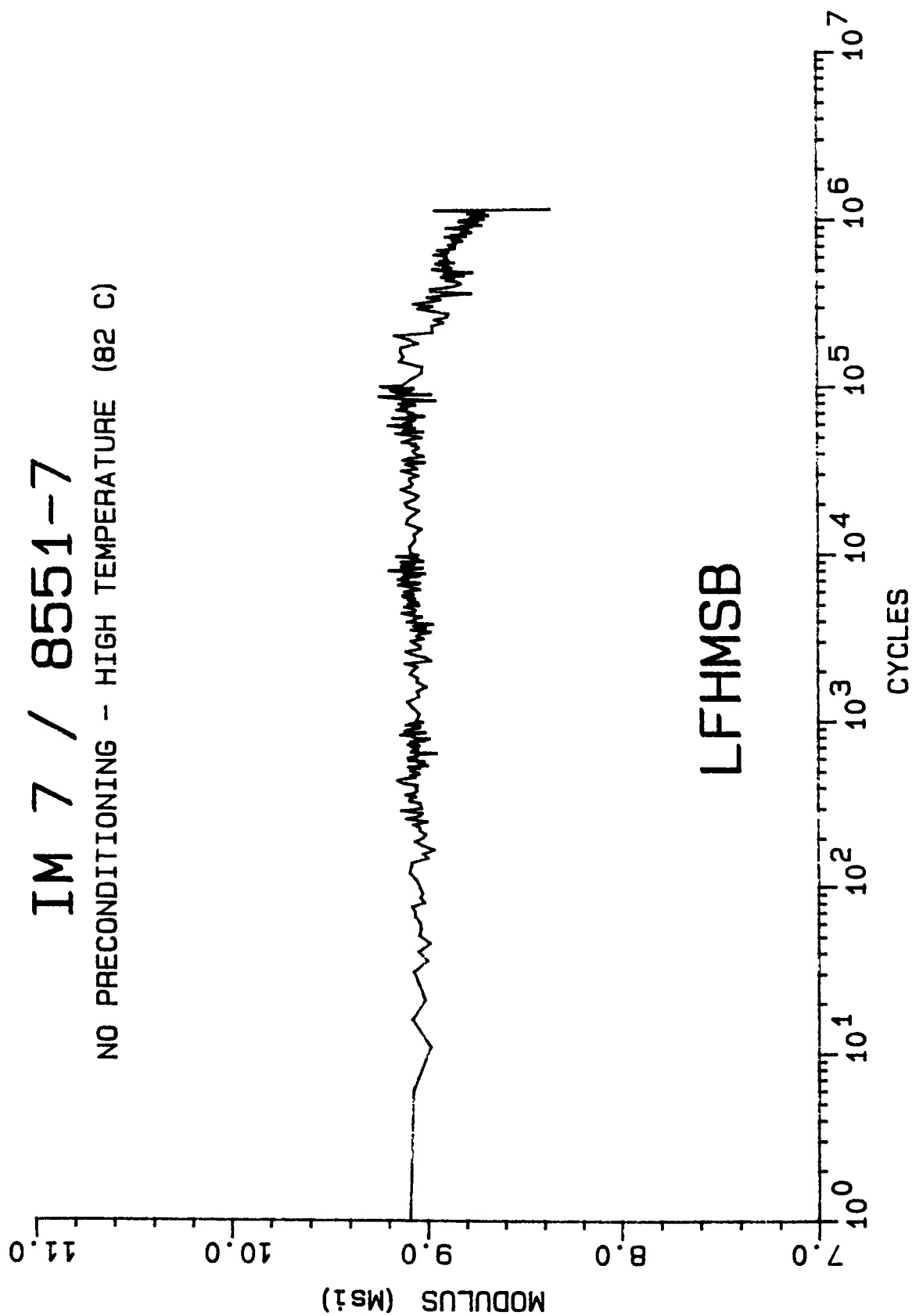
NO PRECONDITIONING - HIGH TEMPERATURE (82 C)



MODULUS DECAY CURVE

IM 7 / 8551-7

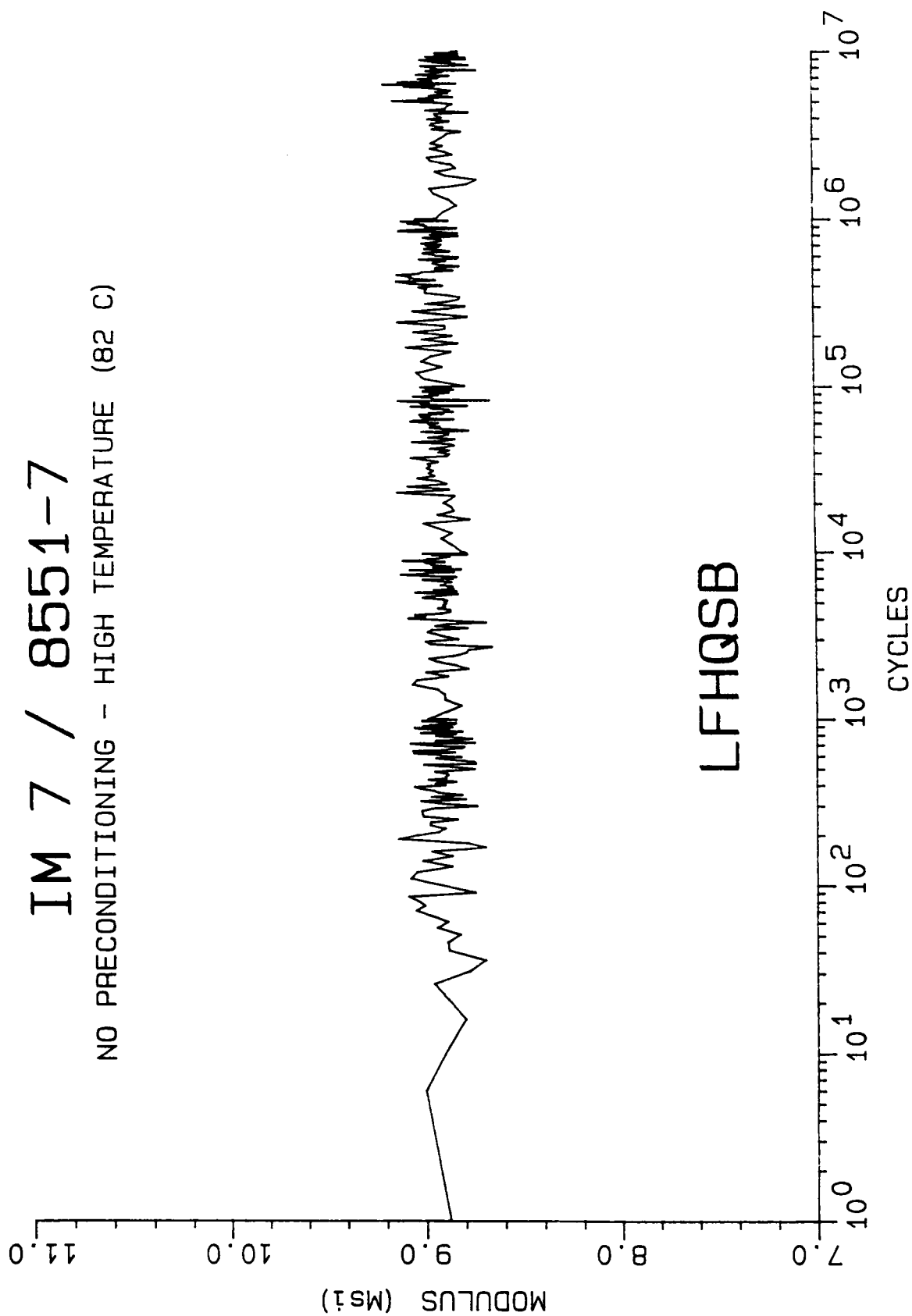
NO PRECONDITIONING - HIGH TEMPERATURE (82 C)



MODULUS DECAY CURVE

IM 7 / 8551-7

NO PRECONDITIONING - HIGH TEMPERATURE (82 C)

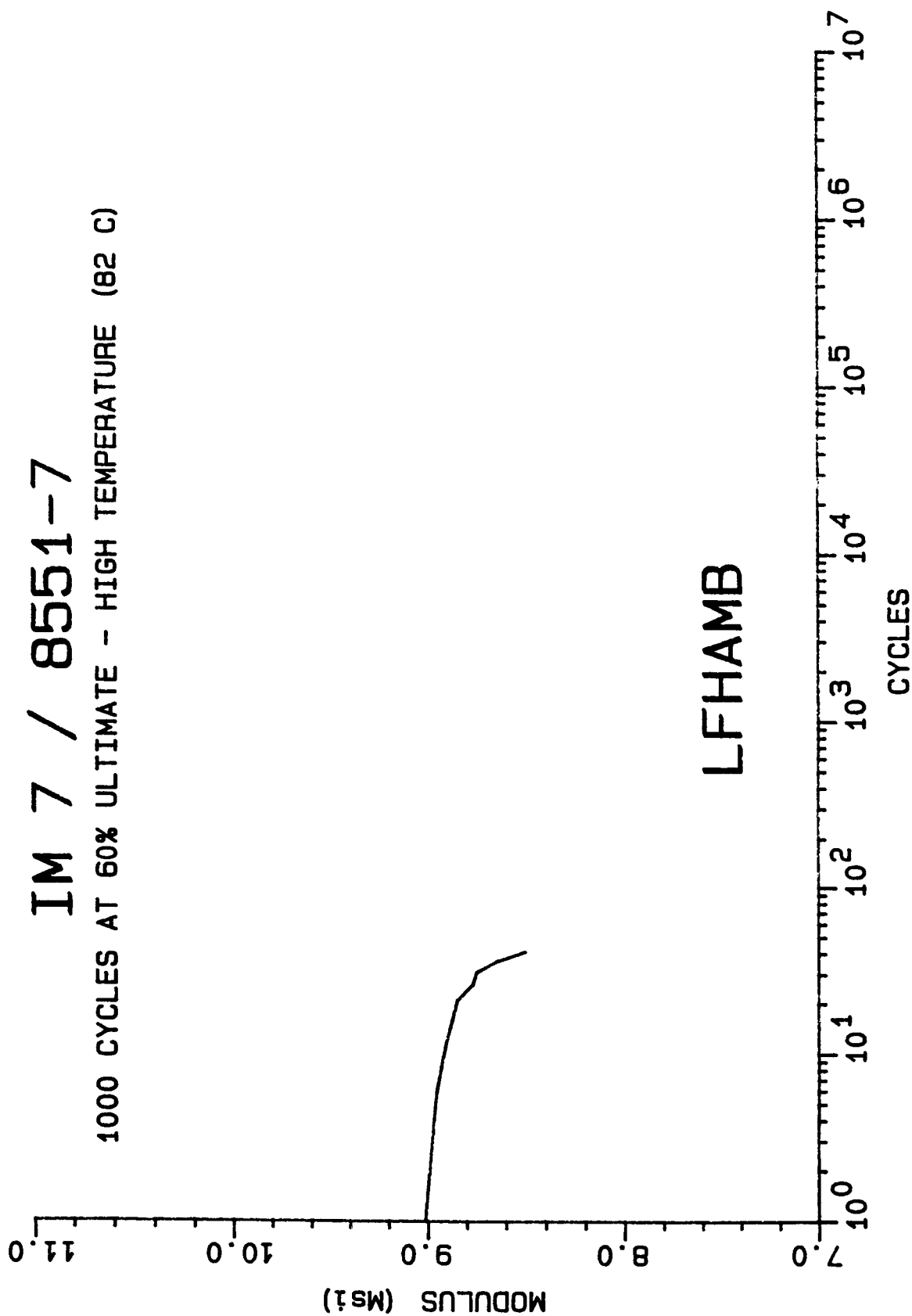


LFHQSB

MODULUS DECAY CURVE

IM 7 / 8551-7

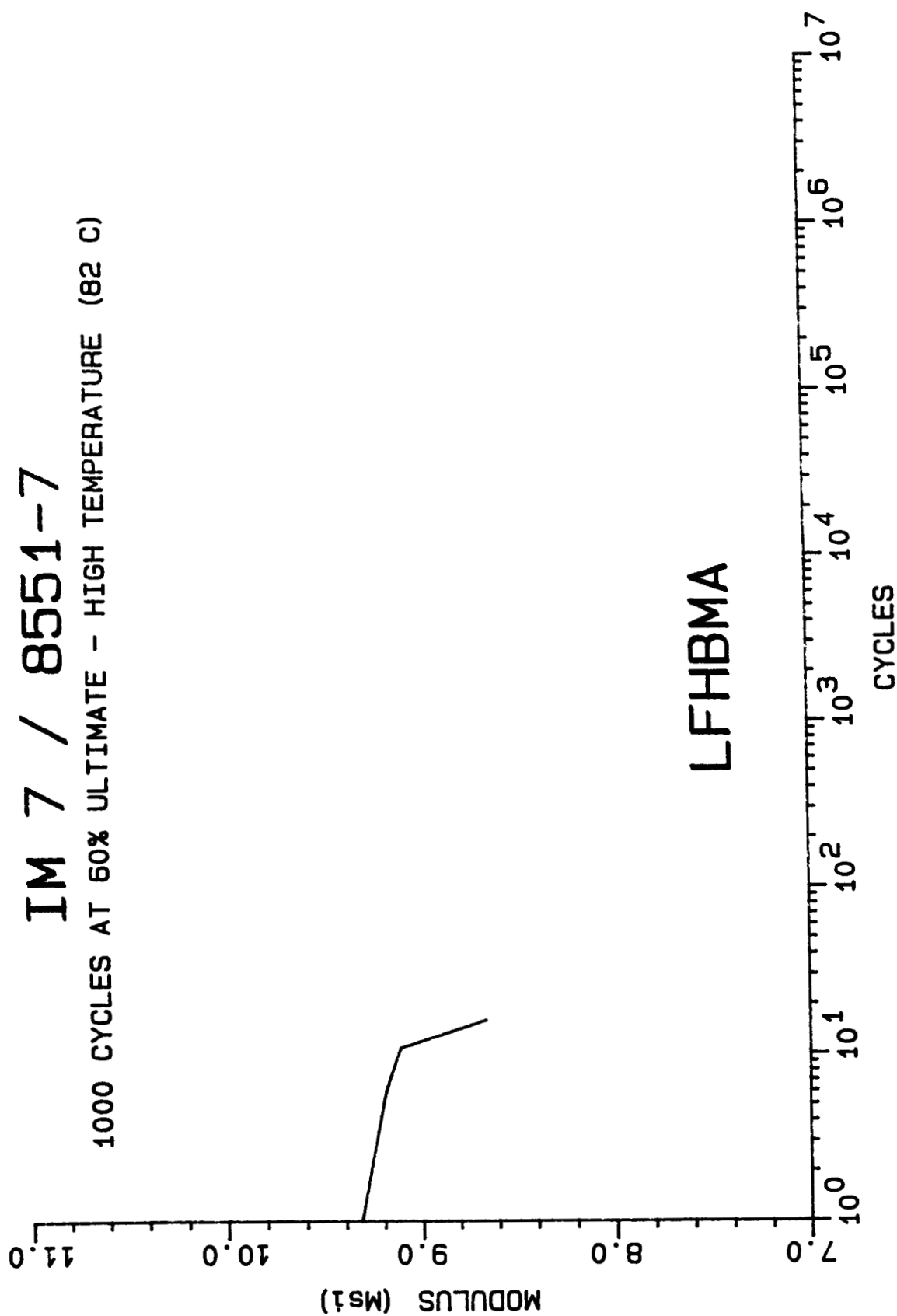
1000 CYCLES AT 60% ULTIMATE - HIGH TEMPERATURE (82 C)



MODULUS DECAY CURVE

IM 7 / 8551-7

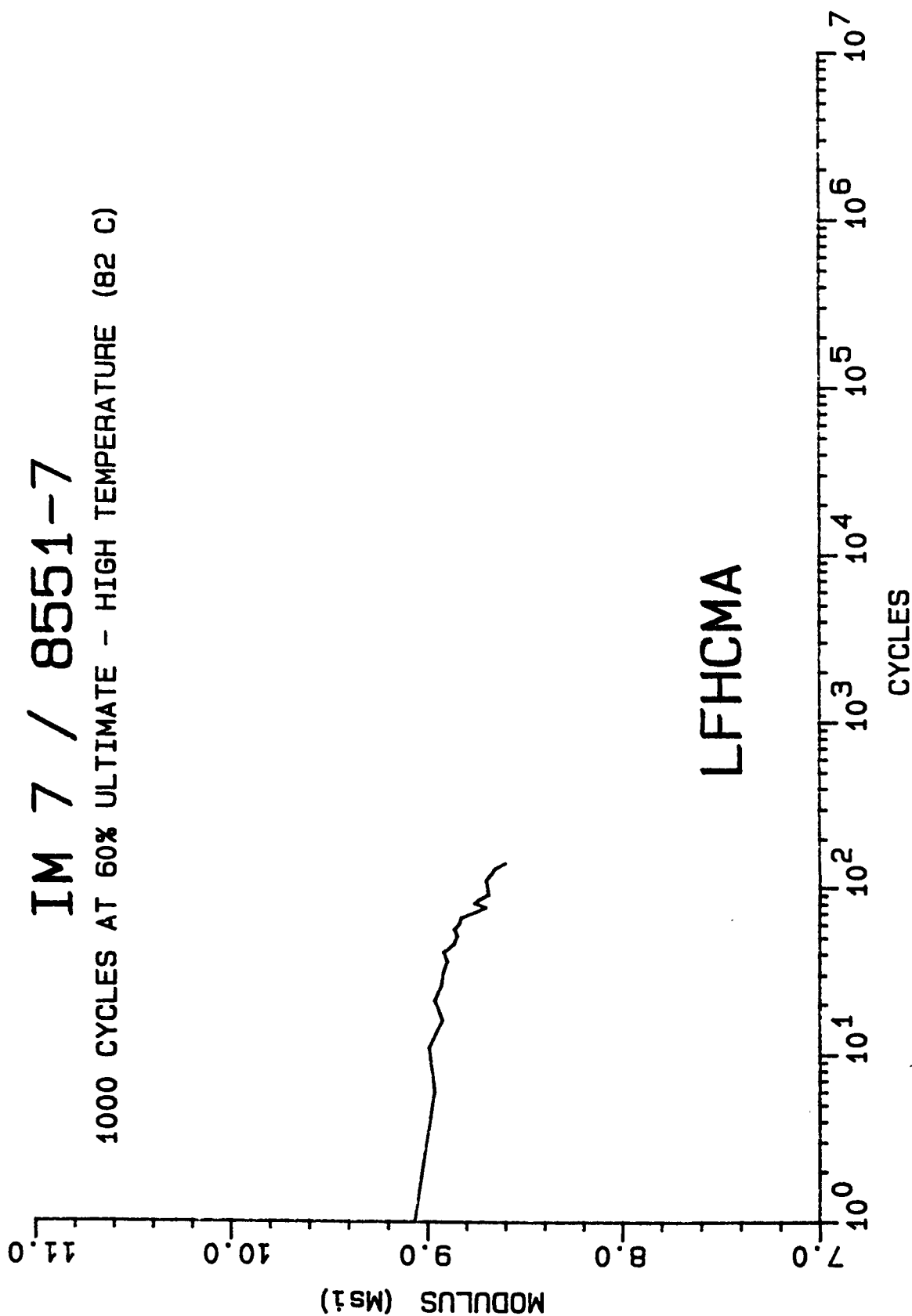
1000 CYCLES AT 60% ULTIMATE - HIGH TEMPERATURE (82 C)



MODULUS DECAY CURVE

IM 7 / 8551-7

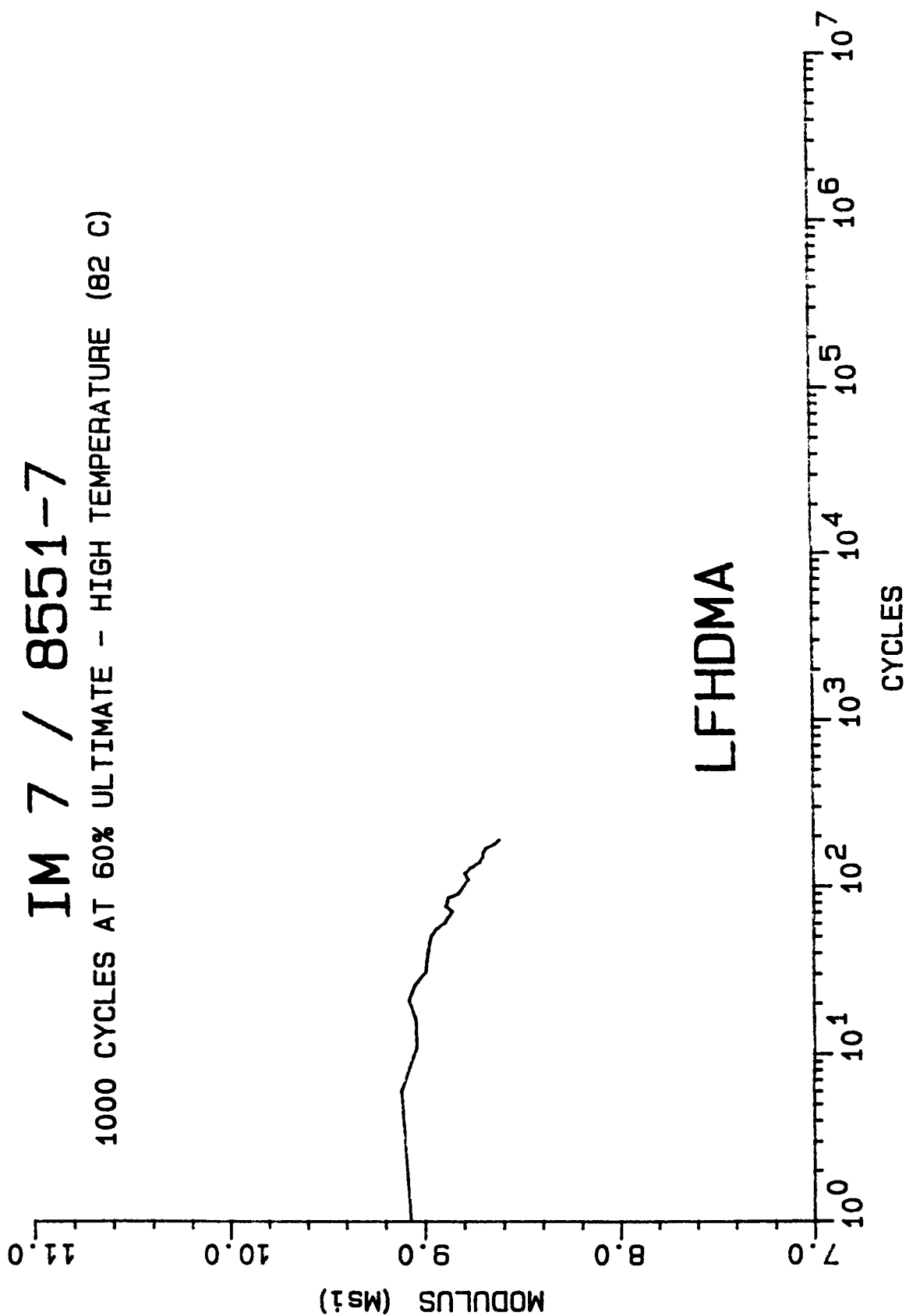
1000 CYCLES AT 60% ULTIMATE - HIGH TEMPERATURE (82 C)



MODULUS DECAY CURVE

IM 7 / 8551-7

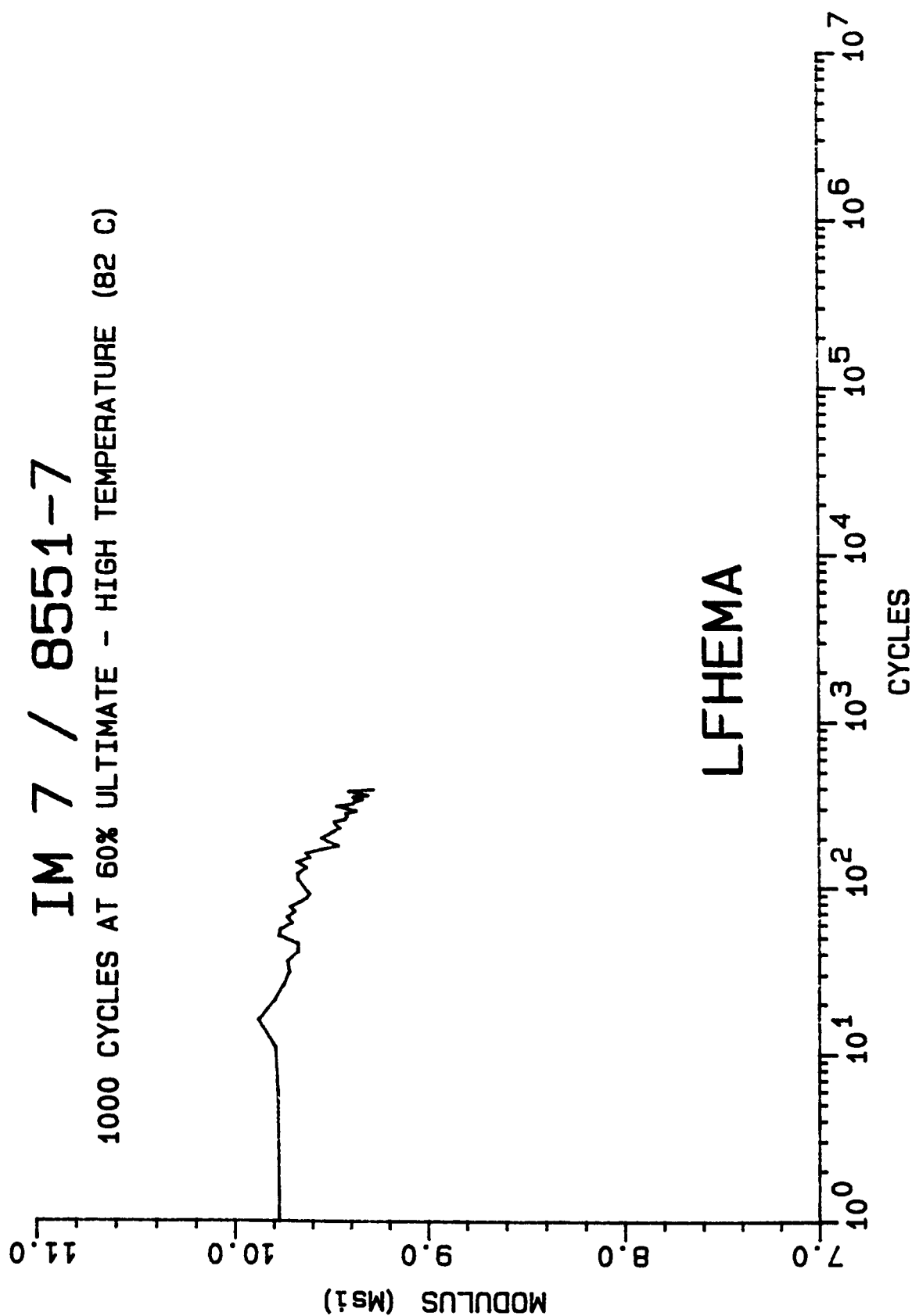
1000 CYCLES AT 60% ULTIMATE - HIGH TEMPERATURE (82 C)



MODULUS DECAY CURVE

IM 7 / 8551-7

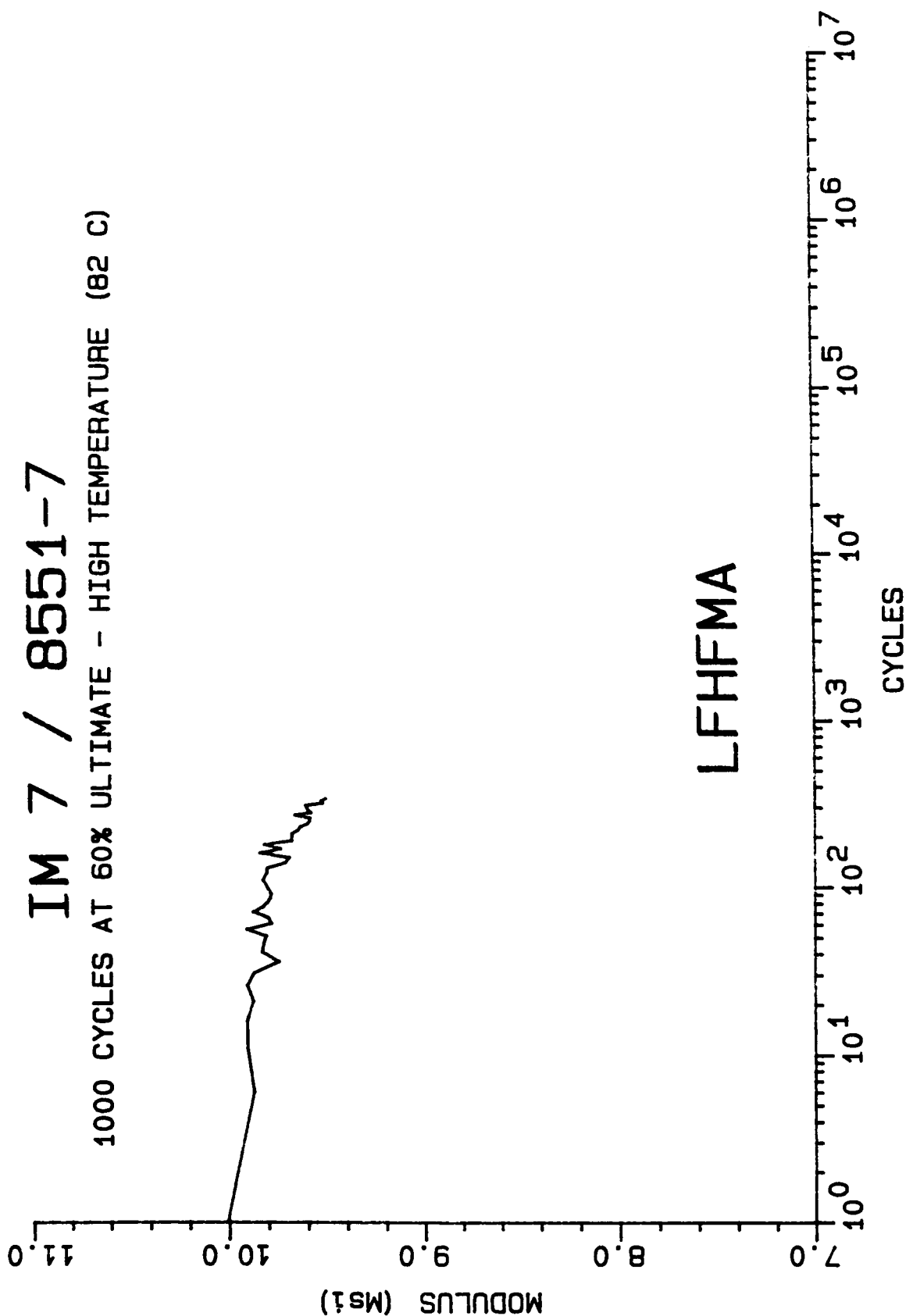
1000 CYCLES AT 60% ULTIMATE - HIGH TEMPERATURE (82 C)



MODULUS DECAY CURVE

IM 7 / 8551-7

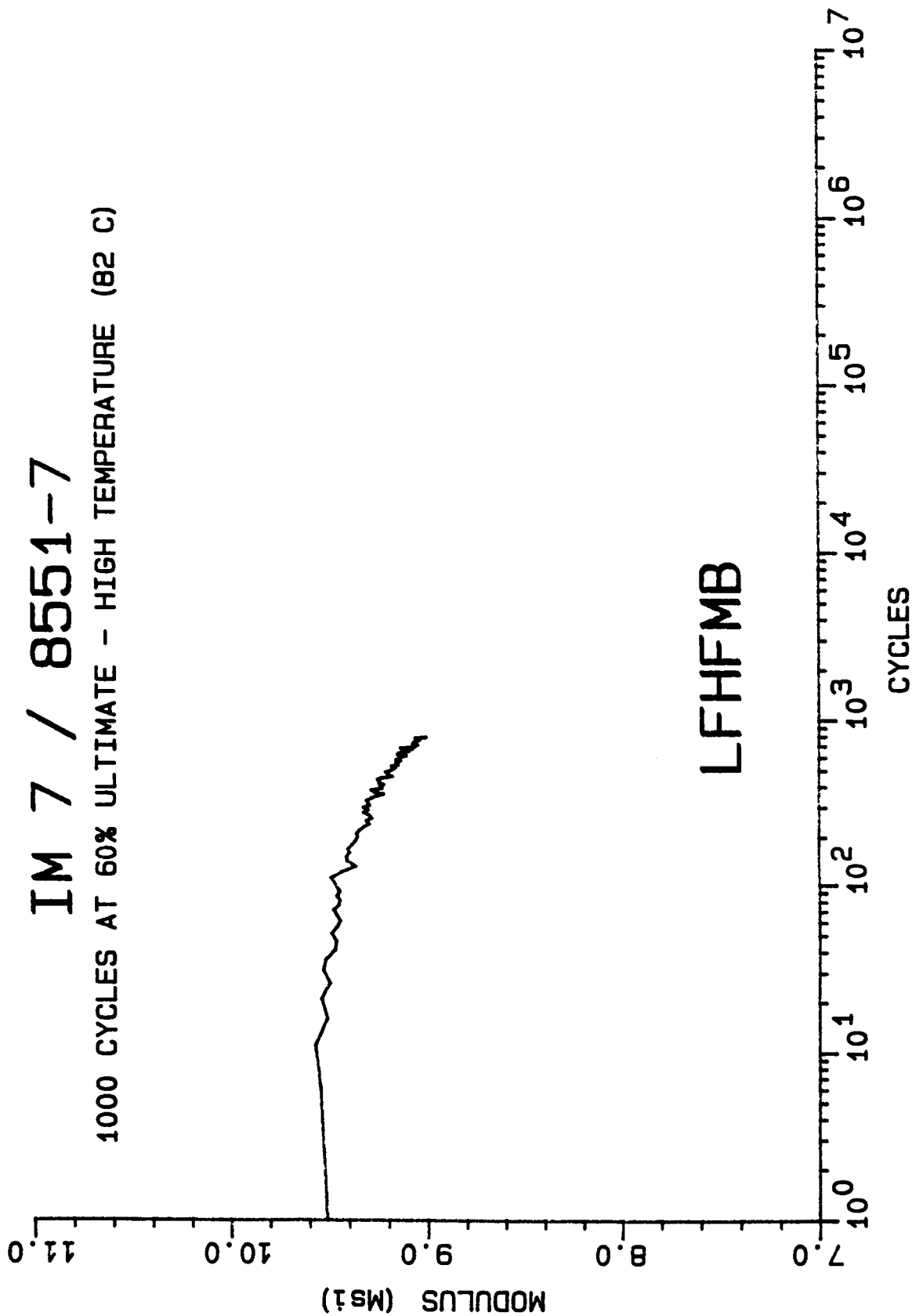
1000 CYCLES AT 60% ULTIMATE - HIGH TEMPERATURE (82 C)



MODULUS DECAY CURVE

IM 7 / 8551--7

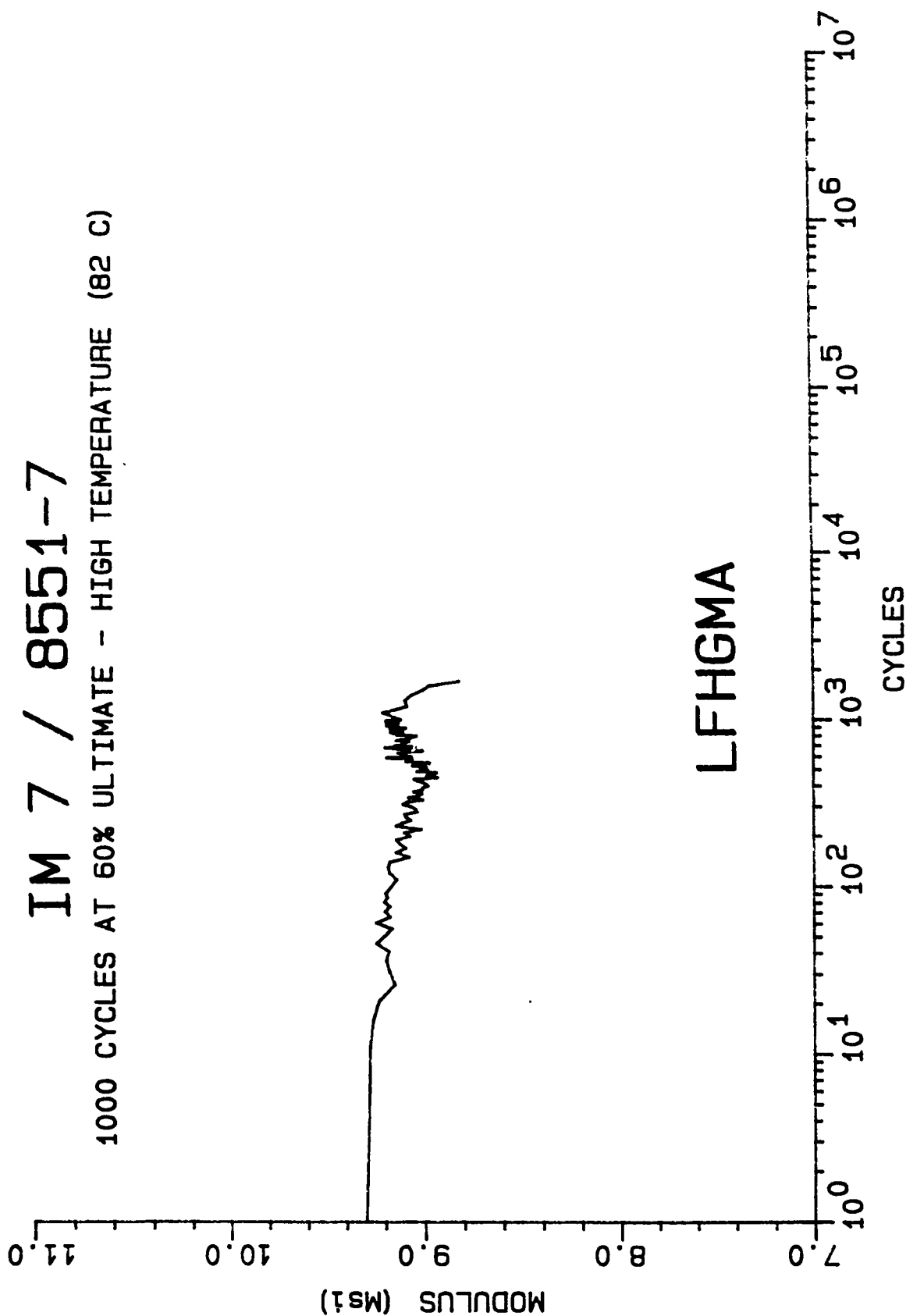
1000 CYCLES AT 60% ULTIMATE - HIGH TEMPERATURE (82 C)



MODULUS DECAY CURVE

IM 7 / 8551-7

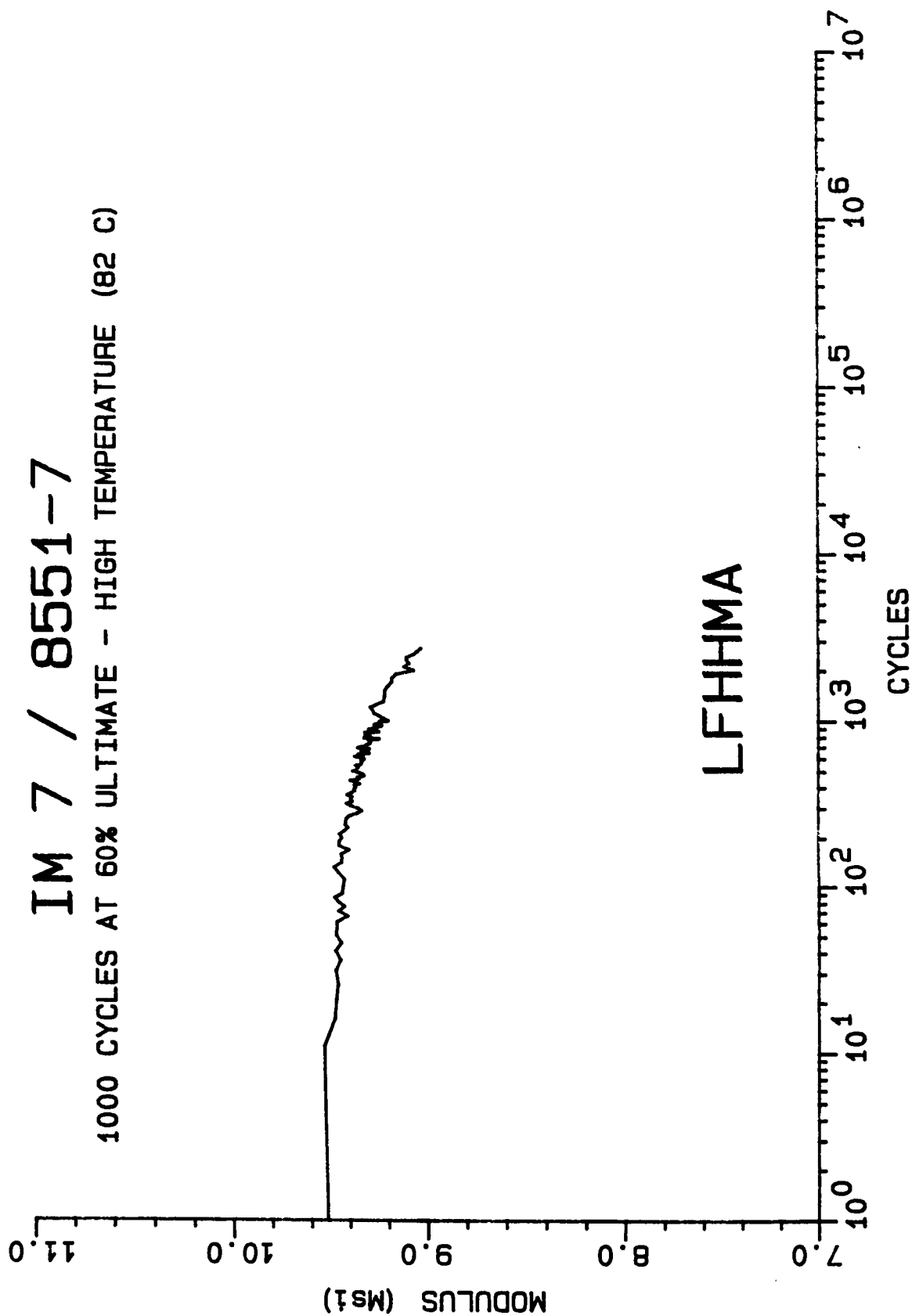
1000 CYCLES AT 60% ULTIMATE - HIGH TEMPERATURE (82 C)



MODULUS DECAY CURVE

IM 7 / 8551-7

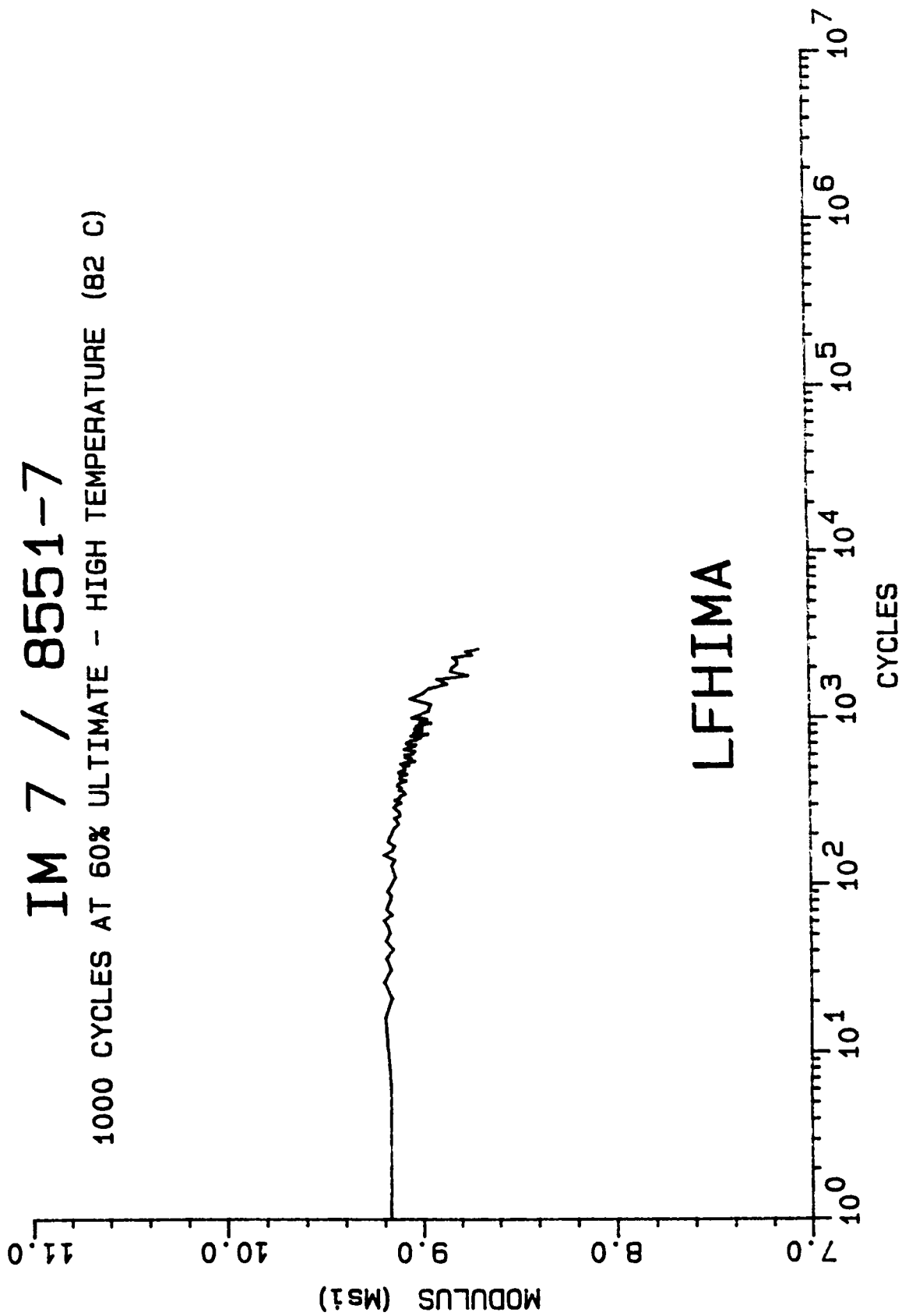
1000 CYCLES AT 60% ULTIMATE - HIGH TEMPERATURE (82 C)



MODULUS DECAY CURVE

IM 7 / 8551-7

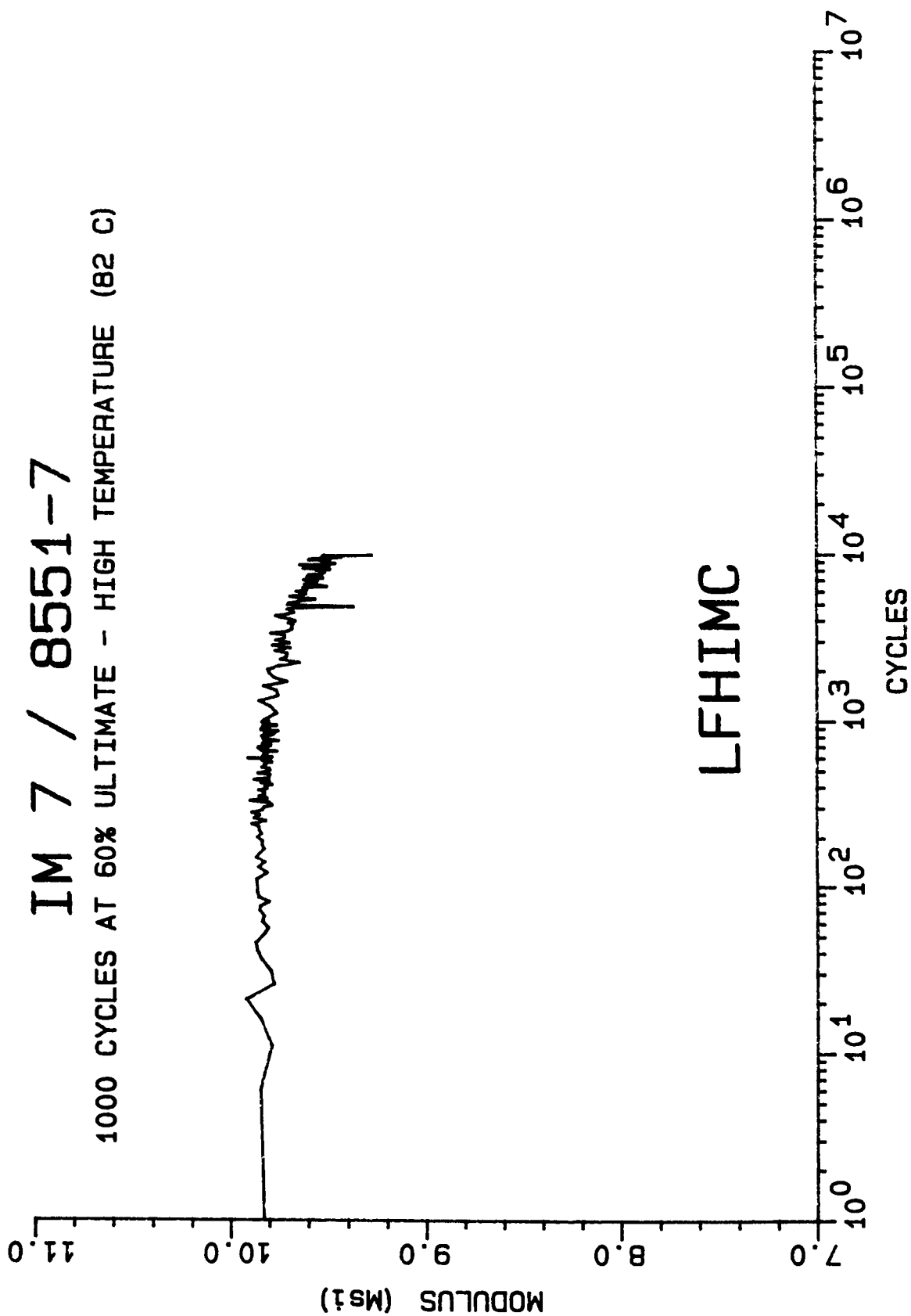
1000 CYCLES AT 60% ULTIMATE - HIGH TEMPERATURE (82 C)



MODULUS DECAY CURVE

IM 7 / 8551-7

1000 CYCLES AT 60% ULTIMATE - HIGH TEMPERATURE (82 C)

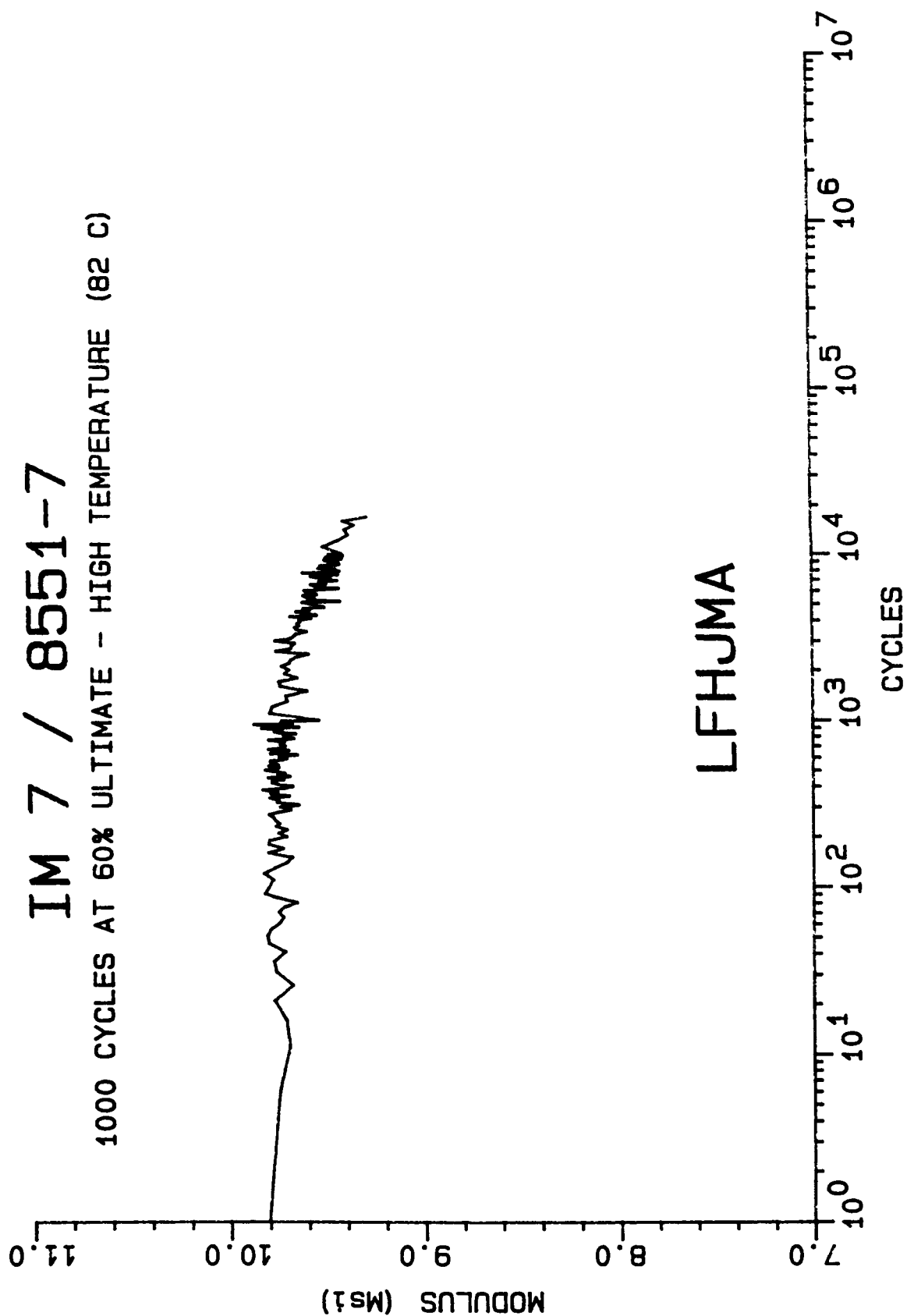


LFHIMC

MODULUS DECAY CURVE

IM 7 / 8551-7

1000 CYCLES AT 60% ULTIMATE - HIGH TEMPERATURE (82 C)

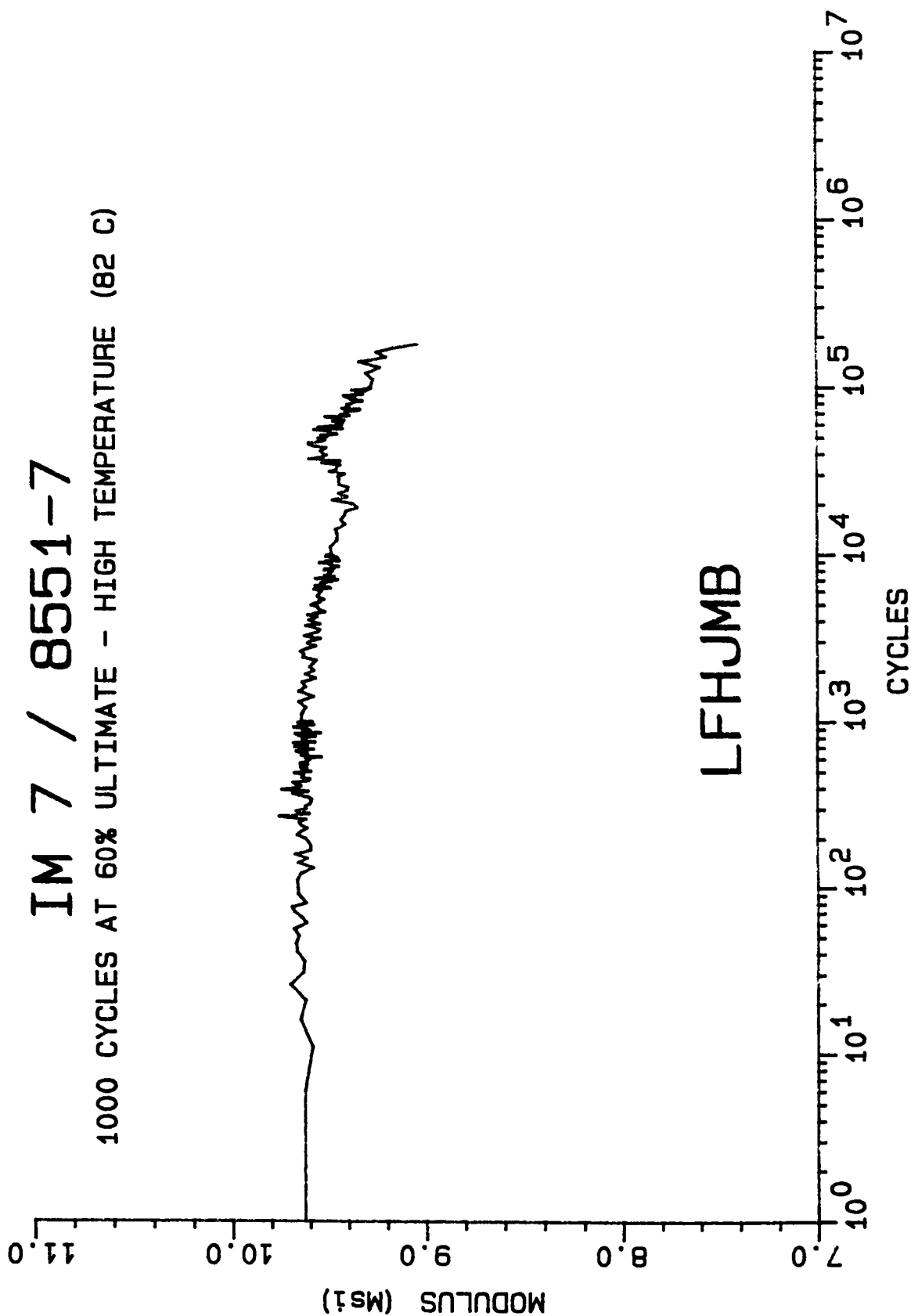


LFHJMA

MODULUS DECAY CURVE

IM 7 / 8551-7

1000 CYCLES AT 60% ULTIMATE - HIGH TEMPERATURE (82 C)

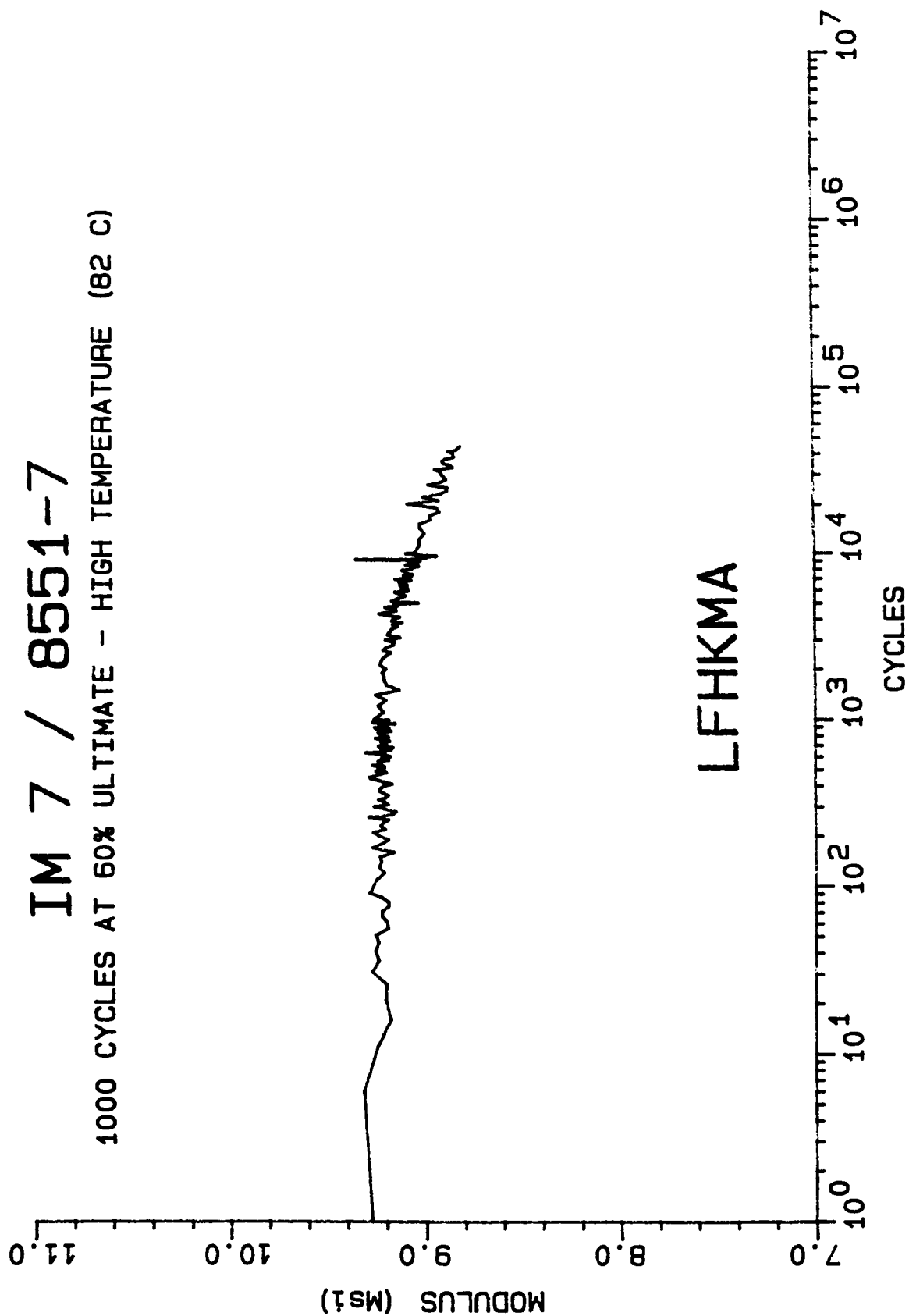


LFHJMB

MODULUS DECAY CURVE

IM 7 / 8551-7

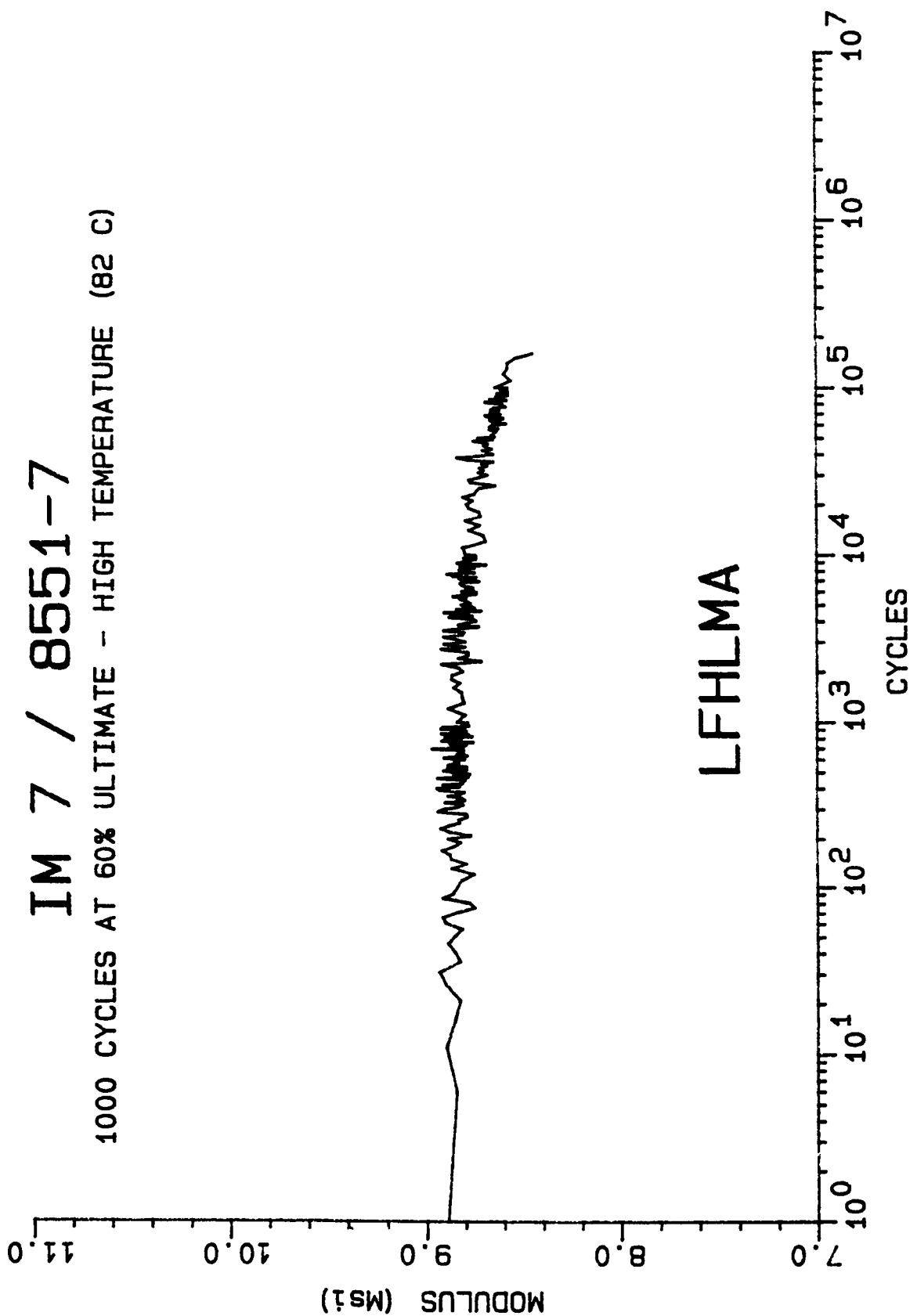
1000 CYCLES AT 60% ULTIMATE - HIGH TEMPERATURE (82 C)



MODULUS DECAY CURVE

IM 7 / 8551-7

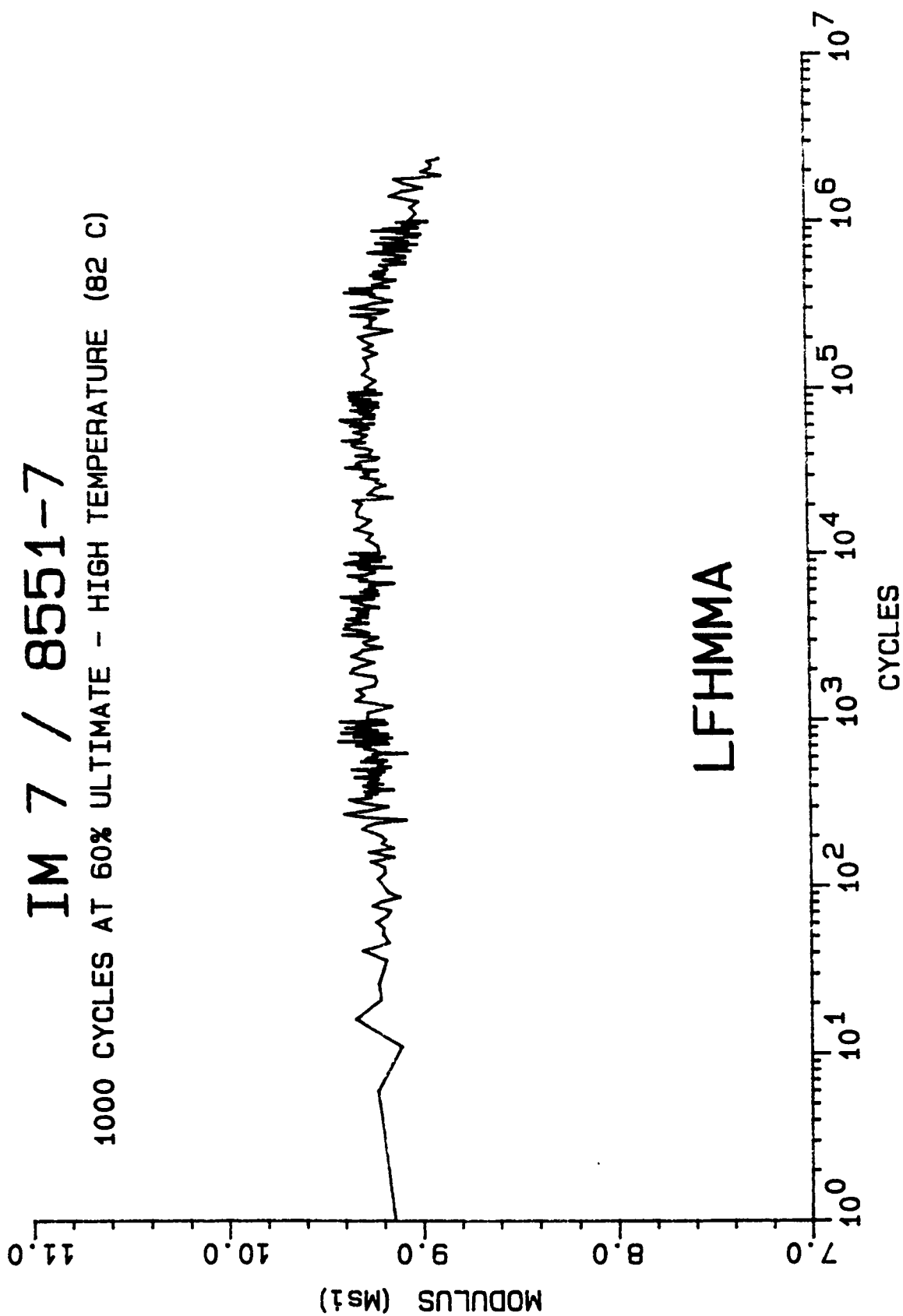
1000 CYCLES AT 60% ULTIMATE - HIGH TEMPERATURE (82 C)



MODULUS DECAY CURVE

IM 7 / 8551-7

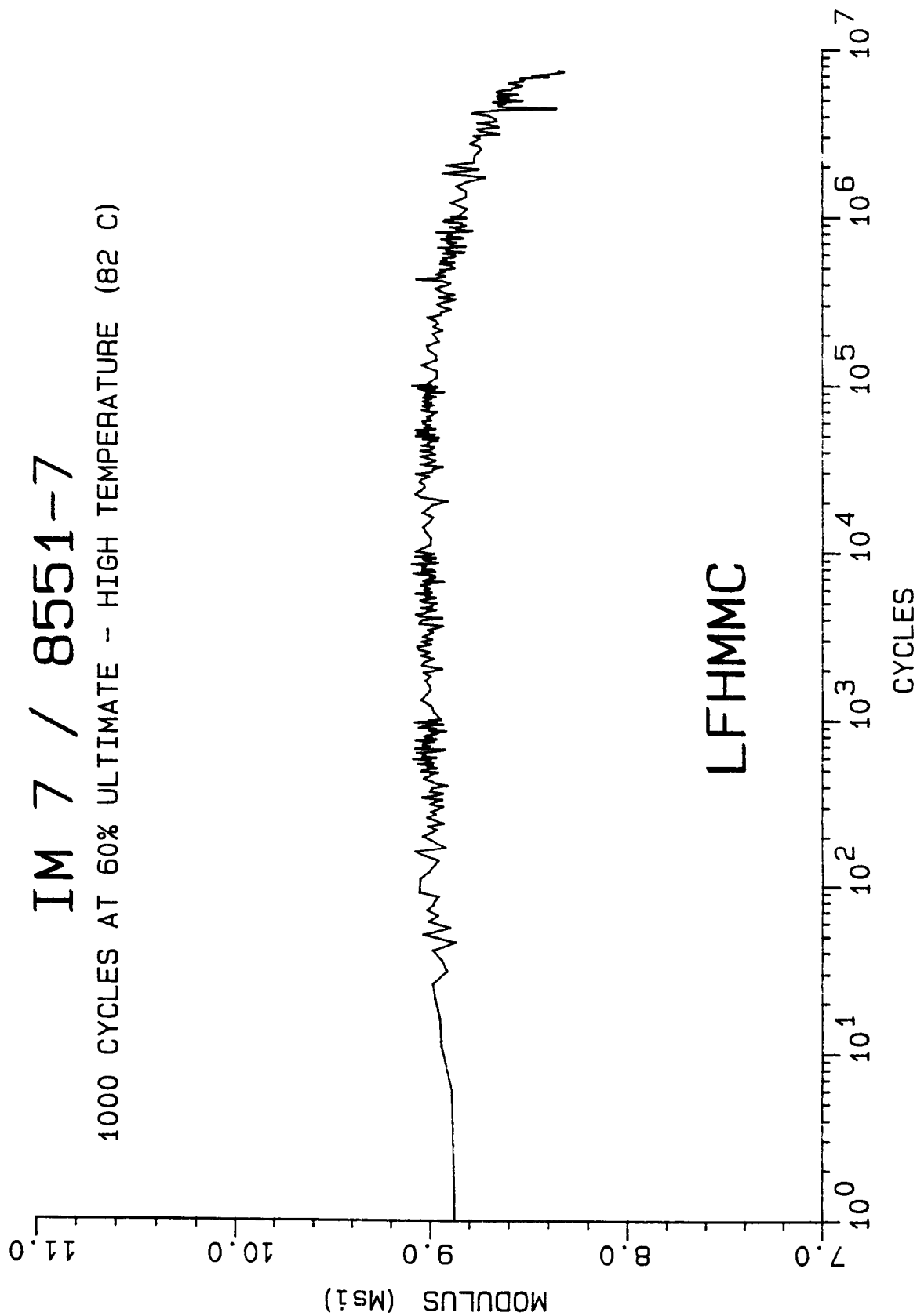
1000 CYCLES AT 60% ULTIMATE - HIGH TEMPERATURE (82 C)



MODULUS DECAY CURVE

IM 7 / 8551-7

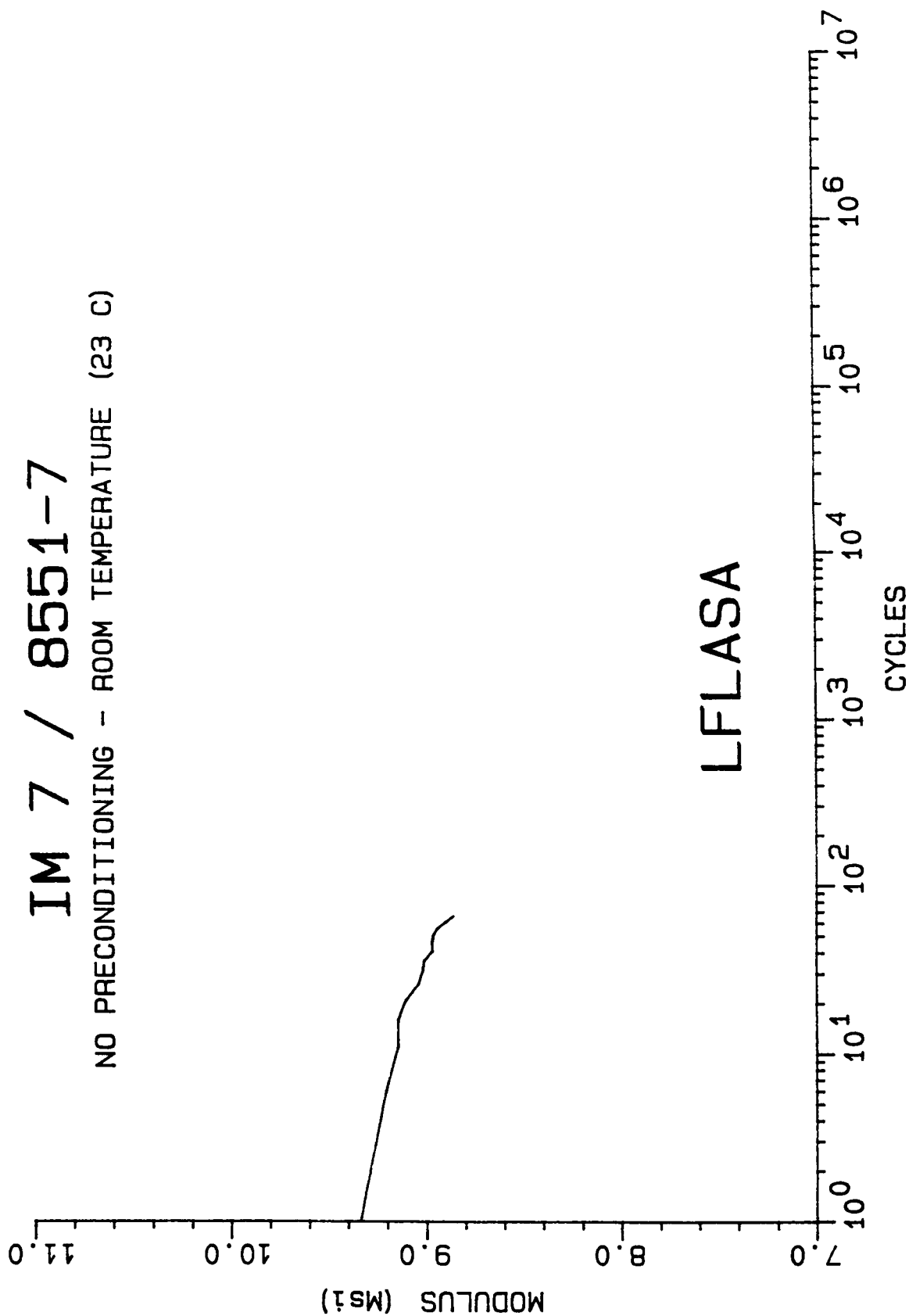
1000 CYCLES AT 60% ULTIMATE - HIGH TEMPERATURE (82 C)



MODULUS DECAY CURVE

IM 7 / 8551-7

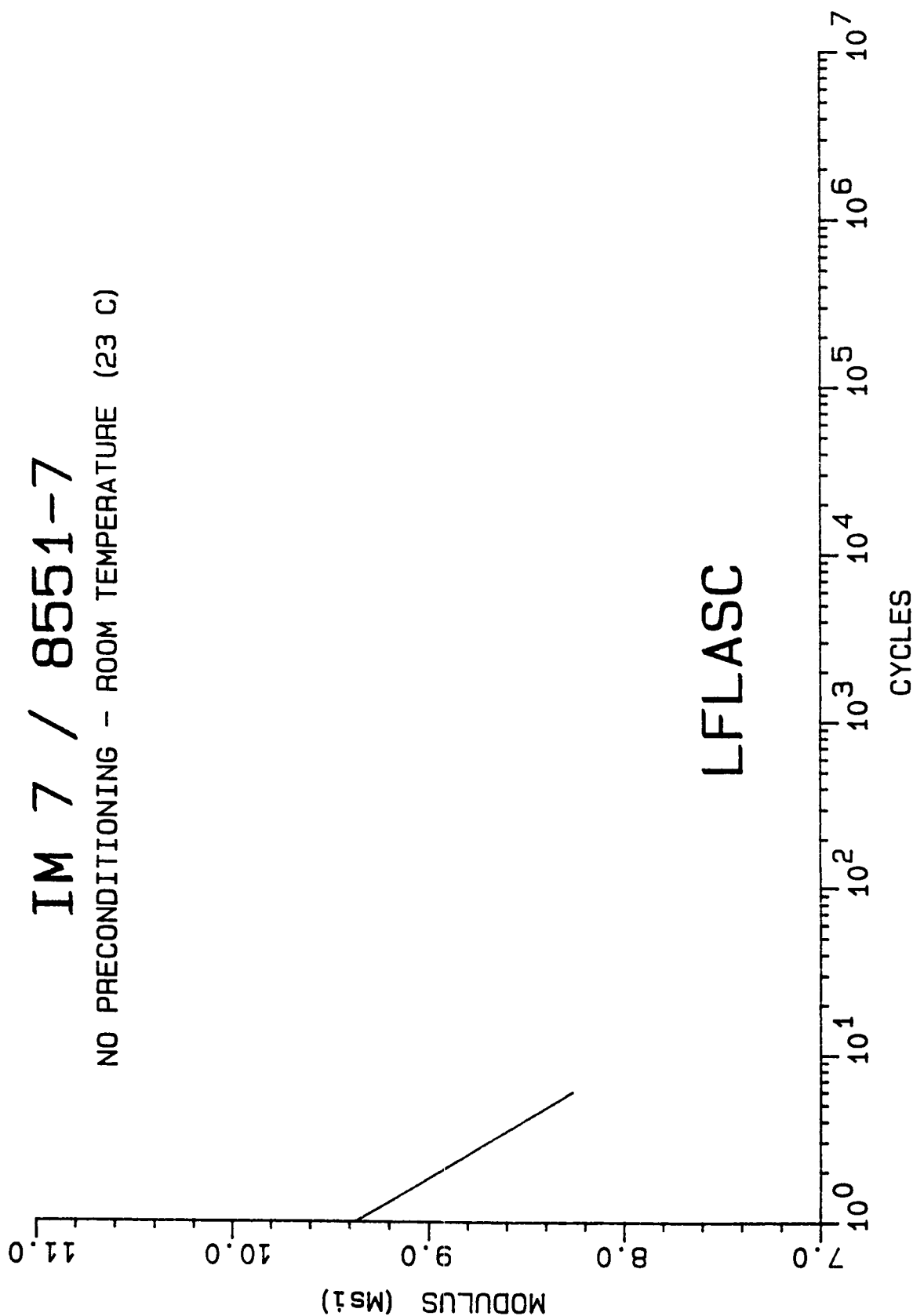
NO PRECONDITIONING - ROOM TEMPERATURE (23 C)



MODULUS DECAY CURVE

IM 7 / 8551-7

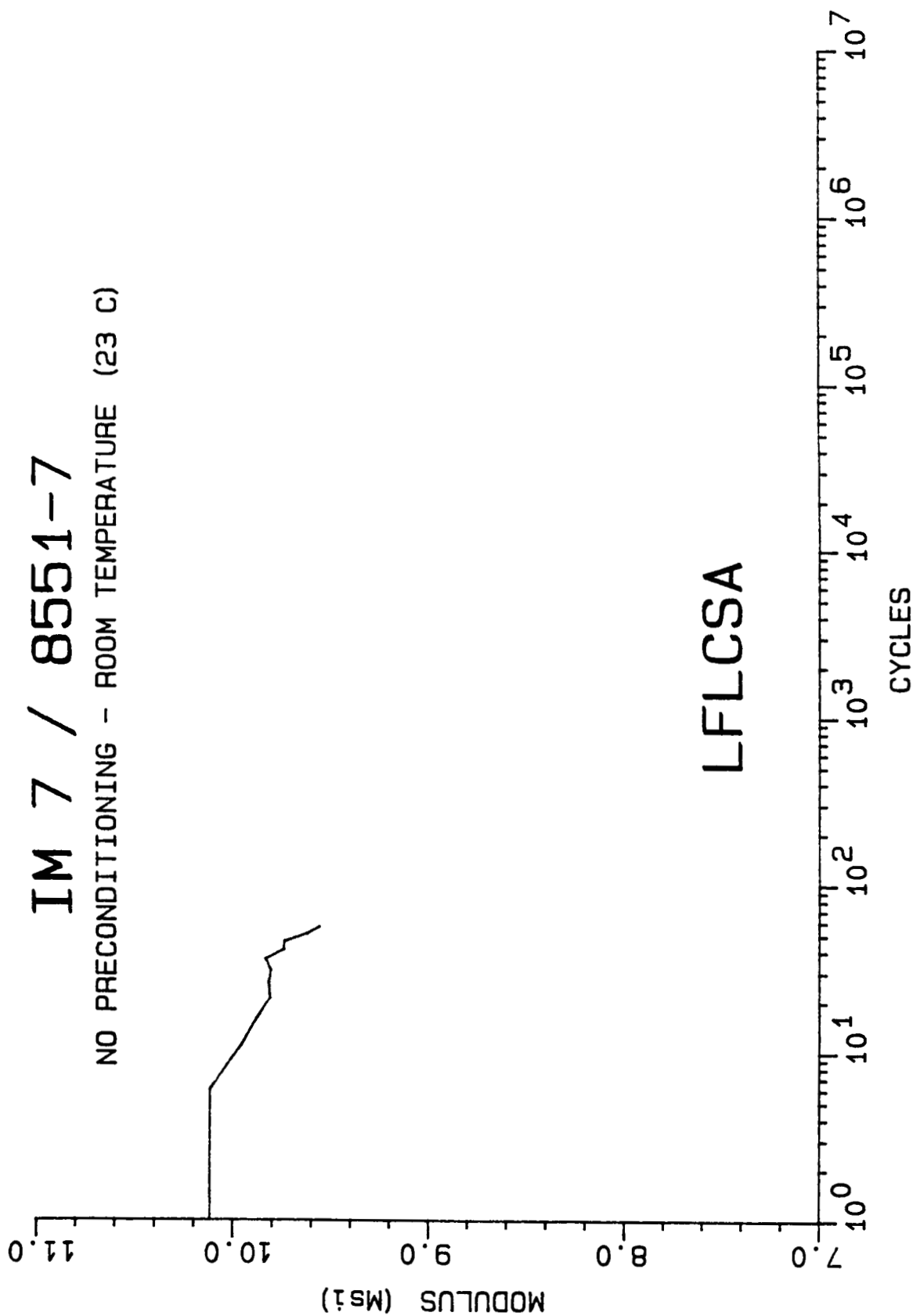
NO PRECONDITIONING - ROOM TEMPERATURE (23 C)



MODULUS DECAY CURVE

IM 7 / 8551-7

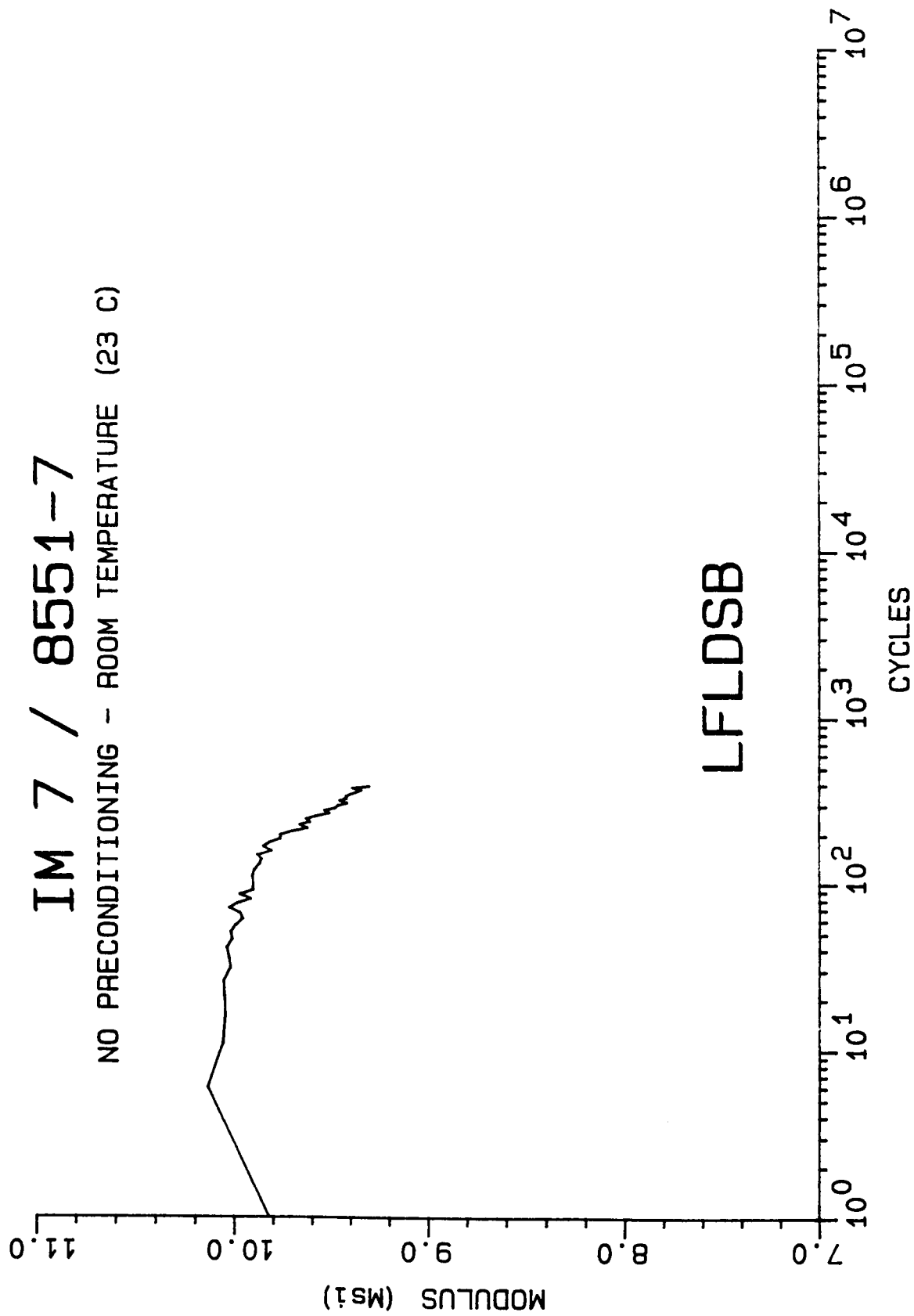
NO PRECONDITIONING - ROOM TEMPERATURE (23 C)



MODULUS DECAY CURVE

IM 7 / 8551-7

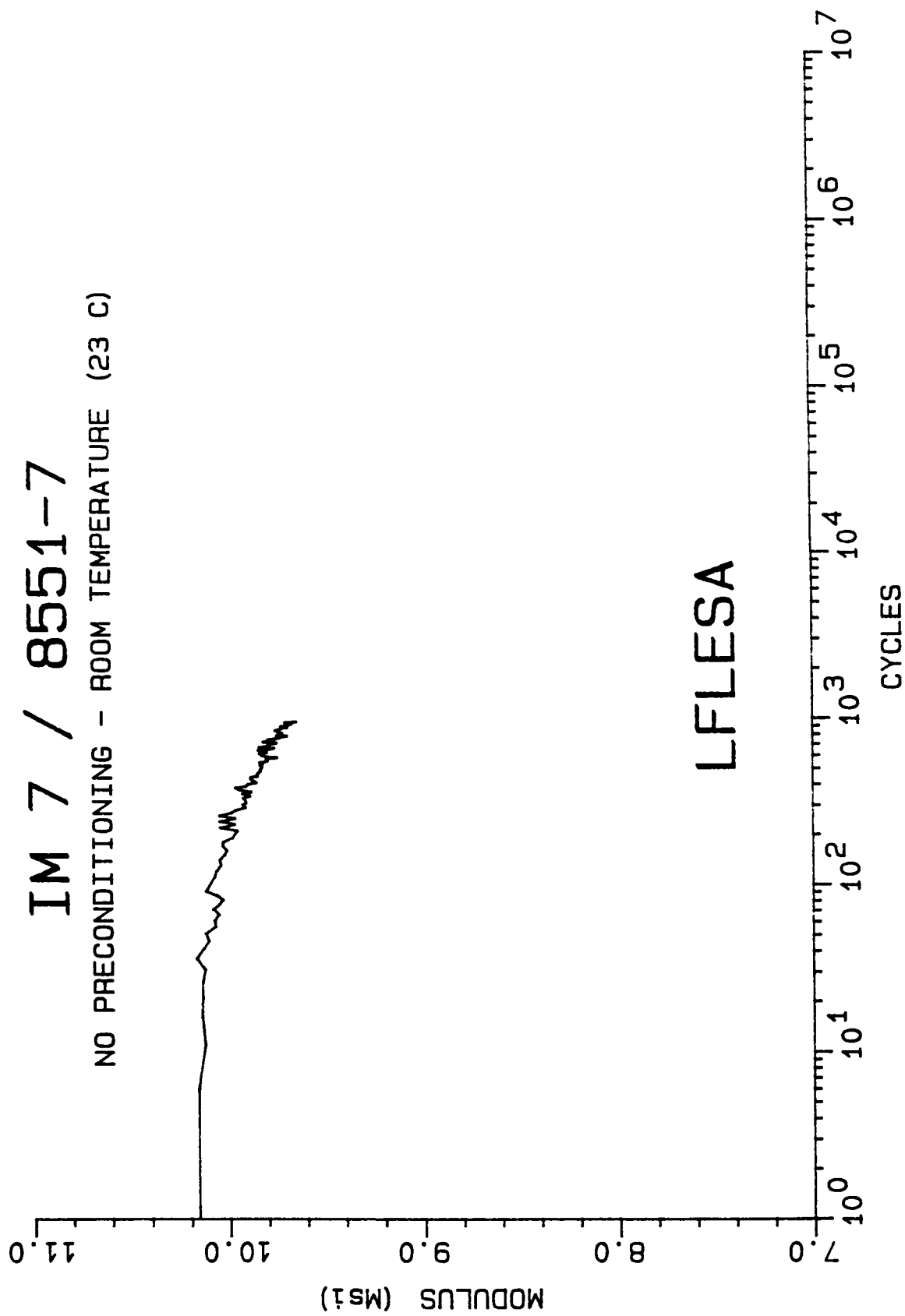
NO PRECONDITIONING - ROOM TEMPERATURE (23 C)



MODULUS DECAY CURVE

IM 7 / 8551-7

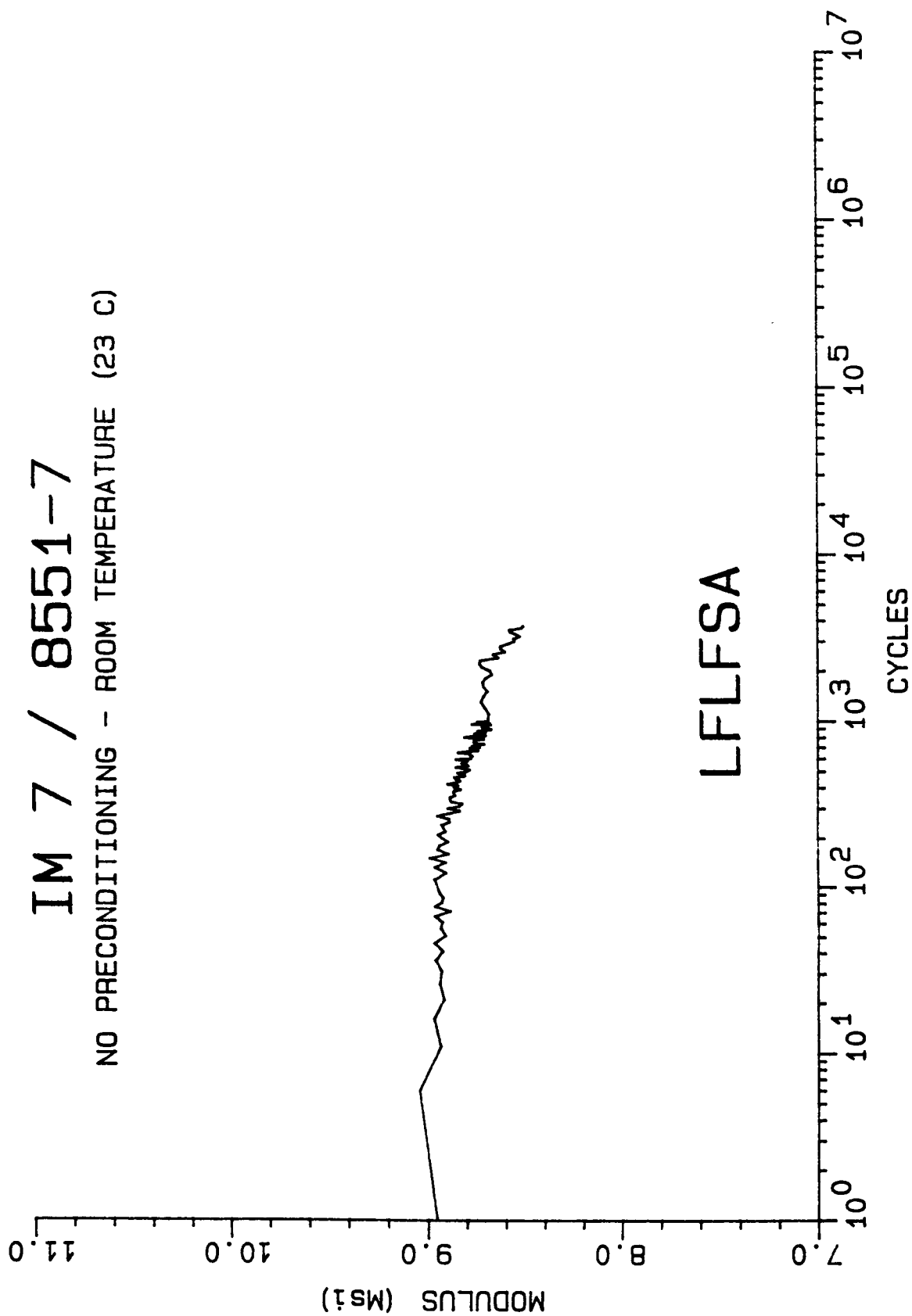
NO PRECONDITIONING - ROOM TEMPERATURE (23 C)



MODULUS DECAY CURVE

IM 7 / 8551-7

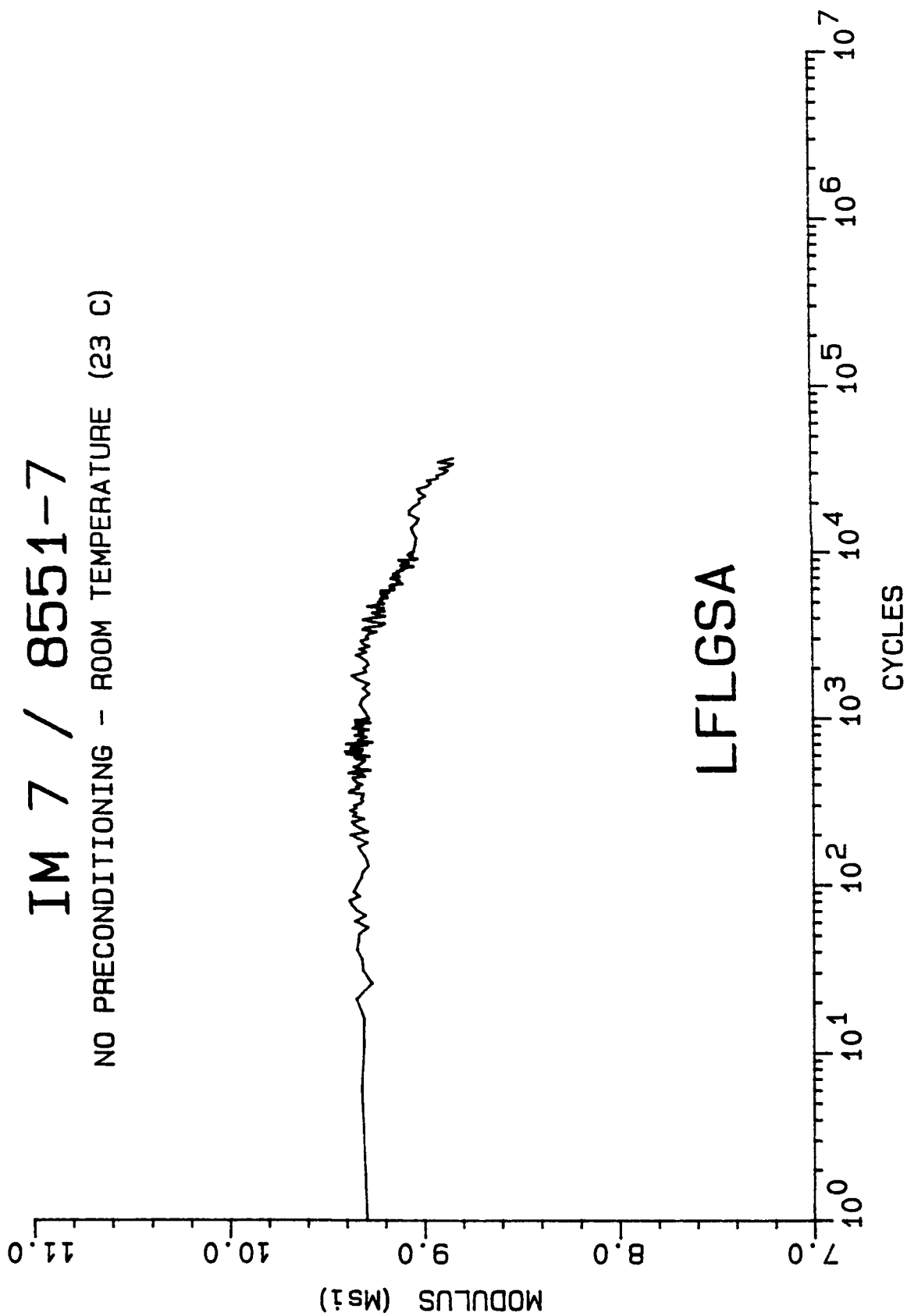
NO PRECONDITIONING - ROOM TEMPERATURE (23 C)



MODULUS DECAY CURVE

IM 7 / 8551-7

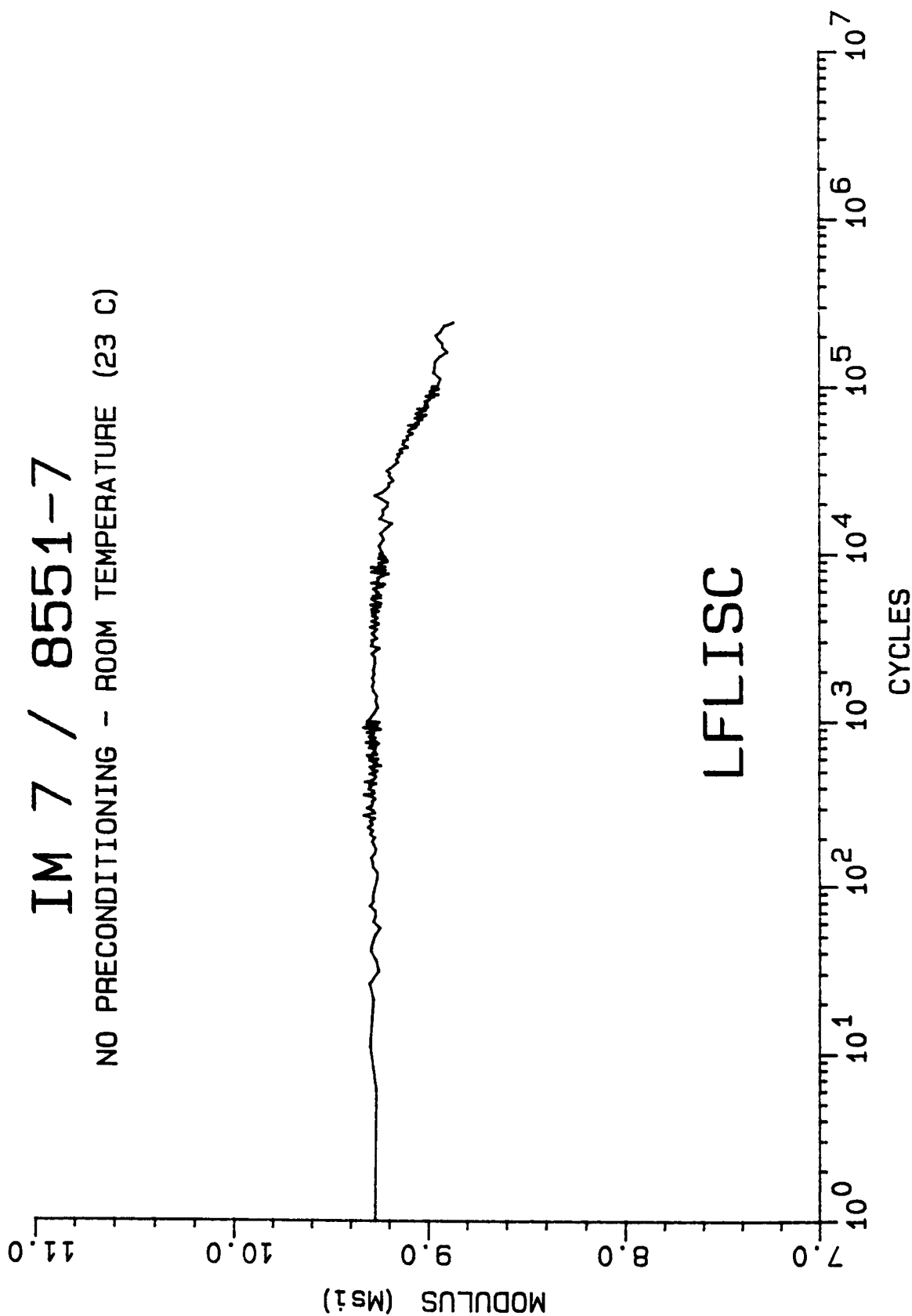
NO PRECONDITIONING - ROOM TEMPERATURE (23 C)



MODULUS DECAY CURVE

IM 7 / 8551-7

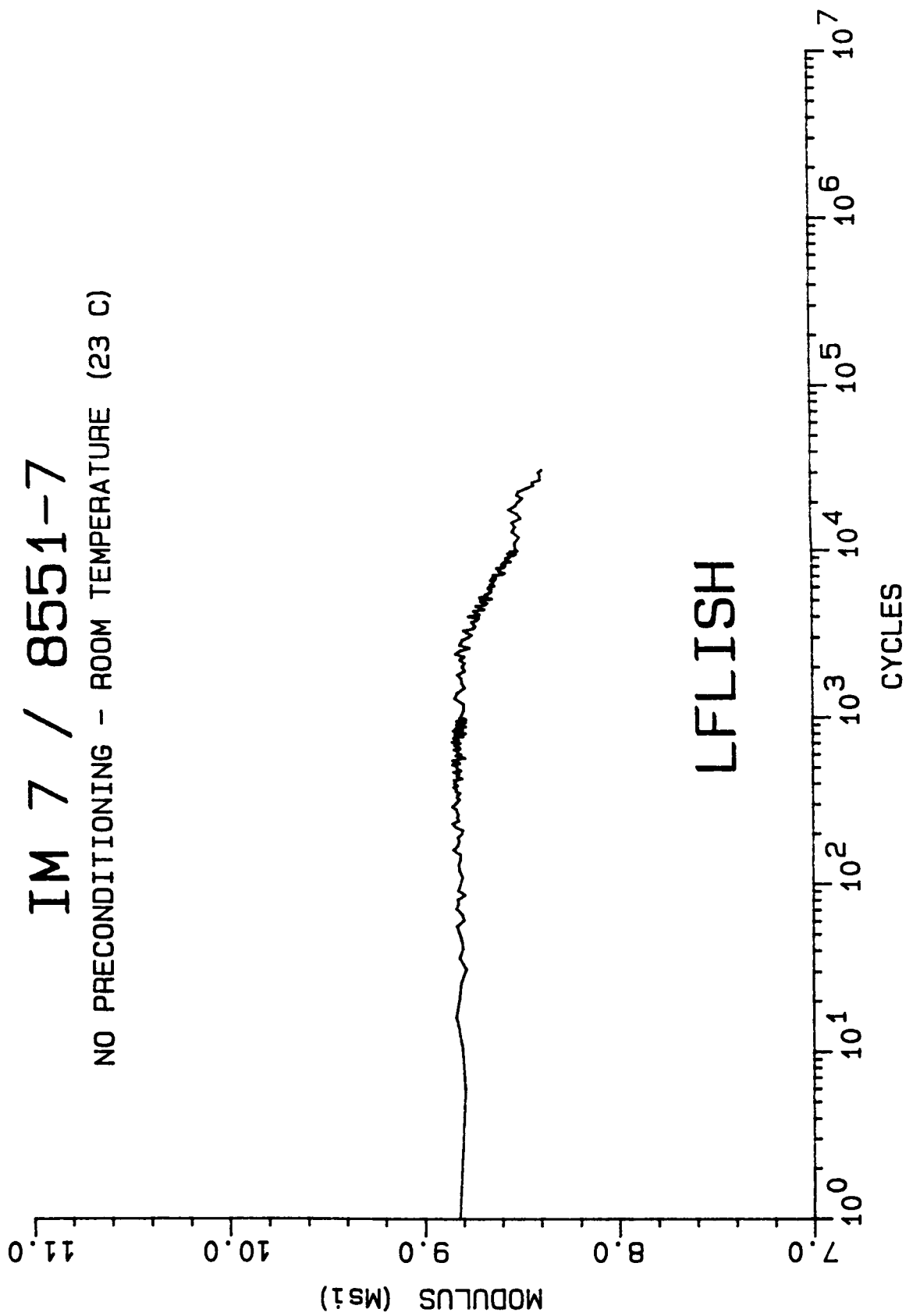
NO PRECONDITIONING - ROOM TEMPERATURE (23 C)



MODULUS DECAY CURVE

IM 7 / 8551-7

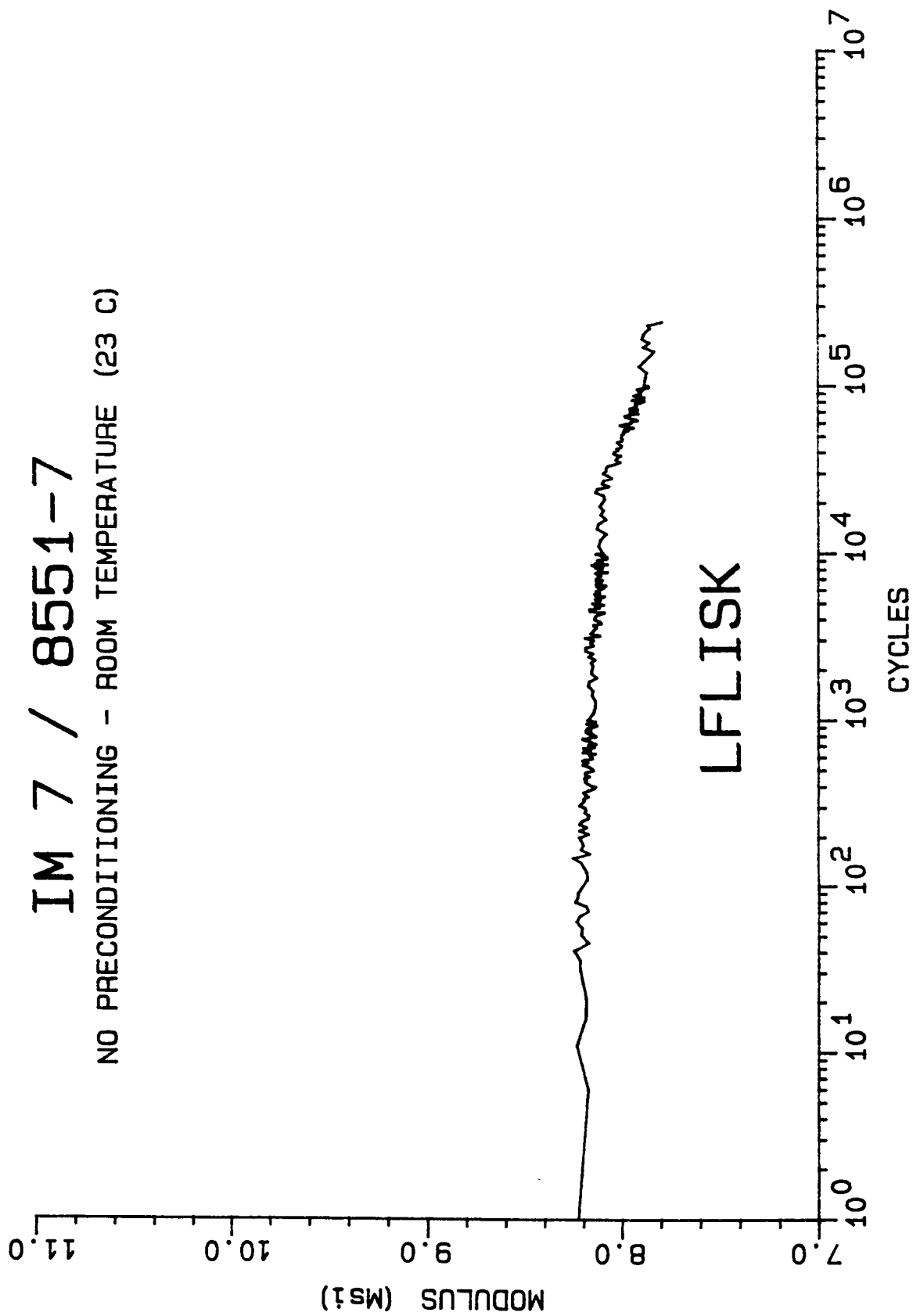
NO PRECONDITIONING - ROOM TEMPERATURE (23 C)



MODULUS DECAY CURVE

IM 7 / 8551-7

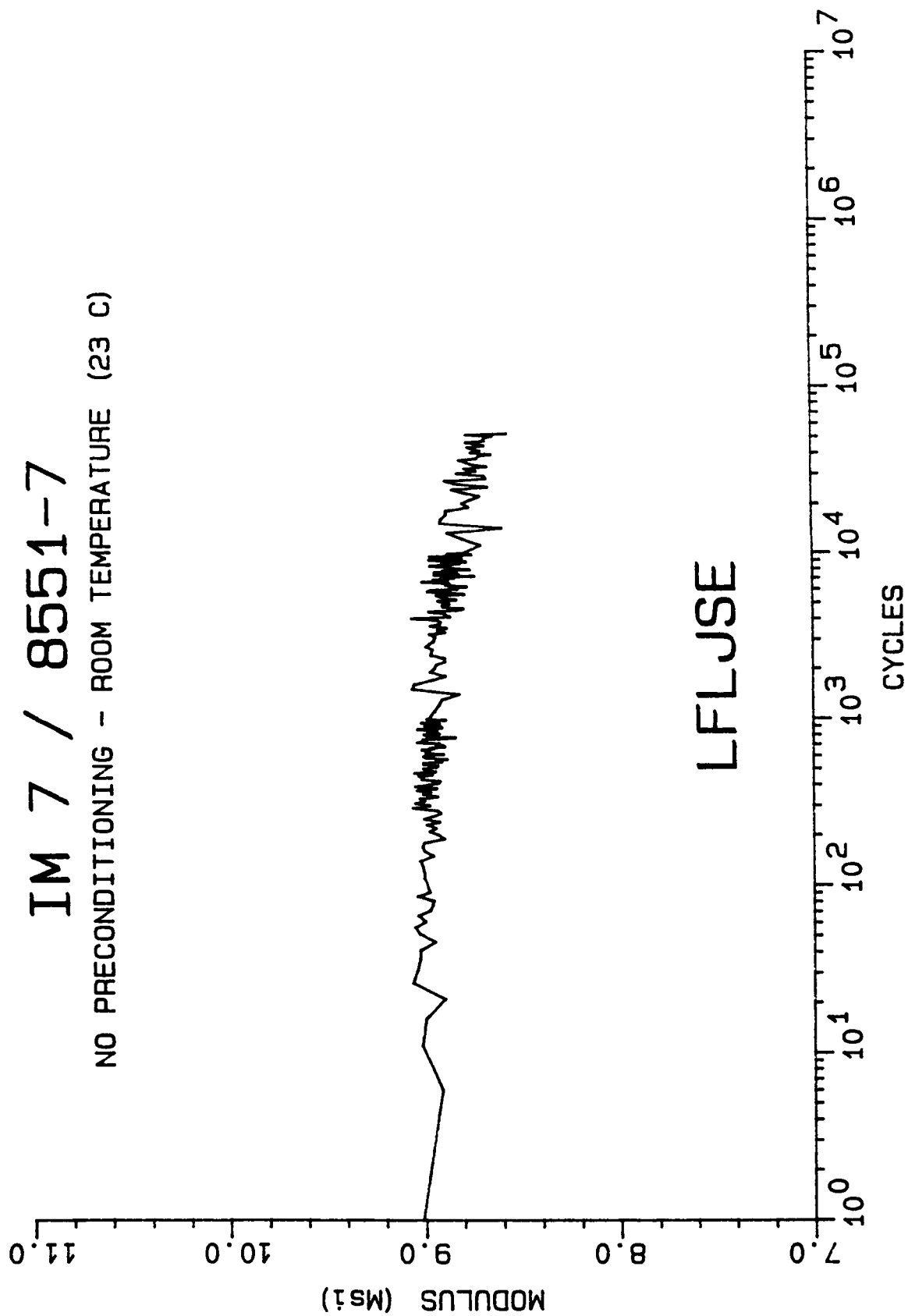
NO PRECONDITIONING - ROOM TEMPERATURE (23 C)



MODULUS DECAY CURVE

IM 7 / 8551-7

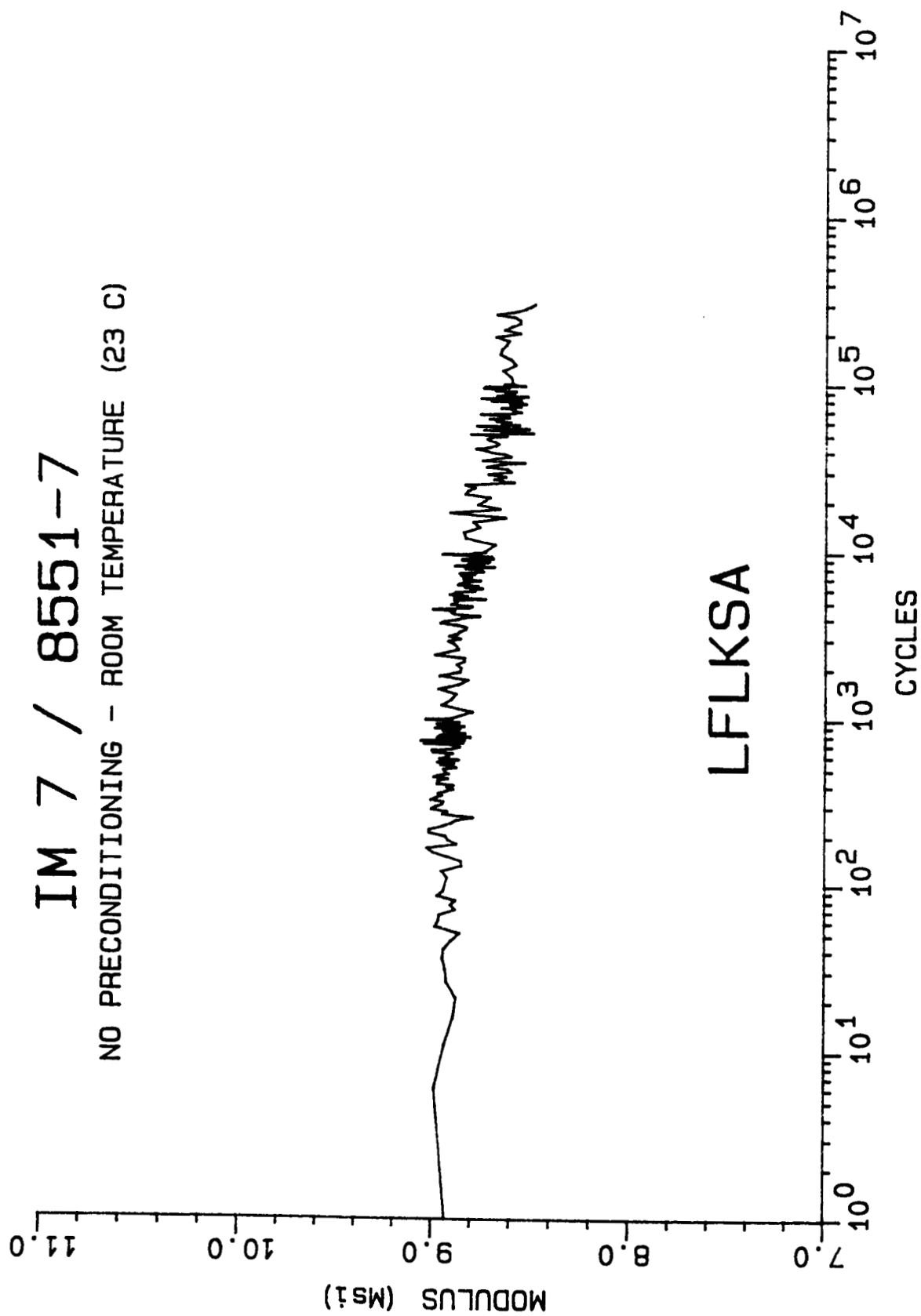
NO PRECONDITIONING - ROOM TEMPERATURE (23 C)



MODULUS DECAY CURVE

IM 7 / 8551-7

NO PRECONDITIONING - ROOM TEMPERATURE (23 C)

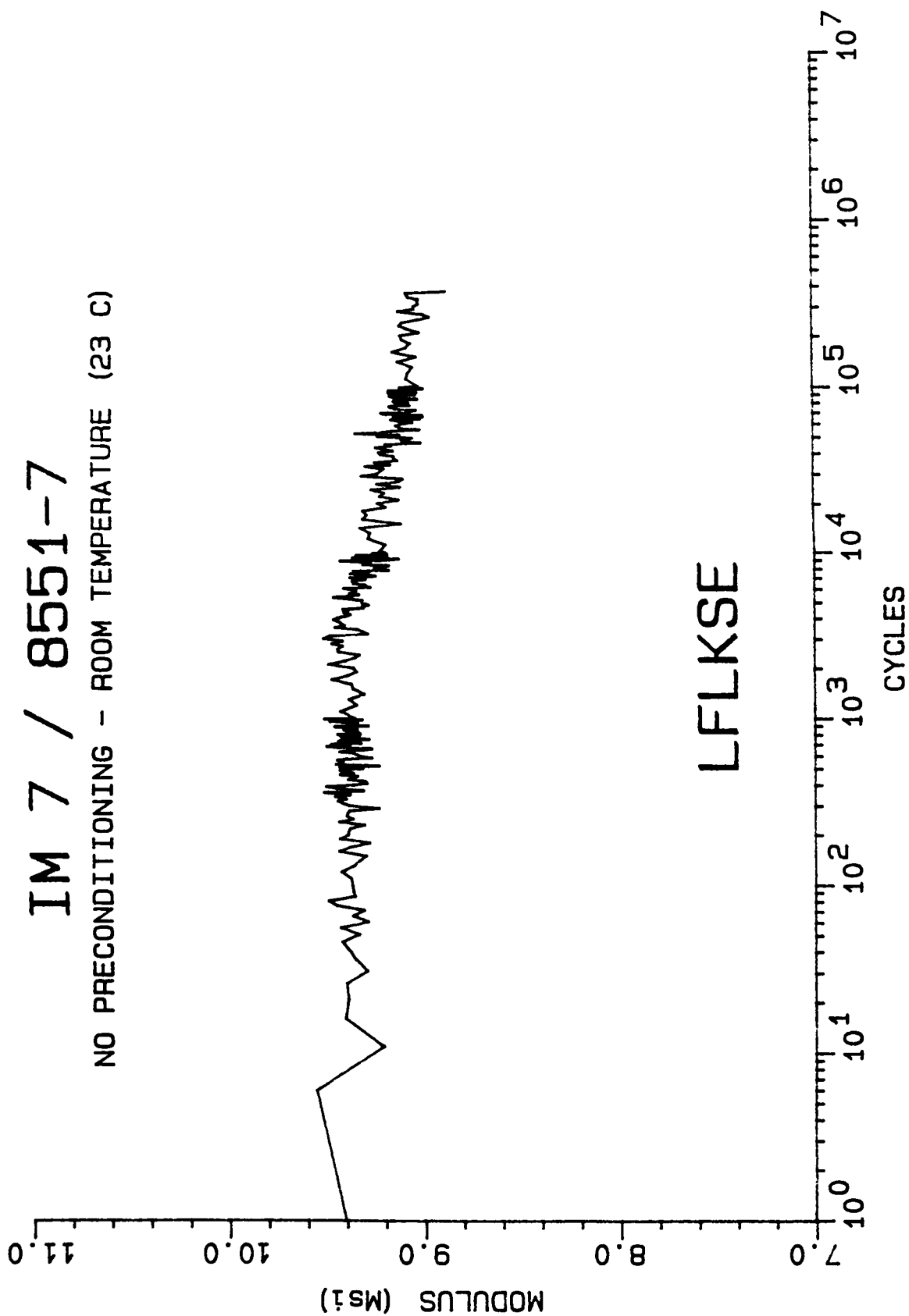


LFLKSA

MODULUS DECAY CURVE

IM 7 / 8551-7

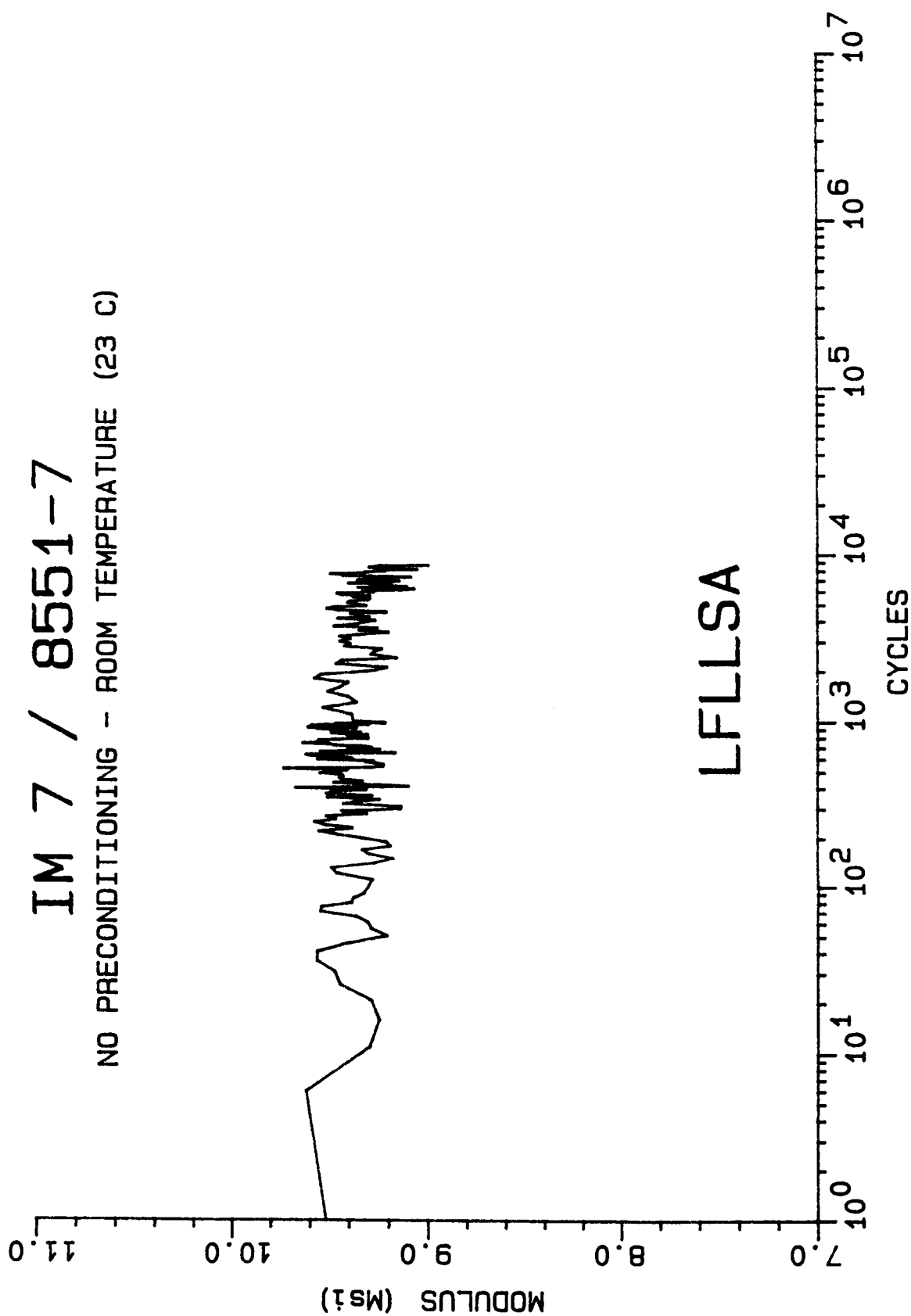
NO PRECONDITIONING - ROOM TEMPERATURE (23 C)



MODULUS DECAY CURVE

IM 7 / 8551-7

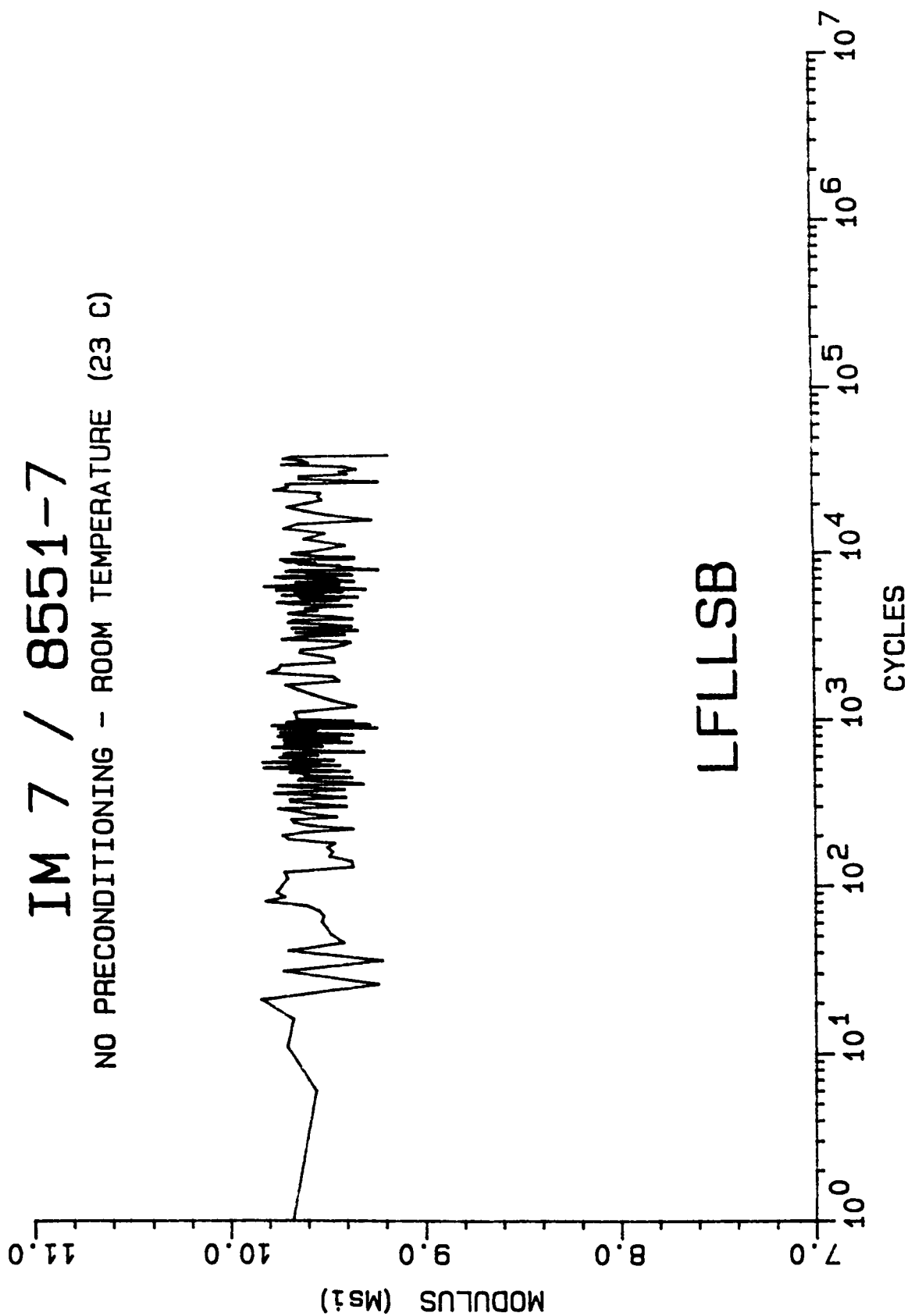
NO PRECONDITIONING - ROOM TEMPERATURE (23 C)



MODULUS DECAY CURVE

IM 7 / 8551-7

NO PRECONDITIONING - ROOM TEMPERATURE (23 C)

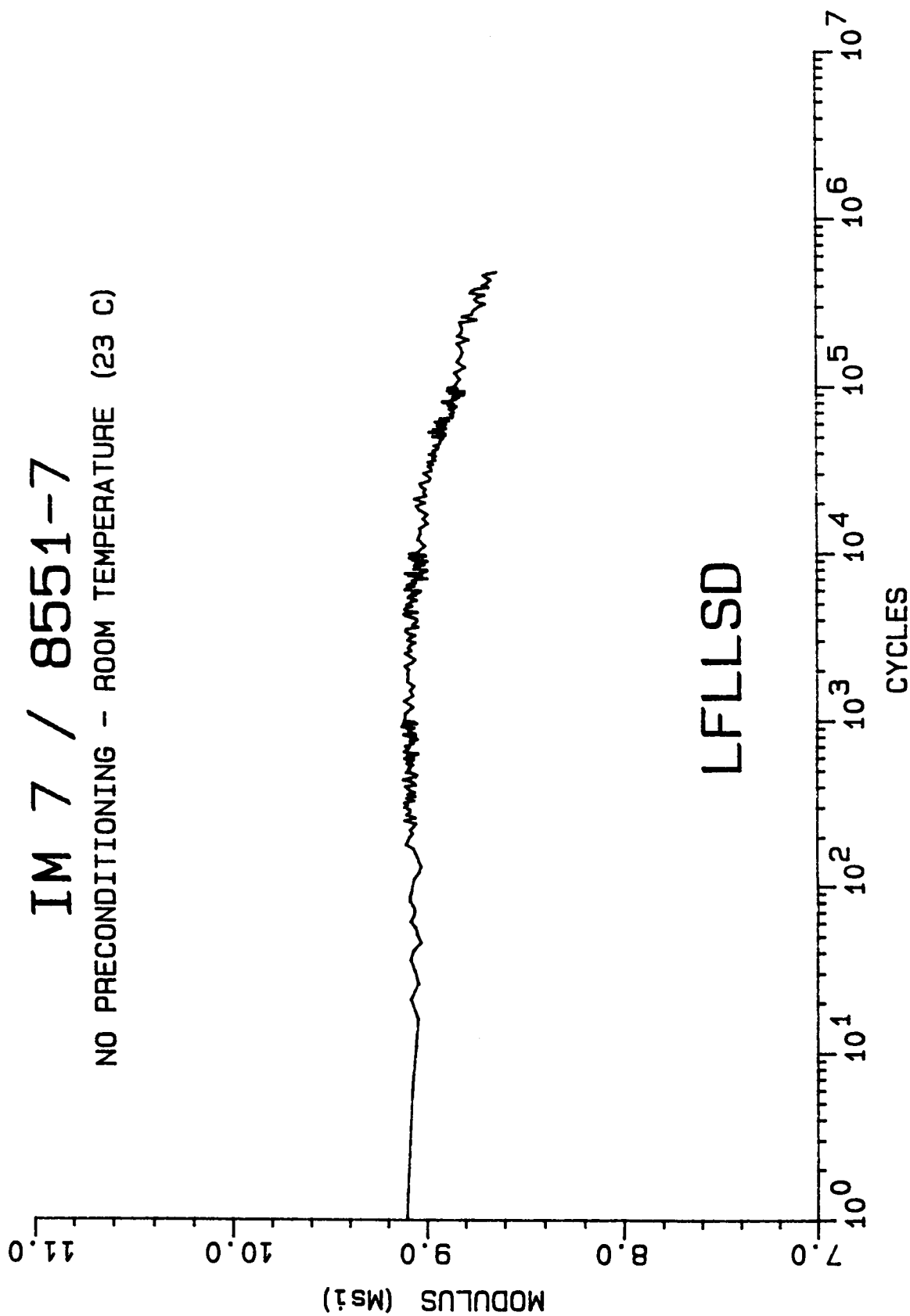


LFLLSB

MODULUS DECAY CURVE

IM 7 / 8551-7

NO PRECONDITIONING - ROOM TEMPERATURE (23 C)



MODULUS DECAY CURVE

IM 7 / 8551-7

NO PRECONDITIONING - ROOM TEMPERATURE (23 C)

